frontiers | Research Topics

Case reports in cardio-oncology 2024

Edited by
Reto Asmis

Published in
Frontiers in Cardiovascular Medicine
Frontiers in Oncology

FRONTIERS EBOOK COPYRIGHT STATEMENT

The copyright in the text of individual articles in this ebook is the property of their respective authors or their respective institutions or funders. The copyright in graphics and images within each article may be subject to copyright of other parties. In both cases this is subject to a license granted to Frontiers.

The compilation of articles constituting this ebook is the property of Frontiers.

Each article within this ebook, and the ebook itself, are published under the most recent version of the Creative Commons CC-BY licence. The version current at the date of publication of this ebook is CC-BY 4.0. If the CC-BY licence is updated, the licence granted by Frontiers is automatically updated to the new version.

When exercising any right under the CC-BY licence, Frontiers must be attributed as the original publisher of the article or ebook, as applicable.

Authors have the responsibility of ensuring that any graphics or other materials which are the property of others may be included in the CC-BY licence, but this should be checked before relying on the CC-BY licence to reproduce those materials. Any copyright notices relating to those materials must be complied with.

Copyright and source acknowledgement notices may not be removed and must be displayed in any copy, derivative work or partial copy which includes the elements in question.

All copyright, and all rights therein, are protected by national and international copyright laws. The above represents a summary only. For further information please read Frontiers' Conditions for Website Use and Copyright Statement, and the applicable CC-BY licence.

ISSN 1664-8714
ISBN 978-2-8325-6897-2
DOI 10.3389/978-2-8325-6897-2

Generative AI statement
Any alternative text (Alt text) provided alongside figures in the articles in this ebook has been generated by Frontiers with the support of artificial intelligence and reasonable efforts have been made to ensure accuracy, including review by the authors wherever possible. If you identify any issues, please contact us.

About Frontiers

Frontiers is more than just an open access publisher of scholarly articles: it is a pioneering approach to the world of academia, radically improving the way scholarly research is managed. The grand vision of Frontiers is a world where all people have an equal opportunity to seek, share and generate knowledge. Frontiers provides immediate and permanent online open access to all its publications, but this alone is not enough to realize our grand goals.

Frontiers journal series

The Frontiers journal series is a multi-tier and interdisciplinary set of open-access, online journals, promising a paradigm shift from the current review, selection and dissemination processes in academic publishing. All Frontiers journals are driven by researchers for researchers; therefore, they constitute a service to the scholarly community. At the same time, the *Frontiers journal series* operates on a revolutionary invention, the tiered publishing system, initially addressing specific communities of scholars, and gradually climbing up to broader public understanding, thus serving the interests of the lay society, too.

Dedication to quality

Each Frontiers article is a landmark of the highest quality, thanks to genuinely collaborative interactions between authors and review editors, who include some of the world's best academicians. Research must be certified by peers before entering a stream of knowledge that may eventually reach the public - and shape society; therefore, Frontiers only applies the most rigorous and unbiased reviews. Frontiers revolutionizes research publishing by freely delivering the most outstanding research, evaluated with no bias from both the academic and social point of view. By applying the most advanced information technologies, Frontiers is catapulting scholarly publishing into a new generation.

What are Frontiers Research Topics?

Frontiers Research Topics are very popular trademarks of the *Frontiers journals series*: they are collections of at least ten articles, all centered on a particular subject. With their unique mix of varied contributions from Original Research to Review Articles, Frontiers Research Topics unify the most influential researchers, the latest key findings and historical advances in a hot research area.

Find out more on how to host your own Frontiers Research Topic or contribute to one as an author by contacting the Frontiers editorial office: frontiersin.org/about/contact

Case reports in cardio-oncology: 2024

Topic editor
Reto Asmis — Wake Forest University, United States

Citation
Asmis, R., ed. (2025). *Case reports in cardio-oncology: 2024*. Lausanne: Frontiers Media SA. doi: 10.3389/978-2-8325-6897-2

Table of contents

05 Case Report: Lung cancer with rare cardiac and other multiple metastases
Li Chen, Jing Zhang and Chunquan Zhang

12 Case Report: Pazopanib-induced acute coronary syndrome
Adithya K. Yadalam, William M. Schultz, Chanhee Han and Anant Mandawat

17 Efficacy and safety of anakinra in radiation-induced acute pericarditis: a case report
Ludovico Luca Sicignano, Celeste Ambra Murace, Antonella Palazzo, Elena Verrecchia, Maria Grazia Massaro, Raffaele Manna and Laura Gerardino

21 A simple goiter of the right ventricle: case report and literature review
Shuai Luo, Xiaoxue Tian, Ting Xu and Jinjing Wang

28 Case Report: Avoiding misdiagnosis in amyloidosis—navigating transthyretin genopositivity and monoclonal gammopathy in a patient with advanced heart failure and spinal stenosis
Xia Wu, Denis Toskic, Ping Zhou, Stephanie Scalia, Xun Ma, Parva Bhatt, Teresa Fogaren, Monika Pilichowska, Knarik Arkun, Jainith Patel, Ron I. Riesenburger, Daniel P. Larson and Raymond L. Comenzo

35 Case report: Primary cardiac undifferentiated sarcoma complicated by esophagus stenosis
Yuxin Ge, Xiaopan Lv, Rui Zhang, Dongxiao Hao, Guifei Si, Yuquan Li, Xuemin Yuan and Xiuping Li

40 Cancer-associated thoracic aorta arterial thrombosis: case report and review of the literature
Miguel Borregón, María Valero, Asia Ferrández, Álvaro Muñoz, Carmen Roque and Javier-David Benítez-Fuentes

47 Aortic intimal sarcoma with abdominal metastasis: case report and management approach
Gongji Yao and Jianwei Xu

52 Diagnostic trap: a case report of intimal sarcoma occurring in the left atrium
Hua Ye, Yuchen Jing, Shuai Luo and Jinjing Wang

59 Severe immune-mediated myocarditis caused by sintilimab combined with gemcitabine: a case report and literature review
Haixia Yang, Menglu Sun, Xiaosha Zhou, Yaxuan Han, Shanshan Zhang, Kelin Zhang and Xiaoyan Zhang

67 Case report: Diversity of imaging in cardiac angiosarcoma: two cases with disparate enhancement and metabolic manifestations
Sinan Chen, Huan Cen, Jie Zhao, Pengcheng Ran, Weihui Lu and Pengtao Sun

73 Multiple cardiac papillary fibroelastomas: a case report and review of the literature
Mostafa Ali, Mohammad Alomari, Magdy M. El-Sayed Ahmed, Pankaj Garg, Anthony N. Pham and Si M. Pham

78 Case Report: A very rare case of diffuse large B-cell lymphoma with cardiac and ovarian involvement
Yadan Du, Yuting Tian, Yawen Chen, Shuaihua Cheng and Jianping Gao

87 Case Report: Primary cardiac diffuse large B-cell lymphoma with sick sinus syndrome and literature review on disease management and therapeutic strategies
Xiaofen Qiu, Li Zhang, Shaojun Zhou, Wenbin Qian, Yun Liang, Huiqing Qiu and Xianggui Yuan

95 Case report: Cardiac myxoid fibrosarcoma: a report of two cases
Weikai Dong, Zhaoqi Du, Dianxiao Liu, Lijuan Yang and Wei Li

frontiers | Frontiers in Cardiovascular Medicine

TYPE Case Report
PUBLISHED 12 September 2024
DOI 10.3389/fcvm.2024.1417906

Check for updates

OPEN ACCESS

EDITED BY
Reto Asmis,
Wake Forest University, United States

REVIEWED BY
Prashanth Ravishankar,
Namida Lab, Inc., United States
Luigi Tarantini,
IRCCS Local Health Authority of Reggio Emilia, Italy

*CORRESPONDENCE
Chunquan Zhang
jxzcq@163.com

†These authors have contributed equally to this work and share first authorship

RECEIVED 15 April 2024
ACCEPTED 30 August 2024
PUBLISHED 12 September 2024

CITATION
Chen L, Zhang J and Zhang C (2024) Case Report: Lung cancer with rare cardiac and other multiple metastases.
Front. Cardiovasc. Med. 11:1417906.
doi: 10.3389/fcvm.2024.1417906

COPYRIGHT
© 2024 Chen, Zhang and Zhang. This is an open-access article distributed under the terms of the Creative Commons Attribution License (CC BY). The use, distribution or reproduction in other forums is permitted, provided the original author(s) and the copyright owner(s) are credited and that the original publication in this journal is cited, in accordance with accepted academic practice. No use, distribution or reproduction is permitted which does not comply with these terms.

Case Report: Lung cancer with rare cardiac and other multiple metastases

Li Chen[1,2†], Jing Zhang[1,2†] and Chunquan Zhang[1,2*]

[1]Department of Ultrasound, The Second Affiliated Hospital of Nanchang University, Nanchang, China, [2]Jiangxi Medical College of Nanchang University, Nanchang, China

Metastasis to the left atrium is exceptionally uncommon, occurring at a rate of only 3.1%. The clinical manifestations of lung cancer metastasizing to the heart can vary widely. They range from paraneoplastic syndrome, dyspnea, and ST-segment elevation on an electrocardiogram to no clinically significant symptoms. Diverging from typical metastatic patterns observed in lung cancer, this case report presents a detailed description, from the perspective of the microenvironment, of a rare instance where lung cancer metastasized to the mediastinal lymph nodes, adrenal glands, brain, and notably, the left atrium, in a non-smoking female patient.

KEYWORDS

left atrial tumors, metastasiscase, case report, microenvironment, diagnostic

1 Introduction

Globally, lung cancer stands as the foremost cause of cancer-related mortality among both men and women, boasting an exceedingly high mortality rate (1). The global increase in lung cancer incidence is primarily driven by male cases, with 85%–90% of these cases closely associated with smoking (2). However, recent studies have revealed a rising incidence of lung cancer among non-smoking women, and it is anticipated that by 2,045, the lung cancer mortality rate in women will surpass that in men (3). It is classified into two main categories: small-cell lung cancer and non-small-cell lung cancer. The predominant sites of metastasis for non-small-cell lung cancer, in descending order, include bone, lung, brain, adrenal gland, liver, and extrathoracic lymph nodes (4). Among these, the likelihood of metastasis to the brain, adrenal gland, and extrathoracic lymph nodes was 28.4%, 16.7%, and 9.5%, respectively (4). Nevertheless, metastasis to the heart is deemed exceptionally rare, with only 3.1% of 4,668 lung cancer patients developing such metastasis in one study (5). This case report is the first to detail, from the perspective of the microenvironment, a female lung cancer case with multiple rare site metastases–including the heart, mediastinal lymph nodes, adrenal glands, and brain–presenting with no significant clinical symptoms other than weight loss.

2 Case report

A 62-year-old non-smoking female presented to our hospital with kidney stones and underwent a comprehensive full-body examination. She self-reported being previously

Abbreviations
NSCLC, non-small-cell lung cancer; ER, endoplasmic reticulum; 18F-FDG PET: 18F-labeled fluorodeoxyglucose positron emission tomography; CCR2, CC- chemokine receptor 2, CXCL12, CXC- chemokine ligand 12; CCR6, CC- chemokine receptor 6; CCL20, CC- chemokine ligand 20; CXCR4, CXC- chemokine receptor 4.

healthy and not experiencing any symptoms, except for a significant recent weight loss. During the physical examination, the patient appeared to be in good overall condition, with a blood pressure reading of 92/51 mmHg, a heart rate of 81 beats per min, a respiratory rate of 19 breaths per min, and no murmurs detected upon cardiopulmonary auscultation. The chest CT scan revealed lung cancer in the upper lobe of the right lung, which was further complicated by hilar and mediastinal lymph node metastasis. The lymphatic vessels surrounding the tumor appeared thickened and nodulated. Transthoracic echocardiography and organ acoustic imaging identified a 5.1 × 3.4 cm metastatic hypoechoic mass in the left atrium, closely associated with the right pulmonary vein (Figure 1). She underwent additional CT contrast imaging of the neck, chest, and upper abdomen, which confirmed the presence of a mass in the left atrium connected to the right upper pulmonary vein (Figure 2). Furthermore, a metastatic nodule was detected in the right adrenal gland. Simultaneously, a contrast-enhanced MRI of the head revealed a circular enhancing nodule located centrally within an oval lesion on the left side, indicative of skull metastasis. To elucidate the pathology, the patient ultimately opted for lung biopsy and immunohistochemical examination, which confirmed the diagnosis of non-small-cell lung cancer (NSCLC). Microscopic examination revealed cancer cells arranged in nests and clusters, demonstrating infiltrative growth, notable heterogeneity among the cancer cells, and proliferation of interstitial fibrous tissue (Figure 3). Following antigen retrieval, blocking, antibody staining, and color development steps in immunohistochemistry, the results indicate that the cancer cells exhibited positivity for CK, focal positivity for CK7, TTF1 (localized), and PD-L1 22C3 TPS (localized), with a Ki-67 proliferation index of approximately 20%. The cells tested negative for NapsinA, P40, P63, CK5/6, and ALK-D5F3. Special stains indicated negative staining for mucus carmine and positive staining for individual cells of AB-PAS.

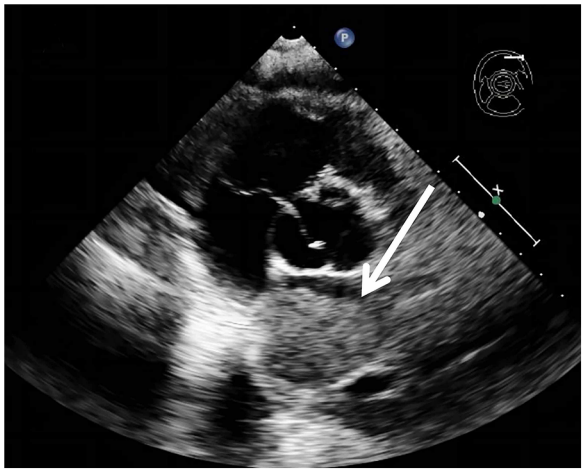

FIGURE 1
A metastatic hypoechoic mass, measuring 5.1 × 3.4 cm, was present in the left atrium, closely adjacent to the right pulmonary vein.

However, the tumor had metastasized to multiple distant sites, progressing to stage IVB, thus eliminating the possibility of surgical intervention. To identify a more appropriate chemotherapy regimen, the patient underwent genetic testing, revealing a fourth exon TP53 frameshift mutation (abundance 48.6%), a KMT2A exon 22 mutation (abundance 25.95%), and an MSH2 exon 16 mutation (abundance 2.6%). The primary method for genetic testing involves fixing, dehydrating, and sectioning the tumor tissue samples obtained from biopsy, followed by DNA extraction and whole-exome sequencing. After careful deliberation, the physician suggested an immunotherapy protocol involving a combination of carboplatin and pemetrexed chemotherapy along with tislelizumab. During the therapy, the patient did not report any significant discomfort. Although the degree of tumor shrinkage still requires further observation, the patient's overall condition remains stable. Specifically, the performance status score is 1, the numerical rating scale is 1, body weight has remained stable, and no significant adverse reactions or complications have emerged. The patient has exhibited a commendable tolerance to this treatment regimen. However, due to the patient's financial constraints and psychological pressures, the patient ultimately decided to discontinue treatment. Specifically, the substantial therapy costs imposed severe stress on her financial situation. Additionally, the patient experienced significant psychological burdens during the therapy, perceiving its prolonged nature and impact on her quality of life, which influenced her decision to cease further treatment. Clinical events have been listed according to the timeline (Table 1).

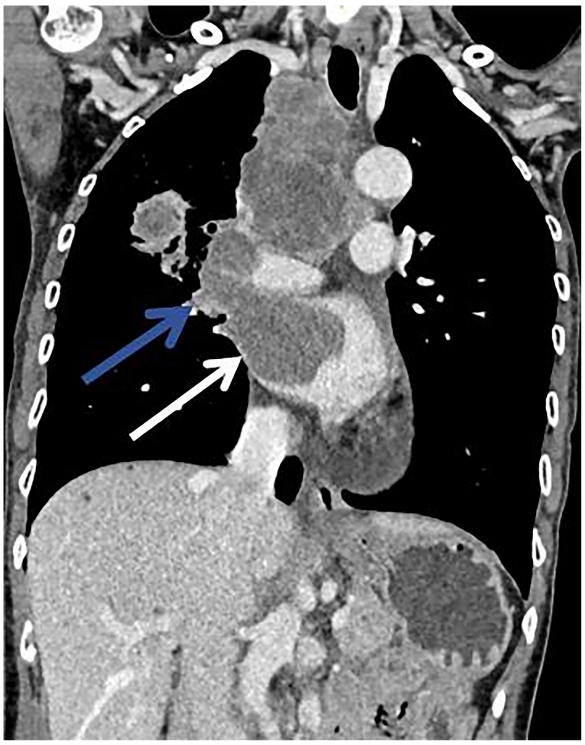

FIGURE 2
There was a mild enhancement filling defect noted in the right upper pulmonary vein (blue arrow) and the left atrium (white arrow).

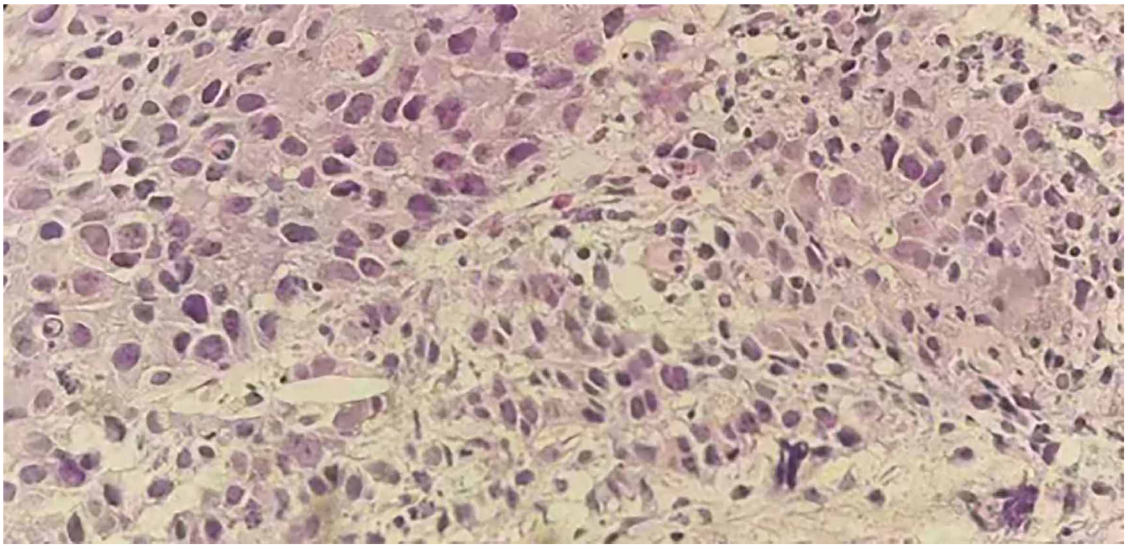

FIGURE 3
Hematoxylin and eosin (H&E) staining on the lung tissue sections reveals nest-like formations of cancer cells, invasive growth patterns, enlarged and deeply stained nuclei, a high nucleus-to-cytoplasm ratio, pronounced atypia of the cancer cells, and stromal fibrosis.

TABLE 1 Based on the timeline, clinical events are listed below.

Time	Evens
April 10, 2023	A transthoracic echocardiogram detected a hypoechoic mass located at the base of the left atrium, measuring approximately 5.1 × 3.4 cm, exhibiting indistinct demarcation from the right pulmonary vein and demonstrating minimal motion throughout the cardiac cycle.
April 11, 2023	Through visceral acoustic imaging, it was confirmed that the left atrial metastasis originated from the right pulmonary vein. A thoracic CT scan diagnosis suggested lung cancer with multiple metastases.
April 13, 2023	Under the guidance of CT laser localization, a lung biopsy was successfully performed.
April 14, 2023	Enhanced CT scans of the neck, chest, and upper abdomen revealed lung cancer with tumor emboli formation in the right upper pulmonary vein and the left atrium, along with metastases to extrathoracic lymph nodes, adrenal glands, and brain. Pathological examination confirmed infiltrating carcinoma in the right lung. The patient received symptomatic treatment with heparin anticoagulation.
April 19, 2023	Immunohistochemistry indicated non-small-cell lung cancer in the right lung.
May 8, 2023	The patient underwent chemotherapy with a combination of carboplatin and pemetrexed chemotherapy along with the tislelizumab and received supportive care, including gastric protection and antiemetics.
May 15, 2023	After this treatment course, the patient's general condition was satisfactory. However, due to personal reasons, she ultimately opted to discontinue further treatment.

3 Discussion

We report a case of a female non-smoker with lung cancer, presenting with metastases to multiple sites, including the left atrium and extrathoracic lymph nodes. Traditionally, the occurrence of lung cancer has been closely associated with male smokers, and the clinical manifestations of left atrial metastases can vary widely, ranging from paraneoplastic syndromes, dyspnea, ST-segment elevation on electrocardiograms, hemoptysis, and weight loss, to the absence of noticeable clinical symptoms (6–9). In contrast to other patients with lung cancer metastasizing to the left atrium, this case involves a female non-smoker who, aside from weight loss, exhibits no other clinical symptoms, which is exceedingly rare (Table 2). In recent years, the incidence of lung cancer among female non-smokers has been rising, potentially linked to exposure to smoke from charcoal, heating, or cooking (1). The increasing incidence of lung cancer among female non-smokers presents a new challenge to current screening programs and strategies, necessitating further adjustments to accommodate this emerging risk group. Remarkably, the patient's circulating tumor cells disseminated directly to the left atrium via the pulmonary veins, an exceedingly rare occurrence (15). Cardiac tumors are categorized into primary cardiac tumors and metastatic cardiac tumors, with metastatic cardiac tumors being 20–30 times more prevalent than primary cardiac tumors (16). However, the reported incidence of left atrial metastatic tumors is only 3.1% (5). The microenvironment, an intricately structured ecosystem consisting of diverse immune cells, cellular stroma, and vascular cells, is widely recognized to play a crucial role in the progression of metastatic tumors (17, 18). It facilitates the dissemination of tumors to distant sites through mechanisms involving inflammatory cytokines, and the Wnt/T-catenin pathway, among others (19). Thus, it plays a central role in tumorigenesis and metastasis (20). In this report, lung cancer cells breached the vascular basement membrane and endothelial barrier to metastasize to the left atrium via the pulmonary vein, a process potentially linked to CC-chemokine receptor 2 (CCR2) signaling by monocytes. CCR2 signaling monocytes transition into mobile

TABLE 2 A review of cases with lung cancer metastasis to the left atrium.

	Our case	Clarket et al. (10)	Nosrati et al. (11)	Xie et al. (12)	Uygur et al. (13)	Cipriano et al. (14)
Gender	Women	Women	Men	Men	Men	Men
Age	62	38	72	59	68	62
Smoker?	NO	NO	YES	Indeterminate	YES	YES
Primary lesion	NSCLC	NSCLC	NSCLC	NSCLC	undifferentiated round cell malignant neoplasm	NSCLC
Clinical characteristics	Weight loss	Cough, shortness of breath, loss of appetite, weig-ht loss	Hemoptysis, fainting	Progressive dys-pnea and exacerbation of bilateral lower extremity edema.	Difficulty breathing, cough	Dyspnea, dry cough, chest and back pain, and weight loss
Diagnostic methods	x-ray, CT, echo-cardiogram, MRI, organ acoustic imaging	x-ray, CT	CT, echocardiogram	CT, echocardiogram, MRI	CT, echocardiogram	CT, echocardiogram
Treatment strategies	carboplatin and pemetrexed chemotherapy along with tislelizumab	radiotherapy, Paclitaxel combined with carboplatin chemotherapy. Pembrolizumab immunotherapy	radiotherapy, Chemotherapy with Etoposide and Cisplatin	Lobectomy, tumor resection, and partial left a-trial resection	Tumor excision, lobectomy, and postoperative chemotherapy	Resection of the cardiac tumor, lobectomy, followed by adjuvant radiotherapy and chemotherapy
Outcome	Discontinuation of treatment	Reduction in tumor size	Deceased	Survived	Survived	Deceased

tumor-associated macrophages and are converted into the chemokine receptor 4 -expressing macrophages upon exposure to transforming growth factor β. CXC-chemokine ligand 12 (CXCL12), secreted by stromal fibroblasts near blood vessels, triggers migrating macrophages and cancer cells to aggregate toward blood vessels (21). Subsequently, the aggregated migrating macrophages transform into perivascular macrophages and enhance vascular permeability by inducing vascular endothelial growth factor A signaling. This results in local disruption of vascular junctions, thereby facilitating the invasion of cancer cells into the vasculature to become circulating tumor cells (22). Circulating tumor cells directly or indirectly interact with various cell types such as blood cells, endothelial cells, and cancer-associated fibroblasts. They manipulate the cellular functions of surrounding normal cells, facilitating the extravasation of circulating tumor cells into the left atrium and leading to the development of left atrial metastases (23). It is also posited that tumor development is closely associated with endoplasmic reticulum (ER) stress (24). In various tumors, the combination of carcinogenesis, transcriptional alterations, and metabolic abnormalities leads to a detrimental microenvironment that disrupts endoplasmic reticulum homeostasis, thereby triggering persistent ER stress. This stress state influences the pro-tumorigenic characteristics of cancer cells and dynamically alters the functions of innate and adaptive immune cells. Abnormal activation of ER stress sensors and their downstream signaling pathways constitutes a critical regulatory factor in tumor growth and metastasis. Research also suggests that inflammation within the tumor microenvironment, particularly that driven by tumor-associated macrophages, is commonly regarded as a significant characteristic of tumors (25). High infiltration of tumor-associated macrophages is often closely associated with poor prognosis in various cancers, such as bladder cancer (26). However, other studies have indicated that in certain instances, the infiltration of tumor-associated macrophages may be associated with a more favorable prognosis (27). This may be related to certain factors within the tumor. In studies of NSCLC, the relationship between macrophages and patient survival has been investigated (28). The research suggests that macrophages within tumor islets may play a role in either promoting tumor growth or exhibiting anti-tumor effects. In contrast, macrophages in the tumor stroma could be associated with tumor progression and adverse prognosis. This indicates that tumor-associated macrophages may hold significant roles in the development and metastasis of NSCLC. Furthermore, tumor-associated macrophages may exhibit varying functions and prognostic implications across different regions of the tumor microenvironment, potentially offering new insights for personalized treatment and prognostic evaluation.

Currently, due to the lack of specific clinical manifestations of left atrial metastases, clinical symptoms cannot serve as direct evidence for the diagnosis of cardiac tumors, often leading to late and incidental discoveries. The diagnosis of cardiac tumors relies on pathological biopsy; however, due to the invasive nature of this method, it is frequently not acceptable to patients (29). In this context, imaging assessment of cardiac tumors has become an increasingly crucial approach. Transthoracic echocardiography is the preferred imaging modality for the evaluation of cardiac tumors, aiding in the differentiation of cardiac tumors from other cardiac conditions. Additionally, with advancements in ultrasound technology, transesophageal echocardiography provides a higher-resolution view of the fine structures of the heart and the pulmonary veins. Uygur et al. (13) reported a case of lung cancer metastasizing to the left atrium, initially diagnosed as an atrial myxoma by transthoracic echocardiography, but subsequently confirmed as a tumor metastatic via the left upper pulmonary vein through transesophageal echocardiography. CT scanning provides a clear depiction of the tumor's specific location and its relationship with surrounding tissues, aiding in

the identification of other metastatic sites and serving as an initial screening for metastasis. However, CT has limitations such as poor soft tissue contrast, radiation exposure, and image artifacts, which may lead to potential misdiagnoses. Cipriano et al. (14) reported a case of cardiac metastasis in which preoperative head CT did not reveal any brain metastases. However, postoperatively, the patient developed seizures, and a subsequent CT scan identified brain metastases. MRI is the standard imaging modality for detecting brain metastases, and, if necessary, patients should undergo multimodal imaging. Bilani et al. (29) investigated the multimodal assessment of cardiac metastases in patients with NSCLC, presenting a detailed clinical case of one patient. The patient's clinical features, along with 18F-labeled fluorodeoxyglucose positron emission tomography (^{18}F-FDG PET) and echocardiography, suggested endocardial metastasis. However, due to the patient's anxiety about the MRI, a further MRI evaluation was declined, and pembrolizumab treatment was chosen instead. Subsequent PET-CT scans, performed two months apart, were negative. Nevertheless, after nine months of treatment, PET-CT revealed a recurrence in the left ventricular area. Ultimately, the patient underwent an MRI, which surprisingly yielded a negative result. The case of Bilani et al. (29) underscores the importance of MRI in the diagnosis of tumor metastases and demonstrates its potential applications in multimodal assessment. This case reinforces the critical role of multimodal imaging in enabling clinicians to accurately ascertain a patient's condition, thereby facilitating the selection of the most suitable treatment plan and ensuring early and effective intervention to minimize the wastage of medical resources. The patient in our case underwent comprehensive evaluations, including echocardiography, contrast-enhanced CT, and MRI, which confirmed the diagnosis of lung cancer and its metastatic lesions. Although the patient exhibited no other clinical symptoms beyond weight loss, which is consistent with current research on cardiac tumors (9), this case warrants special attention compared to cardiac tumors presenting with a range of clinical symptoms. Cases with such subtle clinical symptoms not only have the potential to delay diagnosis and treatment decisions but also underscore the critical importance of emphasizing weight changes and the need for early diagnosis and individualized monitoring in cancer screening.

Rare metastatic lung cancer is generally associated with a poor prognosis. However, with the advent of current highly effective systemic therapies, including immunotherapy, chemotherapy, and radiotherapy, the survival of patients with rare metastatic lung cancer has been significantly extended (30). The study by Niu et al. (31) reveals that a combined approach of systemic therapy (such as chemotherapy and targeted therapy) with local treatments (like tumor resection, radiotherapy, or radiofrequency ablation) can significantly prolong overall survival. This finding underscores the superior benefits of integrated treatment in extending survival, in contrast to relying solely on systemic therapy or supportive care, which yield less favorable outcomes. Jasper et al. (30) further emphasized that this integrated approach not only aids in long-term disease control but also holds the potential for achieving curative outcomes. This indicates that an integrated treatment strategy is particularly crucial for patients with rare metastatic lung cancer, as it not only enhances survival but also offers the possibility of more optimistic therapeutic prospects. Overall, these findings endorse the significance of applying an integrated treatment approach in patients with rare metastatic lung cancer, demonstrating that this method can markedly improve therapeutic outcomes and patient survival rates. Furthermore, it provides compelling evidence for clinical practice, suggesting that healthcare teams should consider the potential advantages of integrated treatment in their treatment plans. Clark et al. (10) achieved tumor reduction in patients with lung cancer accompanied by cardiac metastases through a comprehensive treatment regimen combining radiotherapy, chemotherapy, and immunotherapy. Additionally, Xie et al. (12) and Uygur et al. (13) each reported cases of lung cancer with cardiac metastases where patients survived following surgical resection. These studies challenge the traditional notion that tumors directly extending to the heart are deemed inoperable. This finding suggests that surgical intervention for cardiac metastases may hold genuine therapeutic value, indicating a need to reassess the surgical indications for cardiac metastases and explore related treatment strategies further. In the case presented, the patient experienced widespread metastases, including to the heart. After consulting with experts in cardiology, cardiovascular surgery, and oncology, the patient received a treatment regimen comprising carboplatin and pemetrexed chemotherapy combined with tremelimumab immunotherapy. The patient tolerated this treatment regimen relatively well; however, regrettably, due to economic and psychological pressures, the patient ultimately chose to discontinue further treatment. In this case, a multidisciplinary approach was adopted. With advancements in early cancer detection technologies and effective anticancer therapies, the survival period of lung cancer patients has been significantly extended. However, this also brings challenges related to cardiac issues and elevated cardiovascular risk (32). Cardiovascular disease has been identified as the second leading cause of mortality among patients with NSCLC (33). Particularly for lung cancer patients undergoing cardiotoxic anticancer treatments, a multidisciplinary approach becomes increasingly crucial in their management and care. Baseline cardiovascular risk assessment and evaluation for lung cancer patients should include physical examinations, blood pressure measurements, ECG, lipid profiles, hemoglobin A1c, and smoking status (32). Before initiating anticancer therapy, it is essential to manage cardiovascular risk factors as effectively as possible. During treatment, regular blood pressure monitoring and echocardiographic evaluations should be conducted to detect hypertension and rule out potential cardiomyopathy (34).

Moreover, in this case, metastases to the lymph nodes, adrenal glands, and brain may have the following associations with the microenvironment, respectively. Lymph nodes and lymphatic vessels promote the homing of circulating tumor cells to lymph nodes and their proliferation through lymphangiogenesis and chemokine production in response to signaling molecules secreted by tumor cells and the tumor microenvironment (35).

The development of adrenal metastases is believed to be influenced by CC- chemokine receptor 6 (CCR6) and its receptor CC-chemokine ligand 20 (CCL20). The overexpression of CCL20 in normal tissues adjacent to adrenal metastases establishes a microenvironment that enhances the attraction of circulating tumor cells expressing CCR6 to the adrenal gland (36). Tumor cells after invading the brain phenotypically modify local normal cells from an anti-tumor to a pro-tumor phenotype and undergo T-cell immunosuppression to achieve a suitable tumor microenvironment (37–40). The E2F1-mediated inhibitory pathway of WNT5A expression and the CXCL12/CXC-chemokine receptor 4 (CXCR4) chemokine receptor signaling pathway facilitate the invasion of circulating tumor cells into the brain (41).

The microenvironment plays a pivotal role in both tumorigenesis and metastasis. Consequently, targeted therapy directed at microenvironmental signaling pathways may offer a novel perspective for enhancing cancer treatment efficacy.

4 Conclusion

We report a case of a female lung cancer patient with metastases to the left atrium and extrathoracic lymph nodes et al. Remarkably, this patient remained asymptomatic from the onset of the disease until the development of metastasis, underscoring the growing importance of regular medical checkups for early disease detection. Furthermore, when the primary cancer lesion is identified, it is crucial to conduct multimodal imaging examinations, including those of the heart. Additionally, adopting intervention therapy from a microenvironmental perspective may offer a novel approach to more effective cancer treatment.

Data availability statement

The raw data supporting the conclusions of this article will be made available by the authors, without undue reservation.

Ethics statement

The studies involving humans were approved by Biomedical Research Ethics Committee of the Second Affiliated Hospital of Nanchang University. The studies were conducted in accordance with the local legislation and institutional requirements. The ethics committee/institutional review board waived the requirement of written informed consent for participation from the participants or the participants' legal guardians/next of kin because the patient had verbally consented to the inclusion of her case in the case report and had been discharged. Written informed consent was not obtained from the individual(s) for the publication of any potentially identifiable images or data included in this article because the patient had verbally consented to the inclusion of her case in the case report and had been discharged. Written informed consent was obtained from the participant/patient(s) for the publication of this case report.

Author contributions

LC: Writing – review & editing. JZ: Writing – original draft. CZ: Conceptualization, Data curation, Funding acquisition, Investigation, Methodology, Project administration, Supervision, Writing – review & editing.

Funding

The author(s) declare that no financial support was received for the research, authorship, and/or publication of this article.

Conflict of interest

The authors declare that the research was conducted in the absence of any commercial or financial relationships that could be construed as a potential conflict of interest.

Publisher's note

All claims expressed in this article are solely those of the authors and do not necessarily represent those of their affiliated organizations, or those of the publisher, the editors and the reviewers. Any product that may be evaluated in this article, or claim that may be made by its manufacturer, is not guaranteed or endorsed by the publisher.

Supplementary material

The Supplementary Material for this article can be found online at: https://www.frontiersin.org/articles/10.3389/fcvm.2024.1417906/full#supplementary-material

References

1. Bray F, Ferlay J, Soerjomataram I, Siegel RL, Torre LA, Jemal A. Global cancer statistics 2018: GLOBOCAN estimates of incidence and mortality worldwide for 36 cancers in 185 countries. *CA Cancer J Clin.* (2018) 68:394–424. doi: 10.3322/caac.21492

2. Bade BC, Dela Cruz CS. Lung cancer 2020: epidemiology, etiology, and prevention. *Clin Chest Med.* (2020) 41(1):1–24. doi: 10.1016/j.ccm.2019.10.001

3. Jeon J, Holford TR, Levy DT, Feuer EJ, Cao P, Tam J, et al. Smoking and lung cancer mortality in the United States from 2015 to 2065: a comparative modeling approach. *Ann Intern Med.* (2018) 169(10):684–93. doi: 10.7326/M18-1250

4. Tamura T, Kurishima K, Nakazawa K, Kagohashi K, Ishikawa H, Satoh H, et al. Specific organ metastases and survival in metastatic non-small-cell lung cancer. *Mol Clin Oncol.* (2015) 3:217–21. doi: 10.3892/mco.2014.410

5. Riquet M, Grand B, Arame A, Pricopi CF, Foucault C, Dujon A, et al. Lung cancer invading the pericardium: quantum of lymph nodes. *Ann Thorac Surg*. (2010) 90:1773–7. doi: 10.1016/j.athoracsur.2010.07.039

6. Tyebally S, Chen D, Bhattacharyya S, Mughrabi A, Hussain Z, Manisty C, et al. Cardiac tumors: JACC CardioOncology state-of-the-art review. *JACC CardioOncol*. (2020) 2(2):293–311. doi: 10.1016/j.jaccao.2020.05.009

7. Akgun T, Gulsen K, Cinier G, Pay L, Uslu A, Kup A, et al. Electrocardiographic ccharacteristics of metastatic cardiac tumors presenting with ST-segment elevation. *J Electrocardiol*. (2020) 59:93–9. doi: 10.1016/j.jelectrocard.2019.12.014

8. de Agustin JA, Gomez de Diego JJ, Marcos-Alberca P, Martin Garcia AC, Rodrigo JL, Almeria C, et al. Pulmonary vein stenosis due to invasion of metastatic clear cell sarcoma. *Int J Cardiol*. (2014) 177(3):e115–6. doi: 10.1016/j.ijcard.2014.09.080

9. Lin Z, Xiao H, Liu J, Chen L, Zhang H, Huang Y, et al. Clinical features and prognosis of cardiac metastatic tumors. *BMC Cancer*. (2023) 23(1):1235. doi: 10.1186/s12885-023-11733-1

10. Clark M, Griborio-Guzman AG, Burute NP, Lubbers S, Anthes ML, Sadreddini M, et al. When tissue is not the only issue: poorly differentiated lung squamous-cell carcinoma with adrenal, costochondral, and cardiac metastases—case report. *Front Oncol*. (2023) 13:1117024. doi: 10.3389/fonc.2023.1117024

11. Nosrati A, Nabati M, Vahedi L, Shokri M. Invasion of poorly differentiated large-cell neuroendocrine tumor of the lung through right pulmonary veins into the left atrium: a very rare case report. *J Clin Ultrasound*. (2020) 48(9):560–4. doi: 10.1002/jcu.22844

12. Xie M, Wu W, Lv Q, Wang Y. Lung carcinoma extended to the left atrium through the right inferior pulmonary vein. *Anatol J Cardiol*. (2020) 24(1):E3–4. doi: 10.14744/AnatolJCardiol.2020.58019

13. Uygur B, Celik O, Birant A, Demir AR, Erturk M. Echocardiographic detection of left atrium and left ventricle tumoral invasion via the left upper pulmonary vein, leading to the diagnosis of lung cancer. *J Clin Ultrasound*. (2020) 48(9):565–8. doi: 10.1002/jcu.22824

14. Cipriano F, Dessoti LU, Rodrigues AJ, Vicente WVA, Chahud F, Evora PRB. Report of a lung carcinoma extended to the left atrium through pulmonary vein. *J Thorac Dis*. (2018) 10(1):E46–51. doi: 10.21037/jtd.2017.12.33

15. Li K, Du Y, Li L, Wei DQ. Bioinformatics approaches for anti-cancer drug discovery. *Curr Drug Targets*. (2020) 21:3–17. doi: 10.2174/1389450120666190923162203

16. Maleszewski JJ, Bois MC, Bois JP, Young PM, Stulak JM, Klarich KW. Neoplasia and the heart: pathological review of effects with clinical and radiological correlation. *J Am Coll Cardiol*. (2018) 72:202–27. doi: 10.1016/j.jacc.2018.05.026

17. Kellner J, Sivajothi S, McNiece I. Differential properties of human stromal cells from bone marrow, adipose, liver and cardiac tissues. *Cytotherapy*. (2015) 17:1514–23. doi: 10.1016/j.jcyt.2015.07.009

18. de Visser KE, Joyce JA. The evolving tumor microenvironment: from cancer initiation to metastatic outgrowth. *Cancer Cell*. (2023) 41:374–403. doi: 10.1016/j.ccell.2023.02.016

19. Altorki NK, Markowitz GJ, Gao D, Port JL, Saxena A, Stiles B, et al. The lung microenvironment: an important regulator of tumour growth and metastasis. *Nat Rev Cancer*. (2019) 19:9–31. doi: 10.1038/s41568-018-0081-9

20. Chen Z, Fillmore CM, Hammerman PS, Kim CF, Wong KK. Non-small-cell lung cancers: a heterogeneous set of diseases. *Nat Rev Cancer*. (2014) 14:535–46. doi: 10.1038/nrc3775

21. Arwert EN, Harney AS, Entenberg D, Wang Y, Sahai E, Pollard JW, et al. A unidirectional transition from migratory to perivascular macrophage is required for tumor cell intravasation. *Cell Rep*. (2018) 23:1239–48. doi: 10.1016/j.celrep.2018.04.007

22. Harney AS, Arwert EN, Entenberg D, Wang Y, Guo P, Qian BZ, et al. Real-time imaging reveals local, transient vascular permeability, and tumor cell intravasation stimulated by TIE2hi macrophage-derived VEGFA. *Cancer Discov*. (2015) 5:932–43. doi: 10.1158/2159-8290

23. Pereira-Veiga T, Schneegans S, Pantel K, Wikman H. Circulating tumor cell-blood cell crosstalk: biology and clinical relevance. *Cell Rep*. (2022) 40:111298. doi: 10.1016/j.celrep.2022.111298

24. Chen X, Cubillos-Ruiz JR. Endoplasmic reticulum stress signals in the tumour and its microenvironment. *Nat Rev Cancer*. (2021) 21(2):71–88. doi: 10.1038/s41568-020-00312-2

25. Mantovani A, Sica A. Macrophages, innate immunity and cancer: balance, tolerance, and diversity. *Curr Opin Immunol*. (2010) 22(2):231–7. doi: 10.1016/j.coi.2010.01.009

26. Wu H, Zhang X, Han D, Cao J, Tian J. Tumour-associated macrophages mediate the invasion and metastasis of bladder cancer cells through CXCL8. *PeerJ*. (2020) 8:e8721. doi: 10.7717/peerj.8721

27. El-Arabey AA, Denizli M, Kanlikilicer P, Bayraktar R, Ivan C, Rashed M, et al. GATA3 as a master regulator for interactions of tumor-associated macrophages with high-grade serous ovarian carcinoma. *Cell Signal*. (2020) 68:109539. doi: 10.1016/j.cellsig.2020.109539. Erratum in: Cell Signal. 2022;89:110147. doi: 10.1016/j.cellsig.2021.110147.

28. Dai F, Liu L, Che G, Yu N, Pu Q, Zhang S, et al. The number and microlocalization of tumor-associated immune cells are associated with patient's survival time in non-small cell lung cancer. *BMC Cancer*. (2010) 10:220. doi: 10.1186/1471-2407-10-220

29. Bilani N, Elson L, Martinez F, Sadler D, Nahleh Z, Elimimian E, et al. A multimodal approach to evaluate for cardiac metastasis in a case of non-small cell lung cancer. *Case Rep Oncol*. (2020) 13(1):212–8. doi: 10.1159/000505534

30. Jasper K, Stiles B, McDonald F, Palma DA. Practical management of oligometastatic non-small-cell lung cancer. *J Clin Oncol*. (2022) 40(6):635–41. doi: 10.1200/JCO.21.01719

31. Niu FY, Zhou Q, Yang JJ, Zhong WZ, Chen ZH, Deng W, et al. Distribution and prognosis of uncommon metastases from non-small cell lung cancer. *BMC Cancer*. (2016) 16:149. doi: 10.1186/s12885-016-2169-5

32. de Jesus M, Chanda A, Grabauskas T, Kumar M, Kim AS. Cardiovascular disease and lung cancer. *Front Oncol*. (2024) 14:1258991. doi: 10.3389/fonc.2024.1258991

33. Sun JY, Zhang ZY, Qu Q, Wang N, Zhang YM, Miao LF, et al. Cardiovascular disease-specific mortality in 270,618 patients with non-small cell lung cancer. *Int J Cardiol*. (2021) 330:186–93. doi: 10.1016/j.ijcard.2021.02.025

34. Tan S, Spear E, Sane N, Nelson AJ, Nerlekar N, Segelov E, et al. Blood pressure surveillance in cancer patients treated with immune checkpoint inhibitors. *J Hum Hypertens*. (2023) 37(11):1043–6. doi: 10.1038/s41371-023-00831-z

35. Pereira ER, Jones D, Jung K, Padera TP. The lymph node microenvironment and its role in the progression of metastatic cancer. *Semin Cell Dev Biol*. (2015) 38:98–105. doi: 10.1016/j.semcdb

36. Raynaud CM, Mercier O, Dartevelle P, Commo F, Olaussen KA, de Montpreville V, et al. Expression of chemokine receptor CCR6 as a molecular determinant of adrenal metastatic relapse in patients with primary lung cancer. *Clin Lung Cancer*. (2010) 11:187–91. doi: 10.3816/CLC.2010.n.024

37. Fares J, Fares MY, Khachfe HH, Salhab HA, Fares Y. Molecular principles of metastasis: a hallmark of cancer revisited. *Signal Transduct Target Ther*. (2020) 5:28. doi: 10.1038/s41392-020-0134-x

38. Caffarel MM, Braza MS. Microglia and metastases to the central nervous system: victim, ravager, or something else? *J Exp Clin Cancer Res*. (2022) 41:327. doi: 10.1186/s13046-022-02535-7

39. Quail DF, Joyce JA. Microenvironmental regulation of tumor progression and metastasis. *Nat Med*. (2013) 19:1423–37. doi: 10.1038/nm.3394

40. Ikarashi D, Okimoto T, Shukuya T, Onagi H, Hayashi T, Sinicropi-Yao SL, et al. Comparison of tumor microenvironments between primary tumors and brain metastases in patients with NSCLC. *JTO Clin Res Rep*. (2021) 2:100230. doi: 10.1016/j.jtocrr

41. Li H, Tong F, Meng R, Peng L, Wang J, Zhang R, et al. E2F1-mediated repression of WNT5A expression promotes brain metastasis dependent on the ERK1/2 pathway in EGFR-mutant non-small cell lung cancer. *Cell Mol Life Sci*. (2021) 78:2877–91. doi: 10.1007/s00018-020-03678-6

frontiers | Frontiers in Cardiovascular Medicine

TYPE Case Report
PUBLISHED 24 September 2024
DOI 10.3389/fcvm.2024.1466395

Check for updates

OPEN ACCESS

EDITED BY
Reto Asmis,
Wake Forest University, United States

REVIEWED BY
Giulia Iannaccone,
Catholic University of the Sacred Heart, Italy
Xiaomeng Shi,
Emory University, United States

*CORRESPONDENCE
Anant Mandawat
anant.mandawat@emory.edu

RECEIVED 17 July 2024
ACCEPTED 30 August 2024
PUBLISHED 24 September 2024

CITATION
Yadalam AK, Schultz WM, Han C and Mandawat A (2024) Case Report: Pazopanib-induced acute coronary syndrome.
Front. Cardiovasc. Med. 11:1466395.
doi: 10.3389/fcvm.2024.1466395

COPYRIGHT
© 2024 Yadalam, Schultz, Han and Mandawat. This is an open-access article distributed under the terms of the Creative Commons Attribution License (CC BY). The use, distribution or reproduction in other forums is permitted, provided the original author(s) and the copyright owner(s) are credited and that the original publication in this journal is cited, in accordance with accepted academic practice. No use, distribution or reproduction is permitted which does not comply with these terms.

Case Report: Pazopanib-induced acute coronary syndrome

Adithya K. Yadalam[1], William M. Schultz[1], Chanhee Han[2,3] and Anant Mandawat[1,3]*

[1]Division of Cardiology, Department of Medicine, Emory University School of Medicine, Atlanta, GA, United States, [2]Division of Gynecologic Oncology, Department of Gynecology and Obstetrics, Emory University School of Medicine, Atlanta, GA, United States, [3]Winship Cancer Institute of Emory University, Atlanta, GA, United States

Introduction: Pazopanib is a tyrosine kinase inhibitor approved for the treatment of metastatic renal cell carcinoma and advanced soft-tissue sarcoma that functions by inhibiting vascular endothelial growth factor receptors. Although the package insert and current cardio-oncology guidelines indicate a risk of acute coronary syndrome (ACS) associated with pazopanib, the causative role of pazopanib in arterial thrombosis is unclear due to a lack of focused coronary disease evaluation in oncological clinical trials prior to pazopanib initiation. Herein we present an antecedent ischemic evaluation of a patient who was prescribed pazopanib to demonstrate the first reported case of ACS directly attributable to pazopanib.

Case description: A 65-year-old woman with metastatic leiomyosarcoma presented to the hospital with ACS. Pazopanib had been initiated 8 months prior, and an ischemic evaluation 6 weeks prior to hospitalization indicated mild coronary artery disease (CAD). Emergent cardiac catheterization revealed a large thrombotic occlusion of the mid-left anterior descending coronary artery involving the secondary diagonal artery, which was treated with manual aspiration thrombectomy. Pazopanib was discontinued, and the patient was discharged from the hospital 12 days later.

Discussion: Although pazopanib is associated with ACS, there is a lack of definitive data supporting this association. This case-based demonstration of pazopanib-induced ACS provides a discrete clinical example of this phenomenon. The patient's minimal atherosclerotic burden 6 weeks prior to her presentation for ACS strongly suggests causality attributable to pazopanib. Given the increased risk for ischemic heart disease, careful attention and an individualized risk assessment for CAD should be provided to patients who are prescribed pazopanib.

KEYWORDS

pazopanib, acute coronary syndrome, cardio-oncology, interventional cardiology, case report, coronary artery disease

Introduction

Pazopanib is a tyrosine kinase inhibitor (TKI) approved for the treatment of metastatic renal cell carcinoma and advanced soft-tissue sarcoma (STS) and functions by inhibiting vascular endothelial growth factor (VEGF) receptors (1). Although current European Society of Cardiology (ESC) Cardio-Oncology guidelines classify pazopanib as being associated with a risk for acute coronary syndrome (ACS), evidence is limited and without clear causation (2–7, 9). Herein we present the first reported case of pazopanib-induced ACS in a patient with metastatic STS.

Case description

A 65-year-old woman with a past medical history of hypertension and obesity and without any family history of coronary artery disease (CAD) was diagnosed with Stage IB leiomyosarcoma 2.5 years prior to the index hospitalization for ACS (Figure 1). Her leiomyosarcoma was initially treated with total abdominal hysterectomy, bilateral salpingo-oophorectomy, and bilateral pelvic lymph node dissection. Pathological examination confirmed negative margins and lymph nodes. Recurrent pulmonary metastatic disease was detected 1 year later and treated with docetaxel/gemcitabine. Due to progression of disease despite therapy, doxorubicin was initiated as a second-line treatment 15 months prior to the index hospitalization. An asymptomatic decrease in left ventricular ejection fraction (LVEF) from 60% to 40% with global hypokinesis was observed following doxorubicin therapy, and thus carvedilol was initiated. After a favorable response to a total anthracycline lifetime dose of 508 mg/m^2, pazopanib was initiated 8 months prior to the index hospitalization due to the lifetime dose limitations of doxorubicin. Carvedilol was switched to metoprolol succinate at the time of pazopanib initiation, given the adverse drug–drug interaction between permeability glycoprotein (P-gp) inhibitors, such as carvedilol, and pazopanib, which can result in increased serum exposure to pazopanib (1). Due to persistently reduced LVEF on repeat evaluation, an ischemic evaluation with coronary computed tomography angiography (CCTA) was performed 6 weeks prior to the ACS admission. The CCTA revealed patent coronary arteries and <25% stenosis of the proximal left anterior descending artery (LAD) (Figure 2). The total coronary artery calcium score was 4. Six weeks later, the patient presented for the index ACS hospitalization.

On presentation to the index hospitalization, the patient reported nausea, vomiting, and decreased appetite for 2 days. She

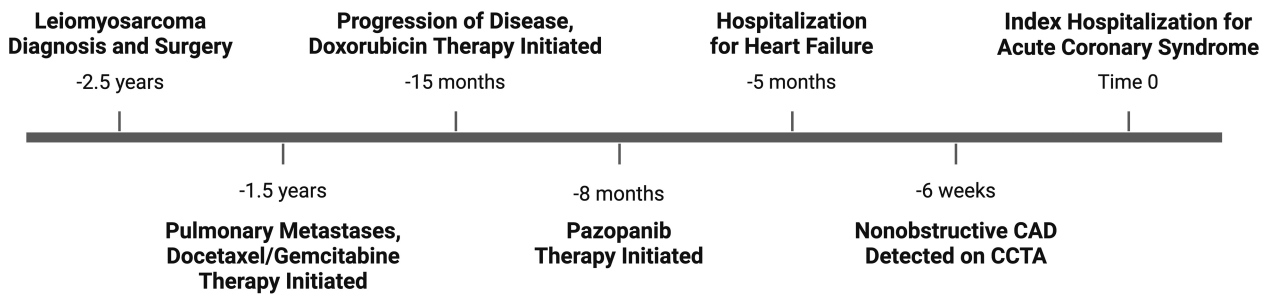

FIGURE 1
Timeline of clinical events. Depiction of important clinical events in chronological order, beginning with diagnosis of leiomyosarcoma and ending with index hospitalization for acute coronary syndrome.

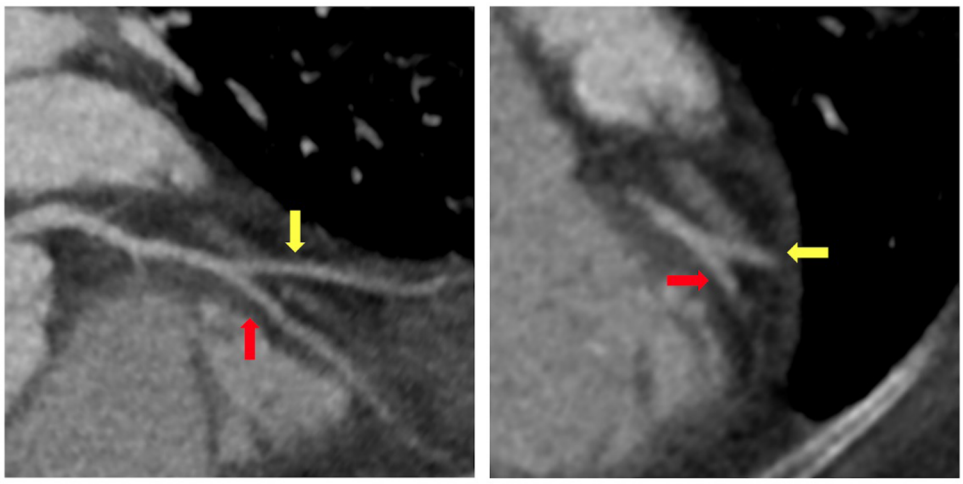

FIGURE 2
Coronary computed tomography angiography. Coronary computed tomography angiography performed 6 weeks prior to index hospitalization for acute coronary syndrome demonstrated minimal coronary atherosclerosis at the bifurcation of the mid-left anterior descending artery (red arrow) and secondary diagonal artery (yellow arrow).

denied a history of alcohol, tobacco, or recreational drug use. Physical examination demonstrated appropriate mentation, regular tachycardia without abnormal heart sounds, vesicular breath sounds, and no peripheral edema. An electrocardiogram showed sinus tachycardia with a heart rate of 103 beats per minute (Figure 3). High-sensitivity troponin-I was >25,000 ng/L (*ref.* <14 ng/L), and the lactate level was 3.4 mmol/L (*ref.* 0.5–2.2 mmol/L). The most recent prior measurement of high-sensitivity troponin-I was 147 ng/L 4 months prior. Liver enzyme and creatinine levels were increased from baseline. Transthoracic echocardiography (TTE) revealed a decrease in LVEF to 10%, left ventricular internal end-diastolic diameter (LVIDd) of 6.2 cm, severe global hypokinesis, and regional wall motion abnormalities within the LAD distribution. No left ventricular thrombus was observed. Pazopanib and carvedilol were held. Emergent cardiac catheterization revealed a large thrombotic occlusion of the mid-LAD involving the secondary diagonal artery, which was treated with manual aspiration thrombectomy (Figure 4). Right heart catheterization revealed elevated right- and left-sided filling pressures and a decreased cardiac index (Fick) of 1.36 L/min/m^2. Her hemodynamic status improved following thrombectomy. The patient's hospital course was complicated by the development of atrial fibrillation with rapid ventricular response, which improved with amiodarone. As the patient's cancer treatment was now limited to a fourth-line therapy with minimal chance of a favorable response, symptom control and supportive therapy were recommended. Pazopanib was discontinued, and the patient was discharged from the hospital 12 days after presentation with a slight improvement in LVEF to 15%–20%. Her discharge medications included aspirin and atorvastatin following her non-ST-elevation myocardial infarction (MI); milrinone, spironolactone, and torsemide for advanced chronic systolic heart failure; and amiodarone and apixaban for atrial fibrillation. The patient was re-hospitalized 3 months later for acute decompensated heart failure following outpatient reduction of her home diuretic dose. During this hospitalization, LVEF was found to have improved to 20%–25%. Upon discharge, her previous home diuretic dose was restored. During post-hospitalization follow-up 1 month later, the patient reported that her heart failure-related symptoms and functional status had improved. Her milrinone dose remains at a stable dose, and she continues to tolerate her regimen of spironolactone, torsemide, amiodarone, and apixaban without issue.

Discussion

The above case represents, to our knowledge, the first causative report of pazopanib-induced ACS in a patient with metastatic STS. Although current ESC guidelines estimate a 1%–10% risk of ACS associated with pazopanib, clinical trials investigating the safety of pazopanib have not convincingly demonstrated a significant association between pazopanib therapy and ACS due to a lack of focused coronary disease evaluation in oncological clinical trials prior to pazopanib initiation (2–7). A single-arm monotherapy trial of pazopanib in patients with metastatic STS previously

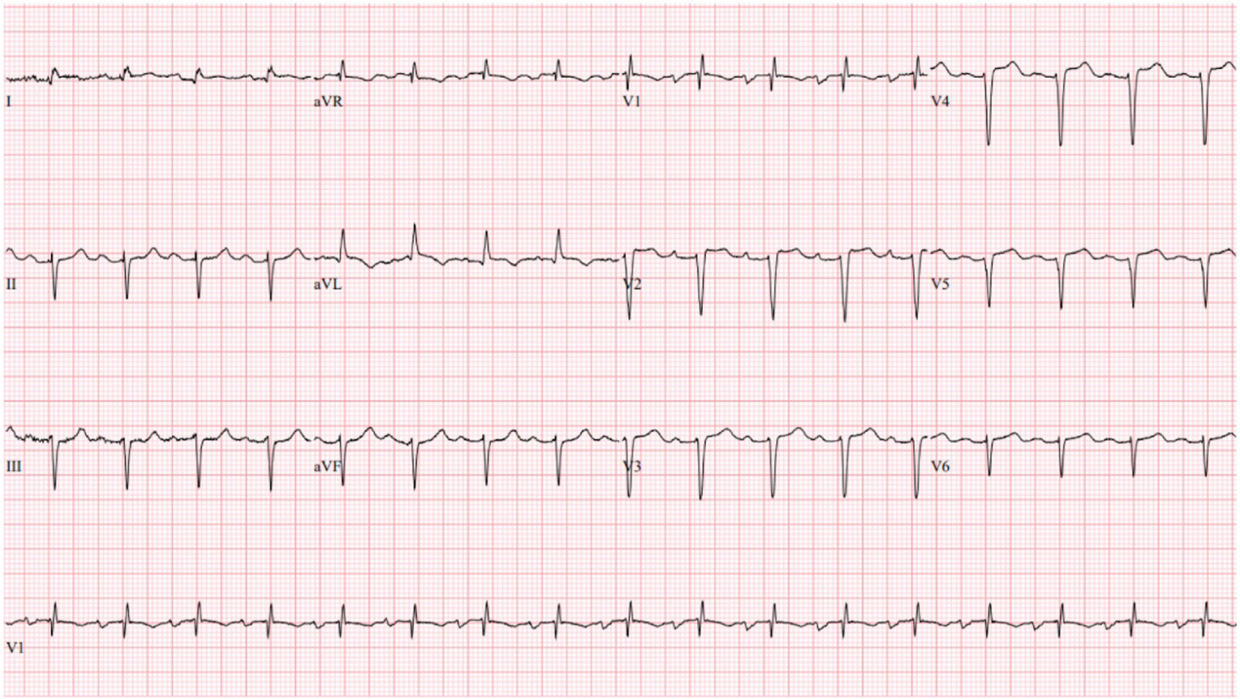

FIGURE 3
Index hospitalization electrocardiogram. The index hospitalization electrocardiogram demonstrated sinus tachycardia (HR 103 beats per minute), left anterior fascicular block, an RSR' pattern in V_1, and non-specific T-wave changes.

observed a 3% ($N = 1/33$) incidence of myocardial infarction incidence; however, the lack of a comparator placebo group makes this finding difficult to contextualize (4). Subsequent randomized, double-blinded, placebo-controlled clinical trials investigating the safety and efficacy of pazopanib in patients with metastatic STS have observed either no ACS events or an MI or ischemia incidence of 2% ($N = 2/240$) in the pazopanib group vs. 0% in the placebo group (Table 1) (5–7). Until now, a case demonstrating a distinct, causal relationship between pazopanib therapy and incident ACS has yet to be described.

Regarding the above case, the patient's patent coronary arteries noted on CCTA 6 weeks prior to her presentation for ACS strongly suggest causality attributable to pazopanib. Moreover, the lack of uncontrolled traditional cardiovascular risk factors or alternative etiologies for ACS further supports this to be a case of pazopanib-induced ACS. Although pazopanib therapy has also been associated with heart failure, the patient's decline in LVEF is substantially more likely a result of anthracycline-induced cardiomyopathy rather than pazopanib, given the temporal relationship with the doxorubicin therapy.

There are several proposed mechanisms for pazopanib-induced thrombosis and myocardial injury. VEGF has been linked to endothelial cell survival and proliferation, as well as the promotion of coronary angiogenesis. Given pazopanib's role in VEGF receptor inhibition, endothelial cell apoptosis and resultant thromboembolic and/or ischemic events are plausible. In addition, pazopanib-induced inhibition of VEGF can create a pro-thrombotic environment through the overproduction of erythropoietin and increased blood viscosity (8).

Although pazopanib use has been associated with ACS, evidence to support this association is lacking. This case provides a discrete example of pazopanib-induced ACS in a patient with non-obstructive CAD demonstrated 6 weeks prior to ACS presentation. Careful attention and an individualized risk

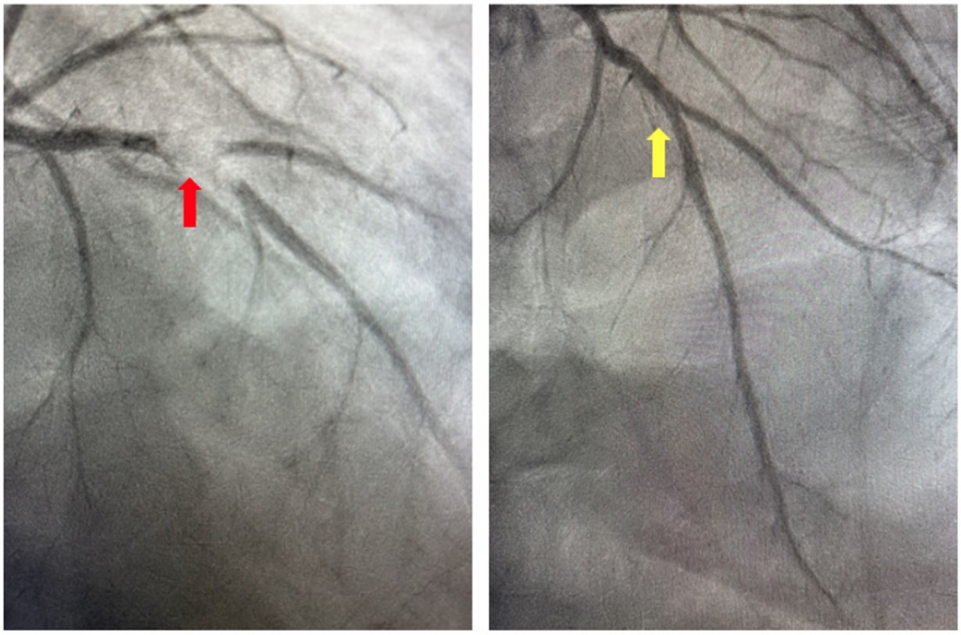

FIGURE 4
Coronary angiogram. Invasive coronary angiography demonstrating thrombotic occlusion of the mid-left anterior descending artery and second diagonal artery prior to manual aspiration thrombectomy (red arrow) and following manual aspiration thrombectomy (yellow arrow).

TABLE 1 Summary of existing evidence regarding pazopanib-associated acute coronary syndrome.

Reference	Study population	Evaluation for coronary artery disease	Results related to ACS
Lim et al. (2010) (4)	$N = 33$ patients with metastatic soft tissue sarcoma	No focused coronary evaluation; excluded patients with a history of MI, PCI ≤12 weeks from enrollment, or hospital admission for UA	MI occurred in 3% ($N = 1/33$) of pazopanib-treatment patients; no placebo arm available for comparison
Sternberg et al. (2010) (9)	$N = 435$ patients with renal cell carcinoma	No focused coronary evaluation; excluded patients with a history of MI, PCI, or UA	MI or ischemia occurred in 2% ($N = 5/290$) of pazopanib-treated patients compared to no events in placebo-treated patients
Van der Graaf et al. (2012) (5)	$N = 372$ patients with soft tissue sarcoma	No focused coronary evaluation; excluded patients with a history of PCI, MI, UA, or CABG ≤6 months from enrollment	MI or ischemia occurred in 2% ($N = 2/240$) of pazopanib-treated patients compared to no events in placebo-treated patients

ACS, acute coronary syndrome; CABG, coronary artery bypass graft; MI, myocardial infarction; PCI, percutaneous coronary intervention; UA, unstable angina.

assessment for CAD should be provided to patients who are prescribed pazopanib, and pazopanib should be permanently discontinued in patients who experience an arterial thromboembolic event. Future studies should examine whether a dose-response relationship exists between pazopanib therapy and adverse cardiovascular events.

Data availability statement

The original contributions presented in the study are included in the article/Supplementary Material, further inquiries can be directed to the corresponding author.

Ethics statement

Written informed consent was obtained from the individual(s) for the publication of any potentially identifiable images or data included in this article.

Author contributions

AY: Conceptualization, Data curation, Formal Analysis, Funding acquisition, Investigation, Methodology, Project administration, Resources, Software, Supervision, Validation, Visualization, Writing – original draft, Writing – review & editing. WS: Data curation, Writing – review & editing. CH: Writing – review & editing. AM: Conceptualization, Investigation, Project administration, Supervision, Visualization, Writing – review & editing.

Funding

The authors declare financial support was received for the research, authorship, and/or publication of this article. AY is supported by the National Heart, Lung and Blood Institute of the National Institutes of Health under award number 5T32HL007745-30.

Acknowledgments

The authors deeply appreciate the participation of the aforementioned patient. Figure 1 was created with Biorender.com.

Conflict of interest

The authors declare that the research was conducted in the absence of any commercial or financial relationships that could be construed as a potential conflict of interest.

Publisher's note

All claims expressed in this article are solely those of the authors and do not necessarily represent those of their affiliated organizations, or those of the publisher, the editors and the reviewers. Any product that may be evaluated in this article, or claim that may be made by its manufacturer, is not guaranteed or endorsed by the publisher.

References

1. Novartis. Votrient (pazopanib) [package insert]. U.S. Food and Drug Administration website. (2009). (revised 26 April 2012). Available online at: https://www.accessdata.fda.gov/drugsatfda_docs/label/2012/022465s-010S-012lbl.pdf (Accessed 16 July 2024).

2. Lyon AR, López-Fernández T, Couch LS, Asteggiano R, Aznar MC, Bergler-Klein J, et al. 2022 ESC guidelines on cardio-oncology developed in collaboration with the European Hematology Association (EHA), the European Society for Therapeutic Radiology and Oncology (ESTRO) and the International Cardio-Oncology Society (IC-OS): developed by the task force on cardio-oncology of the European Society of Cardiology (ESC). *Eur Heart J.* (2022) 43:4229–361. doi: 10.1093/eurheartj/ehac244

3. Iliescu CA, Grines CL, Herrmann J, Yang EH, Cilingiroglu M, Charitakis K, et al. SCAI expert consensus statement: evaluation, management, and special considerations of cardio-oncology patients in the cardiac catheterization laboratory (endorsed by the Cardiological Society of India, and Sociedad Latino Americana de Cardiologia Intervencionista). *Catheter Cardiovasc Interv.* (2016) 87:E202–23. doi: 10.1002/ccd.26379

4. Lim W-T, Ng Q-S, Ivy P, Leong S-S, Singh O, Chowbay B, et al. A phase II study of pazopanib in Asian patients with recurrent/metastatic nasopharyngeal carcinoma. *Clin Cancer Res.* (2011) 17:5481–9. doi: 10.1158/1078-0432.CCR-10-3409

5. van der Graaf WT, Blay J-Y, Chawla SP, Kim D-W, Bui-Nguyen B, Casali PG, et al. Pazopanib for metastatic soft-tissue sarcoma (PALETTE): a randomised, double-blind, placebo-controlled phase 3 trial. *Lancet.* (2012) 379:1879–86. doi: 10.1016/S0140-6736(12)60651-5

6. Kawai A, Araki N, Hiraga H, Sugiura H, Matsumine A, Ozaki T, et al. A randomized, double-blind, placebo-controlled, phase III study of pazopanib in patients with soft tissue sarcoma: results from the Japanese subgroup. *Jpn J Clin Oncol.* (2016) 46:248–53. doi: 10.1093/jjco/hyv184

7. Justice CN, Derbala MH, Baich TM, Kempton AN, Guo AS, Ho TH, et al. The impact of pazopanib on the cardiovascular system. *J Cardiovasc Pharmacol Ther.* (2018) 23:387–98. doi: 10.1177/1074248418769612

8. Scott SS, Greenlee AN, Schwendeman EJ, Mohammad SJ, Naughton MT, Matzko A, et al. Intracellular cardiac signaling pathways altered by cancer therapies. *Cardiovasc Signal Health Dis.* (2022):111–73. doi: 10.1007/978-3-031-08309-9_4

9. Sternberg CN, Davis ID, Mardiak J, Szczylik C, Lee E, Wagstaff J, et al. Pazopanib in locally advanced or metastatic renal cell carcinoma: results of a randomized phase III trial. *J Clin Oncol.* (2010) 28:1061–8. doi: 10.1200/JCO.2009.23.9764

frontiers | Frontiers in Cardiovascular Medicine

TYPE Case Report
PUBLISHED 14 October 2024
DOI 10.3389/fcvm.2024.1491361

Check for updates

OPEN ACCESS

EDITED BY
Reto Asmis,
Wake Forest University, United States

REVIEWED BY
Adolfo Gabriele Mauro,
Virginia Commonwealth University, United States
Matteo Armillotta,
University of Bologna, Italy

*CORRESPONDENCE
Celeste Ambra Murace
celesteambra.murace@guest.policlinicogemelli.it

RECEIVED 04 September 2024
ACCEPTED 26 September 2024
PUBLISHED 14 October 2024

CITATION
Sicignano LL, Murace CA, Palazzo A, Verrecchia E, Massaro MG, Manna R and Gerardino L (2024) Efficacy and safety of anakinra in radiation-induced acute pericarditis: a case report.
Front. Cardiovasc. Med. 11:1491361.
doi: 10.3389/fcvm.2024.1491361

COPYRIGHT
© 2024 Sicignano, Murace, Palazzo, Verrecchia, Massaro, Manna and Gerardino. This is an open-access article distributed under the terms of the Creative Commons Attribution License (CC BY). The use, distribution or reproduction in other forums is permitted, provided the original author(s) and the copyright owner(s) are credited and that the original publication in this journal is cited, in accordance with accepted academic practice. No use, distribution or reproduction is permitted which does not comply with these terms.

Efficacy and safety of anakinra in radiation-induced acute pericarditis: a case report

Ludovico Luca Sicignano[1], Celeste Ambra Murace[2]*, Antonella Palazzo[3], Elena Verrecchia[1], Maria Grazia Massaro[2], Raffaele Manna[2] and Laura Gerardino[1,2]

[1]Department of Aging, Neurological, Orthopedic and Head and Neck Sciences, Agostino Gemelli University Polyclinic (IRCCS), Rome, Italy, [2]Catholic University of the Sacred Heart, Rome, Italy, [3]Comprehensive Cancer Center, Agostino Gemelli University Polyclinic (IRCCS), Rome, Italy

Background: Acute pericarditis represents an inflammatory disease affecting the pericardial layers. In developed countries more than 80% of pericarditis are defined as idiopathic, less frequently they are secondary to other conditions such as infections, rheumatic or systemic inflammatory diseases, cancer, post–cardiac injury syndromes and radiation therapy (RT).
Case presentation: We reported a case of a patient with acute pericarditis that occurred a few hours after chest radiation therapy, performed for breast cancer. After the failure of first-line therapy, we introduced anakinra, an anti- interleukin-1 (IL-1) agent, observing an immediate clinical and instrumental response.
Conclusions: Our experience highlights the efficacy and safety profile of anakinra in early stages of acute pericarditis with an inflammatory phenotype. To the best of our knowledge, there is no data supporting the use of anakinra in the treatment of RT induced acute pericarditis.

KEYWORDS

acute pericarditis, pericardial disease, anakinra, radiation therapy, breast cancer

Introduction

Acute pericarditis represents an inflammatory disease affecting the pericardial layers, with an incidence of 27.7 cases per 100,000 population per year (1). In developed countries more than 80% of pericarditis are defined as idiopathic, less frequently they are secondary to other conditions such as infections, rheumatic or systemic inflammatory diseases, cancer, post–cardiac injury syndromes and radiation therapy (2). In particular, the latter may also represent an obstacle to completing oncological therapy. In those cases, treatment follows recommended guidelines of the European Society of Cardiology, including Nonsteroidal Anti-Inflammatory Drugs (NSAIDs) colchicine and steroids (1). We reported a case of a patient with acute pericarditis that occurred a few hours after chest radiation therapy, performed for breast cancer. After the failure of first-line therapy, we introduced anakinra, an anti-IL1 agent, observing an immediate clinical and instrumental response.

Case description

A 52-years-old woman, with a recent diagnosis of stage IIIC invasive breast cancer, came to our attention in May 2021 for an acute episode of pleuro-pericarditis occurred

during radiation therapy. Her past medical history was significant for depressive and anxious disorder treated with quetiapine and bromazepam. In January 2020 she underwent quadrantectomy with sentinel lymph node biopsy followed by axillary lymph node dissection, which diagnosed pT2 m pN1 (1/11) estrogen and progesterone receptors positive HER2 negative breast cancer. The staging CT scan revealed the presence of a pathological internal mammary lymph node. For this reason, she received anthracycline and taxane based adjuvant chemotherapy, with evidence of radiological partial response on the internal mammary node, followed by letrozole and radiation therapy (RT). In May 2021, after nine doses of RT, she was admitted to hospital for typical chest pain and fever. During the hospitalization, a mild pleuro-pericardial (10 mm) effusion in association with specific electrocardiogram (ECG) abnormalities (Figure 1) and high levels of inflammatory markers [C reactive protein (CRP) 116.7 mg/L, CRP normal value <5 mg/L] were found. Diagnosis of pleuro-pericarditis was made and therapy with ibuprofen 600 mg every 8 h and colchicine 0.5 mg once a day was started. After three days from discharge, she reported a new onset of chest pain and fever and so ibuprofen was uptitrated to 2,400 mg daily. A few days later, she presented to our pericardial clinic complaining about the persistence of symptoms. After ruling out infectious and rheumatic diseases, even if she had received a limited initial radiation dose, we concluded for a diagnosis of suspected radiation-induced acute pericarditis. Therefore, we decided to introduce a different line of therapy and, considering her previous diagnosis of psychiatric disorder, we preferred to use anakinra 100 mg daily over steroids, in agreement with the patient. Thenceforth we observed a rapid resolution of both symptoms and pericardial effusion, with a normalization of inflammatory markers. After one month of treatment, we reduced anakinra to 100 mg every other day and discontinued colchicine, due to neutropenia (neutrophil count 1,200 x 10^9/L). This dosage was maintained for the next three months, with a good efficacy and tolerance. After one month from the temporarily discontinuation, she restarted and completed the radiation therapy program. Since then, she has attended regular follow-up to our clinic, with progressive tapering of anakinra that was monthly reduced by 100/mg every 7 days till the dosage of 100 mg/week. During the follow up, she reported only one recurrence of pericarditis, which occurred after three months from an attempt of drug suspension. Nevertheless, treatment with anakinra showed good safety and efficacy, being well tolerated without serious adverse effects or severe infections. Moreover, several echocardiographic controls resulted normal, excluding constrictive evolution. Furthermore, the patient continued adjuvant endocrine therapy attending regular follow up visits at the oncologic clinic, without any evidence of cancer relapse.

We report an accurate table of the critical events in the patient's medical history (Table 1).

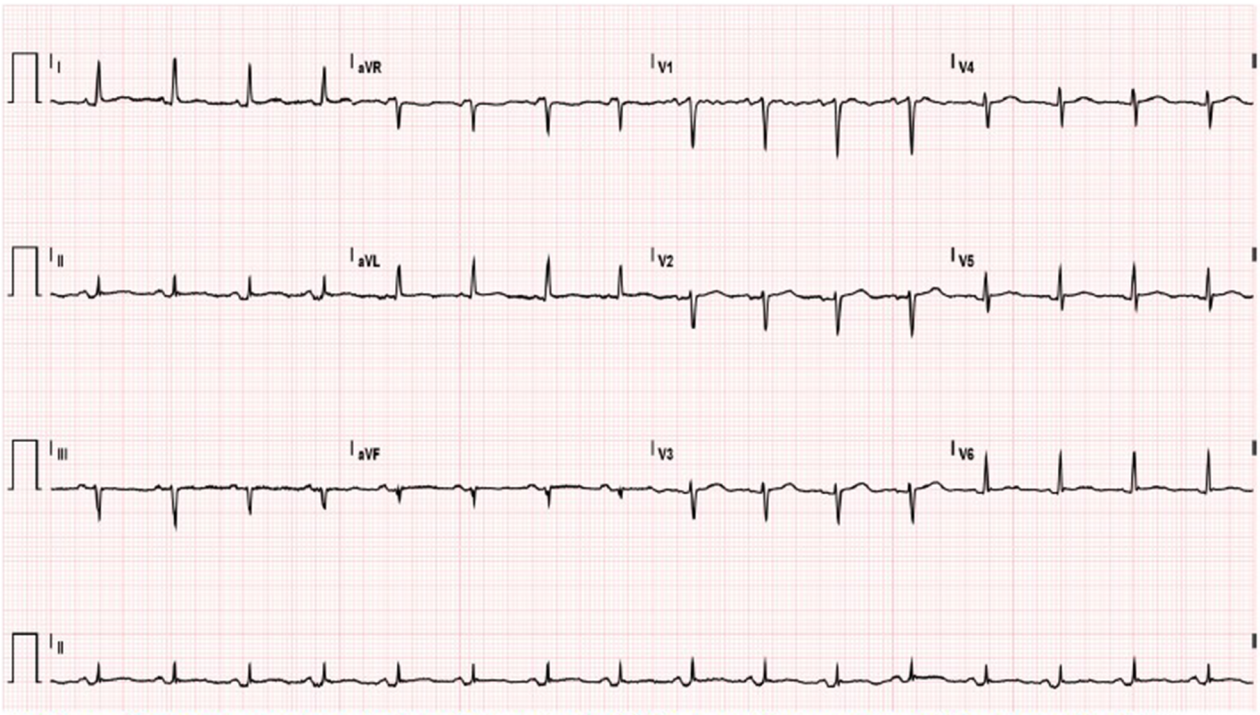

FIGURE 1
Electrocardiogram shows sinus rhythm with heart rate of 97 bpm, PR depression in DII and a specific ST-T.

TABLE 1 Timeline of critical events.

Day 0	Radiation chest therapy and few hours later sign and symptoms of acute pericarditis. Start treatment with Ibuprofen 1,800 mg/day and colchicine 0.5 mg/day.
Day 5	Up titration of therapy with ibuprofen to 2,400 mg/day plus colchicine 0.5 mg/day because of new onset of pericarditis symptoms.
Day 11	Start of anakinra 100 mg/day due to the persistence of sign and symptoms of pericarditis and new increase of PCR (C-reactive protein) values.
Day 30	Restart of radiation therapy program.
Day 42	Decalage of anakinra therapy to 100 mg every other day and suspension of colchicine because of neutropenia.
10 months later	After a progressive tapering, anakinra is suspended and patient is in good clinical conditions.
13 months later	Single recurrence of pericarditis treated with Ibuprofen and colchicine.
Today	Patient is in good clinical conditions, without any evidence of cancer relapse.

Discussion

Despite of improved radiation techniques, RT-related side effects are relatively common, including a wide range of pericardial diseases such as acute pericarditis, pericardial effusion, cardiac tamponade, chronic and constrictive pericarditis, pericardial calcification and fibrosis. Acute pericarditis is a potential manifestation of radiation acute toxicity that may occur as early as a few hours after RT administration, with onset of chest pain, fever, and pericardial friction rub. On the contrary, constrictive pericarditis may occur as delayed complication, even up decades after therapy administration, as an expression of chronic toxicity (3). A recent study reported several pathogenic models through which RT may induce cardiac toxicity, including an inflammatory response mediated by pro-inflammatory cytokines, such as tumor necrosis factor-alpha (TNF-α), interleukin-1 (IL-1) and interleukin-6 (IL-6); endothelial dysfunction and fibrosis (4).

In our clinical case, the patient presented acute pericarditis with an inflammatory phenotype characterized by fever, chest pain, high levels of CRP and moderate pleuro-pericardial effusion. After the failure of first-line therapy, we introduced anakinra, an anti-IL-1 agent, observing an immediate clinical and instrumental response. In our decision making, we excluded the possibility to use corticosteroids, avoiding getting worse patient's psychiatric disorder.

By the current ESC guidelines, anakinra is indicated as the possible treatment for colchicine-resistant and steroid dependent recurrent pericarditis (1). To the state of the art, little evidence supports the use of anakinra in acute pericarditis with evidence of safety and efficacy (5, 6).

Our case is interesting for several reasons. First, it represents an example of the efficacy of anakinra in early stages of acute pericarditis with an inflammatory phenotype. Furthermore, to our knowledge, there is no other evidence in favour of its use in RT-acute pericarditis. Anakinra has proven to be able to control the pericardial disease, inducing a prolonged remission and avoiding progression towards constrictive pericarditis. In addition, our experience highlights a good safety profile of the drug, since we had no major side effects and no serious infections occurred. Moreover, it allowed the patient to resume and complete her oncological treatment, without any recurrence of breast cancer, two years after diagnosis.

In conclusion, anakinra may represent a useful option in the treatment of RT-acute pericarditis, although further studies are needed to confirm this data.

Data availability statement

The original contributions presented in the study are included in the article/Supplementary Material, further inquiries can be directed to the corresponding author.

Ethics statement

Written informed consent was obtained from the individual(s) for the publication of any potentially identifiable images or data included in this article.

Author contributions

LS: Writing – original draft, Writing – review & editing, Conceptualization, Methodology, Project administration, Supervision, Validation, Visualization. CM: Writing – review & editing, Writing – original draft. AP: Writing – review & editing. EV: Conceptualization, Methodology, Resources, Visualization, Writing – original draft, Writing – review & editing. MM: Writing – original draft, Writing – review & editing. RM: Conceptualization, Supervision, Validation, Visualization, Writing – original draft, Writing – review & editing. LG: Conceptualization, Methodology, Project administration, Resources, Supervision, Validation, Visualization, Writing – original draft, Writing – review & editing.

Funding

The author(s) declare that no financial support was received for the research, authorship, and/or publication of this article.

Conflict of interest

The authors declare that the research was conducted in the absence of any commercial or financial relationships that could be construed as a potential conflict of interest.

Publisher's note

All claims expressed in this article are solely those of the authors and do not necessarily represent those of their affiliated organizations, or those of the publisher, the editors and the reviewers. Any product that may be evaluated in this article, or claim that may be made by its manufacturer, is not guaranteed or endorsed by the publisher.

References

1. Adler Y, Charron P. The 2015 ESC guidelines on the diagnosis and management of pericardial diseases. *Eur Heart J*. (2015) 36(42):2873–4. doi: 10.1093/eurheartj/ehv479

2. Chiabrando JG, Bonaventura A, Vecchié A, Wohlford GF, Mauro AG, Jordan JH, et al. Management of acute and recurrent pericarditis: JACC state-of-the-art review. *J Am Coll Cardiol*. (2020) 75(1):76–92. doi: 10.1016/j.jacc.2019.11.021

3. von Kemp BA, Cosyns B. Radiation-induced pericardial disease: mechanisms, diagnosis, and treatment. *Curr Cardiol Rep*. (2023) 25(10):1113–21. doi: 10.1007/s11886-023-01933-3

4. Hufnagle JJ, Andersen SN, Maani EV. *Radiation-Induced Cardiac Toxicity*. Treasure Island, FL: StatPearls Publishing (2023).

5. Wohlford GF, Buckley LF, Vecchié A, Kadariya D, Markley R, Trankle CR, et al. Acute effects of interleukin-1 blockade using anakinra in patients with acute pericarditis. *J Cardiovasc Pharmacol*. (2020) 76(1):50–2. doi: 10.1097/FJC.0000000000000847

6. Sicignano LL, Massaro MG, Savino M, Rigante D, Gerardino L, Manna R. Early introduction of anakinra improves acute pericarditis and prevents tamponade in staphylococcal sepsis. *Intern Emerg Med*. (2021) 16(5):1391–4. doi: 10.1007/s11739-020-02627-2

frontiers | Frontiers in Cardiovascular Medicine

TYPE Case Report
PUBLISHED 18 November 2024
DOI 10.3389/fcvm.2024.1497659

Check for updates

OPEN ACCESS

EDITED BY
Reto Asmis,
Wake Forest University, United States

REVIEWED BY
Maruti Haranal,
U N Mehta Institute of Cardiology and Research, India
Xiaomeng Shi,
Emory University, United States

*CORRESPONDENCE
Jinjing Wang
jinjingwangls@163.com

RECEIVED 17 September 2024
ACCEPTED 28 October 2024
PUBLISHED 18 November 2024

CITATION
Luo S, Tian X, Xu T and Wang J (2024) A simple goiter of the right ventricle: case report and literature review.
Front. Cardiovasc. Med. 11:1497659.
doi: 10.3389/fcvm.2024.1497659

COPYRIGHT
© 2024 Luo, Tian, Xu and Wang. This is an open-access article distributed under the terms of the Creative Commons Attribution License (CC BY). The use, distribution or reproduction in other forums is permitted, provided the original author(s) and the copyright owner(s) are credited and that the original publication in this journal is cited, in accordance with accepted academic practice. No use, distribution or reproduction is permitted which does not comply with these terms.

A simple goiter of the right ventricle: case report and literature review

Shuai Luo, Xiaoxue Tian, Ting Xu and Jinjing Wang*

Department of Pathology, Affiliated Hospital of Zunyi Medical University, Zunyi, Guizhou, China

Background: Cardiac teratoma is extremely rare, accounting for less than 1% of adult cardiac tumors. These teratomas typically occur in the pericardium and myocardium, with intracardiac teratomas being even rarer. Given the limited number of cases, diagnosing and treating intracardiac teratomas remains challenging.
Case demonstration: A 50-year-old man was admitted to the hospital with a 1-month history of chest tightness and shortness of breath after exertion. Color Doppler echocardiography revealed a hyperechoic mass of approximately 58 mm in diameter in the right ventricular cavity and outflow tract. Postoperative pathological examination confirmed a right ventricular monodermal teratoma (goiter). The patient was followed up for 2 years with good overall health and no recurrence.
Conclusions: Intracardiac teratomas are exceedingly uncommon tumors, with the predominant right ventricle involvement being observed across a wide age range. These teratomas are often histologically classified as benign. The early detection of intracardiac teratomas relies on imaging findings, while a definitive diagnosis requires histopathological examination. The primary treatment is surgical resection, which yields a favorable prognosis.

KEYWORDS

right ventricle, teratoma, pathology, goiter, treatment

Background

Cardiac teratoma is an extremely rare condition that represents approximately less than 1% of adult cardiac tumors (1), with only case reports documented in the literature. The clinical manifestations of these teratomas primarily depend on the anatomical location of the tumor, while they can be histopathologically classified as benign or malignant. Cardiac teratomas often arise in the pericardium and myocardium. However, intracardiac teratomas are even rarer, with no more than 10 cases reported to date. According to the World Health Organization definition (2), mature cystic teratomas (MCTs) are composed entirely of mature tissue derived from two or three germ layers (including the ectoderm, mesoderm, and/or endoderm). Conversely, monodermal teratomas, which arise from a single germ layer, are rarer and include goiters, carcinoids, and neuroectodermal tumors. Cardiac teratomas are mainly MCTs (3), with no published cases of intracardiac monodermal teratomas. This case report presents the first documented case of a cardiac monodermal teratoma (goiter), aiming to improve the current understanding of this rarely occurring tumor.

Abbreviations
MCT, mature cystic teratoma; CT, computed tomography; CMR, cardiovascular magnetic resonance.

10.3389/fcvm.2024.1497659

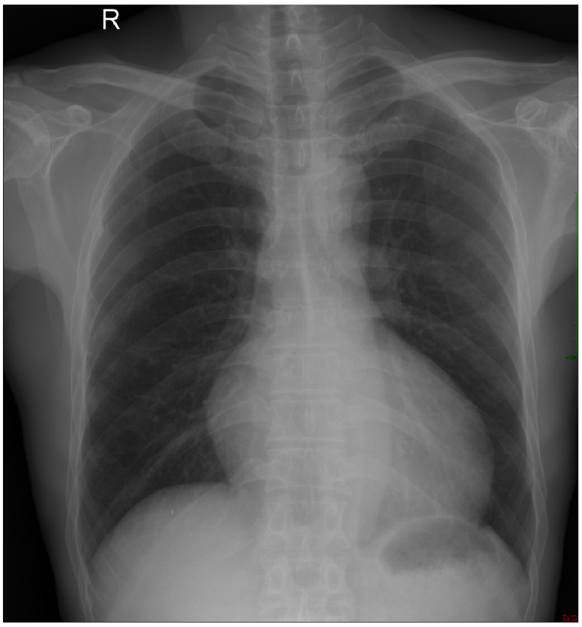

FIGURE 1
Chest radiograph showed an increased transverse diameter of the heart shadow, a smooth bilateral diaphragmatic surface, and a sharp costophrenic angle.

Case demonstration

A 50-year-old male patient was admitted to the hospital with a 1-month history of chest tightness and shortness of breath after exertion, without amaurosis fugax, incontinence, cough, expectoration, cold, and fever. Physical examination revealed an enlarged left heart border, a heart rate of 80 beats/min, a regular heart rhythm, and a rumbling murmur in the apex of the heart.

A chest radiograph (Figure 1) showed an increased transverse diameter of the heart shadow, a smooth bilateral diaphragmatic surface, and a sharp costophrenic angle. Electrocardiography (Figure 2) demonstrated right atrial hypertrophy, complete right bundle branch block, and premature ventricular contraction. Chest computed tomography (CT) (Figure 3) and coronary angiography further demonstrated enlargement of the heart, obvious right atrium and ventricle enlargement, and a massive filling defect of 51 mm × 60 mm in the right ventricle accompanied by uneven density and punctate calcification, which showed enhancement on the contrast-enhanced scan. The left and right coronary arteries arise from the left and right coronary sinus, respectively, and are right-sided dominant. Non-calcified plaque was seen in the distal segment of the right coronary artery, corresponding to mild-to-moderate luminal stenosis. Calcified plaque was found in the proximal segments of the left anterior descending and middle coronary arteries, which

FIGURE 2
Electrocardiography demonstrated right atrial hypertrophy, complete right bundle branch block, and premature ventricular contraction.

FIGURE 3
Contrast-enhanced CT scan showed a massive filling defect in the right ventricle with uneven enhancement (marked with red circles).

corresponded to mild luminal stenosis. Echocardiography indicated that the right atrium and right ventricle were significantly enlarged, while a hyperechoic mass approximately 58 mm × 48 mm in size was observed in the right ventricular cavity and outflow tract (Figure 4). The base of this mass was attached to the basal segment of the anterior septum and showed poor mobility. Furthermore, the inner diameter of the aortic sinus was widened, whereas the inner diameter of the pulmonary artery was normal. The thickness of the interventricular septum and the left and right ventricular walls was normal, while the left ventricular posterior wall exhibited slightly reduced motion. No obvious abnormalities were found in the morphology and structure of the valves. In addition, a Doppler examination revealed moderate eccentric tricuspid regurgitation and mild aortic valve regurgitation. The pulmonary artery systolic pressure was estimated to be approximately 53 mmHg, owing to the tricuspid regurgitation. Mitral flow spectrum showed that peak E was greater than peak A. Based on these findings, the radiologist considered the possibility of thrombosis.

In light of the patient's clinical manifestations of a right ventricular mass, severe tricuspid regurgitation, and cardiac insufficiency, enucleation of the right ventricular tumor and

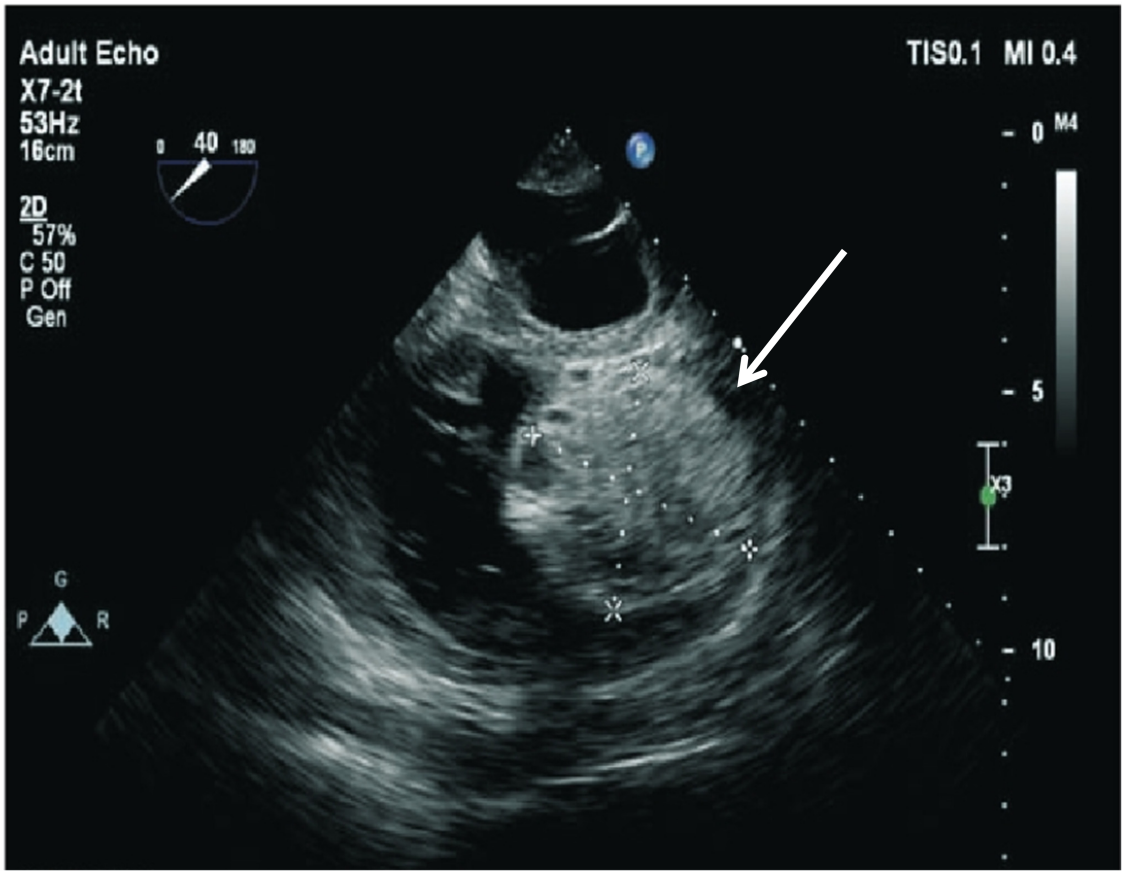

FIGURE 4
An echocardiogram revealing a hyperechoic mass in the right ventricular cavity and outflow tract (white arrow).

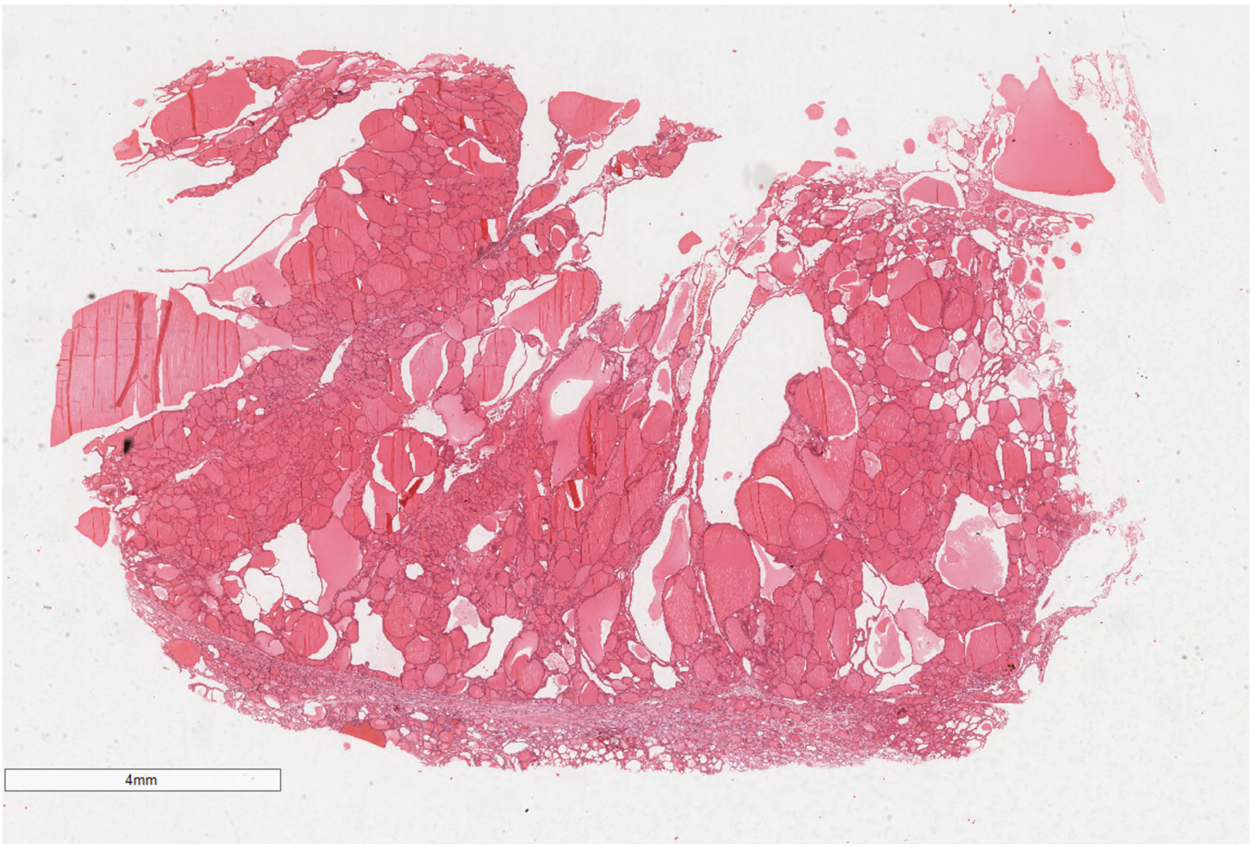

FIGURE 5
The mass was well-circumscribed and consisted almost entirely of normal or hyperplastic thyroid tissue. Hematoxylin and eosin, ×7.

tricuspid valvuloplasty were performed. In this procedure, the right atrium and atrial septum were explored, and a mass of approximately 6 cm × 5 cm was found in the anterior septum of the right ventricle, along with a relatively smooth, pedunculated capsule and a slightly wide base measuring approximately 2.5 cm × 1.5 cm.

Pathological examination revealed a gray-brown oval tissue (6.5 cm × 4.5 cm × 2.5 cm) in size, with a complete capsule, clear boundary, gray-red cut surface, soft texture, local jelly-like, hemorrhage, and calcification.

Histological evaluation showed that the lesions comprised normal or hyperplastic thyroid tissue of varying sizes and mature thyroid follicles (Figure 5). The size of the follicles ranged from microfollicles to giant follicles, and the cavity consisted of eosinophilic glial material. A high magnification view (Figure 6) demonstrated a single layer of low columnar or cuboidal follicular epithelium, bland, with a small proportion of eosinophilic, clear, and mucous cells. Local hemorrhage and cystic degeneration were also visible (Figure 7).

Based on the histopathological features, the tumor, which was composed entirely of thyroid tissue without other teratoma components, was diagnosed as a right ventricular monodermal teratoma (goiter).

After surgical resection of the ventricular mass, the patient was followed up for 2 years, during which he exhibited good overall health and no recurrence.

Discussion

Primary cardiac teratomas are excessively rare, typically developing in the pericardium and myocardium, with intracardiac teratomas being even more uncommon. Currently, only four case reports of teratomas in the ventricular cavity have been published (3–6). Consequently, those previous cases along with the present one lead to five cases (Table 1).

Among these five cases of intracardiac teratoma, three were diagnosed in male patients and two in female patients, with a mean age of 28 years. The tumors had a mean diameter of 4.8 cm, with all cases involving the right ventricle. In terms of clinical manifestations, three patients had syncope, while two presented with palpitation, dyspnea, and chest pain and tightness. Among these five cases, four were primary cardiac teratomas and one was a testicular teratoma metastasized to the heart. Of the four cases of primary cardiac teratomas, three were MCTs and the fourth is the first case of cardiac monodermal teratoma (goiter) documented in the current report. In terms of treatment outcome, three cases of primary

10.3389/fcvm.2024.1497659

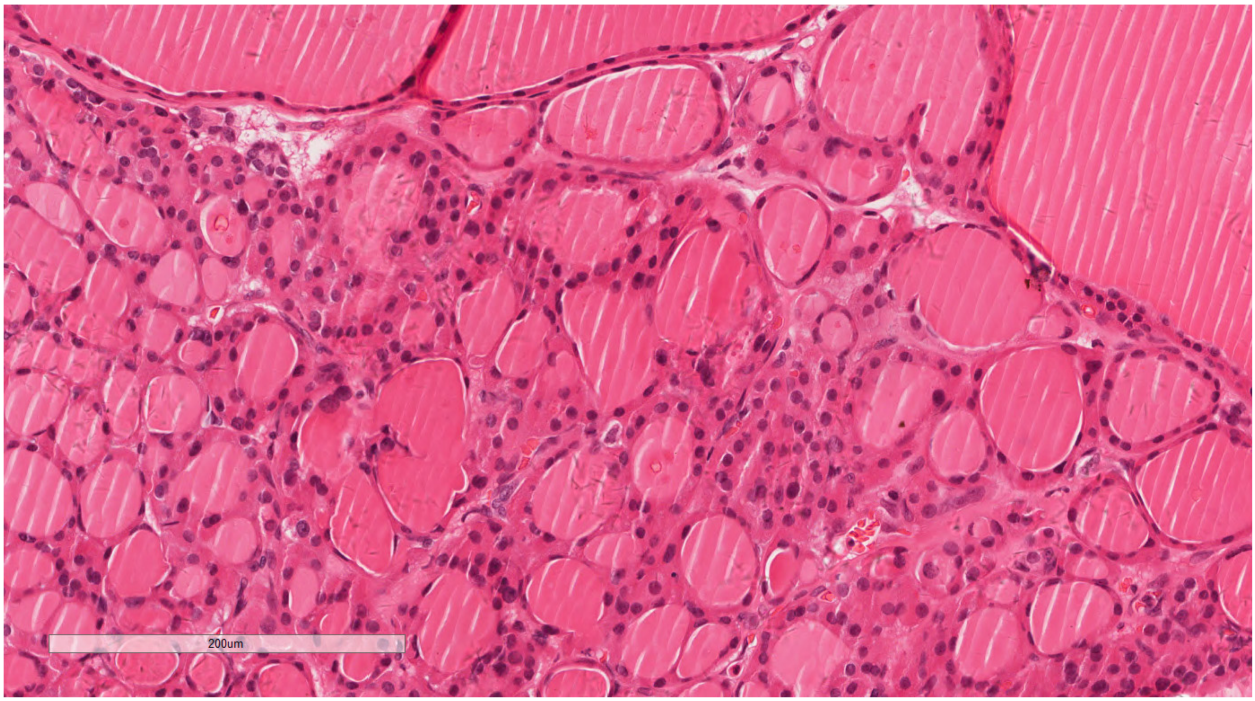

FIGURE 6
A high magnification view demonstrating a single layer of low columnar or cuboidal follicular epithelium, with mild morphology. Hematoxylin and eosin, ×200.

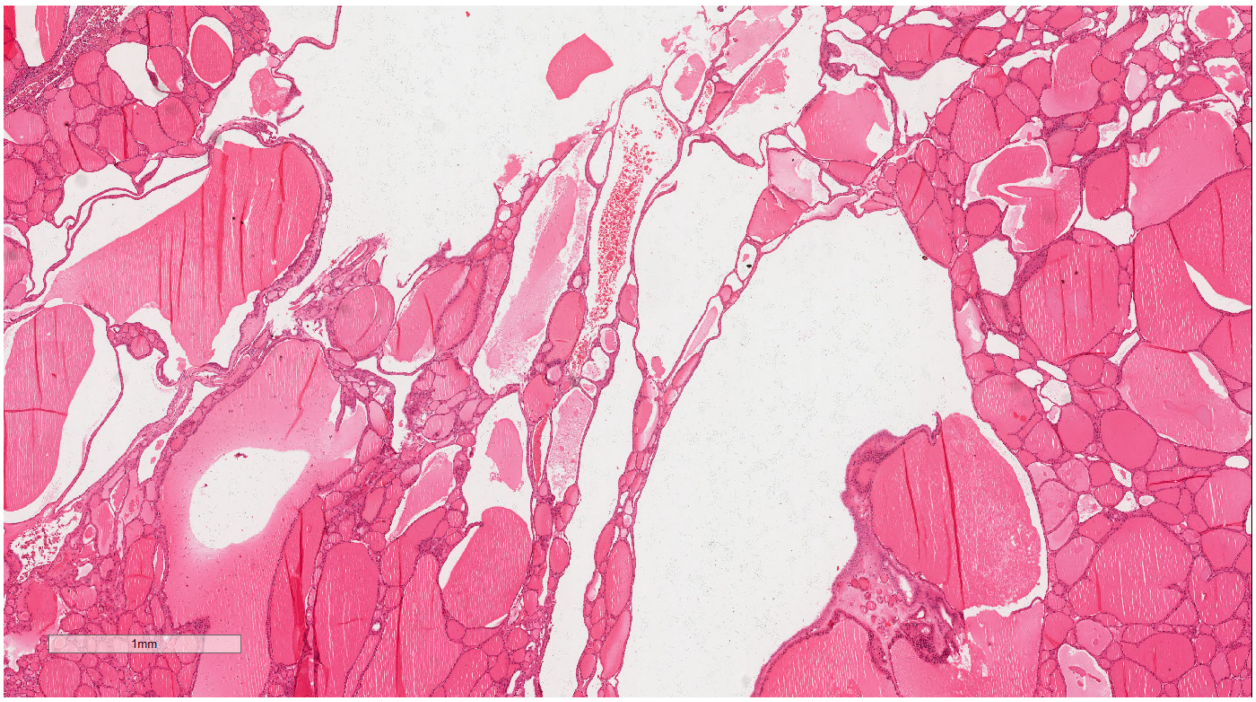

FIGURE 7
The tumor showed local hemorrhage and cystic degeneration. Hematoxylin and eosin, ×22.

TABLE 1 Clinicopathological features of intracardiac teratomas and literature review.

	Time		Sex	Age (years)	Diameter (cm)	Location	Symptoms	Primary (metastasis)	Histologic types	Treatment and prognosis
1	1998	Campagne et al. (3)	F	29	4	Ventricular septum, right ventricle	Syncope	Primary	Mature cystic teratoma	Found at autopsy
2	2019	Farid et al. (5)	F	9 days after birth	1.5	Right ventricle	Recurrent syncope	Primary	Mature cystic teratoma	Recovered well after surgical resection
3	2021	Abdulla et al. (4)	M	22	11.7	Right ventricle	Progressive dyspnea, palpitations, and syncope	Testicular teratoma metastasis	Malignant teratoma of germ cell	Complete regression was achieved after chemotherapy
4	2021	Tao et al. (6)	M	37	1.2	Right ventricle	Chronic chest pain and palpitations worsened	Primary	Mature cystic teratoma	Recovered well after surgical resection
5	2024	This case	M	50	5.8	Right ventricle	After fatigue, chest tightness, shortness of breath	Primary	Monodermal teratoma (goiter)	Recovered well after surgical resection

cardiac benign teratomas showed good results after surgical treatment. In the case of the testicular malignant teratoma metastasized to the heart, complete tumor regression was achieved after chemotherapy. The fifth remaining case was diagnosed at autopsy.

Intracardiac teratomas generally occur over a broad age range, with most cases predominantly developing in the right ventricle of young and middle-aged patients. Furthermore, MCT is the most prevalent histological type. The clinical manifestations of these teratomas are primarily determined by the anatomical location of the tumor rather than its histopathology. The rapid growth of cardiac teratomas may be attributed to the rich blood supply in this region, which provides a conducive environment for tumor growth and increases the likelihood of serious mechanical consequences due to excessive volume. Moreover, different pathogenesis can lead to complications, such as embolism and heart valve impairment, which in turn affect the blood supply function of the heart to cause symptoms of systemic ischemia and hypoxia (7), including syncope, dyspnea, and palpitation. Given that MCTs are the most frequent histological type, this case report is of notable significance as the first documented description of a patient with a cardiac monodermal teratoma (goiter). The most commonly used and valuable methods for the early detection of cardiac-occupying lesions are non-invasive cardiac color Doppler ultrasound and CT, with cardiovascular magnetic resonance (CMR) also emerging as a crucial tool to evaluate cardiac malignant tumors (8). Surgical treatment is the preferred strategy in symptomatic patients, whereas a close follow-up is favored in asymptomatic patients (9).

Conclusion

Intracardiac teratomas are extremely rare tumors that predominantly occur in the right ventricle across a wide age range. These teratomas are usually histologically classified as benign, with clinical manifestations such as ischemia and hypoxia primarily determined according to the anatomical location of the tumor and the degree of obstruction. Symptomatic patients generally undergo surgical treatment, while asymptomatic patients are managed with close follow-up.

Data availability statement

The original contributions presented in the study are included in the article/Supplementary Material, further inquiries can be directed to the corresponding author.

Ethics statement

Written informed consent was obtained from the individual(s) for the publication of any potentially identifiable images or data included in this article.

Author contributions

SL: Resources, Writing – original draft, Writing – review & editing. XT: Resources, Writing – review & editing. TX: Data curation, Writing – review & editing. JW: Data curation, Writing – review & editing.

Funding

The author(s) declare that no financial support was received for the research, authorship, and/or publication of this article.

Acknowledgments

The authors would like to thank all the reviewers who participated in the review and thank Bullet Edits Limited for the linguistic editing and proofreading of the manuscript.

Conflict of interest

The authors declare that the research was conducted in the absence of any commercial or financial relationships that could be construed as a potential conflict of interest.

Publisher's note

All claims expressed in this article are solely those of the authors and do not necessarily represent those of their affiliated organizations, or those of the publisher, the editors and the reviewers. Any product that may be evaluated in this article, or claim that may be made by its manufacturer, is not guaranteed or endorsed by the publisher.

References

1. Ying L, Lin R, Gao Z, Qi J, Zhang Z, Gu W. Primary cardiac tumors in children: a center's experience. *J Cardiothorac Surg*. (2016) 11(1):52. doi: 10.1186/s13019-016-0448-5

2. Organization WH. WHO Classification of Tumours: Female Genital Tumours (2020). (accessed July 5, 2022).

3. Campagne G, Quereda F, Merino G, García A, Herranz Y, Frutos A, et al. Benign intracardiac teratoma detected prenatally. Case report and review of the literature. *Eur J Obstet Gynecol Reprod Biol*. (1998) 80(1):105–8. doi: 10.1016/S0301-2115(98)00066-9

4. Abdulla A, Durand JB, Lopez-Mattei J, Palaskas N. A rare case of testicular teratoma metastasizing to the right ventricle. *JACC Case Rreports*. (2021) 3 (1):117–9. doi: 10.1016/j.jaccas.2020.10.021

5. Farid Y, Chebli L, Seghers V, Dewals W, Sanoussi A, Wauthy P. Obstructive teratoma in the right ventricle of a newborn: a case report. *J Cardiothorac Surg*. (2019) 14(1):55. doi: 10.1186/s13019-019-0874-2

6. Tao Z, Li Y, Zhao Y, Liu D. Incidental finding of an adult intracardiac teratoma. *J Card Surg*. (2021) 36(9):3441–4. doi: 10.1111/jocs.15724

7. Shi L, Wu L, Fang H, Han B, Yang J, Ma X, et al. Identification and clinical course of 166 pediatric cardiac tumors. *Eur J Pediatr*. (2017) 176(2):253–60. doi: 10.1007/s00431-016-2833-4

8. Fussen S, De Boeck BW, Zellweger MJ, Bremerich J, Goetschalckx K, Zuber M, et al. Cardiovascular magnetic resonance imaging for diagnosis and clinical management of suspected cardiac masses and tumours. *Eur Heart J*. (2011) 32 (12):1551–60. doi: 10.1093/eurheartj/ehr104

9. Stiller B, Hetzer R, Meyer R, Dittrich S, Pees C, Alexi-Meskishvili V, et al. Primary cardiac tumours: when is surgery necessary? *Eur J Cardiothorac Surg*. (2001) 20 (5):1002–6. doi: 10.1016/S1010-7940(01)00951-4

frontiers | Frontiers in Cardiovascular Medicine

TYPE Case Report
PUBLISHED 16 December 2024
DOI 10.3389/fcvm.2024.1479676

Check for updates

OPEN ACCESS

EDITED BY
Reto Asmis,
Wake Forest University, United States

REVIEWED BY
Konstantinos Liapis,
Democritus University of Thrace, Greece
Mariana Gospodinova,
University Hospital St. Ivan Rilski, Bulgaria
Ajay Vallakati,
The Ohio State University, United States

*CORRESPONDENCE
Raymond L. Comenzo
✉ raymond.comenzo@tuftsmedicine.org

RECEIVED 12 August 2024
ACCEPTED 25 November 2024
PUBLISHED 16 December 2024

CITATION
Wu X, Toskic D, Zhou P, Scalia S, Ma X, Bhatt P, Fogaren T, Pilichowska M, Arkun K, Patel J, Riesenburger RI, Larson DP and Comenzo RL (2024) Case Report: Avoiding misdiagnosis in amyloidosis—navigating transthyretin genopositivity and monoclonal gammopathy in a patient with advanced heart failure and spinal stenosis.
Front. Cardiovasc. Med. 11:1479676.
doi: 10.3389/fcvm.2024.1479676

COPYRIGHT
© 2024 Wu, Toskic, Zhou, Scalia, Ma, Bhatt, Fogaren, Pilichowska, Arkun, Patel, Riesenburger, Larson and Comenzo. This is an open-access article distributed under the terms of the Creative Commons Attribution License (CC BY). The use, distribution or reproduction in other forums is permitted, provided the original author(s) and the copyright owner(s) are credited and that the original publication in this journal is cited, in accordance with accepted academic practice. No use, distribution or reproduction is permitted which does not comply with these terms.

Case Report: Avoiding misdiagnosis in amyloidosis—navigating transthyretin genopositivity and monoclonal gammopathy in a patient with advanced heart failure and spinal stenosis

Xia Wu[1], Denis Toskic[1,2], Ping Zhou[2], Stephanie Scalia[1], Xun Ma[2], Parva Bhatt[1], Teresa Fogaren[1], Monika Pilichowska[3], Knarik Arkun[3,4], Jainith Patel[4], Ron I. Riesenburger[4], Daniel P. Larson[5] and Raymond L. Comenzo[1,2]*

[1]Division of Hematology-Oncology, Department of Medicine, Tufts Medical Center, Boston, MA, United States, [2]The John Davis Myeloma and Amyloid Program in the Cancer Center, Tufts Medical Center, Boston, MA, United States, [3]Department of Pathology, Tufts Medical Center, Boston, MA, United States, [4]Department of Neurosurgery, Tufts Medical Center, Boston, MA, United States, [5]Department of Laboratory Medicine and Pathology, Mayo Clinic, Rochester, MN, United States

Background: A 63-year-old Black woman presented with progressive exertional dyspnea and chronic lower back pain. The course and findings in her case are instructive.
Case report: Family history was notable for cardiac deaths. An echocardiogram demonstrated ventricular wall thickening with diastolic dysfunction. The patient's N-terminal pro b-type natriuretic peptide level was 1,691 pg/ml with a troponin I level of 0.36 ng/ml. Transthyretin (TTR) sequencing detected a heterozygous V122I variant. The patient's free κ light chain level in serum was 664 mg/L with a ratio of 16.5. Bone marrow analysis showed 20%–30% κ-restricted plasma cells with amyloid deposits. A technetium-99m sodium pyrophosphate scan was performed and was negative. Magnetic resonance imaging of the total spine showed ligamentum flavum (LF) thickening at L4–5, causing severe spinal stenosis. In both the abdominal fat and the LF, liquid chromatography-coupled tandem mass spectrometry confirmed κ-type immunoglobulin light chain (AL) amyloidosis; the quantitative estimate of amyloid content in the LF was 5%. She was diagnosed with AL amyloidosis with Mayo Stage IIIA cardiac and soft tissue involvement, enrolled in the Aquarius trial (NCT05250973) in Cohort 2, and received daratumumab, cyclophosphamide, bortezomib, and dexamethasone. She achieved a partial hematological response with a cardiac response and is now pain-free and fully functional.
Conclusion: In patients with amyloidosis who have both monoclonal gammopathy and a TTR variant, it is imperative to discern the tissue type of the amyloid to deduce the correct diagnosis. ATTR and AL amyloidosis can both cause spinal stenosis with minimal degenerative changes. The LF tissue must be stained for amyloids and, if present, typing must be performed.

KEYWORDS

ATTR amyloidosis, AL amyloidosis, cardiac amyloidosis, ligamentum flavum (LF), differential diagnosis

Introduction

Amyloidosis is a family of diseases driven by misfolded or misassembled precursor proteins that deposit in organs and tissues and cause symptoms. Immunoglobulin light chain (AL) amyloidosis and transthyretin (ATTR) amyloidosis are two common types of systemic amyloidosis and both often involve the heart. With novel agents and new combinations of therapies, the prognosis of both AL and ATTR amyloidosis has improved significantly (1, 2). However, late-stage cardiac involvement and delays in diagnosis are correlated with poor prognosis (3). Therefore, early and accurate diagnosis and subtyping of amyloidosis are critical to ensure appropriate treatment to improve outcomes.

Diagnosis of AL or ATTR amyloidosis can be challenging, especially with cardiac involvement when patients could have similar clinical presentations and echocardiogram findings. In patients with evidence of both monoclonal gammopathy and a TTR mutation, correct subtyping is even more challenging. Given monoclonal gammopathy, clinicians may infer that AL amyloidosis is the diagnosis; however, "Occam's Razor" can be misleading, particularly in Black individuals, among whom monoclonal gammopathies occur at twice the rate observed in white individuals, while mutated TTR genes are present in 3.9% of Black individuals, especially the p.Val122Ile (V122I) mutation (4). Therefore, in the presence of monoclonal gammopathy, tissue typing is mandatory to verify the amyloid composition to achieve the correct diagnosis (5). Here we present an instructive case in point.

Case description

A 63-year-old Black woman from Cameroon presented with progressive fatigue and exertional dyspnea. She reported worsening dyspnea upon exertion for the previous 3 months, particularly during stair climbing. She denied having a cough, chest pain, diarrhea, abdominal pain, dysuria, fever, or weight changes. Her medical history was otherwise notable for worsening chronic lower back pain that was radiating down to her left leg and had been refractory to physical therapy and opioid analgesics. Her family history was notable for cardiac deaths, with her father dying at 59 and her sister in her teens, though details were unclear. Upon presentation, she was afebrile; her blood pressure was 136/84 mmHg, her heart rate was 97 beats per minute, and her oxygen saturation was 99% on room air. Physical examination showed regular heart rate and rhythm with no murmurs and clear lung sounds with no edema, cutaneous lesions, or macroglossia. A transthoracic echocardiogram demonstrated left ventricular wall thickening, interventricular septal thickness at end-diastole (IVSd) of 1.6 cm, ejection fraction of 45%, grade III diastolic dysfunction, and a severely dilated left atrium (Supplementary Figures S1C,D); strain imaging demonstrated an apical sparing pattern (Supplementary Figure S1E), which warranted a work-up for amyloid cardiomyopathy. Laboratory studies revealed that her N-terminal pro b-type natriuretic peptide (NT-proBNP) level was elevated to 1,691 pg/ml (normal range, 0–125) and her troponin I level to 0.36 ng/ml (<0.03). Her clinical picture raised the concern for cardiac amyloidosis; therefore, the patient was screened for monoclonal proteins. Both serum and urine immunofixation electrophoresis (IFE) showed free κ light chains without heavy chains. Serum protein electrophoresis (SPEP) did not show an M spike. Serum protein studies showed an elevated free κ light chain level at 664 mg/L (3.3–19.4) with a κ: λ ratio of 16.5 (0.5–2.0). A clonal plasma cell population of 20%–30% κ restricted CD138-positive cells was detected in the bone marrow, which contained translocation (11; 14), and marrow plasma cell staining was positive for cyclin D1 by immunohistochemistry. Congo red staining and examination in polarized light revealed amyloids in the marrow (Figures 1A,B) and abdominal fat and typing by liquid chromatography-coupled tandem mass spectrometry (LC/MS) confirmed κ-type AL. The sequence of the monoclonal amyloidogenic light chains was further identified to be IGKV1-33 (GenBank accession number: PP112602).

As for the lower back pain, magnetic resonance imaging (MRI) of the lumbar spine showed severe thickening of the ligamentum flavum (LF) at the level of L4–5 and severe narrowing of the spinal canal and bilateral neural foramina (Figures 2A–C). Given the sciatica symptoms refractory to physical therapy and pain medications, the patient underwent an L4–5 laminectomy and onlay arthrodesis, with subsequent relief of her back pain. The removed thickened LF was sent for biopsy and showed positive Congo red staining; LC/MS confirmed κ-type AL (Figures 1C,D) and the calculated amyloid load was 5.5% (Figure 3). The amyloid load was defined as the percentage of LF tissue occupied by amyloids and was quantified using a previously validated machine-learning model developed using Trainable Weka Segmentation (Fiji Version 2.1.0/1.53c) (6). The entire specimen displayed in Figure 3A was utilized for amyloid quantification.

Given the evidence of κ-type AL proteins in the soft tissue forming amyloids, the patient was suspected to have primary AL amyloidosis, with both cardiac involvement and soft tissue involvement. However, ATTR cardiac amyloidosis could not be ruled out without a further work-up given the patient's race and family history of cardiac death. To better identify the driver of cardiac disease, a 1 h technetium-99m (Tc-99m) sodium pyrophosphate (PYP) scan with single photon emission computed tomography (SPECT) was performed and showed grade 0 uptake on planar imaging with a heart-to-contralateral lung ratio of 1.1, which was not consistent with ATTR cardiac amyloidosis (Supplementary Figures S1A,B). We also performed TTR gene sequencing, detecting a heterozygous V122I TTR variant (Figure 1E). Therefore, she was diagnosed with AL amyloidosis with Mayo Stage IIIA cardiac and soft tissue involvement, enrolled in the Aquarius trial (NCT05250973), and received daratumumab, cyclophosphamide, bortezomib, and dexamethasone (Dara-CBD) (7). In addition, the patient also received torsemide and spironolactone for volume and electrolyte management. At the 6-month follow-up, she achieved a partial hematological response following six cycles of Dara-CBD, along

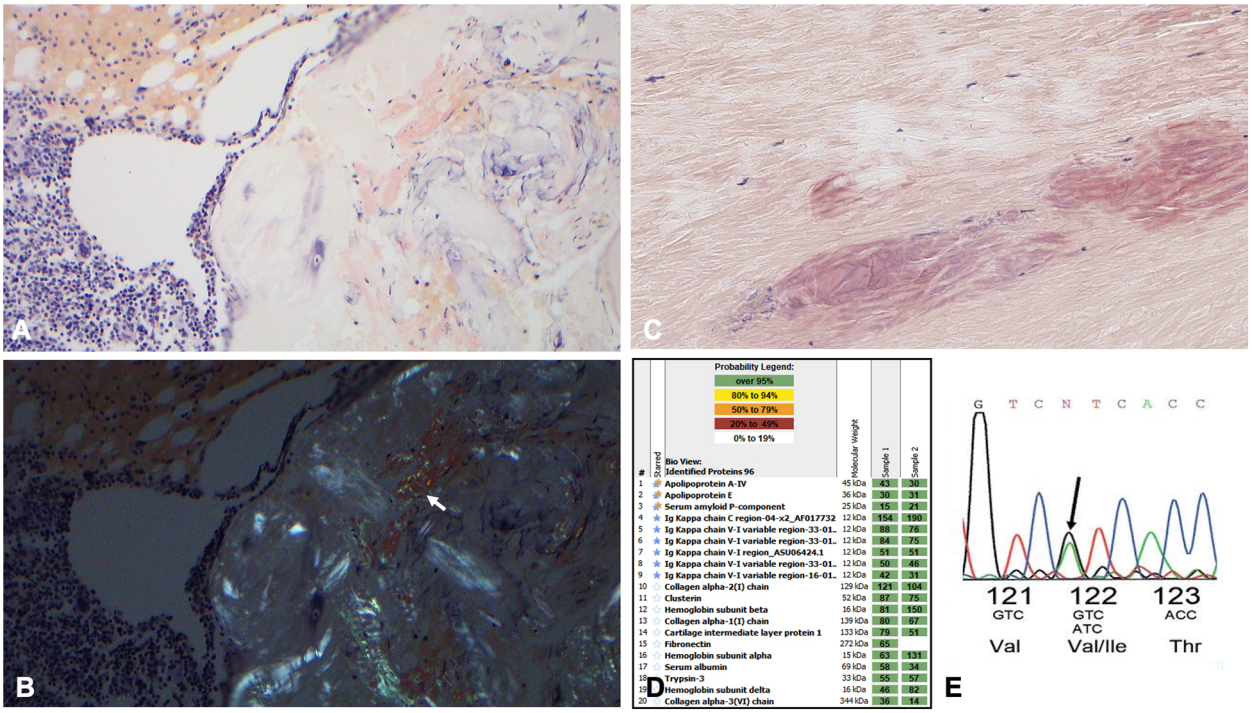

FIGURE 1
(A) 200× Congo red staining highlighting focal amyloid deposition in the patient's bone marrow specimen. **(B)** Corresponding polarized light images of the bone marrow specimen. The arrow is pointing to the apple green birefringence. **(C)** Congo red special staining highlights Congophilic deposits within the ligamentum flavum fibers at 200× magnification; the deposits are a dirty pink salmon color with delicate cracks, along with apple green polarization (not shown), consistent with amyloids. **(D)** The proteomic profile of the ligamentum flavum specimen. The columns labeled "sample" represent two separate analyses from laser micro-dissected Congo red-positive deposits in this case. The proteins highlighted with double stars represent universal amyloid proteins. The proteins highlighted with blue stars represent amyloid-specific markers detected in this case. The numbers in the green boxes correlate with the total number of MS/MS spectra detected of the particular protein in each row. **(E)** The Chromas TTR DNA sequence indicating the substitution of isoleucine (Ile) for valine (Val) at position 122.

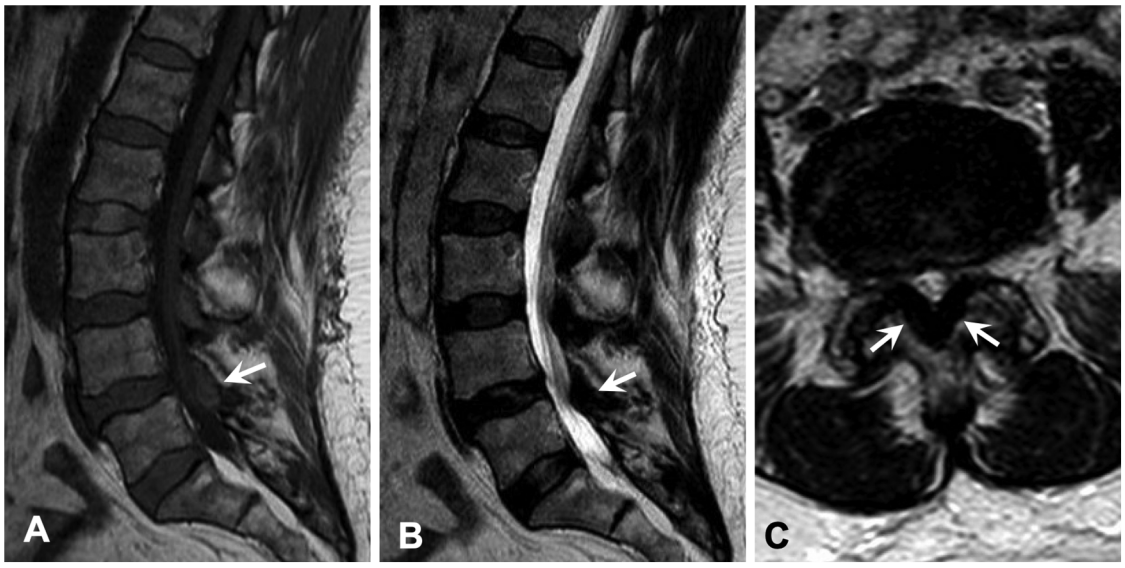

FIGURE 2
Magnetic resonance imaging of the lumbar spine demonstrated severe thickening of the ligamentum flavum at the level of L4–5 (arrow) with associated abnormal T1 hyperintensity, which caused severe narrowing of the spinal canal and bilateral neural foramina. Similar lesions were also seen at the levels of L1–4 to a lesser extent. **(A)** Sagittal T1-weighted image. **(B)** Sagittal T2-weighted image. **(C)** Axial T2-weighted image.

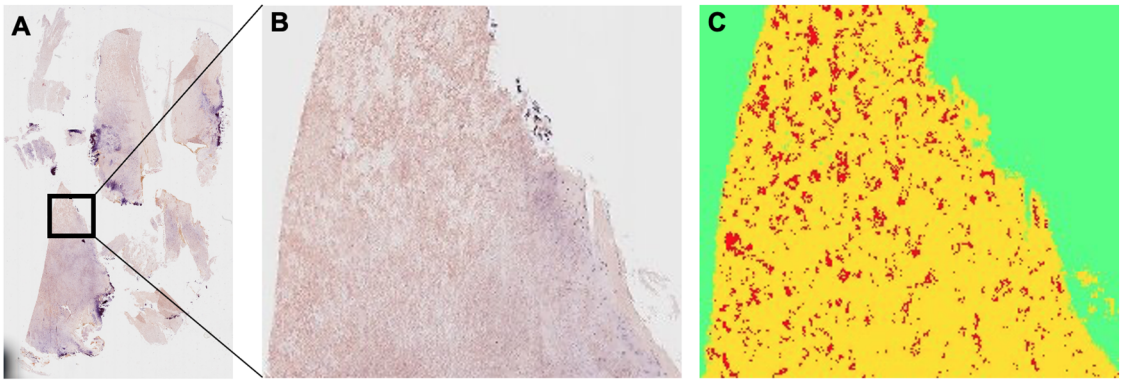

D Color	Object	# of Pixels
Red	Amyloid	60122
Purple	Calcifications	17881
Yellow	Tissue	1016599
Amyloid Load = (Amyloid) / (Amyloid + Calcifications + Tissue) = **0.055 or 5.5%**		

FIGURE 3
(A) Congo red stained slide of ligamentum flavum tissue resected at L4–5. The tissue was scanned under non-polarized light and digitized using a VENTANA DP 200 slide scanner (Roche Diagnostics, Rotkreuz, Switzerland) at 20× magnification and one focus layer. (B) Higher magnification of the Congo red stained ligamentum flavum specimen. (C) The results image generated for the quantification of amyloids and other tissue elements using the Trainable Weka Segmentation model. (D) Table displaying the total number of pixels corresponding to amyloids, calcifications, and tissue in the results image. Amyloid load was calculated as the total number of amyloid pixels divided by the sum of all pixels corresponding to amyloids, calcifications, and tissue.

with a partial cardiac response (8, 9). At the 18-month follow-up, the patient maintained partial hematological and cardiac responses. Her symptoms of back pain and exertional dyspnea had notably alleviated and she was fully functional (Figure 4).

Discussion

Of the cardiac amyloidosis subtypes, AL and wild-type ATTR (ATTRwt) are relatively common, with hereditary ATTR (ATTRm) being less common (10, 11). Differentiating ATTRwt and ATTRm from the AL subtype can be challenging due to their similar patterns of organ involvement; both can present as restrictive cardiomyopathy, carpel tunnel syndrome, autonomic dysfunction, and spinal stenosis. Furthermore, both monoclonal gammopathies and ATTRm occur more frequently in African Americans (12–14). When a patient has evidence of both monoclonal gammopathy and a TTR mutation, it is even more challenging to identify which is the driving cause of symptoms. In a cohort analysis of 197 patients with ATTR amyloidosis, 42% had monoclonal gammopathy with a κ predominance (15).

The diagnosis of amyloidosis is demonstrated by evidence of amyloid deposition either histologically or via highly specific diagnostic imaging studies. In addition, certain imaging studies

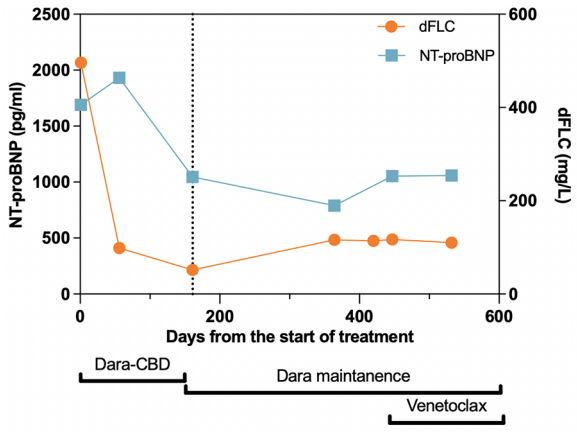

FIGURE 4
Treatment timeline with corresponding cardiac and hematological responses. The vertical dotted line represents the 6-month follow-up time point, at which the patient's hematological and cardiac responses were assessed. At this time, the patient achieved partial hematological and cardiac responses, which were maintained throughout the follow-up period. Dara, daratumumab; CBD, cyclophosphamide, bortezomib, and dexamethasone; dFLC, difference between involved and uninvolved serum free light chains; NT-proBNP, N-terminal of prohormone brain natriuretic peptide.

provide valuable insights into AL amyloidosis. For example, speckle-tracking echocardiography can detect apical sparing, also known as the "cherry on top" pattern, which is an informative feature of cardiac amyloidosis (16). To determine the subtype of amyloidosis, whether AL, ATTR, or another subtype, further studies are warranted in addition to history, physical exam, and other regular work-ups. For instance, SPEP, serum and urine IFE, and a free light chain assay are used to search for evidence of monoclonal proteins; TTR gene sequencing can identify a TTR gene mutation, and Tc-99m PYP and Tc-99m 3,3-diphosphono-1,2-propanodicarboxylic acid (DPD) scans can assist in diagnosing ATTR cardiac amyloidosis. In addition, cardiac magnetic resonance (CMR) imaging plays a crucial role in assisting the diagnoses of AL and ATTR amyloidosis by demonstrating differences in right ventricular size, myocardial strain, and patterns of late gadolinium enhancement (17–20). Moreover, recent studies have highlighted the promising role of CMR imaging in predicting prognosis and monitoring therapeutic responses in patients with AL cardiac amyloidosis (21, 22). Furthermore, LC/MS is the gold standard for amyloid subtyping (23).

Notably, the guidelines have clear recommendations regarding in which order the above diagnostic studies should be performed to diagnose AL, ATTR, or another cardiac amyloidosis appropriately (24). With clinical suspicion of cardiac amyloidosis, the first step is to screen for monoclonal gammopathy with SPEP, serum and urine IFE, and a free light chain assay; if evidence of monoclonal proteins is detected, the next step is a tissue biopsy with Congo red staining and possibly LC/MS to identify the type of amyloidosis; if monoclonal gammopathy is not found, then nuclear scintigraphy can be performed if available with a positive result being diagnostic for ATTR amyloidosis. If this is the case, ATTR genetic testing should also be performed to differentiate between ATTRwt and ATTRm; if the nuclear scintigraphy result is indeterminate, a cardiac biopsy should be considered and, if the result is negative, cardiac amyloidosis is less likely (25, 26). Recently, concerns have been expressed regarding the inappropriate use of Tc-99m PYP scans without completing a monoclonal protein evaluation as they could result in frequent false positive results in cases of AL amyloidosis, which subsequently hinders the real-world value of diagnosing ATTR using a Tc-99m PYP scan (27, 28). Therefore, following the diagnostic steps recommended by the guidelines is of great importance.

In our patient, we applied the same diagnostic algorithm as above but also considered her unique situation to avoid misdiagnosis. With the initial clinical symptoms and findings indicating cardiac and soft tissue amyloidosis, monoclonal protein studies were performed and a subsequent tissue biopsy with LC/MS showed systemic κ-type AL amyloidosis. We could have prematurely concluded that the patient had cardiac amyloidosis driven by amyloidogenic light chains. Nonetheless, taking her race and cardiac family history into account, the patient could have had distinct amyloid subtypes involving separate anatomic sites (ATTR with transthyretin amyloids in the heart), or even a combination of AL and ATTR amyloids in one site (the heart). Such diagnoses are rare yet have been reported in the literature (4, 29). To avoid a misdiagnosis leading to inappropriate treatment, Tc-99m PYP SPECT was performed, and with a grade 0 on planar imaging and a heart-to-contralateral lung ratio of 1.1, the cardiac amyloidosis was considered to be caused by AL instead of ATTR. Therefore, our case is instructive because it serves as a valuable supplement to the existing diagnostic algorithms in specific situations. It highlights the importance of incorporating an individualized approach, even when following established diagnostic algorithms, to achieve an accurate diagnosis of the type of amyloidosis and prevent potential mistreatment.

Notably, our patient also has a heterozygous V122I TTR variant, predisposing her to ATTRm amyloidosis. While our patient's current amyloidosis is light chain-driven, it is important to understand the possibility that two amyloid types may be present in one individual (4). In our patient, the V122I TTR variant may predispose her to develop hereditary ATTR cardiac amyloidosis in the future; however, there are currently no established guidelines for surveillance in such cases. Sidiqi et al. analyzed 1,094 patients with LC/MS-confirmed amyloids and identified nine (0.82%) patients who had two amyloid types. All nine patients had ATTR amyloids and six had AL amyloids (30). In such a case, a repeat Tc-99m-PYP scan and a repeat biopsy with amyloid typing should be considered to further evaluate the possible development of ATTR amyloidosis.

Studies have shown that amyloid deposits are commonly found in the LF of patients with spinal stenosis (31), with ATTR subtypes accounting for nearly 80% (32). In rare cases, patients can have both ATTR and AL amyloid deposits in the LF (33). In our case, the LF tissue had an amyloid load of 5.5%, a finding consistent with prior reports (34). Patients with ATTRwt amyloids in their LF have been shown to have less severe disc degeneration compared to patients with lumbar stenosis without amyloids. This suggests that amyloids may play a separate role in LF thickening compared to the degeneration of intervertebral discs (35). While the exact mechanisms by which AL and ATTR amyloids contribute to the thickening of the LF are relatively unknown, a positive association between amyloid load and the thickness of the LF has been established (34). Therefore, in patients with systemic amyloidosis who present with lower back pain, it is reasonable to consider potential amyloid deposits in the LF that cause LF thickening and spinal stenosis, and a histopathological work-up of the LF might assist a further diagnosis.

Conclusion

In patients with suspected cardiac amyloidosis, screening for monoclonal gammopathy is required prior to further consideration of Tc-99m-PYP scans. However, in patients with cardiac amyloidosis who present with both monoclonal gammopathies and a TTR variant, it is imperative to ascertain the tissue type of the amyloids and to employ diagnostic modalities such as Tc-99m-PYP scans to deduce the correct

diagnosis. In elderly patients who may have both monoclonal gammopathies and wild-type ATTR amyloidosis, the same guidance applies. Meanwhile, ATTR and AL amyloids can both cause spinal stenosis with minimal degenerative changes shown in spinal MRI. LF tissue must be stained for amyloids and, if present, typing must be performed.

Data availability statement

The original contributions presented in the study are included in the article/Supplementary Material, further inquiries can be directed to the corresponding author.

Ethics statement

The studies involving humans were approved by The Health Sciences Institutional Review Board, Tufts Medical Center. The studies were conducted in accordance with the local legislation and institutional requirements. The participants provided their written informed consent to participate in this study. Written informed consent was obtained from the individual(s) for the publication of any potentially identifiable images or data included in this article.

Author contributions

XW: Conceptualization, Data curation, Formal Analysis, Investigation, Methodology, Project administration, Visualization, Writing – original draft, Writing – review & editing. DT: Conceptualization, Data curation, Methodology, Project administration, Writing – review & editing. PZ: Data curation, Methodology, Project administration, Resources, Visualization, Writing – review & editing. SS: Data curation, Formal Analysis, Methodology, Project administration, Visualization, Writing – review & editing. XM: Data curation, Formal Analysis, Project administration, Resources, Validation, Writing – review & editing. PB: Conceptualization, Data curation, Resources, Supervision, Writing – review & editing. TF: Data curation, Methodology, Resources, Writing – review & editing. MP: Conceptualization, Data curation, Formal Analysis, Project administration, Resources, Writing – review & editing. KA: Formal Analysis, Methodology, Resources, Visualization, Writing – review & editing. JP: Visualization, Writing – original draft, Writing – review & editing. RR: Methodology, Supervision, Validation, Writing – review & editing. DL: Conceptualization, Methodology, Visualization, Writing – review & editing. RC: Conceptualization, Investigation, Resources, Supervision, Visualization, Writing – original draft, Writing – review & editing.

Funding

The author(s) declare financial support was received for the research, authorship, and/or publication of this article. This work was supported by the NIH/National Institute of Aging grant [R21-AG070502 (RC) and R01-CA279808 (RC)] and the Janssen QuickFire Challenge Idea grant. For their continued support of the Tufts Medicine Myeloma and Amyloid Research Fund, we thank all of the donors including the Sidewater Family Fund, the Amyloidosis Foundation, David and Barbara Levine (in memoriam), and the Demarest Lloyd Jr Foundation.

Acknowledgments

We would like to thank Jason Theis for providing the proteomic profile of the ligamentum flavum specimen.

Conflict of interest

The authors declare that the research was conducted in the absence of any commercial or financial relationships that could be construed as a potential conflict of interest.

Publisher's note

All claims expressed in this article are solely those of the authors and do not necessarily represent those of their affiliated organizations, or those of the publisher, the editors and the reviewers. Any product that may be evaluated in this article, or claim that may be made by its manufacturer, is not guaranteed or endorsed by the publisher.

Supplementary material

The Supplementary Material for this article can be found online at: https://www.frontiersin.org/articles/10.3389/fcvm.2024.1479676/full#supplementary-material

References

1. Antonopoulos AS, Panagiotopoulos I, KouroutzoglouA, Koutsis G, Toskas P, Lazaros G, et al. Prevalence and clinical outcomes of transthyretin amyloidosis: a systematic review and meta-analysis. *Eur J Heart Fail.* (2022) 24(9):1677–96. doi: 10.1002/ejhf.2589

2. Muchtar E, Gertz MA, Kumar SK, Lacy MQ, Dingli D, Buadi FK, et al. Improved outcomes for newly diagnosed AL amyloidosis between 2000 and 2014: cracking the glass ceiling of early death. *Blood.* (2017) 129(15):2111–9. doi: 10.1182/blood-2016-11-751628

3. Oubari S, Naser E, Papathanasiou M, Luedike P, Hagenacker T, Thimm A, et al. Impact of time to diagnosis on Mayo stages, treatment outcome, and survival in patients with AL amyloidosis and cardiac involvement. *Eur J Haematol.* (2021) 107 (4):449–57. doi: 10.1111/ejh.13681

4. Comenzo RL, Zhou P, Fleisher M, Clark B, Teruya-Feldstein J. Seeking confidence in the diagnosis of systemic AL (Ig light-chain) amyloidosis: patients can have both monoclonal gammopathies and hereditary amyloid proteins. *Blood*. (2006) 107 (9):3489–91. doi: 10.1182/blood-2005-10-4148

5. Gertz MA. Immunoglobulin light chain amyloidosis: 2020 update on diagnosis, prognosis, and treatment. *Am J Hematol*. (2020) 95(7):848–60. doi: 10.1002/ajh.25819

6. Wang AY, Sharma V, Saini H, Tingen JN, Flores A, Liu D, et al. Machine learning quantification of amyloid deposits in histological images of ligamentum flavum. *J Pathol Inform*. (2022) 13:100013. doi: 10.1016/j.jpi.2022.100013

7. Dispenzieri A, Gertz MA, Kyle RA, Lacy MQ, Burritt MF, Therneau TM, et al. Serum cardiac troponins and N-terminal pro-brain natriuretic peptide: a staging system for primary systemic amyloidosis. *J Clin Oncol*. (2004) 22(18):3751–7. doi: 10.1200/JCO.2004.03.029

8. Palladini G, Dispenzieri A, Gertz MA, Kumar S, Wechalekar A, Hawkins PN, et al. New criteria for response to treatment in immunoglobulin light chain amyloidosis based on free light chain measurement and cardiac biomarkers: impact on survival outcomes. *J Clin Oncol*. (2012) 30(36):4541–9. doi: 10.1200/JCO.2011.37.7614

9. Muchtar E, Dispenzieri A, Wisniowski B, Palladini G, Milani P, Merlini G, et al. Graded cardiac response criteria for patients with systemic light chain amyloidosis. *J Clin Oncol*. (2023) 41(7):1393–403. doi: 10.1200/JCO.22.00643

10. Kaku M, Berk JL. Neuropathy associated with systemic amyloidosis. *Semin Neurol*. (2019) 39(5):578–88. doi: 10.1055/s-0039-1688994

11. Westermark GT, Fändrich M, Westermark P. AA Amyloidosis: pathogenesis and targeted therapy. *Annu Rev Pathol*. (2015) 10:321–44. doi: 10.1146/annurev-pathol-020712-163913

12. Atkin C, Reddy-Kolanu V, Drayson MT, Sapey E, Richter AG. The prevalence and significance of monoclonal gammopathy of undetermined significance in acute medical admissions. *Br J Haematol*. (2020) 189(6):1127–35. doi: 10.1111/bjh.16487

13. Connors LH, Prokaeva T, Lim A, Théberge R, Falk RH, Doros G, et al. Cardiac amyloidosis in African Americans: comparison of clinical and laboratory features of transthyretin V122I amyloidosis and immunoglobulin light chain amyloidosis. *Am Heart J*. (2009) 158(4):607–14. doi: 10.1016/j.ahj.2009.08.006

14. Jacobson DR, Alexander AA, Tagoe C, Garvey WT, Williams SM, Tishkoff S, et al. The prevalence and distribution of the amyloidogenic transthyretin (TTR) V122I allele in Africa. *Mol Genet Genomic Med*. (2016) 4(5):548–56. doi: 10.1002/mgg3.231

15. Phull P, Sanchorawala V, Connors LH, Doros G, Ruberg FL, Berk JL, et al. Monoclonal gammopathy of undetermined significance in systemic transthyretin amyloidosis (ATTR). *Amyloid*. (2018) 25(1):62–7. doi: 10.1080/13506129.2018.1436048

16. Wali E, Gruca M, Singulane C, Cotella J, Guile B, Johnson R, et al. How often does apical sparing of longitudinal strain indicate the presence of cardiac amyloidosis? *Am J Cardiol*. (2023) 202:12–6. doi: 10.1016/j.amjcard.2023.06.022

17. Dungu JN, Valencia O, Pinney JH, Gibbs SD, Rowczenio D, Gilbertson JA, et al. CMR-based differentiation of AL and ATTR cardiac amyloidosis. *JACC Cardiovasc Imaging*. (2014) 7(2):133–42. doi: 10.1016/j.jcmg.2013.08.015

18. Kristen AV, aus dem Siepen F, Scherer K, Kammerer R, Andre F, Buss SJ, et al. Comparison of different types of cardiac amyloidosis by cardiac magnetic resonance imaging. *Amyloid*. (2015) 22(2):132–41. doi: 10.3109/13506129.2015.1020153

19. Ridouani F, Damy T, Tacher V, Derbel H, Legou F, Sifaoui I, et al. Myocardial native T2 measurement to differentiate light-chain and transthyretin cardiac amyloidosis and assess prognosis. *J Cardiovasc Magn Reson*. (2018) 20(1):58. doi: 10.1186/s12968-018-0478-3

20. Slivnick JA, Tong MS, Nagaraja HN, Elamin MB, Wallner A, O'Brien A, et al. Novel cardiovascular magnetic resonance model to distinguish immunoglobulin light chain from transthyretin cardiac amyloidosis. *Cardiovasc Imaging*. (2021) 14 (1):302–4. doi: 10.1016/j.jcmg.2020.07.030

21. Boretto P, Patel NH, Patel K, Rana M, Saglietto A, Soni M, et al. Prognosis prediction in cardiac amyloidosis by cardiac magnetic resonance imaging: a systematic review with meta-analysis. *Eur Heart J Open*. (2023) 3(5):oead092. doi: 10.1093/ehjopen/oead092

22. Martinez-Naharro A, Patel R, Kotecha T, Karia N, Ioannou A, Petrie A, et al. Cardiovascular magnetic resonance in light-chain amyloidosis to guide treatment. *Eur Heart J*. (2022) 43(45):4722–35. doi: 10.1093/eurheartj/ehac363

23. Lavatelli F, Vrana JA. Proteomic typing of amyloid deposits in systemic amyloidoses. *Amyloid*. (2011) 18(4):177–82. doi: 10.3109/13506129.2011.630762

24. Hanna M, Ruberg FL, Maurer MS, Dispenzieri A, Dorbala S, Falk RH, et al. Cardiac scintigraphy with technetium-99m-labeled bone-seeking tracers for suspected amyloidosis: JACC review topic of the week. *J Am Coll Cardiol*. (2020) 75 (22):2851–62. doi: 10.1016/j.jacc.2020.04.022

25. Krepp JM, Katz R, Volke R, Ryan A, Panjrath G. Amyloid heart disease module 1: diagnosis. *Br J Cardiol*. (2021). doi: 10.5837/bjc.2021.015

26. Benson M, Dasgupta N, Rao R. Diagnosis and screening of patients with hereditary transthyretin amyloidosis (hATTR): current strategies and guidelines. *Ther Clin Risk Manag*. (2020) 16:749–58. doi: 10.2147/TCRM.S185677

27. Poterucha TJ, Elias P, Bokhari S, Einstein AJ, DeLuca A, Kinkhabwala M, et al. Diagnosing transthyretin cardiac amyloidosis by technetium Tc 99 m pyrophosphate: a test in evolution. *Cardiovasc Imaging*. (2021) 14(6):1221–31. doi: 10.1016/j.jcmg.2020.08.027

28. Yan CL, Thakkar Rivera N, Hoffman J. Inappropriate use of technetium-99m pyrophosphate scanning for the evaluation of transthyretin amyloidosis. *Amyloid*. (2024) 31(1):76–8. doi: 10.1080/13506129.2023.2267162

29. Jhaveri T, Sarosiek S, Ruberg FL, Siddiqi O, Berk JL, Sanchorawala V. Once AL amyloidosis: not always AL amyloidosis. *Amyloid*. (2018) 25(2):139–40. doi: 10.1080/13506129.2018.1449104

30. Sidiqi MH, McPhail ED, Theis JD, Dasari S, Vrana JA, Drosou ME, et al. Two types of amyloidosis presenting in a single patient: a case series. *Blood Cancer J*. (2019) 9(3):30. doi: 10.1038/s41408-019-0193-9

31. Wang AY, Patel J, Kanter M, Olmos M, Maurer MS, McPhail ED, et al. The emerging significance of amyloid deposits in the ligamentum flavum of spinal stenosis patients: a review. *World Neurosurg*. (2023) 177:88–97. doi: 10.1016/j.wneu.2023.06.037

32. Marchi F, Kessler C, Distefano D, Terzi di Bergamo L, Fumagalli L, Averaimo M, et al. Prevalence of amyloid in ligamentum flavum of patients with lumbar spinal stenosis. *Amyloid*. (2023) 30:1–8. doi: 10.1080/13506129.2023.2230516

33. Godara A, Wang AY, Arkun K, Fogaren T, Qamar AS, McPhail ED, et al. Unraveling a rare cause of spinal stenosis: coexistent AL and ATTR amyloidosis involving the ligamentum flavum. *Surg Neurol Int*. (2022) 13:12. doi: 10.25259/SNI_1235_2021

34. Wang AY, Saini H, Tingen JN, Sharma V, Flores A, Liu D, et al. The relationship between wild-type transthyretin amyloid load and ligamentum flavum thickness in lumbar stenosis patients. *World Neurosurg*. (2022) 164:e113–8. doi: 10.1016/j.wneu.2022.04.008

35. Wang AY, Kanter M, Olmos M, McPhail ED, Safain MG, Kryzanski J, et al. Lumbar stenosis due to wild-type transthyretin amyloid–induced thickening of the ligamentum flavum: a separate etiology from degeneration of intervertebral discs? *J Neurosurg Spine*. (2022) 1(aop):1–7. doi: 10.3171/2022.5.SPINE22362

frontiers | Frontiers in Oncology

TYPE Case Report
PUBLISHED 21 January 2025
DOI 10.3389/fonc.2024.1530403

Check for updates

OPEN ACCESS

EDITED BY
Reto Asmis,
Wake Forest University, United States

REVIEWED BY
Tomo Svaguša,
Clinical Hospital Dubrava, Croatia
Cherry Bansal,
Tantia University, India

*CORRESPONDENCE
Xuemin Yuan
lyxhyxm@163.com

RECEIVED 18 November 2024
ACCEPTED 30 December 2024
PUBLISHED 21 January 2025

CITATION
Ge Y, Lv X, Zhang R, Hao D, Si G, Li Y, Yuan X and Li X (2025) Case report: Primary cardiac undifferentiated sarcoma complicated by esophagus stenosis. *Front. Oncol.* 14:1530403. doi: 10.3389/fonc.2024.1530403

COPYRIGHT
© 2025 Ge, Lv, Zhang, Hao, Si, Li, Yuan and Li. This is an open-access article distributed under the terms of the Creative Commons Attribution License (CC BY). The use, distribution or reproduction in other forums is permitted, provided the original author(s) and the copyright owner(s) are credited and that the original publication in this journal is cited, in accordance with accepted academic practice. No use, distribution or reproduction is permitted which does not comply with these terms.

Case report: Primary cardiac undifferentiated sarcoma complicated by esophagus stenosis

Yuxin Ge[1], Xiaopan Lv[1], Rui Zhang[1], Dongxiao Hao[1], Guifei Si[1], Yuquan Li[1], Xuemin Yuan[2*] and Xiuping Li[2]

[1]School of Clinical Medicine, Shandong Second Medical University, Weifang, Shandong, China, [2]Department of Gastroenterology, Linyi People's Hospital, Linyi, Shandong, China

In this study, we present the case of a 38-year-old woman who was diagnosed with primary cardiac undifferentiated sarcoma after hospital admission. Following postoperative treatment that included radiotherapy and immunotherapy, the patient developed esophagus stenosis.

KEYWORDS

cardiac undifferentiated sarcoma, endoscopy, esophagus stenosis, immunohistochemistry, pathology

Introduction

Primary cardiac tumors are rare with an incidence between 0.0017% and 0.28% (1). Twenty-five percent of cardiac tumors are malignant, and nearly 20% of these are sarcomas. Among these, Cardiac angiosarcomas constitute 37% of cardiac sarcomas, while undifferentiated sarcomas account for less than 24%, leiomyosarcomas constitute 8% to 9% of cardiac sarcomas, and rhabdomyosarcomas account for 4% to 7%. In addition, Osteosarcoma, fibrosarcoma, liposarcoma, and synovial sarcoma represent a small proportion of cardiac sarcomas (2, 3). Cardiac sarcomas are often asymptomatic until advanced, and even then produce non-specific symptoms such as palpitations, shortness of breath, dyspnea, chest pain, syncope, anemia, and weight loss (4–6). As a result, they can easily be misdiagnosed as other conditions, such as pneumonia or pericarditis (4). The dismal prognosis results from extensive local invasion or distant metastases at presentation. The initial diagnosis of cardiac sarcoma primarily relies on imaging techniques such as echocardiography, MRI and PET-CT, although a definitive histopathological diagnosis is essential (7, 8). In this report, we described a case that underwent initial cardiac tumor resection, and was confirmed to be undifferentiated sarcoma based on pathological findings. Following postoperative treatment that included radiotherapy and immunotherapy, the patient developed esophagus stenosis. To the best of our knowledge, this is the first case report detailing a primary cardiac undifferentiated sarcoma complicated by esophagus stenosis.

Case reports

A 38-year-old female patient was admitted to the hospital on December 9, 2023 with complaints of "palpitations for 1 week." She did not report any significant chest tightness, wheezing, or other noteworthy symptoms. She was healthy in the past and had no family history of hereditary disease. An outpatient echocardiogram revealed a large left atrium with a medium to strong echo mass (69 mm x 41 mm) attached to the roof of the left atrium. The mass had an irregular shape with uneven internal echogenicity and was partially protruding into the left ventricle near the mitral valve (Figure 1A). Cardiac mass resection was performed on December 12, 2023. The right atrium and interatrial septum were incised, revealing a large tumor (7 cm x 5 cm x 5 cm), and the tumor is somewhat resilient in texture (such as palpating the nose tip), that occupied the left atrium and extended into the openings of the left and right pulmonary veins. The tumor was completely excised along its attachment to the surrounding tissues. The postoperative immunohistochemical analysis revealed the following results: CK (focal +), SMA (focal +), Desmin (focal +), S-100 (–), SOX 10 (–), CD34 (vascular +), Ki67-MIB1 (50%), Vimentin (+), MyoD1 (–), Myogenin (–), CD68 (+). (Figures 2A–G), confirmed that the tumor was consistent with cardiac sarcoma, undifferentiated sarcoma. The patient's recovery following surgery was uneventful. However, on January 25, 2024, cardiac MRI revealed abnormal signals in the posterior wall of the left atrium, raising concerns of tumor recurrence (Figure 1B). Radiotherapy was started in February, 2024, (18 times, Radiation dose: 3x18Gy) and was completed on March 1, 2024. In accordance with the guidelines from the Chinese Society of Clinical Oncology for the Diagnosis and Treatment of Soft Tissue Sarcoma, the patient began oral anlotinib (10 mg QD) during radiotherapy. Regular immunotherapy with cindarizumab (administered once every 21 days) commenced on February 28, 2024. In April 2024, the patient was readmitted due to dysphagia. Gastroscopy indicated that the distance between the esophagus and the incisor was approximately 28 cm, revealing an esophagus ulcer covered with white exudate, narrowing of the lumen, and obstruction preventing endoscopic passage (Figure 3A). Mediastinal CT showed that after left atrial surgery, the posterior wall of the left atrium and the posterior esophagus were thickened (Figures 1C, D). PET-CT revealed thickening of the left atrial wall and the esophagus wall, with increased FDG metabolism (Figures 4A, B). On August 8, 2024, follow-up gastroscopy demonstrated an esophagus ulcer located about 30 cm from the incisor, consistent with an inability to pass the endoscope (Figure 3B). The comprehensive analysis considered the patient's recurrence of cardiac undifferentiated sarcoma and invasion of the esophagus, resulting in esophagus stenosis. After consulting with the cardiovascular surgeon, the patient was informed about the necessity and risks of undergoing another surgical procedure. However, the patient and his family ultimately refused further surgical treatment. For treatment, a multidisciplinary team, including oncologists and gastroenterologists, recommended esophagus stent implantation, which was successfully performed on August 28, 2024 (Figures 3C, D). The procedure was uneventful, and the patient's swallowing capability was deemed acceptable. As of the time of writing, the patient remains alive and independent.

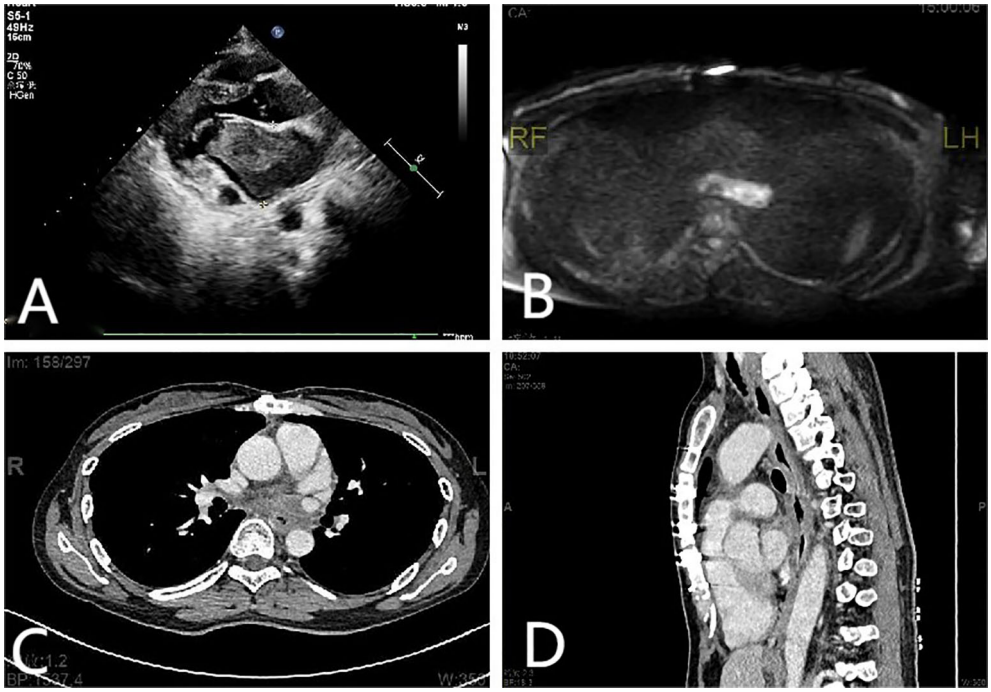

FIGURE 1
(A) Echocardiographic findings: A mass measuring approximately 69 mm × 41 mm was identified in the anterior wall of the left atrium. **(B)** Cardiac MRI scan findings: abnormal signals in the posterior wall of the left atrium. **(C, D)** Mediastinal CT scan findings: the posterior wall of the left atrium and the posterior esophagus were thickened. The gap between the esophagus and the left atrium disappeared, and tumor cell infiltration of the esophagus was considered.

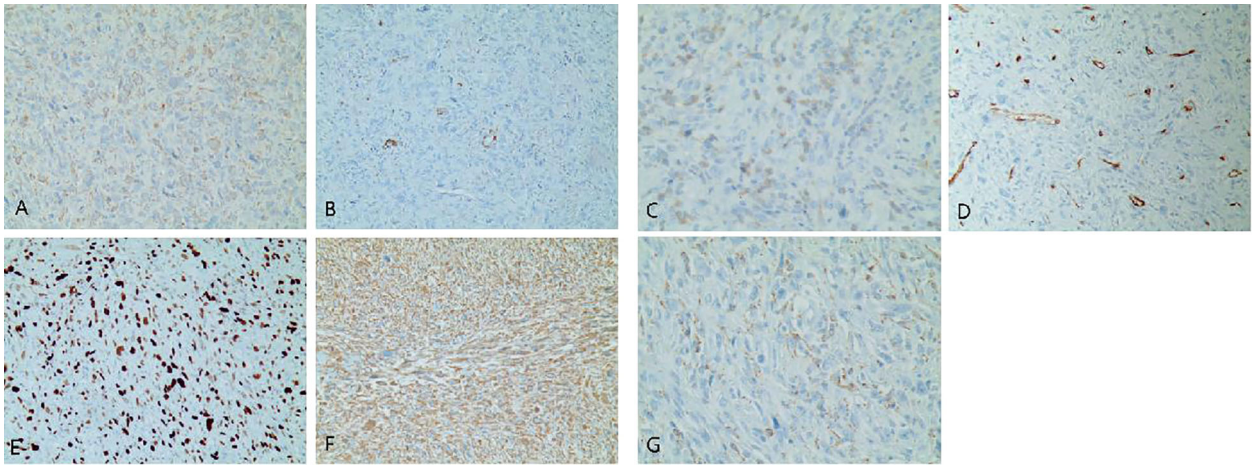

FIGURE 2
(A–G) Immunohistochemistry of the left atrium mass. **(A)** CK (focal +). **(B)** SMA (focal +). **(C)** Desmin (focal +). **(D)** CD34 (vascular +). **(E)** Ki67-MIB1 (50%). **(F)** Vimentin (+). **(G)** CD68 (+).

Discussion

The incidence of primary cardiac tumors ranges from 0.0017% to 0.28% (1). These sarcomas typically have a poor prognosis, as they are often widely disseminated and prone to hematogenous metastasis to the lungs or liver by the time of diagnosis (9, 10). Undifferentiated sarcoma, the most aggressive type of cardiac malignant tumor, accounts for approximately 12% of all primary cardiac sarcomas and is associated with an extremely poor prognosis (11). Due to their local aggressiveness, complete resection of undifferentiated sarcomas is often not feasible, with only about 12% of patients achieving R0 resection (complete response) (12). Despite aggressive treatment, the median overall survival for patients with cardiac sarcomas is low, typically ranging from 6 to 12 months (13). Notably, patients who receive multimodal therapy may experience better survival outcomes

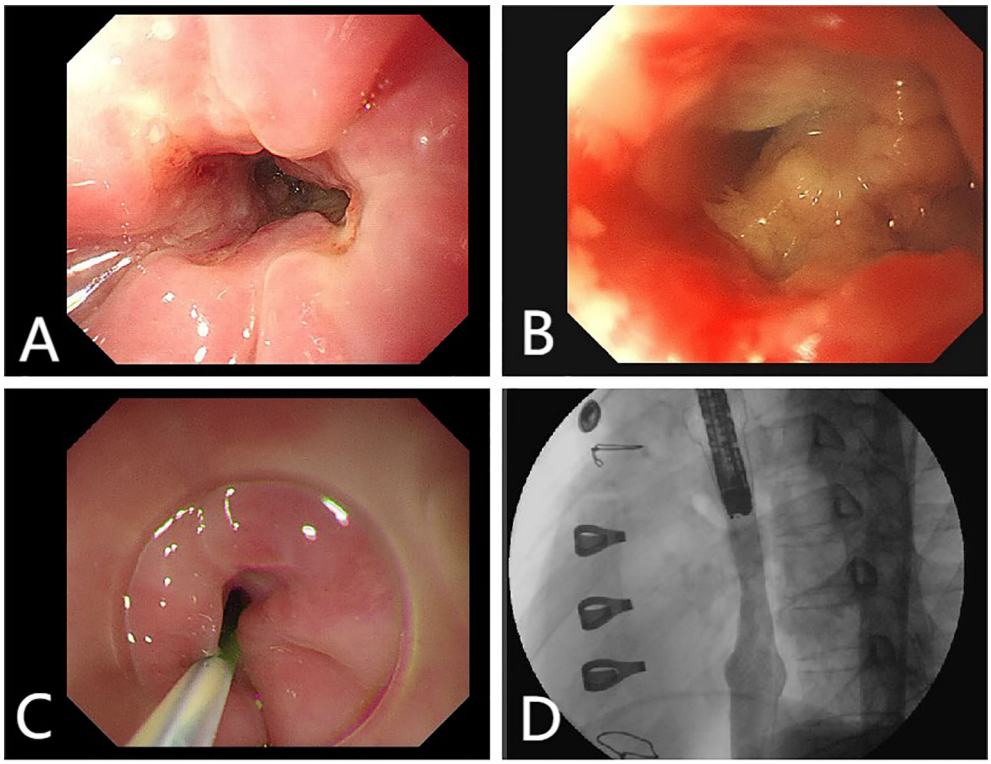

FIGURE 3
(A) Endoscopy reveals an esophagus ulcer covered with white exudate, narrowing of the lumen. **(B)** Endoscopy reveals an esophagus ulcer. **(C, D)** Esophagus stent implantation.

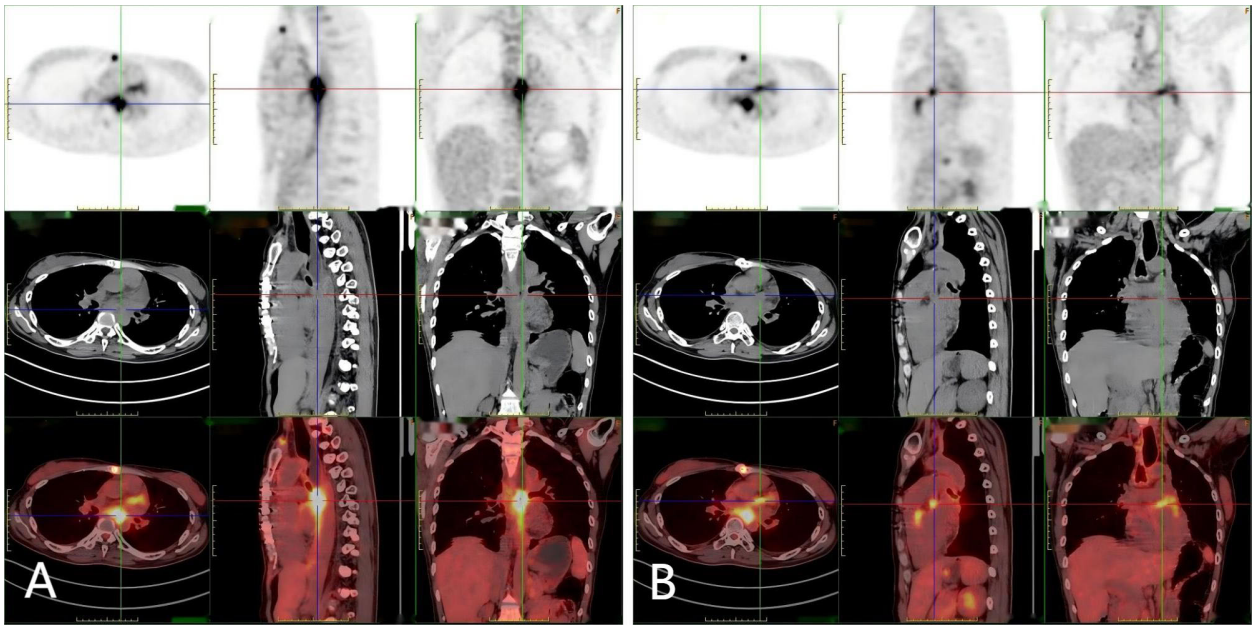

FIGURE 4
(A, B) A ^{18}F-FDG-PET-CT scan: Hypermetabolic lesion in the left atrium wall and esophagus.

compared to those who undergo surgery alone (14). The treatment of undifferentiated sarcoma necessitates a multidisciplinary approach, often derived from case reports and series, due to a lack of robust data, randomized clinical trials, or standardized treatment protocols (15, 16). In this case, the patient was pathologically confirmed as undifferentiated sarcoma after cardiac mass resection, and active intervention was immediately taken, including radiotherapy, immunization and targeted therapy. Currently, the patient is experiencing esophagus stenosis, ^{18}FDG-PET-CT showed a hypermetabolic lesion in the left atrium wall and esophagus, so we considered the possibility of recurrence and invasion of cardiac malignant tumors (17). However, pathological results did not confirm any malignancy, which may be attributed to the effects of prior radiotherapy. Research indicates that the incidence of esophagus stenosis is 1%-2% when the radiation dose is less than 60 Gy, increasing to 5%-6% when the radiation dose exceeds 60 Gy (18). Studies have found that there is a significant correlation between radiotherapy dose and the occurrence of esophagus stenosis. As the radiation dose increases, the degree of fibrosis in the esophageal muscle layer and submucosa progressively worsens, thereby elevating the risk of esophageal stenosis (19, 20). Therefore, the specific causes need to be further examined. Finally, the patient underwent esophagus stent implantation. The procedure was successful, and the patient reported improved swallowing function postoperatively. From the review of literature, we conclude that although surgical intervention was necessary for resection of the tumor, it is important to identify malignant tumors early, in order to enable patients to undergo radiotherapy or chemotherapy as soon as possible. In addition, We believe that cardiac MRI examinations should be enhanced prior to surgery to provide better guidance during the procedure. In this case, the cardiac MRI was not adequately improved before the operation, which reflects our oversight. In the future, we should adopt a more rigorous approach to diagnosis and treatment, ensuring that preoperative examination and evaluation are thoroughly optimized. The treatment of undifferentiated cardiac sarcoma requires a multidisciplinary approach. Advances in anti-tumor immunotherapy, targeted therapy, and chemotherapy offer new options for managing cardiac sarcomas. Moving forward, more basic and clinical research is needed to develop additional treatment strategies for this disease, ultimately aiming to extend patient survival.

Data availability statement

The original contributions presented in the study are included in the article/supplementary material. Further inquiries can be directed to the corresponding author.

Ethics statement

Written informed consent was obtained from the individual(s) for the publication of any potentially identifiable images or data included in this article.

Author contributions

YG: Conceptualization, Writing – original draft, Writing – review & editing. XLv: Data curation, Writing – original draft.

RZ: Formal analysis, Writing – original draft. DH: Visualization, Writing – original draft. GS: Supervision, Validation, Writing – original draft. YL: Software, Writing – original draft. XY: Supervision, Writing – review & editing. XLi: Supervision, Writing – review & editing.

Funding

The author(s) declare financial support was received for the research, authorship, and/or publication of this article. This work was supported by grants from the Linyi People's Hospital Innovation Team Development Project (LYSRMYY-KCTD-008).

Acknowledgments

We express our gratitude to the patients and their families for providing informed consent to use their personal data.

Conflict of interest

The authors declare that the research was conducted in the absence of any commercial or financial relationships that could be construed as a potential conflict of interest.

Generative AI statement

The author(s) declare that no Generative AI was used in the creation of this manuscript.

Publisher's note

All claims expressed in this article are solely those of the authors and do not necessarily represent those of their affiliated organizations, or those of the publisher, the editors and the reviewers. Any product that may be evaluated in this article, or claim that may be made by its manufacturer, is not guaranteed or endorsed by the publisher.

References

1. Morphet JA. A 30-year analysis of cardiac neoplasms at autopsy. *Can J Cardiol*. (2006) 22:80. doi: 10.1016/S0828-282X(06)70247-1

2. Hoffmeier A, Sindermann JR, Scheld HH, Martens S. Cardiac tumors–diagnosis and surgical treatment. *Dtsch Arztebl Int*. (2014) 111:205–11. doi: 10.3238/arztebl.2014.0205

3. Tyebally S, Chen D, Bhattacharyya S, Mughrabi A, Hussain Z, Manisty C, et al. Cardiac tumors: JACC cardioOncology state-of-the-art review. *JACC CardioOncol*. (2020) 2:293–311. doi: 10.1016/j.jaccao.2020.05.009

4. Dulal Karki S, Westhoff M, Maschek H, Augustyniak J, Gupta V, Welter S. A rare diagnostic challenge in a female patient with a rapid recurrent pleural effusion: Autopsy revealed cardiac angiosarcoma with bilateral pleural and pulmonary metastases. *A Case Rep Int J Surg Case Rep*. (2021) 78:278–83. doi: 10.1016/j.ijscr.2020.12.034

5. Alizadehasl A, Hakimian H, Dokhani N, Pouraliakbar H, Firoozbakhsh P. Early presentation of undifferentiated pleomorphic cardiac sarcoma. *Radiol Case Rep*. (2024) 19:4308–11. doi: 10.1016/j.radcr.2024.06.088

6. Guerra-Raygada M, Saavedra-Sanchez AJ, Hidalgo-Avendaño D, Bermudez-Pelaez MF, Guevara-Lazo D, Nombera-Aznaran N. From dyspnea to diagnosis, unmasking undifferentiated cardiac sarcoma: a case report. *Egypt Heart J*. (2024) 76:86. doi: 10.1186/s43044-024-00520-3

7. Maraj S, Pressman GS, Figueredo VM. Primary cardiac tumors. *Int J Cardiol*. (2009) 133:152–6. doi: 10.1016/j.ijcard.2008.11.103

8. Oh SJ, Yeom SY, Kim KH. Clinical implication of surgical resection for the rare cardiac tumors involving heart and great vessels. *J Korean Med Sci*. (2013) 28:717–24. doi: 10.3346/jkms.2013.28.5.717

9. Ramlawi B, Leja MJ, Abu Saleh WK, Al Jabbari O, Benjamin R, Ravi V, et al. Surgical treatment of primary cardiac sarcomas: review of a single-institution experience. *Ann Thorac Surg*. (2016) 101:698–702. doi: 10.1016/j.athoracsur.2015.07.087

10. Centofanti P, Di Rosa E, Deorsola L, Dato GM, Patanè F, La Torre M, et al. Primary cardiac tumors: early and late results of surgical treatment in 91 patients. *Ann Thorac Surg*. (1999) 68:1236–41. doi: 10.1016/S0003-4975(99)00700-6

11. Randhawa JS, Budd GT, Randhawa M, Ahluwalia M, Jia X, Daw H, et al. Primary cardiac sarcoma: 25-year cleveland clinic experience. *Am J Clin Oncol*. (2016) 39:593–9. doi: 10.1097/COC.0000000000000106

12. Siontis BL, Zhao L, Leja M, McHugh JB, Shango MM, Baker LH, et al. Primary cardiac sarcoma: A rare, aggressive Malignancy with a high propensity for brain metastases. *Sarcoma*. (2019) 2019:1960593. doi: 10.1155/2019/1960593

13. Truong PT, Jones SO, Martens B, Alexander C, Paquette M, Joe H, et al. Treatment and outcomes in adult patients with primary cardiac sarcoma: the British Columbia Cancer Agency experience. *Ann Surg Oncol*. (2009) 16:3358–65. doi: 10.1245/s10434-009-0734-8

14. Nakamura-Horigome M, Koyama J, Eizawa T, Kasai H, Kumazaki S, Tsutsui H, et al. Successful treatment of primary cardiac angiosarcoma with docetaxel and radiotherapy. *Angiology*. (2008) 59:368–71. doi: 10.1177/0003319707308212

15. Abbas HA, Amini B, Wang WL, Ravi V. Maneuvering the management of a rare case of primary undifferentiated cardiac sarcoma. *Am J Case Rep*. (2020) 21:e918878. doi: 10.12659/AJCR.918878

16. Sun YP, Wang X, Gao YS, Zhao S, Bai Y. Primary cardiac sarcoma complicated with cerebral infarction and brain metastasis: A case report and literature review. *Cancer biomark*. (2017) 21:247–50. doi: 10.3233/CBM-170448

17. Utsunomiya Y, Miyake KK, Fukushima S, Kinoshita H, Ikeda Y, Matsumoto M, et al. (18)F-FDG PET/CT in left atrial undifferentiated pleomorphic sarcoma with osteosarcomatous differentiation. *J Cardiol Cases*. (2024) 29:30–4. doi: 10.1016/j.jccase.2023.09.005

18. Morichau-Beauchant M, Touchard G, Battandier D, Maire P, Fontanel JP, Daban A, et al. Chronic radiation-induced esophagitis after treatment of oropharyngolaryngeal cancer: a little-known anatomo-clinical entity. *Gastroenterol Clin Biol*. (1983) 7:843–50.

19. Roeder F, Nicolay NH, Nguyen T, Saleh-Ebrahimi L, Askoxylakis V, Bostel T, et al. Intensity modulated radiotherapy (IMRT) with concurrent chemotherapy as definitive treatment of locally advanced esophageal cancer. *Radiat Oncol*. (2014) 9:191. doi: 10.1186/1748-717X-9-191

20. Afifi A, Powerski M, Jechorek D, Brunner TB, Weigt J, Venerito M. Radiation-induced damage in the upper gastrointestinal tract: clinical presentation, diagnostic tests and treatment options. *Best Pract Res Clin Gastroenterol*. (2020) 48-49:101711. doi: 10.1016/j.bpg.2020.101711

frontiers | Frontiers in Cardiovascular Medicine

TYPE Case Report
PUBLISHED 29 January 2025
DOI 10.3389/fcvm.2025.1480310

Check for updates

OPEN ACCESS

EDITED BY
Reto Asmis,
Wake Forest University, United States

REVIEWED BY
Omer Iqbal,
Loyola University Chicago, United States
Kirtipal Bhatia,
Mount Sinai Morningside, United States

*CORRESPONDENCE
Miguel Borregón
✉ miguelborregonrivilla@gmail.com

RECEIVED 13 August 2024
ACCEPTED 07 January 2025
PUBLISHED 29 January 2025

CITATION
Borregón M, Valero M, Ferrández A, Muñoz Á, Roque C and Benítez-Fuentes J-D (2025) Cancer-associated thoracic aorta arterial thrombosis: case report and review of the literature.
Front. Cardiovasc. Med. 12:1480310.
doi: 10.3389/fcvm.2025.1480310

COPYRIGHT
© 2025 Borregón, Valero, Ferrández, Muñoz, Roque and Benítez-Fuentes. This is an open-access article distributed under the terms of the Creative Commons Attribution License (CC BY). The use, distribution or reproduction in other forums is permitted, provided the original author(s) and the copyright owner(s) are credited and that the original publication in this journal is cited, in accordance with accepted academic practice. No use, distribution or reproduction is permitted which does not comply with these terms.

Cancer-associated thoracic aorta arterial thrombosis: case report and review of the literature

Miguel Borregón[1]*, María Valero[1], Asia Ferrández[1], Álvaro Muñoz[1], Carmen Roque[2] and Javier-David Benítez-Fuentes[1]

[1]Department of Medical Oncology, Hospital General Universitario de Elche, FISABIO, Alicante, Spain, [2]Department of Radiology, Hospital General Universitario de Elche, FISABIO, Alicante, Spain

Background: Arterial thrombosis is an uncommon complication in cancer patients, often overshadowed by venous thromboembolic events. Its occurrence in patients with solid tumors on active antineoplastic treatment poses a significant clinical challenge.
Key clinical question: Given the lack of consensus on the optimal therapy for arterial thrombosis in cancer patients, the best practices for managing an aortic thrombus, and the benefit of low molecular weight heparin (LMWH) must be reviewed.
Clinical approach: We present the case of a 70-year-old female with stage IVA lung adenocarcinoma who developed an aortic thrombus during chemo-immunotherapy. The thrombus was successfully treated with LMWH, avoiding further complications, and allowing for the continuation of her cancer therapy.
Conclusions: This case highlights the importance of early detection and management of arterial thrombus in cancer patients. LMWH proved effective in resolving the thrombus, underscoring its role in managing such complications.

KEYWORDS

cancer-associated thrombosis (CAT), venous thromboembolism (VTE), arterial thromboembolism (ATE), low molecular weight heparin (LMWH), small cell lung carcinoma (SCLC) and cisplatin

Introduction

Cancer-associated thrombosis (CAT) is a well-recognized complication in cancer patients, contributing significantly to morbidity and mortality in this population. Thrombosis in cancer patients is multifactorial, involving tumor-related factors, patient characteristics, and treatment modalities (1). While venous thromboembolism (VTE) is the most common type of CAT, arterial thromboembolism (ATE), although less frequent, poses a critical risk, leading to severe cardiovascular events, including myocardial infarction, cerebrovascular events, and peripheral artery disease (2).

The pathophysiology of ATE in cancer involves complex interactions between pro-thrombotic states induced by malignancy, endothelial damage, and hypercoagulability exacerbated by cancer treatments (3). Different epidemiological studies indicate that cancer patients have an elevated risk of ATE compared to the general population (4). However, information related to its management is scarce (3).

The case discussed herein involves a 70-year-old woman with a history of limited stage small cell lung carcinoma (SCLC) treated with radical chemo-radiotherapy in 2008 and a recent diagnosis of stage IVA adenocarcinoma of the lung in December 2023. Her current treatment includes a combination of chemotherapy and immunotherapy (maintenance

pemetrexed and pembrolizumab). After a partial response to treatment, the patient developed an arterial thrombus in the ascending aorta. This complication highlights the potential risk for serious thrombotic complications in cancer patients, the importance of cardiovascular monitoring and prompt treatment of CAT in oncology patients.

Case description

A timeline of the key events in this case is presented in Table 1. A 70-year-old Caucasian woman with a significant past medical history presented with asymptomatic aortic thrombosis. Her personal history includes a former smoking habit (35 pack-years, ceased in 2008), hypertension, dyslipidemia, osteoporosis under oral zoledronic acid treatment, and actinic keratosis on the nose. Her surgical history includes resection of breast fibroadenomas and a basal cell carcinoma excision from the right shoulder in 2006. She had no previous medical history of thrombosis.

The patient's oncological history is notable for two metachronous neoplasms. In July 2008, she was diagnosed with limited stage SCLC of the right lung with a 9.5 cm right anterior mediastinal lymph node mass, which compressed the superior cava vein, a 4.5 cm subpleural right lung mass, and enlarged subcarinal nodes. She underwent five cycles chemotherapy with cisplatin (80 mg/m^2 IV infusion) and etoposide (100 mg/m^2 IV infusion) every 3 weeks and concurrent radiotherapy 50.4 Gy in 30 sessions on the pulmonary mass and the affected lymph nodes. In January 2009 she received prophylactic cranial irradiation (PCI), 30 Gy in 10 sessions. She achieved a major partial response and was followed up until March 2020 with no evidence of progression, when she was discharged from oncology following an unremarkable FDG-PET scan.

In December 2023, she was diagnosed with stage IVA (cT2b cN1 cM1a) adenocarcinoma of the lung, characterized by a 5 cm necrotic mass in inferior right lobe (SuvMax 10.9), a small node located in lingula (SuvMax 4.5), and two right hilar adenopathies (SuvMax 6.6). The biopsy sample was negative for PD-L1 expression, and driver mutations. She started first-line treatment with carboplatin (AUC 5 IV infusion), pemetrexed (500 mg/m^2 IV infusion) and pembrolizumab (200 mg IV infusion) every 3 weeks. After four cycles, an FDG-PET scan in March 2024 showed a partial response, and maintenance therapy with pemetrexed (500 mg/m^2 IV infusion) and pembrolizumab (200 mg IV infusion) was initiated.

On June 5, 2024, during a routine follow-up visit, she was diagnosed with an asymptomatic ascending aorta arterial thrombus after completing four cycles of pemetrexed and pembrolizumab maintenance therapy. The thoraco-abdominal CT scan for her tumor evaluation, carried out on May 31, 2024, revealed a new hypodense nodular image adhered to the anterior wall of the ascending thoracic aorta, consistent with an 8 mm thrombus (Figures 1–3). The CT scan also noted chronic post-radiation changes in the right lung and a stable subpleural necrotic mass in the right lower lobe, with no evidence of new mediastinal adenopathy or pleural/pericardial effusion.

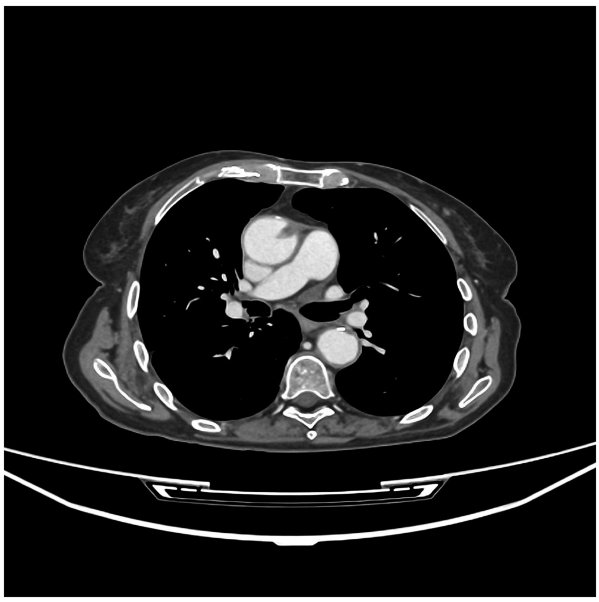

FIGURE 1
Transversal CT-scan plane showing the 8 mm thrombus in the ascending aorta.

As risk factors for the thrombus development, besides her oncology history, the patient had also been diagnosed 2 weeks before with a fracture of the sacrum. It was related to her osteoporosis and an accidental fall at home days before. Magnetic resonance performed on May 22, 2024, described a vertical and bilateral sacral ala fracture, with marrow edema, with no tumoral component. She was experiencing severe pain and was prescribed transdermal fentanyl.

Given the thrombus diagnosis, the oncology team suspended the patient's maintenance therapy and consulted the cardiology team, that evaluated the patient on the same day. Cardiology evaluation found no chest pain, signs of heart failure, syncope,

TABLE 1 Timeline of key events.

July 2008	Second semester 2008	January 2009	December 2023	First trimester 2024	March 2023	Second trimester 2024	May 31, 2024	June 5, 2024	June 14, 2024
Limited stage small cell lung carcinoma	Cisplatin + etoposide + concurrent thoracic radiotherapy	Prophylactic cranial irradiation	Stage IVA adenocarcinoma of the lung	Carboplatin + pemetrexed + pembrolizumab	Partial response	Pemetrexed + pembrolizumab maintenance	Ascending thoracic aorta thrombus	LMWH 1 mg kg	Thrombus is resolved

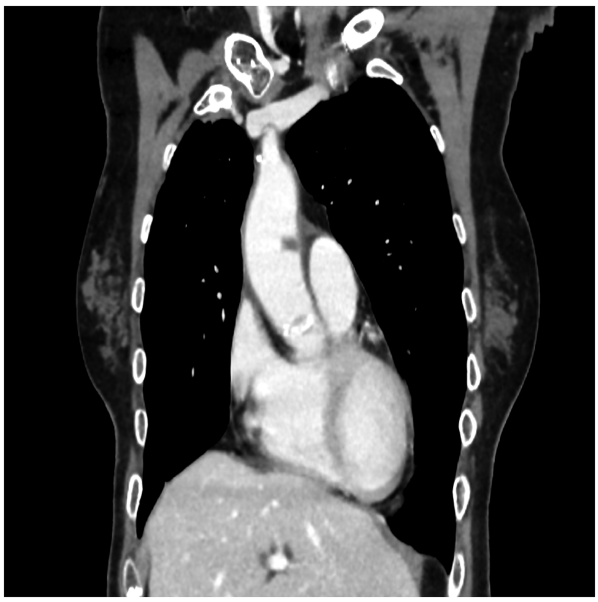

FIGURE 2
Coronal CT-scan plane showing the 8 mm thrombus in the ascending aorta.

FIGURE 3
Sagittal CT-scan plane showing the 8 mm thrombus in the ascending aorta.

palpitations, or neurological symptoms. An echocardiogram revealed a non-dilated and non-hypertrophic left ventricle with preserved ejection fraction and no segmental wall motion abnormalities. There was moderate bi-atrial dilation, a normal-sized aortic root (31 mm) and ascending aorta (36 mm) without alterations. A small nodule was visualized where the aortic thrombus was located in the CT. No pericardial effusion or intracavitary thrombus were seen. For therapeutic decision-making, we conducted a thorough review of the literature regarding ATE treatment in cancer patients. In most published case reports, asymptomatic ATE has been managed with LMWH. Therefore, we decided to start enoxaparin 1 mg/kg every 12 hours.

Two weeks later, on June 14, 2024, a follow-up CT scan of the chest to monitor the aortic thrombus showed its complete resolution (Figures 4–6). Due to the patient's preference to avoid twice-daily injections, her anticoagulation therapy was changed to bemiparin 115 IU/Kg every 24 hours and she resumed her treatment with pemetrexed and pembrolizumab. The patient reported no new symptoms and developed no complications related to the anticoagulation therapy. At the three-month follow-up, she remained asymptomatic.

Discussion

This case highlights the importance of vigilant cardiovascular monitoring in cancer patients, especially those undergoing active treatment, due to the heightened risk of thrombotic events. Early identification and prompt management of arterial thrombosis are critical in improving outcomes in this vulnerable population. Our patient was exposed to several well-known risk factors for thrombotic events, including her past SCLC, her current adenocarcinoma of the lung, the chemotherapy, thoracic radiotherapy and PCI in 2008, her current treatment with chemotherapy and immunotherapy, and her recent sacrum fracture. However, our patient did not exhibit the typical clinical presentation of VTE. Instead, she developed an ATE in the ascending aorta, which is particularly challenging to treat due to its critical location and associated compromise. The literature on managing ATEs is scarce, underscoring the need for individualised assessment and management in each case.

Cancer patients experience an increased risk of thromboembolic events due to a hypercoagulable state induced by the malignancy itself, as well as by the therapeutic interventions they undergo. It has been reported that the risk of VTE increases four- to six-fold in cancer patients receiving chemotherapy (5, 6), and especially in the case of ATE it can lead to catastrophic outcomes (7). Risk factors for ATE in the general population are severe atherosclerosis, aortic aneurysm, cardiovascular surgery, uncontrolled diabetes mellitus and polytrauma (8–10). Some ATE risk factors documented in cancer patients are: the first month after diagnosis of cancer, hypertension, smoking, pre-existing cardiovascular diseases, age over 65 years, previous history of ATE, distant metastasis and chemotherapy (11). While ATE in cancer patients is less common than VTE, both conditions share overlapping pathophysiological mechanisms (12). Recognized cancer-related mechanisms contributing to these complications include tumour

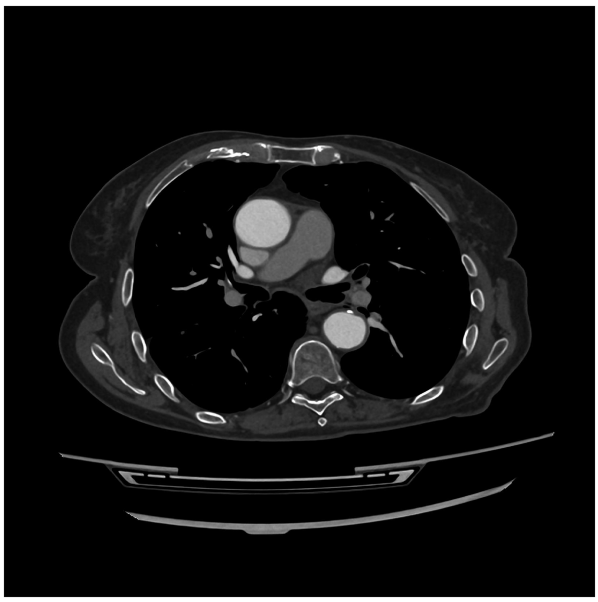

FIGURE 4
Transversal CT-scan plane showing the resolution of the 8 mm thrombus in the ascending aorta.

FIGURE 6
Sagittal CT-scan plane showing the resolution of the 8 mm thrombus in the ascending aorta.

FIGURE 5
Coronal CT-scan plane showing the resolution of the 8 mm thrombus in the ascending aorta.

cell-induced activation of coagulation pathways, a decrease in anticoagulant molecules, structural or functional changes in the vascular wall, endothelial damage, platelet activation, alterations in the fibrinolytic system, and the release of cytokines such as vascular endothelial growth factor (VEGF), tumour necrosis factor (TNF)-α, and interleukin-1β (13–18).

Antineoplastic agents, including hormone therapy, chemotherapy, and immunotherapy play an additional role, further exacerbating the risk by inducing endothelial injury and enhancing procoagulant activity (19, 20). Radiotherapy has also been suggested as a risk factor for VTE development. In a prospective study focused on curative intent radiotherapy, Daguenet et al. found an incidence rate of VTE 6 months post-radiotherapy of 2% (21).

Cisplatin and carboplatin are some of the frequently used chemotherapy drugs associated with ATE. It has been speculated that cisplatin may enhance tissue factor activity and platelet activation and elevate the von Willebrand factor, which can cause endothelial injury and potentiate arterial thrombosis. Dehydration and hypomagnesemia, are factors related to cisplatin treatment that might also contribute to thrombosis (22–25).

Some clinical cases specifically explore the relationship between cisplatin and ATE. Table 2 summarizes these cases. Chin et al. described the case of one patient with limited stage SCLC treated with cisplatin and etoposide, who was diagnosed with an aortic arch thrombus and its improvement when started on LMWH (26). Weijl et al. studied the incidence of thrombosis in 179 germ cell cancer patients treated with cisplatin and bleomycin, finding it to be approximately 8.4% (18). Of these events, three (16.7%) were arterial events, including two cerebral ischemic strokes and one lower limb arterial thrombosis. Numico et al. found in 108 stage III-IV NSCLC patients treated with cisplatin and gemcitabine chemotherapy a VTE incidence of approximately 17.6% (27). Of these events, ten were arterial events (2 myocardial infarctions, 7 lower limb arterial thrombosis, and 1 cerebral ischemic stroke). Dieckmann et al. reported the case of a

TABLE 2 Clinical cases exploring the relationship between cisplatin and arterial thromboembolism (ATE).

Author	Publication	Cancer type	Chemotherapy	Site of ATE	Timing of ATE	Outcomes
Chin et al. (26)	2010	1 patient with limited stage SCLC	Cisplatin + etoposide	Aortic arch thrombus	First restaging scan	Improvement on LMWH
Weijl et al. (18)	2000	179 patients with germ cell cancer	Cisplatin + bleomycin-based CT	2 strokes, 1 lower limb ATE	Between the start and 6 weeks after CT	Incidence of ATE 1,7%
Numico et al. (27)	2005	108 patients with stage III-IV NSCLC	Cisplatin + gemcitabine	2 myocardial infarctions, 7 lower limb ATEs, 1 stroke	Between 4 days and 234 days after the start of CT	Incidence of ATE 9,2%
Dieckmann et al. (28)	2009	1 patient with advanced seminoma	Cisplatin + etoposide + bleomycin	Descending thoracic aorta and infrarenal aorta	First restaging scan after 2 cycles of CT	Improvement on LMWH, AAS and warfarin
Apiyasawat et al. (29)	2003	1 patient with stage IIB cervical cancer	RT + cisplatin + 5-fluorouracil	Aortic distal arch and femoral artery emboli	The same day receiving CT	Successful surgical thrombectomy
Ito et al. (30)	2013	1 patient with stage IV gastric cancer	Cisplatin-based CT	Descending thoracic aorta and infrarenal abdominal aorta	First restaging scan	Successfully treated with intravenous heparin and warfarin
Morlese et al. (31)	2007	1 patient with localized oesophageal adenocarcinoma	Preoperative cisplatin + 5-fluorouracil	Large thrombus in the abdominal aorta	The day after receiving his first cycle	Surgical embolectomy, finally died 7 days later
Moore et al. (32)	2011	All (932) patients with cisplatin-based CT in 2008	Cisplatin-based CT	14 patients with ATE, 5 patients with ATE + VTE	Between the start and 4 weeks after CT	Incidence of ATE 8,3%, and ATE + VTE 3%

AAS, acetylic salicylic acid; ATE, arterial thromboembolism; CT, chemotherapy; LMWH, low molecular weight heparin; SCLC, small cell lung carcinoma; NSCLC, non-small cell lung carcinoma; RT, radiotherapy; VTE, venous thromboembolism.

man with advanced seminoma receiving cisplatin, etoposide and bleomycin chemotherapy who developed thrombotic deposits in the descending thoracic aorta and in the infrarenal abdominal aorta respectively. He was placed on anticoagulant therapy and 6 months after completion of chemotherapy, thrombotic deposits had completely resolved (28). Apiyasawat et al. reported the case of a patient that developed a thrombus in the distal arch of the aorta when she was receiving radiotherapy, cisplatin and 5-fluorouracil for stage IIB cervical cancer (29). Numerous vascular emboli were occluding her distal common femoral artery. The patient underwent successful surgical thrombectomy. Ito et al. described a patient suffering a thrombosis in the descending arch of the thoracic aorta and the infrarenal abdominal aorta during cisplatin-based chemotherapy for stage IV gastric cancer that was successfully treated with intravenous heparin and warfarin (30). Morlese et al. described a case of spontaneous arterial thrombosis in a 42-year-old male with localised oesophageal adenocarcinoma the day after receiving his first cycle of preoperative cisplatin-5-fluorouracil chemotherapy (31). It was identified a large thrombus in the abdominal aorta, beginning in the mid-aorta, just superior to the origin of the renal arteries, and continuing distally into both common iliac vessels. The patient received a surgical embolectomy and bilateral lower limb fasciotomies, but she finally died 7 days later due to small bowel infarction. Moore et al. performed a large retrospective analysis of all patients treated with cisplatin-based chemotherapy at *Memorial Sloan-Kettering Cancer Center* in 2008. Among 932 patients, 169 (18.1%) experienced a VTE and/or an ATE event during cancer treatment or within 4 weeks after finishing it. Most of them suffered VTE, but arterial thrombosis alone was found in 8.3% of these patients, and co-occurrence of ATE and VTE in 3.0% (32).

The patient we present in this case report has a history of thoracic radiotherapy for her previous SCLC, another notable risk factor for ATE development. A *post-hoc* analysis from the *COMPASS-CAT trial*, whose primary objective was to study a predictive model for VTE diagnosis in cancer, was focused on 361 patients with early, locally advanced, or metastatic breast, lung, colon, or ovarian cancer who received radiotherapy. At a median follow up of 6 months, 33 patients (9.1%) developed a VTE event. After applying a competing risk model, radiotherapy remained significantly associated with increased risk for VTE (HR 2.47, 95% CI: 1.47–4.12, $p = 0.001$) (33). Radiation injury has been demonstrated to cause acute and late alterations in the endothelium, favouring vascular events, as it has been studied in patients with central nervous system tumours presenting radionecrosis (34–36). Rishi et al. published the case of a 54-year-old male suffering extensive abdominal aortic thrombus along with involvement of left common iliac, saphenous-popliteal, and tibial arteries as well as moderate stenosis coronary arteries three days after receiving her first cycle of cisplatin-based chemotherapy given concurrently with radiotherapy for squamous cell carcinoma of the base of tongue (37).

Another risk factor for CAT development exhibited by the patient of our clinical case is her current exposure to pembrolizumab, as immune checkpoint inhibitors (ICI) have been associated with VTE and ATE risk in cancer patients (38–41). Moik et al. in the *Vienna General Hospital* conducted a retrospective study focused on patients treated with ICI. Melanoma, lung cancer and renal cancer were the most common types of cancer included. Nivolumab, pembrolizumab and ipilimumab were the most frequent ICI included. A total of 47.6% patients were also treated with radiation therapy. Cumulative incidences of VTE and ATE were 12.9% and 1.8% respectively (38). Based on the same hypothesis, Sussman et al.

conducted a retrospective study of 228 patients with melanoma receiving ICI between 2015 and 2017 at the *Cleveland Clinic*. Fifty-one thrombotic events occurred in 47 patients (20.6%), including 37 VTE and 14 ATE (39). Roopkumar et al. conducted a retrospective cohort study including 1.686 patients who received ICI for a variety of malignancies to determine the incidence of VTE. VTE occurred in 404 patients (24%) and was associated with decreased overall survival [HR = 1.22 (95% CI 1.06–1.41), $p < 0.008$]. Patients developing VTE expressed significantly higher pretreatment levels of myeloid-derived suppressor cells, interleukin 8, and soluble vascular cell adhesion protein 1, postulated as drivers in VTE pathogenesis (40).

The information regarding the management of ATE in cancer patients is scarce and it should involve a multidisciplinary approach. Standard treatment modalities remain controversial. Systemic anticoagulation alone, aortic thromboendarterectomy, open-surgery for thrombus removal, or endovascular placement of stent grafts has been suggested (41–45). Goto et al. published the case of a 51-year-old woman with early esophageal cancer who presented an aortic mural thrombus. She was started on intravenous heparin and later changed to warfarin and three months later the thrombus had disappeared (46). Han et al. described a patient presenting ascending aortic thrombosis occurring 9 days after cisplatin-based chemotherapy for his lung cancer. He was successfully treated with LMWH and warfarin (47).

Conclusion

Although less frequent than VTE, ATE in cancer patients requires prompt recognition and management due to its severe potential consequences. This case describes an ascending aortic ATE in a cancer patient successfully treated with LMWH. Anticoagulation with LMWH resolved the thrombus, demonstrating its efficacy in managing CAT. LMWH for ATE in cancer patients may prevent further vascular complications, and allow for the continuation of the antineoplastic treatment. We hypothesize that if there are no life-threatening symptoms and no contraindications, based on the scarce available evidence, multidisciplinary evaluation, anticoagulation with LMWH alone and a close follow-up could be a good option for cancer-related ATE.

Data availability statement

The original contributions presented in the study are included in the article/Supplementary Material, further inquiries can be directed to the corresponding author.

Ethics statement

Written informed consent was obtained from the individual(s) for the publication of any potentially identifiable images or data included in this article.

Author contributions

MB: Conceptualization, Data curation, Formal Analysis, Funding acquisition, Investigation, Methodology, Project administration, Resources, Software, Supervision, Validation, Visualization, Writing – original draft, Writing – review & editing. MV: Conceptualization, Investigation, Writing – original draft. AF: Software, Supervision, Writing – review & editing. ÁM: Conceptualization, Data curation, Formal Analysis, Funding acquisition, Methodology, Resources, Validation, Writing – review & editing. CR: Conceptualization, Methodology, Project administration, Supervision, Writing – original draft. JB: Conceptualization, Data curation, Formal Analysis, Funding acquisition, Investigation, Methodology, Project administration, Resources, Software, Supervision, Validation, Visualization, Writing – original draft, Writing – review & editing.

Funding

The author(s) declare financial support was received for the research, authorship, and/or publication of this article. “Foundation for the Promotion of Health and Biomedical Research in the Valencian Region (FISABIO)” has funded this research.

Conflict of interest

The authors declare that the research was conducted in the absence of any commercial or financial relationships that could be construed as a potential conflict of interest.

Publisher’s note

All claims expressed in this article are solely those of the authors and do not necessarily represent those of their affiliated organizations, or those of the publisher, the editors and the reviewers. Any product that may be evaluated in this article, or claim that may be made by its manufacturer, is not guaranteed or endorsed by the publisher.

References

1. Khorana AA, Mackman N, Falanga A, Pabinger I, Noble S, Ageno W, et al. Cancer-associated venous thromboembolism. *Nat Rev Dis Primers*. (2022) 8(1):11. doi: 10.1038/s41572-022-00336-y

2. Gervaso L, Dave H, Khorana AA. Venous and arterial thromboembolism in patients with cancer: *JACC: CardioOncology* state-of-the-art review. *JACC CardioOncol*. (2021) 3(2):173–90. doi: 10.1016/j.jaccao.2021.03.001

3. De Stefano V. Arterial thrombosis and cancer: the neglected side of the coin of Trousseau syndrome. *Haematologica*. (2018) 103(9):1419–21. doi: 10.3324/haematol.2018.197814

4. Zamorano JL, Lancellotti P, Muñoz DR, Aboyans V, Asteggiano R, Galderisi M, et al. 2016 ESC position paper on cancer treatments and cardiovascular toxicity developed under the auspices of the ESC committee for practice guidelines: the task

force for cancer treatments and cardiovascular toxicity of the European Society of Cardiology (ESC). *Eur Heart J*. (2016) 37(36):2768–801. doi: 10.1093/eurheartj/ehw211

5. Khorana AA, Kuderer NM, Culakova E, Lyman GH, Francis CW. Development and validation of a predictive model for chemotherapy-associated thrombosis. *Blood*. (2008) 111:4902–7. doi: 10.1182/blood-2007-10-116327

6. Streiff MB, Holmstrom B, Angelini D, Ashrani A, Elshoury A, Fanikos J, et al. Cancer-associated venous thromboembolic disease, version 2.2021, NCCN clinical practice guidelines in oncology. *J Natl Compr Canc Netw*. (2021) 19(10):1181–201. doi: 10.6004/jnccn.2021.0047

7. Erbel R, Aboyans V, Boileau C, Bossone E, Di Bartolomeo R, Eggebrecht H, et al. ESC guidelines on the diagnosis and treatment of aortic diseases: document covering acute and chronic aortic diseases of the thoracic and abdominal aorta of the adult. The task force for the diagnosis and treatment of aortic diseases of the European Society of Cardiology. *Eur Heart J*. (2014) 35(41):2873–926. doi: 10.1093/eurheartj/ehu281

8. Cañadas V, Vilacosta I, Luaces M, Bustos A, Ferreirós J, Aragoncillo P, et al. Thrombosis of an apparently normal thoracic aorta and arterial embolism. *Rev Esp Cardiol*. (2008) 61:196–200. doi: 10.1157/13116207

9. Hahn TL, Dalsing MC, Sawchuk AP, Cikrit DF, Lalka SG. Primary aortic mural thrombus: presentation and treatment. *Ann Vasc Surg*. (1999) 13:52–9. doi: 10.1007/s100169900220

10. Vaideeswar P, Deshpande JR. Non-atherosclerotic aorto-arterial thrombosis: a study of 30 cases at autopsy. *J Postgrad Med*. (2001) 47:8–14.

11. Pernod G, Cohen A, Mismetti P, Sanchez O, Mahé I; INNOVTE CAT Working Group. Cancer-related arterial thromboembolic events. *Arch Cardiovasc Dis*. (2024) 117(1):101–13. doi: 10.1016/j.acvd.2023.11.007

12. Aronson D, Brenner B. Arterial thrombosis and cancer. *Thromb Res*. (2018) 164(Suppl 1):S23–8. doi: 10.1016/j.thromres.2018.01.003

13. Lowe GDO. Common risk factors for both arterial and venous thrombosis. *Br J Haematol*. (2008) 140:488–95. doi: 10.1111/j.1365-2141.2007.06973.x

14. Alsamman M, Pothen J, Inoyatov M, Cruz Salcedo EM, Ramesh C. Aortic thrombus extending to left subclavian in a patient with diffuse venous thromboembolism on aromatase inhibitor therapy. *Cureus*. (2021) 13(7):e16698. doi: 10.7759/cureus.16698

15. Alcocer J, Ascaso M, Quintana E, Sandoval E, Castellá M. Operative management of ascending aorta thrombus and bilateral pulmonary embolism in the setting of breast cancer. *J Card Surg*. (2021) 36(4):1550–3. doi: 10.1111/jocs.15347

16. Previtali E, Bucciarelli P, Passamonti SM, Martinelli I. Risk factors for venous and arterial thrombosis. *Blood Transfus*. (2011) 9:120–38. doi: 10.2450/2010.0066-10

17. Haddad T, Greeno E. Chemotherapy-induced thrombosis. *Thromb Res*. (2006) 118:555–68. doi: 10.1016/j.thromres.2005.10.015

18. Weijl N, Rutten M, Zwinderman A, Keizer J, Nooy M, Rosendaal F, et al. Thromboembolic events during chemotherapy for germ cell cancer: a cohort study and review of the literature. *J Clin Oncol*. (2000) 18(10):2169–78. doi: 10.1200/JCO.2000.18.10.2169

19. Ay C, Pabinger I, Cohen AT. Cancer-associated venous thromboembolism: burden, mechanisms, and management. *Thromb Haemost*. (2017) 117(2):219–30. doi: 10.1160/TH16-08-0615

20. Wang TF, Khorana AA, Carrier M. Thrombotic complications associated with immune checkpoint inhibitors. *Cancers (Basel)*. (2021) 13(18):4606. doi: 10.3390/cancers13184606

21. Daguenet E, Maison M, Tinquaut F, Giroux EA, Bertoletti L, Suchaud JP, et al. Venous thromboembolism and radiation therapy: the final radiation-induced thrombosis study analysis. *Cancer Med*. (2022) 11(8):1753–62. doi: 10.1002/cam4.4559

22. Mathews J, Goel R, Evans WK, Shamji F, Stewart DJ. Arterial occlusion in patients with peripheral vascular disease treated with platinum-based regimens for lung cancer. *Cancer Chemother Pharmacol*. (1997) 40:19–22. doi: 10.1007/s002800050619

23. Walsh J, Wheeler H, Geczy C. Modulation of tissue factor on human monocytes by cisplatin and adriamycin. *Br J Haematol*. (1992) 81(4):480–8. doi: 10.1111/j.1365-2141.1992.tb02978.x

24. Cool R, Herringon J, Wong L. Recurrent peripheral arterial thrombosis induced by cisplatin and etoposide. *Pharmacotherapy*. (2002) 22(9):1200–4. doi: 10.1592/phco.22.13.1200.33524

25. Licciarello J, Moake J, Rudi C, Karp D, Hong W. Elevated plasma von Willebrand factor levels and arterial occlusive complications associated with cisplatin-based chemotherapy. *Oncology*. (1985) 42:296–300. doi: 10.1159/000226049

26. Chin SO, Lee JJ, Hwang YH, Han JJ, Maeng CH, Baek SK, et al. Aortic thrombosis resolved with enoxaparin in a patient treated with cisplatin-based regimen for small cell lung cancer. *Int J Hematol*. (2010) 91(5):892–6. doi: 10.1007/s12185-010-0571-3

27. Numico G, Garrone O, Dongiovanni V, Silvestris N, Colantonio I, Di Costanzo G, et al. Prospective evaluation of major vascular events in patients with nonsmall cell lung carcinoma treated with cisplatin and gemcitabine. *Cancer*. (2005) 103(5):994–9. doi: 10.1002/cncr.20893

28. Dieckmann KP, Gehrckens R. Thrombosis of abdominal aorta during cisplatin-based chemotherapy of testicular seminoma—a case report. *BMC Cancer*. (2009) 9:459. doi: 10.1186/1471-2407-9-459

29. Apiyasawat S, Wongpraparut N, Jacobson L, Berkowitz H, Jacobs LE, Kotler MN. Cisplatin induced localized aortic thrombus. *Echocardiography*. (2003) 20(2):199–200. doi: 10.1046/j.1540-8175.2003.03002.x

30. Ito S, Nakamura Y, Noumi T, Sasaki Y. Acute aortic thrombosis during cisplatin based chemotherapy for gastric cancer. *Intern Med*. (2013) 52(9):973–5. doi: 10.2169/internalmedicine.52.9337

31. Morlese JF, Jeswani T, Beal I, Wylie P, Bell J. Acute ventricular and aortic thrombosis post chemotherapy. *Br J Radiol*. (2007) 80(952):e75–7. doi: 10.1259/bjr/26948582

32. Moore RA, Adel N, Riedel E, Bhutani M, Feldman DR, Tabbara NE, et al. High incidence of thromboembolic events in patients treated with cisplatin-based chemotherapy: a large retrospective analysis. *J Clin Oncol*. (2011) 29(25):3466–73. doi: 10.1200/JCO.2011.35.5669

33. Temraz S, Moukalled N, Gerotziafas GT, Elalamy I, Jara-Palomares L, Charafeddine M, et al. Association between radiotherapy and risk of cancer associated venous thromboembolism: a sub-analysis of the COMPASS-CAT study. *Cancers (Basel)*. (2021) 13(5):1033. doi: 10.3390/cancers13051033

34. Yoshii Y. Pathological review of late cerebral radionecrosis. *Brain Tumor Pathol*. (2008) 25(2):51–8. doi: 10.1007/s10014-008-0233-9

35. Gonzalez J, Kumar AJ, Conrad CA, Levin VA. Effect of bevacizumab on radiation necrosis of the brain. *Int J Radiat Oncol Biol Phys*. (2007) 67(2):323–6. doi: 10.1016/j.ijrobp.2006.10.010

36. Levin VA, Bidaut L, Hou P, Kumar AJ, Wefel JS, Bekele BN, et al. Randomized double-blind placebo-controlled trial of bevacizumab therapy for radiation necrosis of the central nervous system. *Int J Radiat Oncol Biol Phys*. (2011) 79(5):1487–95. doi: 10.1016/j.ijrobp.2009.12.061

37. Rishi A, Ghoshal S. Acute multiple arterial thrombosis after cisplatin in base of tongue carcinoma: case report. *Head Neck*. (2013) 35(9):E269–71. doi: 10.1002/hed.23123

38. Moik F, Chan WSE, Wiedemann S, Hoeller C, Tuchmann F, Aretin MB, et al. Incidence, risk factors, and outcomes of venous and arterial thromboembolism in immune checkpoint inhibitor therapy. *Blood*. (2021) 137(12):1669–78. doi: 10.1182/blood.2020007878

39. Sussman TA, Li H, Hobbs B, Funchain P, McCrae KR, Khorana AA. Incidence of thromboembolism in patients with melanoma on immune checkpoint inhibitor therapy and its adverse association with survival. *J Immunother Cancer*. (2021) 9(1):e001719. doi: 10.1136/jitc-2020-001719

40. Roopkumar J, Swaidani S, Kim AS, Thapa B, Gervaso L, Hobbs BP, et al. Increased incidence of venous thromboembolism with cancer immunotherapy. *Med*. (2021) 2(4):423–34. doi: 10.1016/j.medj.2021.02.002

41. Toyama M, Nakayama M, Hasegawa M, Yuasa T, Sato B, Ohno O. Direct oral anticoagulant therapy as an alternative to surgery for the treatment of a patient with a floating thrombus in the ascending aorta and pulmonary embolism. *J Vasc Surg Cases Innov Tech*. (2018) 4(2):170–2. doi: 10.1016/j.jvscit.2018.03.002

42. Choukroun EM, Labrousse LM, Madonna FP, Deville C. Mobile thrombus of the thoracic aorta: diagnosis and treatment in 9 cases. *Ann Vasc Surg*. (2002) 16:714–22. doi: 10.1007/s10016-001-0314-2

43. Zhang WW, Abou-Zamzam AM, Hashisho M, Killeen JD, Bianchi C, Teruya TH. Staged endovascular stent grafts for concurrent mobile/ulcerated thrombi of thoracic and abdominal aorta causing recurrent spontaneous distal embolization. *J Vasc Surg*. (2008) 47:193–6 doi: 10.1016/j.jvs.2007.07.050

44. Tsilimparis N, Hanack U, Pisimisis G, Yousefi S, Wintzer C, Rückert RI. Thrombus in the non-aneurysmal, non-atherosclerotic descending thoracic aorta—an unusual source of arterial embolism. *Eur J Vasc Endovasc Surg*. (2011) 41:450–7. doi: 10.1016/j.ejvs.2010.11.004

45. Shames ML, Rubin BG, Sanchez LA, Thompson RW, Sicard GA. Treatment of embolizing arterial lesions with endoluminally placed stent grafts. *Ann Vasc Surg*. (2002) 16:608–12. doi: 10.1007/s10016-001-0278-2

46. Goto I, Okamoto R, Sawai T, Takasaki A, Takeuchi T, Matsuo H, et al. A case of aortic thrombosis and embolism preceding the progression of early esophageal cancer. *J Cardiol Cases*. (2013) 7(5):e123–5. doi: 10.1016/j.jccase.2012.12.008

47. Hahn SJ, Oh JY, Kim JS, Kim DY. A case of acute aortic thrombosis after cisplatin-based chemotherapy. *Int J Clin Oncol*. (2011) 16(6):732–6. doi: 10.1007/s10147-011-0205-7

frontiers | Frontiers in Oncology

TYPE Case Report
PUBLISHED 12 February 2025
DOI 10.3389/fonc.2025.1508691

Check for updates

OPEN ACCESS

EDITED BY
Reto Asmis,
Wake Forest University, United States

REVIEWED BY
Ulrich Ronellenfitsch,
Medical Faculty of the Martin-Luther-University Halle-Wittenberg, Germany
Hirotaka Suto,
Hyogo Cancer Center, Japan

*CORRESPONDENCE
Jianwei Xu
13807057836@163.com

RECEIVED 09 October 2024
ACCEPTED 22 January 2025
PUBLISHED 12 February 2025

CITATION
Yao G and Xu J (2025) Aortic intimal sarcoma with abdominal metastasis: case report and management approach. *Front. Oncol.* 15:1508691. doi: 10.3389/fonc.2025.1508691

COPYRIGHT
© 2025 Yao and Xu. This is an open-access article distributed under the terms of the Creative Commons Attribution License (CC BY). The use, distribution or reproduction in other forums is permitted, provided the original author(s) and the copyright owner(s) are credited and that the original publication in this journal is cited, in accordance with accepted academic practice. No use, distribution or reproduction is permitted which does not comply with these terms.

Aortic intimal sarcoma with abdominal metastasis: case report and management approach

Gongji Yao[1,2] and Jianwei Xu[1,2]*

[1]Department of Intervention, Huzhou Central Hospital, The Fifth School of Clinical Medicine of Zhejiang Chinese Medical University, Huzhou, Zhejiang, China, [2]Department of Intervention, Huzhou Central Hospital, The Affiliated Central Hospital of Huzhou University, Huzhou, Zhejiang, China

Background: Aortic intimal sarcoma is an exceptionally rare malignancy with a poor prognosis. Tumors are predominantly located in the abdominal aorta, thoracic aorta, and thoracoabdominal aorta. Abdominal metastasis of aortic sarcoma is rarely documented, and effective treatment regimens are lacking.

Case presentation: A 55-year-old female presented with recurrent abdominal pain and a history of hypertension and mesenteric thrombosis. Initial arterial computed tomography angiography (CTA) revealed multiple thrombi with significant luminal narrowing, leading to a diagnosis of aortic thrombosis. She was referred to the First Affiliated Hospital of Zhejiang University for surgical intervention. Pathological analysis confirmed a diagnosis of aortic intimal sarcoma with MDM2 positivity. One month later, the patient developed severe abdominal pain, and positron emission tomography-computed tomography (PET-CT) showed accumulation in the small intestine, jejunum, and back muscles. Palliative tumor removal was performed, and the patient received chemotherapy with platinum drugs and epirubicin. Post-treatment PET-CT indicated no significant tumor staining or progression.

Discussion: Aortic intimal sarcoma is a rare neoplasm with limited treatment options. MDM2 overexpression is commonly observed, but similar histological features can appear in other conditions, making diagnosis challenging. Imaging modalities, including MRI and PET-CT, are crucial for diagnosis and monitoring. Current treatment strategies are non-standardized, but small-molecule inhibitors targeting MDM2 show promise. This case highlights the potential effectiveness of combined surgical and chemotherapeutic approaches for managing abdominal metastasis of aortic intimal sarcoma and provides a foundation for future clinical trials.

KEYWORDS

aortic intimal sarcoma, abdominal metastasis, MDM2, chemotherapy, PET-CT, MRI, case report

Introduction

Aortic intimal sarcoma is an exceptionally rare aorta tumor with a grim prognosis. Predominant tumor locations include the abdominal aorta (40%), thoracic aorta (20%), and thoracoabdominal aorta (10%) (1, 2). However, abdominal metastasis of aortic sarcoma is scarcely documented. Currently, there is no effective treatment regimen available (2, 3). We present a rare case of primary aortic sarcoma with abdominal metastasis and its subsequent treatment. Herein, we report a case of primary aortic intimal sarcoma with abdominal metastasis and its treatment strategy.

Case presentation

A 55-year-old female patient was admitted to the hospital with a primary complaint of "recurrent abdominal pain for over a month, worsened for the past hour." The patient denies smoking or alcohol consumption but has a history of hypertension and a history of mesenteric thrombosis diagnosed one month prior. Upon admission, her blood pressure was 180/110 mmHg, with all other vital signs within normal range. Arterial computed tomography angiography (CTA) revealed The aortic arch, the superior segment of the descending aorta, the inferior segment of the abdominal aorta, the bilateral iliac arteries, and the distal internal portion of the superior mesenteric artery. A filling defect is present in the balance sheet, and the local lumen exhibits severe stenosis (Figure 1A). The attending physician diagnosed her condition as aortic thrombosis. She was urgently transferred to the First Affiliated Hospital of Zhejiang University for surgical treatment, After meticulous surgical disinfection under general anesthesia, the patient received a longitudinal incision in the bilateral groin, and the bilateral common femoral artery was liberated. Following systemic heparinization (intravenous injection of 100U/kg heparin), the

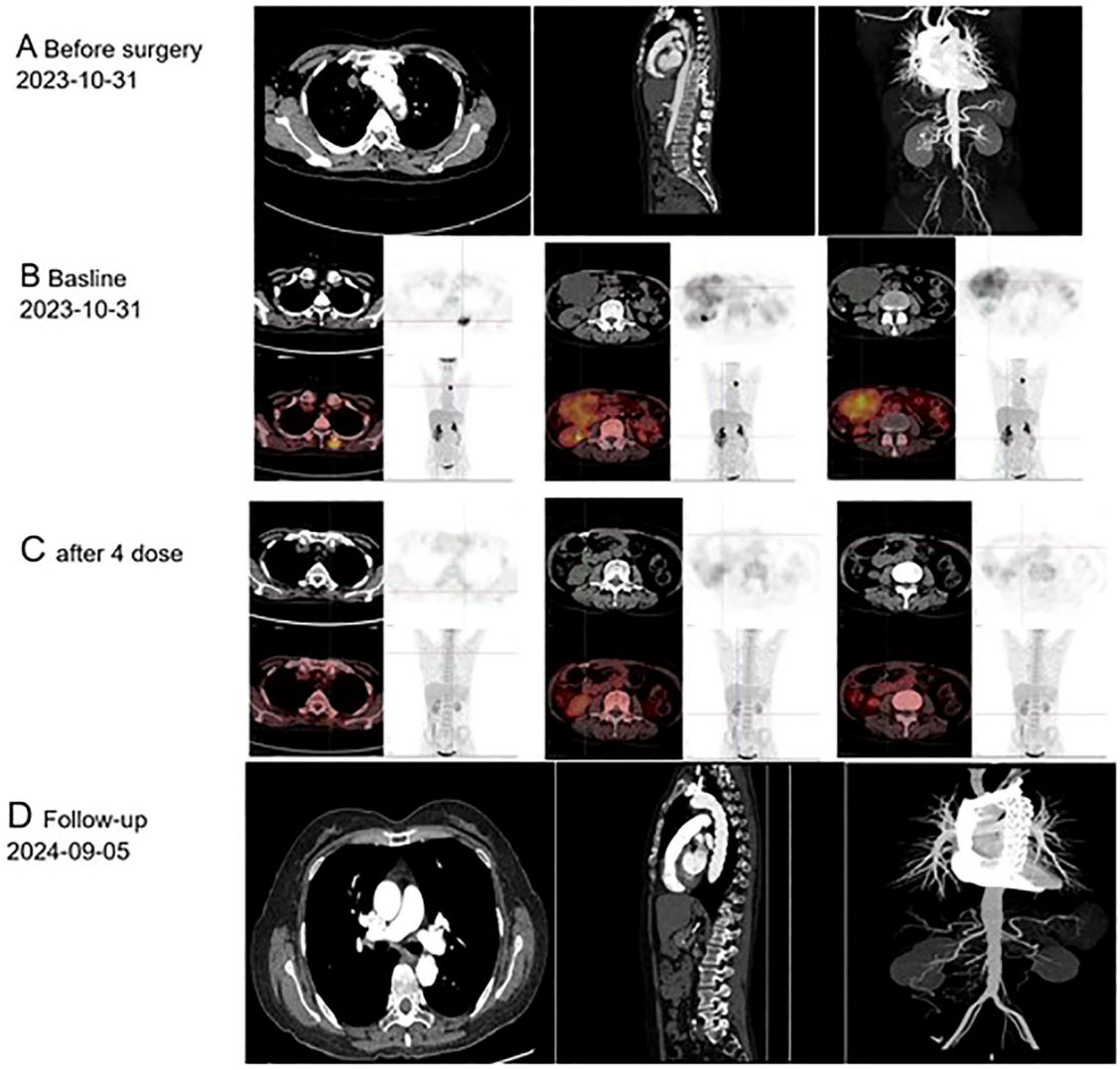

FIGURE 1
Imaging findings of primary endovascular sarcoma: **(A)** Computed Tomography conducted prior to October 31, 2023; **(B)** Positron Emission Tomography performed before December 14, 2023; **(C)** Positron Emission Tomography following four cycles of postoperative chemotherapy; **(D)** Follow-up care, September 5th, 2024.

femoral artery approach catheter was utilized to access the thoracic aorta. Angiography disclosed large filling defects in the descending aorta and distal occlusion of the superior mesenteric artery. Occlusion was present from the lower abdominal aorta to the bifurcation of both iliac arteries. Once the CODA balloon was sent to the thoracic aorta along the catheter guide wire, the balloon was inflated, and the thrombus was withdrawn. Reimaging indicated that the filling defect of the thoracic aorta was reduced compared to previous imaging, and a covered stent of 26-22 *160mm was placed at the distal end of the left subclavian artery. Again, the abdominal aorta was accessed via the bilateral femoral artery approach, and a considerable amount of jelly-like neoplasms were removed through the thrombectomy catheter. The abdominal aorta, bilateral common iliac artery, and external iliac artery were found to have smooth blood flow. After the bilateral femoral artery incision was trimmed, the intima was exfoliated, and the bilateral common femoral artery incision was sutured. The femoral artery pulsated well upon opening the blood flow. The bilateral groin incisions were sutured layer by layer. Frozen section analysis identified the presence of aortic intimal sarcoma (Figures 2A, B), and the tumor was resected with clear margins. The tumor cells were positive for vimentin and MDM2 (Figures 2C, D), confirming the diagnosis of aortic intimal sarcoma.

After a month, she returned to the hospital with a recent onset of sharp, acute, and persistent abdominal pain. Positron Emission Tomography-Computed Tomography (PET-CT) showed fluorodeoxyglucose (FDG) accumulation in the small intestine, part of the jejunum, and back muscles (Figure 1B). The patient was transferred to the Department of Vascular Surgery for palliative tumor removal. Following general anesthesia, the patient was positioned in a supine posture and a 15-cm incision was executed in the mid-abdomen. During the surgical procedure, a palpable mass was discerned in the ascending mesocolon (approximately 10*10 cm), which permeated the mesocolon and invaded the jejunum. 40 cm distant from the Treitz ligament, several enlarged lymph nodes were detectable in the mesentery, concurrent with adhesion of the omentum and small intestine. Moreover, 5.0*5.0 masses were identified subcutaneously on the back. In light of the intraoperative observations, resection of the abdominal and back masses, local resection of the small intestine, jejune-jejunal side-to-side anastomosis, and lysis of intestinal adhesions were carried out. Histopathological examination confirmed intimal sarcoma, Weakly positive for vimentin, staining positive for MDM2 (Figures 2C, D). Two weeks after surgery, the patient received chemotherapy with Cisplatin (38 mg, Days 1-3) combined with epirubicin (110 mg, Day 1) every three weeks without radiation treatment. After four cycles of this regimen, the patient's symptoms were completely resolved with no adverse events. PET-CT revealed No fluorodeoxyglucose accumulation (FDG) was observed in the operative area (Figure 1C). The patient has exhibited no tumor progression and has been under our follow-up care from October 1, 2023, to September 20, 2024 (Figure 1D). So we think The local surgical treatment combined with chemotherapy may represent an effective approach for peritoneal metastasis of primary aortic intimal sarcoma. However, further cases are required to substantiate this conclusion.

Discussion

Aortic intimal sarcoma is an exceptionally rare neoplasm, and due to the rarity and limited clinical data available on this disorder, the majority of patients are diagnosed at advanced stages, resulting in a poor prognosis. The median survival for affected individuals is approximately 16 months (range: 0–168 months) (1, 2), with 3-year and 5-year survival rates at approximately 11.2% and 8%, respectively. The male to female ratio among patients is about 2:1, with the average age at diagnosis being 60 years (range: 48–85 years) (2). The principal clinical manifestations include vascular embolism or occlusion, primarily caused by arterial emboli.

Here, we report a case of aortic sarcoma in a 55-year-old female patient with abdominal metastasis, presenting with severe abdominal pain and symptoms of arterial embolization, which led to an initial misdiagnosis. During the patient's first surgery, pathological examination revealed MDM2 positivity. The diagnosis of primary aortic sarcoma was established based on its location, pathological findings, and medical history. Approximately

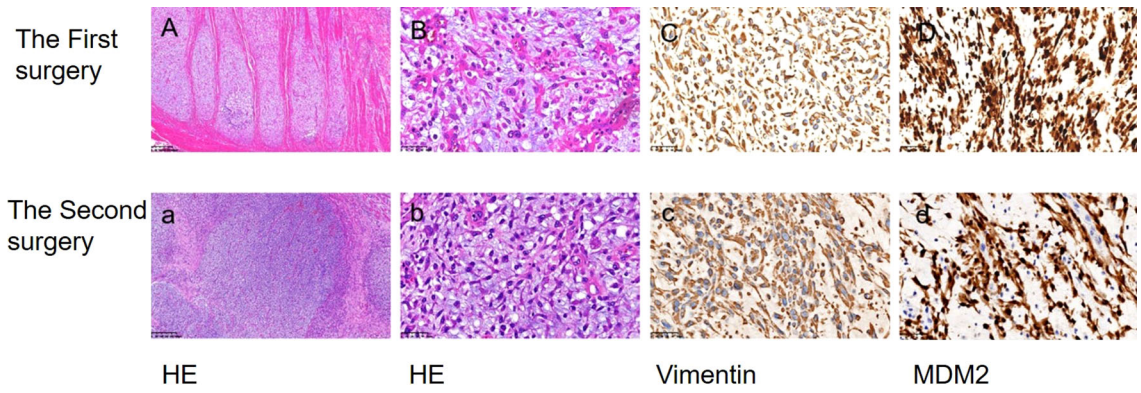

FIGURE 2
The morphological characteristics and immunohistochemical findings of biopsy specimens were examined. Hematoxylin and eosin staining (HE) revealed the presence of endometrial sarcoma cells (**A, a** ×100; **B, b** ×400). Immunohistochemical analysis demonstrated positive expression of Vimentin and MDM2 (**C, c**; **D, d** ×400).

one month after surgery, the patient experienced a recurrence of severe abdominal pain. PET-CT scans were conducted on the small intestine and back muscles, followed by resective procedures in these areas and chemotherapy administration two weeks later.

Histologically, MDM2 overexpression is noted in most cases; however, similar histological features can occur in other conditions that are not specific to this diagnosis. Therefore, the diagnosis primarily relies on correlating clinical manifestations with imaging findings (4). Vimentins are class-III intermediate filaments found in various non-epithelial cells, especially mesenchymal cells. vimentin as an exclusive marker on sarcoma circulating tumor cells regardless of the tissue origin of the sarcoma (5). In Burke and Virmani's analysis of nine cases of aortic intimal sarcoma, vimentin expression was positive (6). Therefore, we hold the belief that the main immune characteristics of aortic endovascular sarcoma are as follows: 1. Vimentins derived from the interstitial tissue should be positive; 2. Endometrial sarcomas typically exhibit poor differentiation and nonspecific characteristics, with MDM2 expression observed in over 70% of cases (7). To more accurately differentiate types of sarcomas, it is essential to conduct smooth muscle staining and epithelial marker staining. These procedures are indeed necessary when positive MDM2 is identified, as they provide critical diagnostic information.

Some studies suggest that magnetic resonance angiography using gadolinium is the most sensitive imaging modality. Magnetic resonance imaging is crucial as tumors often resemble atherosclerotic plaques on CT imaging, making differentiation difficult (2, 8). In previous studies, PET-CT was primarily used in cases with a high suspicion of early metastasis. In pulmonary endothelial sarcoma, FDG-PET imaging typically demonstrates high F-18 uptake, with a reported mean maximum standardized uptake value (SUVmax) of 7.63 ± 2.21 (9, 10). Another study established a cutoff value of 3.5 for SUVmax to differentiate between cardiac malignancies and benign tumors (11). Wittram et al. observed that the SUVmax values for pulmonary embolism ranged from 0.45 to 3.03 (12). It has been reported that single PET-CT findings are insufficient to definitively differentiate between endometrial sarcoma and pulmonary embolism (13)]. Consequently, the interpretation of PET/CT results should be integrated with additional relevant clinical and imaging information for a comprehensive evaluation. Based on the following,we thinkThis imaging model PET-CT may be useful in: (1) estimating disease stage and tumor burden; (2) Postoperative follow-up to evaluate the residual tumor; (3) Evaluation of early response to neoadjuvant and adjuvant therapy (9).

Given the rarity of aortic sarcoma, no standardized treatment protocols currently exist (2). In the instance of localized disease with no evidence of metastasis, radical resection seems to be the most efficacious treatment option (14). In pulmonary endometrial stromal sarcomas, both doxorubicin and ifosfamide combination chemotherapy regimens have demonstrated efficacy, contingent upon the histological subtype of these tumors (15). Other drugs like carboplatin, epirubicin, cyclophosphamide, gemcitabine, dacarbazine, eposide, and vinorelbine have also demonstrated a positive effect in some cases of pulmonary endometrial stromal sarcomas (16). The patient had a history of hypertension and had undergone two surgical procedures, resulting in a significant cardiac burden. To mitigate this burden, Epirubicinand cisplatin was selected due to its lower cardiotoxicity.

Due to its overexpression of MDM2, small-molecule inhibitors targeting MDM2 may be a potential treatment option. In a recent open-label phase 1b/2 study of MDM2 inhibitors, 20% of patients showed sustained survival for over 15 months (17). However, this study was limited to only 10 cases and had several limitations, so it cannot definitively establish the efficacy of targeted therapy. We present a case of intimal sarcoma with abdominal metastasis treated through a combination of surgical intervention and postoperative chemotherapy. While it is difficult to exclude potential synergistic effects from this combined treatment on favorable outcomes, these findings provide a foundation for clinical trials exploring therapies for Aortic intimal sarcoma.

Data availability statement

The raw data supporting the conclusions of this article will be made available by the authors, without undue reservation.

Ethics statement

The studies involving humans were approved by Ethics Committee of Huzhou Central Hospital. The studies were conducted in accordance with the local legislation and institutional requirements. The participants provided their written informed consent to participate in this study. Written informed consent was obtained from the individual(s) for the publication of any potentially identifiable images or data included in this article.

Author contributions

GY: Writing – original draft, Writing – review & editing. JX: Writing – original draft, Writing – review & editing.

Funding

The author(s) declare that no financial support was received for the research, authorship, and/or publication of this article.

Conflict of interest

The authors declare that the research was conducted in the absence of any commercial or financial relationships that could be construed as a potential conflict of interest.

Generative AI statement

The author(s) declare that no Generative AI was used in the creation of this manuscript.

Publisher's note

All claims expressed in this article are solely those of the authors and do not necessarily represent those of their affiliated organizations, or those of the publisher, the editors and the reviewers. Any product that may be evaluated in this article, or claim that may be made by its manufacturer, is not guaranteed or endorsed by the publisher.

References

1. Mo H, Kwon H-M, Choi J-S, Ahn SJ, Lee Y-S. Multiple embolic infarction due to a primary aortic intimal sarcoma. *J Stroke*. (2016) 18:358–60. doi: 10.5853/jos.2016.00311

2. Scharl M, Bode B, Rushing E, Knuth A, Rordorf T. Uncommon case of brain metastasis in a patient with a history of heavy smoking. *Curr Oncol*. (2014) 21:e728–31. doi: 10.3747/co.21.1880

3. Bartolomé SA, Inaraja-Pérez G-C, Elbaile AJ, Brito MO, Buisán Bardaji JM. Intimal angiosarcoma of the descending aorta presenting as atheroembolism: case report and description of intravascular biopsy. *J Vasc Surg cases Innov Tech*. (2023) 9:101230. doi: 10.1016/j.jvscit.2023.101230

4. Neuville A, Collin F, Bruneval P, Parrens M, Thivolet F, Gomez-Brouchet A, et al. Intimal sarcoma is the most frequent primary cardiac sarcoma: clinicopathologic and molecular retrospective analysis of 100 primary cardiac sarcomas. *Am J Surg Pathol*. (2014) 38:461–9. doi: 10.1097/PAS.0000000000000184

5. Satelli A, Mitra A, Cutrera JJ, Devarie M, Xia X, Ingram DR, et al. Universal marker and detection tool for human sarcoma circulating tumor cells. *Cancer Res*. (2014) 74:1645–50. doi: 10.1158/0008-5472.CAN-13-1739

6. Nishida N, Yutani C, Ishibashi-Ueda H, Tsukamoto Y, Ikeda Y, Nakamura Y. Histopathological characterization of aortic intimal sarcoma with multiple tumor emboli. *Pathol Int*. (2000) 50:923–7. doi: 10.1046/j.1440-1827.2000.01144.x

7. Zhao C, Chen D, Wu K, Song Y, Rotzinger DC, Danesi TH, et al. Intimal sarcoma of the aortic valve and ascending aorta: a case report. *J Thorac Dis*. (2024) 16:8126–32. doi: 10.21037/jtd-24-1550

8. Ropp AM, Burke AP, Kligerman SJ, Leb JS, Frazier AA. Intimal sarcoma of the great vessels. *Radiographics*. (2021) 41:361–79. doi: 10.1148/rg.2021200184

9. Ito K, Kubota K, Morooka M, Shida Y, Hasuo K, Endo H, et al. Diagnostic usefulness of 18F-FDG PET/CT in the differentiation of pulmonary artery sarcoma and pulmonary embolism. *Ann Nucl Med*. (2009) 23:671–6. doi: 10.1007/s12149-009-0292-y

10. von Falck C, Meyer B, Fegbeutel C, Länger F, Bengel F, Wacker F, et al. Imaging features of primary sarcomas of the great vessels in CT, MRI and PET/CT: a single-center experience. *BMC Med Imaging*. (2013) 13:25. doi: 10.1186/1471-2342-13-25

11. Rahbar K, Seifarth H, Schäfers M, Stegger L, Hoffmeier A, Spieker T, et al. Differentiation of Malignant and benign cardiac tumors using 18F-FDG PET/CT. *J Nucl Med*. (2012) 53:856–63. doi: 10.2967/jnumed.111.095364

12. Wittram C, Scott JA. 18F-FDG PET of pulmonary embolism. *AJR Am J Roentgenol*. (2007) 189:171–6. doi: 10.2214/AJR.06.0640

13. Suto H, Suto M, Inui Y, Okamura A. Difficulty in distinguishing pulmonary arterial intimal sarcoma from pulmonary thromboembolism using FDG PET/CT. *In Vivo*. (2022) 36:1519–22. doi: 10.21873/invivo.12861

14. Abularrage CJ, Weiswasser JM, White PW, Arora S, Sidawy AN. Aortic angiosarcoma presenting as distal arterial embolization. *Ann Vasc Surg*. (2005) 19:744–8. doi: 10.1007/s10016-005-5436-5

15. Pervaiz N, Colterjohn N, Farrokhyar F, Tozer R, Figueredo A, Ghert M. A systematic meta-analysis of randomized controlled trials of adjuvant chemotherapy for localized resectable soft-tissue sarcoma. *Cancer*. (2008) 113:573–81. doi: 10.1002/cncr.v113:3

16. Assi T, Kattan J, Rassy E, Moussa T, Nassereddine H, Honore C, et al. A comprehensive review on the diagnosis and management of intimal sarcoma of the pulmonary artery. *Crit Rev Oncol Hematol*. (2020) 147:102889. doi: 10.1016/j.critrevonc.2020.102889

17. Koyama T, Shimizu T, Kojima Y, Sudo K, Okuma HS, Shimoi T, et al. Clinical activity and exploratory resistance mechanism of milademetan, an MDM2 inhibitor, in intimal sarcoma with MDM2 amplification: an open-label phase ib/II study. *Cancer Discovery*. (2023) 13:1814–25. doi: 10.1158/2159-8290.CD-23-0419

frontiers | Frontiers in Cardiovascular Medicine

TYPE Case Report
PUBLISHED 13 February 2025
DOI 10.3389/fcvm.2025.1509505

Check for updates

OPEN ACCESS

EDITED BY
Reto Asmis,
Wake Forest University, United States

REVIEWED BY
Didem Oguz,
University of Health Sciences, Türkiye
Tareg Bey,
University of Texas MD Anderson Cancer Center, United States

*CORRESPONDENCE
Jinjing Wang
✉ yeauh0209@126.com

RECEIVED 11 October 2024
ACCEPTED 29 January 2025
PUBLISHED 13 February 2025

CITATION
Ye H, Jing Y, Luo S and Wang J (2025) Diagnostic trap: a case report of intimal sarcoma occurring in the left atrium. Front. Cardiovasc. Med. 12:1509505. doi: 10.3389/fcvm.2025.1509505

COPYRIGHT
© 2025 Ye, Jing, Luo and Wang. This is an open-access article distributed under the terms of the Creative Commons Attribution License (CC BY). The use, distribution or reproduction in other forums is permitted, provided the original author(s) and the copyright owner(s) are credited and that the original publication in this journal is cited, in accordance with accepted academic practice. No use, distribution or reproduction is permitted which does not comply with these terms.

Diagnostic trap: a case report of intimal sarcoma occurring in the left atrium

Hua Ye, Yuchen Jing, Shuai Luo and Jinjing Wang*

Department of Pathology, Affiliated Hospital of Zunyi Medical University, Zunyi, Guizhou, China

Background: Intimal Sarcoma (IS) is an exceptionally rare and highly aggressive mesenchymal tumor with an uncertain origin. Its clinical and pathological characteristics are challenging to differentiate from other tumors based merely on histological and cytological morphology. Additionally, the immunohistochemical phenotype lacks specificity. Genomically, IS is distinguished by the amplification of the Mouse Double Minute 2 homolog (MDM2) gene. Presently, there are significant obstacles in clinical diagnosis and differential diagnosis of this condition.
Case demonstration: A 49-year-old male patient was hospitalized due to cough and dyspnea. An echocardiogram indicated a myxoma, leading to the performance of a partial cardiac tumor resection. Post-surgical pathological analysis revealed numerous spindle-shaped tumor cells organized in bundles. The cells displayed significant atypia, areas of necrosis, myxoid degeneration, and pathological mitotic figures. Immunophenotyping indicated positivity for Vimentin, Smooth Muscle Actin, and MDM2, focal positivity for ETS-Related Gene, and a Ki-67 index of 40%, with other markers being negative. Fluorescence *in situ* Hybridization genetic testing confirmed MDM2 gene amplification. The diagnosis was established as IS of the left atrium, World Health Organization grade 2. Post-surgery, six cycles of chemotherapy were administered. An 11-month follow-up period revealed tumor recurrence and progression, with multiple lesions but no distant metastases.
Conclusions: A rare case of cardiovascular IS located in the left atrium has been documented. Diagnosing this condition poses significant challenges based solely on histological, cytomorphological, and immunophenotypic characteristics, as differentiation from angiosarcoma, malignant mesothelioma, synovial sarcoma, and myxofibrosarcoma is difficult. Consequently, diagnosing IS necessitates a comprehensive approach that integrates clinical presentation, echocardiography, and pathological examinations, encompassing morphology, immunohistochemistry, and genomic analysis. Surgical resection remains the primary treatment option. However, the rate of postoperative recurrence is high, and the prognosis remains poor. Adjuvant chemotherapy and radiotherapy are suggested. In advanced cases, comprehensive immunotherapy methods may be employed to enhance patient survival rates and quality of life.

KEYWORDS

diagnosis, immunotherapy, intimal sarcoma, left atrium, MDM2, vascular

Abbreviations
IS, intimal sarcoma; MDM2, mouse double minute 2 homolog; CT, computed tomography; BNP, brain natriuretic peptide; ICIs, immune checkpoint inhibitors.

Background

Cardiac tumors are exceedingly rare, with malignant variants having an even lower incidence, constituting approximately 10% of all cardiac tumors (1, 2). Among primary malignant cardiac tumors, 95% are sarcomas (3). The World Health Organization (WHO) (2015) histopathological classification of cardiac tumors categorizes the histological subtypes of cardiac sarcomas into angiosarcoma, fibrosarcoma, synovial sarcoma, leiomyosarcoma, rhabdomyosarcoma, malignant fibrous histiocytoma, undifferentiated sarcoma, and others. Intimal sarcoma (IS) is classified as a malignant tumor with uncertain differentiation, with its pathogenesis remaining unclear and possibly originating from multipotent mesenchymal cells (4).

Additionally, IS is an exceptionally rare and highly malignant mesenchymal tumor of unknown origin, typically occurring in the intima of large vessels within the systemic or pulmonary circulation (5). It is currently hypothesized to originate from subendothelial intimal mesenchymal cells (6), proliferating into the lumen and locally invading the vessel wall. Furthermore, it can also form tumor emboli that obstruct blood vessels or metastasize distally along small pulmonary arteries (7). Most ISs are poorly differentiated, with immunohistochemical and electron microscopic studies suggesting fibroblastic or myofibroblastic differentiation. A rare instance of cardiovascular IS occurring in the left atrium is documented here, characterized by an acute onset and non-specific clinical manifestations. Due to the rarity of this condition, most information is derived from individual pathological reports.

Case demonstration

A 49-year-old male patient was hospitalized presenting a 20-day history of cough and shortness of breath, which had exacerbated over the past week. The initial diagnosis indicated small pleural effusion and pneumonia. Oral medication did not lead to any improvement, and there was no significant change in weight. Auscultation revealed scattered moist rales in both lungs without wheezing. Heart sounds were normal, with no enhancement or weakening. No additional heart sounds or murmurs were detected in the valve areas, and there was no pericardial friction rub. Palpation revealed mild tenderness below the xiphoid process without rebound tenderness or muscle tension. Symptomatic treatment, including cough suppression and anti-infection therapy, was administered. Ultrasound examination and thoracocentesis and paracentesis and abdominal effusion indicated bilateral pleural effusion (left side encapsulated). A chest thin-layer computed tomography (CT) scan with 3D reconstruction revealed bilateral pleural effusion, small pericardial effusion, and multiple enlarged mediastinal lymph nodes. Elevated levels of brain natriuretic peptide (BNP) were observed, with N-terminal pro-B-type natriuretic peptide at 1,016.2 pg/ml. Echocardiography (Figure 1) indicated a left atrial mass, suggestive of myxoma, obstructive mitral stenosis, mild tricuspid regurgitation, pulmonary hypertension, and small pericardial effusion. Global heart failure was assessed as class II-III (according to the New York Heart Association). Coronary CT angiography showed mild stenosis in the middle segment of the left anterior descending artery, close to the interventricular groove.

The patient's condition was critical, necessitating continuous oxygen therapy and cardiac monitoring. A median sternotomy was performed to partially resect the cardiac tumor with the assistance of cardiopulmonary bypass during open heart surgery. Intraoperative exploration revealed a solid mass, approximately 40 mm × 30 mm, in the left atrium, attached to the orifice of the left atrial appendage. Multiple nodules of varying sizes, with the largest measuring about 10 mm × 5 mm, were observed on the left atrial wall and the posterior leaflet of the mitral valve. The solid mass exhibited a fish-flesh appearance upon cross-section. Based on intraoperative findings, malignancy was suspected. An intraoperative frozen section biopsy suggested a malignant tumor of mesenchymal origin. Complete tumor resection was not feasible during surgery, and the metastatic lesions on the left atrial wall and mitral valve could not be removed.

Pathological examination

Gross examination: A grayish-white mass of tissue, measuring 40 mm × 40 mm × 10 mm, was noted. The cut surface was grayish-white, solid, and had medium consistency.

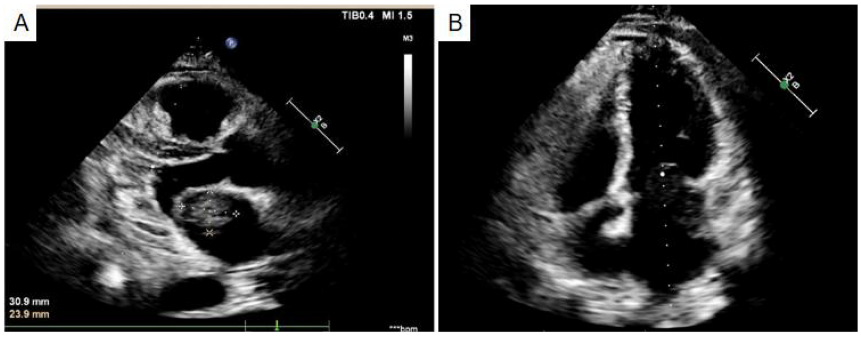

FIGURE 1
Echocardiography indicated a left atrial mass (A), suggestive of myxoma, obstructive mitral stenosis (B).

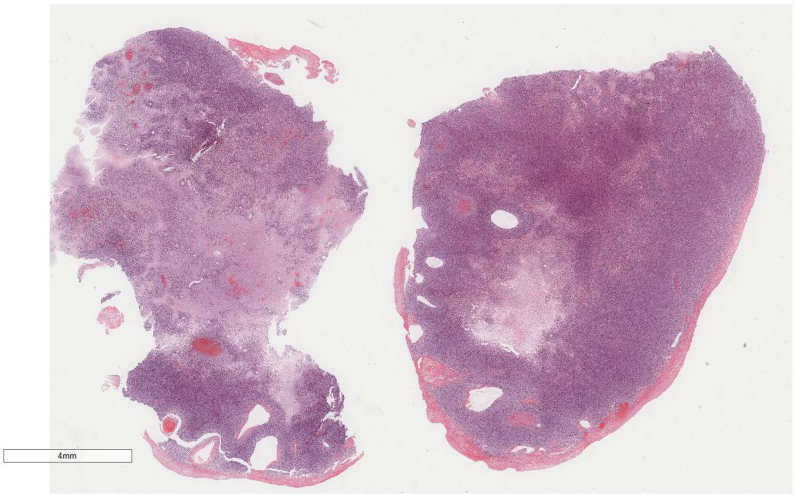

FIGURE 2
At low magnification, the tumor was elliptic and the boundary was clear. H&E × 5.

Microscopic examination (Figure 2): Microscopically, numerous spindle-shaped tumor cells were seen, arranged in fascicular or interlacing patterns (Figure 3). These cells showed significant atypia, with prominent nucleoli and abundant eosinophilic cytoplasm. Focal necrosis and myxoid degeneration were present (Figure 4). The stroma was relatively abundant and exhibited increased vascularity. Multinucleated tumor giant cells were identified in some regions. Mitotic figures were frequently observed, with 4–10 per 10 high-power fields (HPF), including atypical mitoses (Figure 5).

Immunophenotype: Vimentin (+), Smooth Muscle Actin (SMA) (+), Mouse Double Minute 2 homolog (MDM2) (+) (Figure 6), ETS-related gene (ERG) (focally +), Epithelial Membrane Antigen (EMA) (—), Desmin (—), Cluster of Differentiation 31 (CD31) (—), Cluster of Differentiation 34 (CD34) (—), S100 protein (S-100) (—), Ki-67 (Figure 7) proliferation index (40%, +), PD-L1 (22C3):1 point (Figure 8).

Gene detection (Figure 9): A dual-color probe of MDM2/Chromosome Enumeration Probe 12 (CEP12) was utilized, where orange-red signals (R) denoted the MDM2 gene and green signals (G) denoted CEP12. Fifty cells were counted. The MDM2 signals totaled 617, averaging 12.34 per cell, while the CEP12 signals totaled 123, averaging 2.46 per cell. The average ratio of MDM2/CEP12 signals was calculated as 5.02 (>2). The MDM2 amplification status, determined by FISH (fluorescence *in situ* hybridization), was confirmed to be positive.

Pathological diagnosis: IS of the left atrium, WHO grade 2.

Postoperatively, intensive care and specialized nursing were provided. Dynamic blood gas analysis was conducted, and measures to prevent incision infection were implemented. Symptomatic supportive treatments were administered, including hemostasis, acid suppression, expectoration, and myocardial nutrition. Vasoactive drugs were utilized to maintain circulatory stability. Five days post-surgery, a chest CT scan revealed postoperative changes in the sternum, small fluid accumulation in the anterior mediastinum and

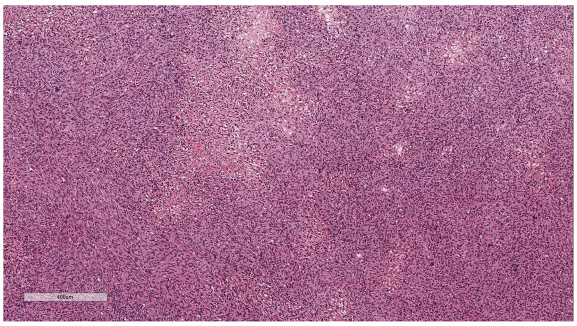

FIGURE 3
Numerous spindle-shaped tumor cells were seen, arranged in fascicular or interlacing patterns. H&E × 50.

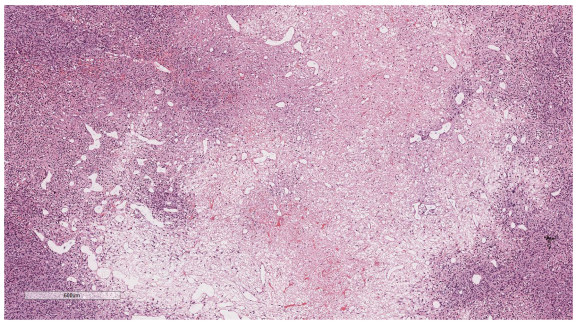

FIGURE 4
Focal necrosis and myxoid degeneration were present. H&E × 40.

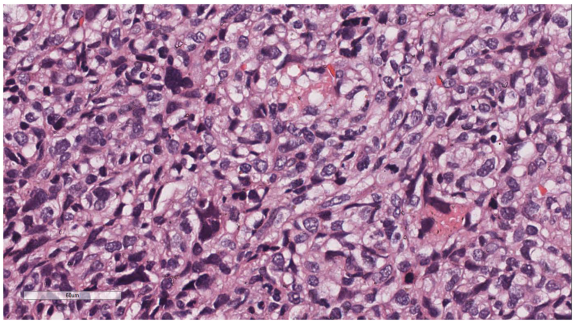

FIGURE 5
Multinucleated tumor giant cells were identified in some regions. Mitotic figures were frequently observed, with 4–10 per 10 high-power fields (HPF), including atypical mitoses. H&E × 400.

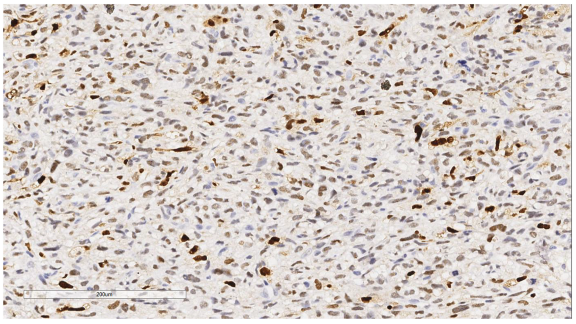

FIGURE 6
Immunohistochemistry reveals a tumor cells MDM2 (+). EnVision, ×200.

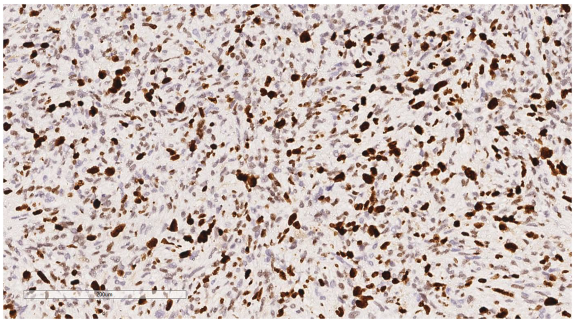

FIGURE 7
Immunohistochemistry reveals a tumor cells Ki-67 proliferation index (40%, +). EnVision, ×200.

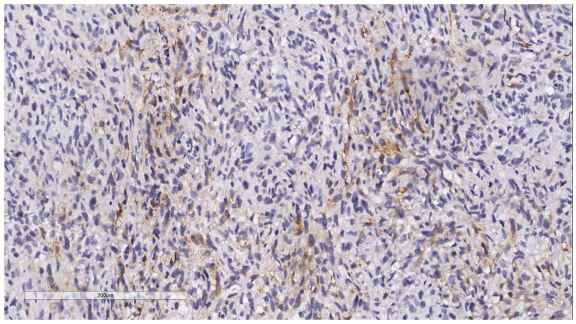

FIGURE 8
Immunohistochemistry reveals a tumor cells PD-L1 (22C3): 1 point. EnVision, ×200.

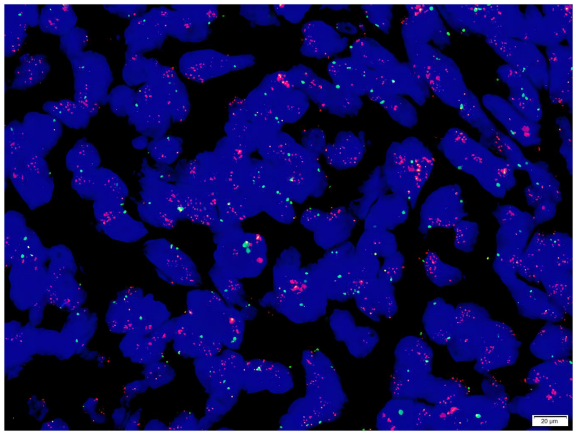

FIGURE 9
The average ratio of MDM2/CEP12 signals was calculated as 5.02 (>2). The MDM2 amplification status, determined by FISH (fluorescence *in situ* hybridization), was confirmed to be positive.

pericardium, pneumonia in both lungs with partial atelectasis in the lower lobes, small bilateral pleural effusions, and enlarged mediastinal lymph nodes. Echocardiography indicated post-partial cardiac tumor resection status with an irregular echo measuring approximately 15 mm × 8 mm near the left atrial appendage, without significant movement. Mild regurgitation of the mitral, tricuspid, and pulmonary valves was observed. Left ventricular systolic function: left ventricular ejection fraction was 60% and fractional shortening was 32%. The electrocardiogram indicated atrial premature beats.

The patient underwent six cycles of chemotherapy within six months following surgery. Each month, a course of chemotherapy was administered, comprising "doxorubicin hydrochloride liposome 55.0 mg + ifosfamide 3.25 g + mesna 0.6 g". Based on medical advice, the patient was admitted to the hospital for treatment of a "cardiac tumor" three months after the final chemotherapy session. The patient reported experiencing chest tightness and shortness of breath at rest, as well as a reduced quality of life. Cardiac ultrasound indicated a solid space-occupying lesion in the left atrium, multiple irregular solid echo masses on the left atrial wall, with the largest measuring approximately 44 mm × 25 mm, left atrial enlargement, poor mobility of the posterior mitral valve leaflet with slightly increased forward flow velocity at the valve orifice, and mild mitral and tricuspid regurgitation. Chest CT revealed

proliferative foci, calcified foci, and multiple fibrotic foci in the upper and lower lobes of both lungs, with increased small lymph nodes in the mediastinum. The oncology department initially planned to administer second-line chemotherapy or immunotherapy according to guidelines. However, the patient reported a poor physical condition, making it difficult to tolerate further chemotherapy. Additionally, due to financial constraints, the patient was unable to afford immunotherapy costs and refused further anti-tumor treatment.

Discussion

Primary malignant cardiac tumors are rare, typically occurring in any part of the heart, though they are more frequently found in the right cardiac system, particularly in the right atrium (8). The case presented in this study involves an IS in the left atrium, an exceedingly rare location. Patients with this condition generally report symptoms such as cough, chest tightness, and shortness of breath, which are often non-specific. A minority may exhibit signs of heart failure, including lower limb edema and dyspnea, complicating the differentiation from other cardiopulmonary diseases. By the time a definitive diagnosis is achieved, the disease has often advanced to the middle or late stages.

Cardiac color Doppler echocardiography can illustrate the movement of the tumor and its impact on hemodynamics, offering a valuable tool for early detection and definitive diagnosis of cardiac tumors (9). Cardiac computed tomography (CCT) can visually show the initial location, extent of the lesion and its adjacent relationship with the surrounding tissue, and observe the perfusion and density of the cardiac space-occupying lesion, which is helpful to evaluate the course of the adjacent coronary artery and pulmonary large vessels, and provide more comprehensive and accurate imaging information for surgery. Cardiac Magnetic Resonance Imaging (CMRI) can noninvasively evaluate the function of the left ventricle and each myocardial segment, display the myocardial perfusion and the location and area of myocardial infarction, and then judge the myocardial activity, which is of great significance in cardiac occupying lesions (10). In imaging, primary cardiac angiosarcoma shows homogeneous or heterogeneous density in plain CT images, and heterogeneous centritic enhancement in enhanced CT images, which can be initially differentiated from benign tumors such as myxoma (11).

In this case, a preoperative cardiac ultrasound revealed a mass in the left atrium, initially suspected to be a myxoma. Nevertheless, the pathological results from surgery remain the gold standard for definitive diagnosis. During partial resection of the cardiac tumor, a solid fish-flesh-like mass measuring approximately 40 mm × 30 mm was observed in the left atrium. Intraoperative frozen section pathology suggested a malignant tumor of mesenchymal origin. Under HE microscopy, the tumor cells appeared spindle-shaped, arranged in an interlacing or fascicular pattern, with significant atypia, distinct nucleoli, and abundant eosinophilic cytoplasm. Areas of patchy necrosis and myxoid degeneration were noted, along with the proliferation of interstitial blood vessels. Some regions showed multinucleated giant tumor cells, with frequent mitotic figures (4–10 per 10 HPF), including atypical mitoses. Immunohistochemical staining showed positivity for Vimentin, SMA, and MDM2, scattered positivity for ERG, negativity for EMA, Desmin, CD31, CD34, and S-100, and Ki-67 positivity in 40% of cells.

The following differential diagnoses should be considered (12):

(1) Angiosarcoma: Microscopically, spindle-shaped or ovoid tumor cells form irregular vascular lumina that interconnect and communicate. These spaces are typically lined by atypical endothelial cells, with occasional multinucleated forms observed. Immunohistochemical markers CD31, CD34, ERG, D2-40, and Factor VIII are positive.
(2) Malignant mesothelioma: Microscopic examination reveals epithelioid tumor cells in papillary or nodular patterns. Occasionally, the tumor displays biphasic characteristics, with spindle cells and mesothelial-like cells coexisting. These cells have abundant eosinophilic cytoplasm, large nuclei with a vesicular or hyperchromatic appearance, and no mitotic figures. Immunohistochemical markers Calretinin and CK5/6 are positive, while adenocarcinoma markers are negative.
(3) Synovial sarcoma: Microscopically, spindle-shaped tumor cells exhibit a biphasic pattern with alternating dense and edematous areas. The cells are small and compact, with occasional lymphocytic infiltration. Epithelioid cells are arranged in clusters or nests, with gland-like structures occasionally observed.
(4) Myxofibrosarcoma: Microscopically, sarcomas tend to have a spindle or short spindle cell pattern, which be asteroidal in mucous area. The nuclei presents rotundity and hyperchromatic, and mitotic figure is rare. Immunohistochemical markers MUC4, DOG1 are positive, CD99, BCL-2 are expressed occasionally, while Desmin, S-100, EMA, CD34 are negative. However, Intimal sarcoma is poorly differentiated malignant tumor, which is difficult to distinguish from other malignancies only in terms of tissue and cell morphology, and the immunohistochemical phenotype lacks specificity, vimentin 、 SMA are positive, others are mostly negative (13). Therefore, in order to further clarify the diagnosis, we sought the help of genomics.

A review of domestic and international literature reveals that genomic studies on cardiac IS are scarce. Regarding molecular alterations, it has been clearly established that IS is characterized by MDM2 amplification (14). MDM2, a proto-oncogene located in the 12q12-15 region near the CDK4, GLI-1, DDIT3, and HMGA2 genes, functions as a negative regulator of TP53 (15). It encodes an oncoprotein acting as an E3 ubiquitin ligase, targeting the p53 protein for proteasomal degradation, thereby circumventing the regulatory effects of the tumor suppressor gene p53 on cell growth (16). Furthermore, reports have indicated that besides MDM2 gene amplification, IS may also exhibit amplifications of CDK4, PDGFRA, GLI-1, HMGA2, DDIT3, and KIT6 (12, 17). Some studies have identified deletions of TP53, RB1, PTEN, CDKN2A, and CDKN2B in IS (18), as

well as loss of p16 expression, which may contribute to disease progression (19). In the present case, molecular testing revealed MDM2 gene amplification, providing a new therapeutic target for the patient. However, the possibility of additional gene therapy targets cannot be excluded.

Currently, no definitive effective treatment regimen exists for this disease, either domestically or internationally. Early diagnosis and surgery are recommended. For cases without distant metastasis, complete surgical resection is the primary choice. However, achieving complete surgical removal is challenging, and the postoperative recurrence rate is high, resulting in poor prognosis (20). Heart transplantation is considered for tumors that have not invaded the myocardial tissue (21). If treatment outcomes are unsatisfactory, the patient's survival period is conservatively estimated at only 6–18 months (22). In this case, the tumor could not be entirely removed during surgery, and metastases in the left atrial wall and mitral valve could not be excised. During an 11-month follow-up, the patient reported poor results after six rounds of chemotherapy, experiencing symptoms such as chest tightness and shortness of breath at rest, with a diminished quality of life. Cardiac color Doppler ultrasound showed enlarged and multiple tumors. Given the patient's condition, the oncology department suggested immunotherapy as a treatment approach.

PD-1 antibodies are currently the most widely used immune checkpoint therapy drugs in clinical practice (23). However, soft tissue sarcomas are immunologically characterized as "cold tumors," and immune checkpoint inhibitors (ICIs) have not shown particularly promising efficacy for soft tissue sarcomas. Current clinical studies on immune checkpoint drugs (such as SARC028 and Alliance A091401) indicate that these drugs are only effective for certain soft tissue sarcomas (24, 25). In this case, the patient's PD-L1 (22C3) score combined with a positive score of 1. PD-1 monoclonal antibody treatment could be considered, but immune checkpoint therapy often takes effect slowly, while sarcomas progress rapidly. Therefore, combining other methods to enhance the efficacy of immune checkpoint therapy is necessary (26), such as small molecule multi-target tyrosine kinase inhibitors and Group A streptococcus preparations. Soft tissue sarcomas are not the optimal tumor type for immune checkpoint therapy, and the development of ICIs is not mature in China. Thus, how to rationally apply ICIs and further integrate them into the comprehensive treatment paradigm for soft tissue sarcomas is a direction that should be pursued in the future, with the hope of bringing more treatment opportunities for patients with advanced soft tissue sarcomas. However, the patient reported poor economic conditions and refused comprehensive immunotherapy.

Conclusion

A rare case of IS in the left atrium is presented. Cardiac IS, an uncommon malignant tumor of the heart, has an unclear origin, potentially involving a unique pathogenic mechanism. Given its atypical clinical presentation and pathological features, it necessitates heightened attention from clinicians and pathologists to avoid misdiagnosis and mistreatment. Future research should focus on enhancing understanding of this disease, thoroughly investigating its immunopathological and molecular pathological changes, and identifying additional genetic targets and immune checkpoints. These advancements would provide new evidence for the classification, diagnosis, and treatment of cardiac malignancies.

Data availability statement

The original contributions presented in the study are included in the article/Supplementary Material, further inquiries can be directed to the corresponding author.

Ethics statement

Written informed consent was obtained from the individual(s) for the publication of any potentially identifiable images or data included in this article.

Author contributions

HY: Resources, Writing – original draft, Writing – review & editing. YJ: Resources, Writing – review & editing. SL: Data curation, Writing – review & editing. JW: Resources, Writing – review & editing.

Funding

The author(s) declare that no financial support was received for the research, authorship, and/or publication of this article.

Acknowledgments

The authors would like to thank all the reviewers who participated in the review and thank Bullet Edits Limited for the linguistic editing and proofreading of the manuscript.

Conflict of interest

The authors declare that the research was conducted in the absence of any commercial or financial relationships that could be construed as a potential conflict of interest.

Generative AI statement

The author(s) declare that no Generative AI was used in the creation of this manuscript.

Publisher's note

All claims expressed in this article are solely those of the authors and do not necessarily represent those of their affiliated organizations, or those of the publisher, the editors and the reviewers. Any product that may be evaluated in this article, or claim that may be made by its manufacturer, is not guaranteed or endorsed by the publisher.

References

1. Crispi F, Martinez JM. 94-cardiac tumors. *Obstetr Imaging Fetal Diagn Care*. (2018):416–8.e1. doi: 10.1016/B978-0-323-44548-1.00094-2

2. Saraiva J, Antunes PE, Carvalho L, Antunes MJ. Primary malignant cardiac tumors: surgical results. *Rev Port Cardiol*. (2016) 35(4):199–204. doi: 10.1016/j.repc.2015.11.005

3. Basso C, Rizzo S, Valente M, Thiene G. Cardiac masses and tumours. *Heart*. (2016) 102(15):1230–45. doi: 10.1136/heartjnl-2014-306364

4. Travis WD, Brambilla E, Nicholson AG, Yatabe Y, Austin JHM, Beasley MB, et al. *WHO Classification of Tumours of the Lung, Pleura, thymus and Heart*. 4th ed. Lyon: IARC Press (2015). p. 300–48.

5. Dewaele B, Floris G, Finalet-Ferreiro J, Fletcher CD, Coindre JM, Gillou L, et al. Coactivated platelet-derived growth factor receptor α and epidermal growth factor receptor are potential therapeutic targets in intimal sarcoma. *Cancer Res*. (2010) 70:7304–14. doi: 10.1158/0008-5472.CAN-10-1543

6. Bode-Lesniewska B, Debiec-Rychter M, Tavora F. WHO Classification of Tumours Editorial Board. In: Fletcher CDM, Bridge JA, Hogendoorn PCW, Mertens F, editors. *WHO Classification of Tumours of Soft Tissue and Bone*. Lyon, France: IARC Press (2020). Intimal sarcoma; p. 315–7.

7. Vinod P, Jabri A, Hegde V, Lahorra J, Cutler D. Functional mitral stenosis: imposture of primary cardiac intimal sarcoma. *Cardiol Res*. (2018) 9(5):307–13. doi: 10.14740/cr748w

8. Burke A. Primary malignant cardiac tumors. *Sem Diagn Pathol*. (2008) 25(1):39–46. doi: 10.1053/j.semdp.2007.10.006

9. Spartalis M, Tzatzaki E, Spartalis E, Moris D, Athanasiou A, Kyrzopoulos S, et al. Primary cardiac intimal sarcoma masquerading as mitral stenosis. *Clin Caserep*. (2017) 5(8):1422–3. doi: 10.1002/ccr3.1089

10. Chen Y, Li Y, Zhang N, Shang J, Li X, Liu J, et al. Clinical and imaging features of primary cardiac angiosarcoma. *Diagnostics (Basel)*. (2020) 10(10):776. doi: 10.3390/diagnostics10100776

11. Ye N, Lan L, Hu H, Liu J, Xu H. Case report: the diagnostic challenge of primary cardiac intimal sarcoma. *Front Cardiovasc Med*. (2023) 10:1089636. doi: 10.3389/fcvm.2023.1089636

12. Neuville A, Collin F, Bruneval P, Parrens M, Thivolet F, Gomez-Brouchet A, et al. Intimal sarcoma in the most frequent primary cardiac sarcoma: clinicopathologic and molecular retrospective analysis of 100 primary cardiac sarcomas. *Am J Surg Pathol*. (2014) 38:461–9. doi: 10.1097/PAS.0000000000000184

13. Nassereddine H, Sciot R, Debiec-Rychter M, Aydin S, Libbrecht L. Cardiac intimal sarcoma: a case report of a rare tumor with peculiar histopathological findings. *Ann Pathol*. (2019) 39(6):440–3. doi: 10.1016/j.annpat.2019.08.001

14. Sciot R. MDM2 Amplified sarcomas: a literature review. *Diagnostics*. (2021) 11:496. doi: 10.3390/diagnostics11030496

15. Agaram NP, Zhang L, Sung Y-S, Singer S, Stevens T, Prieto-Granada CN, et al. GLI1-amplifications Expand the spectrum of soft tissue neoplasms defined by GLI1 gene fusions. *Mod Pathol*. (2019) 32:1617–26. doi: 10.1038/s41379-019-0293-x

16. Feeley KP, Adams CM, Mitra R, Eischen CM. MDM2 Is required for the survival and growth of p53-deficient cancer cells. *Cancer Res*. (2017) 77(14):3823–33. doi: 10.1158/0008-5472.CAN-17-0809

17. Ito Y, Maeda D, Yoshida M, Yoshida A, Kudo-Asabe Y, Nanjyo H, et al. Cardiac intimal sarcoma with PDGFRbeta mutation and co-amplification of PDGFRalpha and MDM2: an autopsy case analyzed by whole-exome sequencing. *Virchows Arch*. (2017) 471:423–8. doi: 10.1007/s00428-017-2135-x

18. Roszik J, Khan A, Conley AP, Livingston JA, Groisberg R, Ravi V, et al. Unique aberrations in intimal sarcoma identified by next-generation sequencing as potential therapy targets. *Cancers (Basel)*. (2019) 11:1283. doi: 10.3390/cancers11091283

19. Giner F, Machado I, Rubio-Martínez LA, López-Guerrero JA, Claramunt-Alonso R, Navarro S, et al. Intimal sarcoma with MDM2/CDK4 amplification and p16 overexpression: a review of histological features in primary tumor and Xenograft, with immunophenotype and molecular profiling. *Int J Mol Sci*. (2023) 24(8):7535. doi: 10.3390/ijms24087535

20. Aboud A, Farha K, Hsieh WC, Brasch F, Ensminger S, Gummert J, et al. Prognostic factors for long-term survival after surgical resection of primary cardiac sarcoma. *Thorac Cardiovasc Surg*. (2019) 67(8):665–71. doi: 10.1055/s-0039-1692409

21. Coelho PN, Banazol NG, Soares RJ, Fragata JI. Long-term survival with heart transplantation for fibrosarcoma of the heart. *Ann Thorac Surg*. (2010) 90(2):635–6. doi: 10.1016/j.athoracsur.2010.01.078

22. Karavasilis V, Seddon BM, Ashley S, Al-Muderis O, Fisher C, Judson I. Significant clinical benefit of first-line palliative chemotherapy in advanced soft-tissue sarcoma: retrospective analysis and identification of prognostic factors in 488 patients. *Cancer*. (2008) 112(7):1585–91. doi: 10.1002/cncr.23332

23. Qin S, Xu L, Yi M, Yu S, Wu K, Luo S. Novel immune checkpoint targets: moving beyond PD-1 and CTLA-4. *Mol Cancer*. (2019) 18(1):155. doi: 10.1186/s12943-019-1091-2

24. Tawbi HA, Burgess M, Bolejack V, Van Tine BA, Schuetze SM, Hu J, et al. Pembrolizumab in advanced soft-tissue sarcoma and bone sarcoma (SARC028): a multicentre, two-cohort, single-arm, open-label, phase 2 trial. *Lancet Oncol*. (2017) 18(11):1493–501. doi: 10.1016/S1470-2045(17)30624-1

25. Seligson ND, Chen JL, Goodrich AC, Van Tine BA, Campbell JD, Richards AL, et al. A multicenter, randomized, non-comparative, phase II study of nivolumab ± ipilimumab for patients with metastatic sarcoma (Alliance A091401): expansion cohorts and correlative analyses. *J Immunother Cancer*. (2024) 12(9):e009472. doi: 10.1136/jitc-2024-009472

26. Pollack SM, Redman MW, Baker KK, Wagner MJ, Schroeder BA, Loggers ET, et al. Assessment of doxorubicin and pembrolizumab in patients with advanced anthra-cycline-naive sarcoma: a phase 1/2 nonrandomized clinical trial. *JAMA Oncol*. (2020) 6(11):1778–82. doi: 10.1001/jamaoncol.2020.3689

frontiers | Frontiers in Cardiovascular Medicine

TYPE Case Report
PUBLISHED 09 April 2025
DOI 10.3389/fcvm.2025.1559173

Check for updates

OPEN ACCESS

REVIEWED BY
Beshay Zordoky,
University of Minnesota Twin Cities, United States
Tareg Bey,
University of Texas MD Anderson Cancer Center, United States

*CORRESPONDENCE
Haixia Yang
yhx2015111@163.com
Xiaoyan Zhang
xiaoyanzhang878@126.com

RECEIVED 12 January 2025
ACCEPTED 25 March 2025
PUBLISHED 09 April 2025

CITATION
Yang H, Sun M, Zhou X, Han Y, Zhang S, Zhang K and Zhang X (2025) Severe immune-mediated myocarditis caused by sintilimab combined with gemcitabine: a case report and literature review.
Front. Cardiovasc. Med. 12:1559173.
doi: 10.3389/fcvm.2025.1559173

COPYRIGHT
© 2025 Yang, Sun, Zhou, Han, Zhang, Zhang and Zhang. This is an open-access article distributed under the terms of the Creative Commons Attribution License (CC BY). The use, distribution or reproduction in other forums is permitted, provided the original author(s) and the copyright owner(s) are credited and that the original publication in this journal is cited, in accordance with accepted academic practice. No use, distribution or reproduction is permitted which does not comply with these terms.

Severe immune-mediated myocarditis caused by sintilimab combined with gemcitabine: a case report and literature review

Haixia Yang[1]*, Menglu Sun[1], Xiaosha Zhou[1], Yaxuan Han[1], Shanshan Zhang[1], Kelin Zhang[2] and Xiaoyan Zhang[1]*

[1]Department of Radiation Oncology, Xi'an Chest Hospital Affiliated to Northwest University, Xi'an, China, [2]Department of Cardiovascular Medicine, Xi'an Chest Hospital Affiliated to Northwest University, Xi'an, China

Following the approval of sintilimab for lung cancer immunotherapy in China in June 2021, real-world clinical practice has confirmed its efficacy and safety. Although there have been limited reports of immune-related myocarditis associated with sintilimab, no fatal cases have been reported to date. This case report focuses on a 71-year-old male patient with lung squamous cell carcinoma who developed severe immune-mediated myocarditis after receiving sintilimab in combination with gemcitabine. The patient presented with immune myocarditis combined with acute myocardial infarction. Due to delayed diagnosis, the outcome was unfavorable. This case is a warning to clinicians for early identification, rapid diagnosis and standardized use of glucocorticoids and immunosuppressants in sindilizumab induced myocarditis and emphasize the importance of multidisciplinary collaboration in managing such rare but serious adverse events.

KEYWORDS

lung cancer, sintilimab, immune myocarditis, multidisciplinary collaboration, delayed diagnosis, case report

Introduction

In recent years, immunotherapy has emerged as a crucial treatment modality for lung cancer, providing new hope by blocking tumor immune escape and activating the body's immune system. Immune checkpoint inhibitors such as PD-1 and PD-L1 have significantly improved treatment outcomes (1). However, immune myocarditis, a rare but fatal adverse reaction, poses a significant challenge to immunotherapy. The incidence of ICI-related myocarditis ranges from 0.27 to 1.14% (2), and it is often severe and life-threatening. The reported incidence of ICIs-related myocarditis is low (<1%), but it can be life-threatening with a mortality rate of up to 60% (3, 4). Early diagnosis is difficult, especially in patients with concurrent cardiovascular diseases, leading to misdiagnosis and missed diagnoses (5). Sintilimab, a humanized monoclonal antibody against PD-1, was approved in China in 2021 for treating non-small cell lung cancer. It effectively blocks the interaction between PD-1 and PD-L1 and PD-L2, enhancing anti-tumor activity. While generally safe, reports of immune myocarditis are limited, and no fatal cases have been reported (6–11). We conducted an extensive search in PubMed, Web of science, CNKI and Wanfang databases by employing the keywords "sintilimab", "lung cancer", and "myocarditis". Through this meticulous search process, a total of seven case reports related to sintilimab induced autoimmune myocarditis in lung cancer patients

were carefully selected. It is notable that all the cases demonstrated either significant improvement or complete cure following proactive and aggressive treatment (see Table 1). This paper specifically presents a case where a patient with lung squamous cell carcinoma and underlying cardiovascular diseases experienced a severe immune-related myocarditis that tragically led to death after receiving the combination therapy of sintilimab and gemcitabine. The primary objective of presenting this case is to heighten clinicians' awareness and comprehension of this exceptionally rare complication. Moreover, it aims to offer valuable guidance for early diagnosis and the implementation of appropriate treatment strategies, with the ultimate goal of enhancing patient outcomes and prognosis.

Case presentation

A 71-year-old male was diagnosed with left superior lobe squamous cell carcinoma (cT4N3Mx) on September 20, 2023. Genetic or PDL-1 testing was not carried out. From October to November 2023, he received radiotherapy for lung and mediastinal lesions, with a target dose of 54Gy and an average cardiac dose of 3.4Gy, achieving a partial response (PR). From December 2023 to July 2024, he underwent 5 cycles of albumin-bound paclitaxel + cisplatin chemotherapy, among which the 4th cycle was combined with recombinant human endostatin (Endu). Due to cardiac reactions related to Endu, the treatment was not completed, and the efficacy was stable disease (SD). In October 2024, the disease progressed (PD), resulting in gemcitabine + sintilimab treatment starting on October 21, 2024. Baseline assessment before immunotherapy revealed normal myocardial injury markers and BNP. ECG showed sinus rhythm, unbiased electrical axis, low extremity conduction voltage, complete right bundle branch block, and prolonged Q-TcF interval. Cardiac ultrasound indicated reduced left ventricular diastolic relaxation function but normal systolic function (EF 63%).

Thyroid function was not tested. The anti-tumor situation is presented in Figure 1, and chest CT images are shown in Figure 2. Previous medical history. The patient has a documented history of cerebral infarction for over a decade, characterized by mild right-sided limb weakness and intermittent numbness in the upper extremities. In May 2024, the patient received a clinical diagnosis of coronary heart disease without undergoing coronary computed tomography angiography (CTA).

The patient is on long-term management with aspirin and atorvastatin.

On November 28, 2024, the patient manifested shortness of breath, accompanied by cough, yellow sputum, fatigue, and bilateral knee pain. However, these symptoms were initially not given sufficient attention. On December 1, 2024, the patient's shortness of breath deteriorated significantly, resulting in emergency hospital admission. The electrocardiogram indicated abnormal Q waves in leads II, III, aVF, and V1-V6, along with ST-segment elevation, suggesting acute myocardial infarction (see Figure 3A). There was a reduced stroke amplitude in the anterior wall, posterior wall, and anterior interventricular septum. Markers of myocardial injury were significantly elevated, such as hypersensitive troponin at 6456.6 pg/ml (reference range: 0–34.2 pg/ml), BNP at 650.8 pg/ml (reference range: 0–100 pg/ml), and myoglobin > 1,200 ng/ml (reference range: 0–146.9 ng/ml) (see Figure 4). Considering the potential for coronary artery stenosis to cause acute myocardial infarction (AMI), a consultation with a cardiologist was sought. However, immune-related myocarditis could not be ruled out. Given that corticosteroid administration in AMI may compromise infarct healing and repeated high-dose corticosteroid therapy could increase the risk of ventricular rupture or aneurysm formation, initial treatment comprised antiplatelet agents (aspirin, clopidogrel), cardioprotective medications (Coenzyme Q10, polarizing solution, nicotinamide), ventricular rate control drugs (metoprolol tartrate, esmolol), heart failure management drugs (recombinant human brain natriuretic peptide), and anti-infective agents (piperacillin-tazobactam, meropenem), without the use of corticosteroids. Additionally, anticoagulant therapy was not initiated owing to the patient's elevated risk of gastrointestinal bleeding secondary to long-term aspirin use. On December 2, 2024, the patient's symptoms of chest tightness and shortness of breath persisted. Coronary angiography was carried out, revealing a 40% stenosis in the left main trunk, a 50% stenosis in the proximal intima of the left anterior descending branch with distal antegrade blood flow at TIMI-3 grade, a 50% stenosis in the proximal circumflex branch, an 85% stenosis in the distal circumflex branch with distal antegrade blood flow at TIMI-3 grade, and patency in the right coronary artery. Although coronary angiography showed no significant stenosis requiring a stent placement (see Figure 5), the patient's ECG and cardiac indicators suggested acute myocardial infarction. Further evaluation of the cause of acute myocardial infarction using IVUS, OCT, or FFR was warranted. This type of myocardial infarction is associated with microvascular dysfunction, coronary artery spasm, plaque rupture, or other rare conditions. The patient may have had acute myocardial infarction combined with immune myocarditis.

As a result, treatment was promptly initiated with 20 g of intravenous human immunoglobulin and 360 mg of methylprednisolone sodium succinate. On December 3, 2024, the patient presented with a poor mental state and intermittent chest tightness as well as shortness of breath. The BNP levels rose to 1,460.7 pg/ml, a marked increase compared to December 1, 2024. The hypersensitive troponin remained at 6,387.5 pg/ml, while myoglobin exceeded 1,200 ng/ml (see Figure 4). Echocardiography revealed an EF of 51% using the biplane method, while Pulse Doppler demonstrated an E/A ratio less than 1. These findings suggest a reduction in left ventricular diastolic function. The dosage of methylprednisolone sodium succinate was adjusted to 240 mg twice daily, and the immunoglobulin shock therapy was continued. At 10:12 AM on December 3, 2024, the patient experienced a sudden loss of consciousness accompanied by hypotensive shock. Immediate interventions included initiating mechanical ventilation support, performing endotracheal intubation, central venous catheterization, urinary catheter insertion, invasive ventilator-assisted respiration, and administration of vasopressors. By 11:36 AM, the patient's vital signs had stabilized; however, he

TABLE 1 Characteristics of reported cases of sintilimab-induced myocarditis in lung cancer patients.

Author, year	Age/ sex	PT/ stage	ICI and Concomitant drugs	Onset of myocarditis	Clinical presentation	ADR	Diagnostic method	Cardiac biomarkers	ECG	Treatment
Lin Y et al., 2022	66/M	Ade/IV	TC + Sintilimab	3 weeks after 1 cycle	Chest pain, shortness of breath	Myocarditis	ECG, UCG, CAG	TnI, CK, CK- MB, NT-proBNP↑	V5 - V9 ST↑	MP, IG
Chen X et al., 2024	33/F	Ade/IV	PC + Sintilimab	2 days after 3 cycles	Shortness of breath, productive cough	Myocarditis	ECG, Chest CT	α - HBDH, cTn, CK-MB, NT-proBNP↑	Tachycardia	MP, De
Bi H et al., 2021	68/M	SCC/IIIb	TC + Sintilimab	6 days after 3 cycles	Productive cough, progressive dysphagia	Myocarditis	ECG, CAG	CK, CK-MB, hs-cTnl, BNP↑	CRBBB, Ⅱ°AVB, diffuse ST segment depression	MP
Xing Q et al., 2020	68/M	Ade/NA	Sintilimab	4 days after 2 cycles	Fatigue, myalgia, shortness of breath, progressive muscle weakness	Myocarditis, myositis, rhabdomyolysis	ECG, UCG	CPK, Myo, TnT, anti-AChR-Ab↑	CRBBB, Ⅲ°AVB	MP, IG, Mestinon, PE, TPM
Xia J et al., 2024	66/M	Ade/IVb	PN + Sintilimab	2 weeks after 2 cycles	Double eyelid ptosis, chest tightness	Myocarditis, hepatitis, pneumonia	ECG, UCG, CTA, Chest CT	CK-MB, Myo, ultra-TNI, NT-proBNP, AST, ALT↑	CRBBB, LAH, LAD, ST-T changes	MP, IG
Hu Y et al., 2023	60/M	SCC/ Ⅰ A3	TC + Sintilimab	after 2 cycles	No symptoms	Myocarditis	CTA, ECG, UCG, CMR, Chest CT, myocardial biopsy	TnT, NT-proBNP↑	Normal sinus rhythm	MP
Zhang Y et al., 2023	58/M	Ade/IVb	PC + Sintilimab	after 1cycle	No symptoms	Myocarditis, myasthenia gravis, myositis	ECG, UCG, CAG, MPI, CMR, EMG	hsTNI, CK, CK-MB, Myo↑	Sinus rhythm, type A pre-excitation syndrome	MP
The present case report	71/M	SCC/ $T_4N_3M_x$	G + Sintilimab	17 days after 1cycle	Shortness of breath, cough, yellow sputum, fatigue, bilateral knee pain	Myocarditis	ECG, UCG, CAG	BNP, CK-MB, ultra-Tnl, Myo↑	Abnormal Q waves, ST-segment elevation	MP, IG

PT, pathological types; ICI, immune checkpoint inhibitors; M, male; Ade, adenocarcinoma; ECG, electrocardiograph; UCG, ultrasonic cardiogram; CAG, coronary arteriography; CMR, cardiac magnetic resonance; F, female; CTA, computed tomography angiography; SCC, squamous cell carcinoma; IG, immunoglobulin; MP, methylprednisolone; CRBBB, complete right bundle branch block; AVB, atrioventricular block; LAH, left anterior hemiblock; LAD, left axis deviation; PE, plasma exchange; ST, sinus tachycardia; APB, atrial premature beats; AT, atrial tachycardia.

10.3389/fcvm.2025.1559173

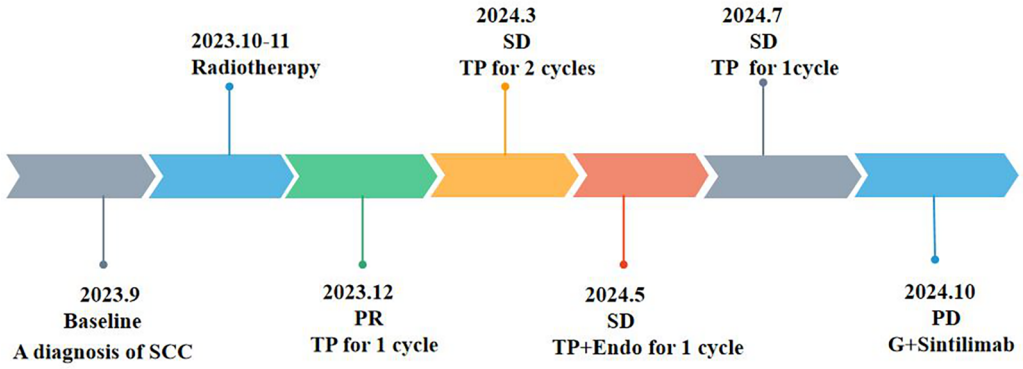

FIGURE 1
Chronology of integrated antitum or therapy.

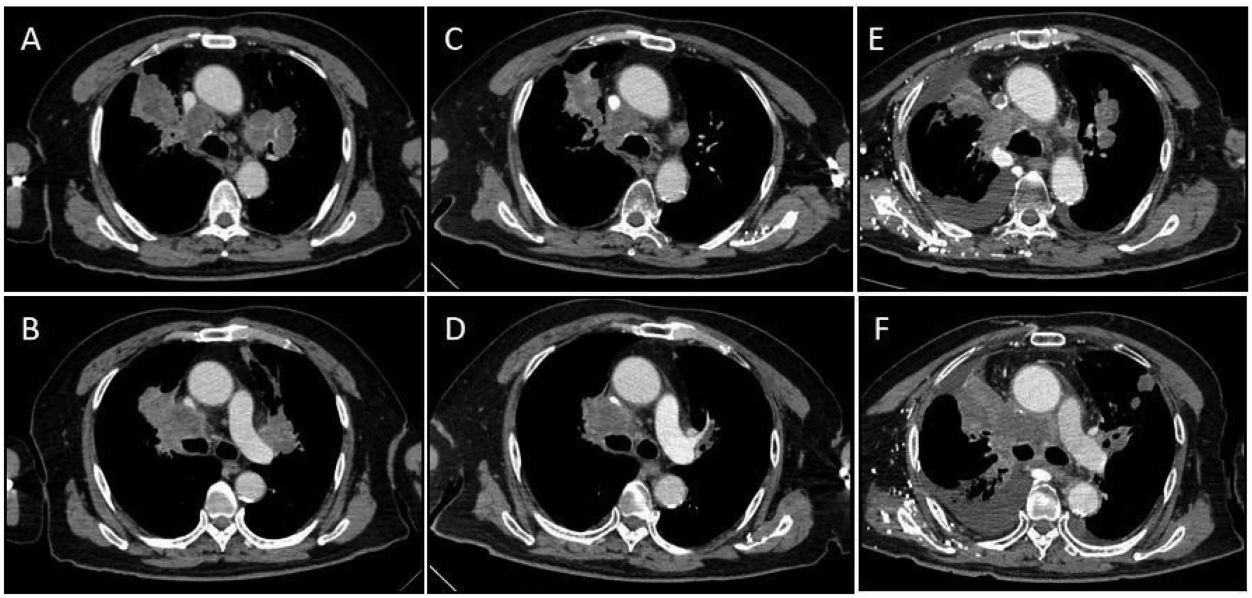

FIGURE 2
Comparison of chest CT images at different stages. (A,B) Initial diagnosis, (C,D) post-radiotherapy, (E,F) pre-immunotherapy with sintilimab.

remained in an unconscious state. High-dose corticosteroids, intravenous immunoglobulin, antimicrobial agents, and anti-shock measures were continued. As of December 4, 2024, the patient remained intubated and dependent on mechanical ventilation without regaining consciousness. Serial measurements revealed a decrease in BNP to 625.6 pg/ml, hypersensitive troponin to 4,117.3 pg/ml, and myoglobin to 702.3 ng/ml, all of which were lower than previous levels (see Figure 4). An electrocardiogram (ECG) revealed an ectopic rhythm, left axis deviation, wide QRS tachycardia (excluding ventricular tachycardia), and a prolonged QTcF interval (see Figure 3C). On December 5, 2024, the hypersensitive troponin level further decreased to 2,561.4 pg/ml; however, both BNP (956.4 pg/ml) and myoglobin (811.5 ng/ml) remained elevated compared to previous levels (see Figure 4). The ECG findings included sinus rhythm, normal electrical axis, sinus tachycardia, complete right bundle branch block, limb lead low voltage, and widespread ST-T changes. Please refer to the clinical context provided in Figure 3D. Due to the family's decision to discontinue treatment, the patient was discharged from the hospital on December 5, 2024, and subsequently passed away on the same day.

Discussion

This paper reports on the diagnosis, treatment, and outcome of grade 4 immune-related myocarditis in a patient with squamous cell carcinoma of the lung after undergoing chemoradiotherapy combined with sintilimab and gemcitabine. It typically

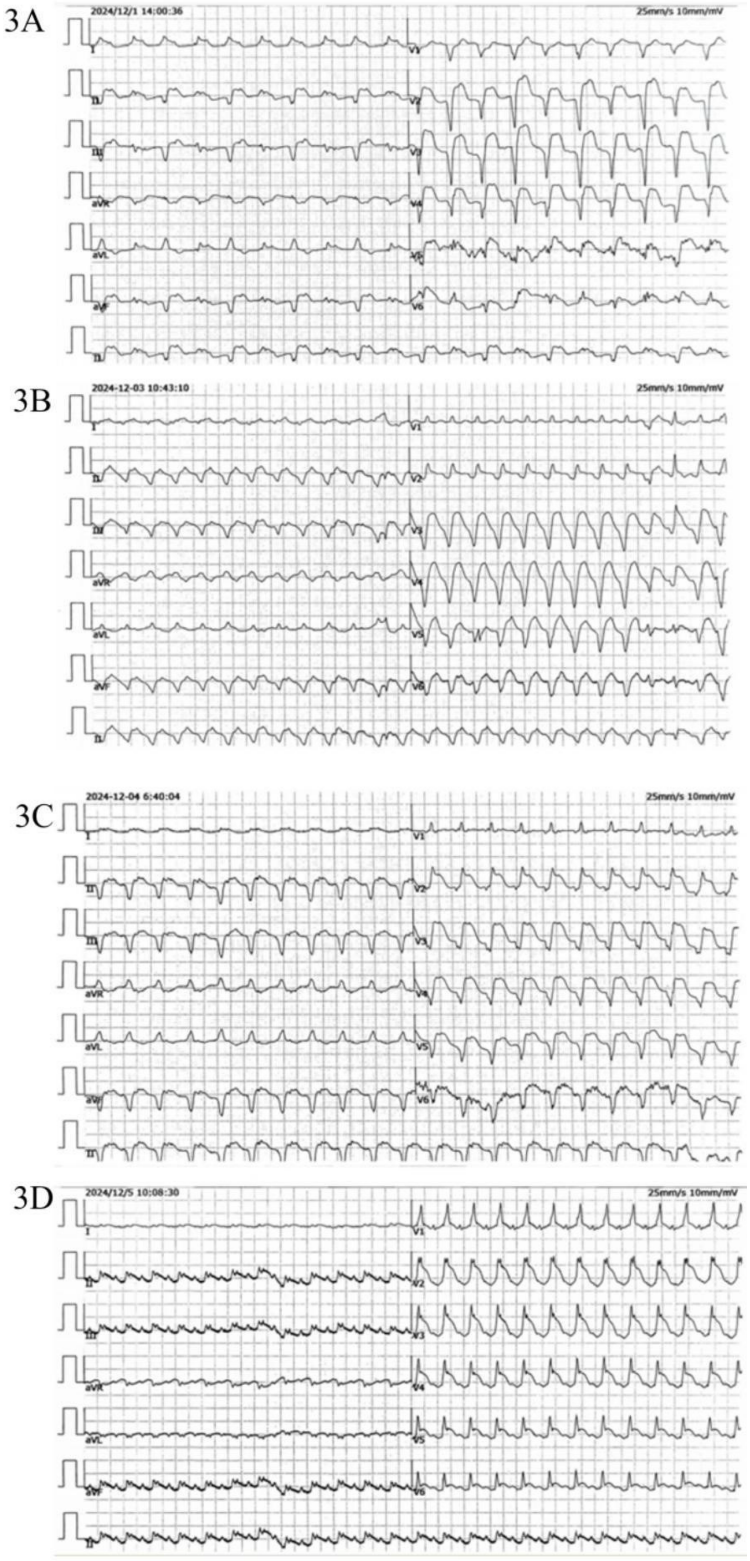

FIGURE 3
ECG **(A)** extensive ST-T changes are observed in leads II, III, aVF, and V1-V6, with the presence of abnormal Q waves and ST segment elevation (2024/12/1). **(B,C)** Ectopic rhythm mean ventricular rate, wide QRS tachycardia. **(D)** Sinus rhythm with sinus tachycardia, complete right bundle branch block, and widespread STT changes across multiple leads.

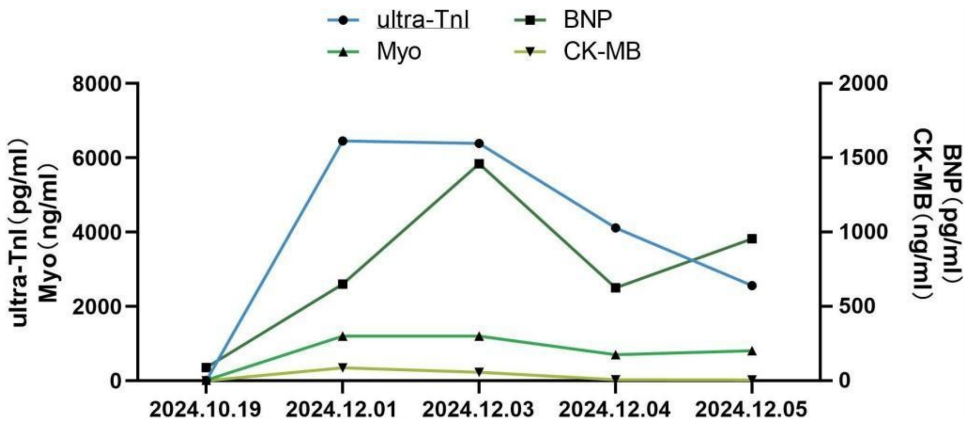

FIGURE 4
Alterations in serum myocardial markers during myocarditis ultra-TnI, high sensitivity cardiac troponin I; BNP, B-type natriuretic peptide; Myo, myoglobin; CK-MB, creatine kinase MB.

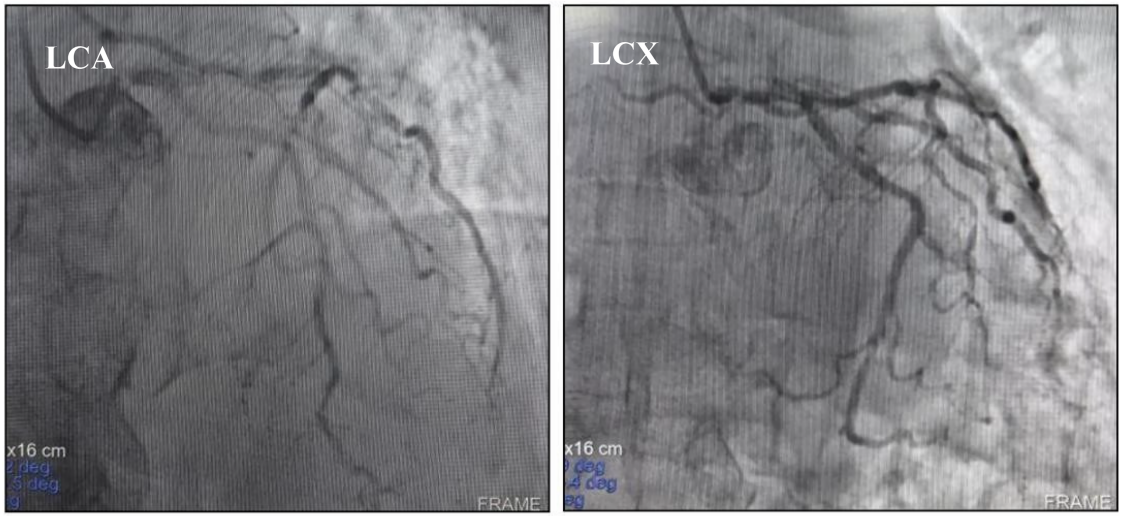

FIGURE 5
Coronary angiography did not support coronary artery disease as the cause of acute myocardial infarction. LCA, left coronary artery; LCX, proximal circular artery.

demonstrates the severity, complexity of diagnosis, and challenging nature of the treatment of this disease. We reflect upon the deficiencies in the diagnosis and treatment process, propose optimization strategies for risk assessment, diagnosis and treatment, and caution clinicians to be highly vigilant about this rare complication throughout the entire process of lung cancer immunotherapy, emphasizing early identification and precise intervention to enhance patient prognosis. In this case, the patient developed immune-associated myocarditis 38 days following administration of sintilimab. The underlying mechanism is likely related to the activation of T lymphocytes by sintilimab. Specifically, T lymphocytes activated by immune checkpoint inhibitors (ICIs) may recognize shared myocardial antigens, resulting in lymphocytic infiltration of the myocardium and subsequent myocarditis (8). When employing ICIs to treat lung cancer patients, clinicians should conduct a comprehensive evaluation and remain highly vigilant regarding the occurrence of immune-associated myocarditis (12, 13). This patient had a 50-year history of smoking and documented histories of cardiovascular and cerebrovascular diseases, coronary heart disease, as well as prior chest radiotherapy and chemotherapy before undergoing immunotherapy. Collectively, these factors constitute significant risk factors for immune-mediated myocarditis. Hence, the risk assessment of immune myocarditis before treatment with sintilimab was inadequate. Furthermore, neither the patients nor their family members demonstrated a robust understanding of monitoring symptoms potentially indicative of myocarditis, such as chest tightness, shortness of

breath, dyspnea, and fatigue, following immunotherapy. Consequently, they were unable to seek medical attention promptly, leading to missed opportunities for early intervention and delayed treatment (14). Injury markers, complicating the diagnostic process. In this case, autoimmune myocarditis coexisted with acute myocardial infarction, which increased the difficulty of diagnosis and treatment. This observation is in line with previous reports, which suggest that immune-associated myocarditis often lacks specific clinical, laboratory, or radiographic diagnostic criteria and must be carefully differentiated from other cardiovascular diseases (15, 16, 25). During the diagnosis, a comprehensive assessment of the patient's medication history, clinical symptoms, cardiac biomarkers, ECG findings, and imaging results is indispensable. Myocardial biopsy should be contemplated if necessary to confirm the diagnosis (17, 24). In this case, the patient rapidly deteriorated after admission, experiencing hemodynamic instability and shock. Endotracheal intubation and resuscitative measures were performed, but dependence on mechanical ventilation made an emergent cardiac biopsy impossible.

The suboptimal treatment outcomes of this patient can be ascribed to two main factors. Firstly, the inherent severity of immune-related myocarditis is marked by its rapid progression. Once it occurs, a considerable number of cardiomyocytes are damaged, causing a sharp decline in cardiac function. Secondly, early diagnosis presents considerable challenges, as myocardial inflammation often reaches an advanced stage by the time it is detected. As a result, the optimal window for intervention is missed, and the current therapeutic options remain limited. While immunomodulatory agents can partially alleviate immune hyperplasia, they are insufficient in completely reversing multifactorial myocardial damage, leading to an adverse prognosis. This highlights the perilous nature and therapeutic complexity of immune-related myocarditis, which is in line with the previously reported high mortality rates (18, 19).

Once immune-related myocarditis is diagnosed, high-dose corticosteroids are considered as the first stage of immunosuppressive therapy (20). Intravenous Methylprednisolone of 1,000 mg/day is recommended as a pulse dose, usually for three days, followed by 1 mg/kg daily either intravenously or orally. The American Society of Clinical Oncology guidelines recommend a tapering of at least 4–6 weeks.

However, specific tapering should be tailored on a case-by-case basis (21). Zhang et al. found that the time of initiation of steroid treatment impacted MACE-free survival, whereby patients receiving corticosteroids within 24 h, regardless of dosage, showed the best outcome, and patients receiving corticosteroids after 72 h, regardless of dosage, showed the worst outcome (22). In this case, the delayed diagnosis of immune-related myocarditis led to missed opportunities for optimal treatment. High-dose methylprednisolone sodium succinate and intravenous immunoglobulin were not administered until five days after symptom onset. Despite aggressive therapeutic interventions, the patient's condition rapidly deteriorated, resulting in a fatal outcome. Furthermore, earlier consideration of immunosuppressants such as infliximab, mycophenolate mofetil (MMF), or tacrolimus, either individually or in combination, along with timely life support treatment, might have potentially improved clinical outcomes. Additionally, insufficient initial dosage of glucocorticoids indicate that clinicians need to enhance their understanding of ICIS-related deadly myocarditis. In summary, preimmunotherapy risk assessment is crucial for elderly patients with a history of cardiovascular and cerebrovascular diseases as well as thoracic radiotherapy and chemotherapy. Timely diagnosis of immune-associated myocarditis is essential to prevent missed treatment opportunities. Furthermore, in the event of deteriorating conditions, it is imperative to promptly optimize the treatment plan and implement multiple measures concurrently. Future research should be focused on further exploring the pathogenesis of immune-related myocarditis and seeking more accurate and effective early diagnostic approaches and personalized treatment plans. In the face of complex diseases, it is crucial to strengthen multidisciplinary collaboration among oncology, cardiology, rheumatology, and other departments to lower the mortality rate of severe immune myocarditis (5, 23).

Data availability statement

The datasets presented in this article are not readily available because of ethical and privacy restrictions. Requests to access the datasets should be directed to the corresponding author/s.

Ethics statement

The studies involving humans were approved by Clinical Research Ethics Committee of Xi 'an Chest Hospital affiliated to Northwest University. The studies were conducted in accordance with the local legislation and institutional requirements. The participants provided their written informed consent to participate in this study. Written informed consent was obtained from the individual(s) for the publication of any potentially identifiable images or data included in this article.

Author contributions

HY: Conceptualization, Funding acquisition, Writing – original draft. MS: Methodology, Data curation, Writing – original draft. XZ: Writing – review & editing, Formal analysis, Data curation, Conceptualization. YH: Conceptualization, Writing – original draft, Data curation. SZ: Formal analysis, Data curation, Writing – review & editing. KZ: Writing – review & editing, Validation. XZ: Conceptualization, Data curation, Investigation, Methodology, Writing – review & editing.

Funding

The author(s) declare that financial support was received for the research and/or publication of this article. This study was

supported by Science and Technology Project of Xi'an City, Shaanxi Province (No. 21YXYJ0076).

Conflict of interest

The authors declare that the research was conducted in the absence of any commercial or financial relationships that could be construed as a potential conflict of interest.

Publisher's note

All claims expressed in this article are solely those of the authors and do not necessarily represent those of their affiliated organizations, or those of the publisher, the editors and the reviewers. Any product that may be evaluated in this article, or claim that may be made by its manufacturer, is not guaranteed or endorsed by the publisher.

References

1. Guo H, Zhang J, Qin C, Yan H, Luo X, Zhou H. Advances and challenges of first-line immunotherapy for non-small cell lung cancer: a review. *Medicine (Baltimore)*. (2024) 103(3):e36861. doi: 10.1097/MD.0000000000036861

2. Moslehi J, Lichtman AH, Sharpe AH, Galluzzi L, Kitsis RN. Immune checkpoint inhibitor-associated myocarditis: manifestations and mechanisms. *J Clin Invest*. (2021) 131(5):e145186. doi: 10.1172/JCI145186

3. Shalata W, Abu-Salman A, Steckbeck R, Mathew Jacob B, Massalha I, Yakobson A. Cardiac toxicity associated with immune checkpoint inhibitors: a systematic review. *Cancers (Basel)*. (2021) 13(20):5218. doi: 10.3390/cancers13205218

4. Moslehi JJ, Salem JE, Sosman JA, Lebrun-Vignes B, Johnson DB. Increased reporting of fatal immune checkpoint inhibitor-associated myocarditis. *Lancet*. (2018) 391(10124):933. doi: 10.1016/S0140-6736(18)30533-6

5. Frascaro F, Bianchi N, Sanguettoli F, Marchini F, Meossi S, Zanarelli L, et al. Immune checkpoint inhibitors-associated myocarditis: diagnosis, treatment and current status on rechallenge. *J Clin Med*. (2023) 12(24):7737. doi: 10.3390/jcm12247737

6. Bi H, Ren D, Wang Q, Ding X, Wang H. Immune checkpoint inhibitor-induced myocarditis in lung cancer patients: a case report of sintilimab-induced myocarditis and a review of the literature. *Ann Palliat Med*. (2021) 10(1):793–802. doi: 10.21037/apm-20-2449

7. Chen Y, Jia Y, Liu Q, Shen Y, Zhu H, Dong X, et al. Myocarditis related to immune checkpoint inhibitors treatment: two case reports and literature review. *Ann Palliat Med*. (2021) 10(7):8512–7. doi: 10.21037/apm-20-2620

8. Hu Y, Liu C, Jin S, Yi Z, Wang C, Pan X, et al. A case of subclinical immune checkpoint inhibitor-associated myocarditis in non-small cell lung cancer. *BMC Pulm Med*. (2023) 23(1):119. doi: 10.1186/s12890-023-02417-4

9. Lin Y, Yuan X, Chen L. Immune myocarditis related to sintilimab treatment in a patient with advanced lung adenocarcinoma: a case report. *Front Cardiovasc Med*. (2022) 9:955527. doi: 10.3389/fcvm.2022.955527

10. Xia J, Wen Y, Xiao M, Ye D, Gao Y, Tang D, et al. Sequential severe immune-related adverse events induced by PD-1 inhibitor: a case report and literature review. *Front Oncol*. (2024) 14:1391698. doi: 10.3389/fonc.2024.1391698

11. Xing Q, Zhang ZW, Lin QH, Shen LH, Wang PM, Zhang S, et al. Myositis-myasthenia gravis overlap syndrome complicated with myasthenia crisis and myocarditis associated with anti-programmed cell death-1 (sintilimab) therapy for lung adenocarcinoma. *Ann Transl Med*. (2020) 8(5):250. doi: 10.21037/atm.2020.01.79

12. Sase K, Fujisaka Y, Shoji M, Mukai M. Cardiovascular complications associated with contemporary lung cancer treatments. *Curr Treat Options Oncol*. (2021) 22(8):71. doi: 10.1007/s11864-021-00869-6

13. Herrmann J. Adverse cardiac effects of cancer therapies: cardiotoxicity and arrhythmia. *Nat Rev Cardiol*. (2020) 17(8):474–502. doi: 10.1038/s41569-020-0348-1

14. Li Y, Liu PJ, Zhang ZL, Wang YN. Cardiac imaging techniques for the assessment of immune checkpoint inhibitor-induced cardiotoxicity and their potential clinical applications. *Am J Cancer Res*. (2022) 12(8):3548–60.

15. Chiang CH, Chiang CH, Ma KS, Hsia YP, Lee YW, Wu HR, et al. The incidence and risk of cardiovascular events associated with immune checkpoint inhibitors in Asian populations. *Jpn J Clin Oncol*. (2022) 52(12):1389–98. doi: 10.1093/jjco/hyac150

16. Pradhan R, Nautiyal A, Singh S. Diagnosis of immune checkpoint inhibitor-associated myocarditis: a systematic review. *Int J Cardiol*. (2019) 296:113–21.

17. Michel L, Rassaf T, Totzeck M. Biomarkers for the detection of apparent and subclinical cancer therapy-related cardiotoxicity. *J Thorac Dis*. (2018) 10(Suppl 35): S4282–95. doi: 10.21037/jtd.2018.08.15

18. Turker I, Johnson DB. Immune checkpoint inhibitor-related myocarditis: current understanding and potential diagnostic and therapeutic strategies. *Expert Opin Drug Saf*. (2023) 22(10):909–19. doi: 10.1080/14740338.2023.2254218

19. Vergara A, De Felice M, Cesaro A, Gragnano F, Pariggiano I, Golia E, et al. Immune-Checkpoint inhibitor-related myocarditis: where we are and where we will go. *Angiology*. (2024) 75(10):909–20. doi: 10.1177/00033197231201929

20. Hu JR, Florido R, Lipson EJ, Naidoo J, Ardehali R, Tocchetti CG, et al. Cardiovascular toxicities associated with immune checkpoint inhibitors. *Cardiovasc Res*. (2019) 115(5):854–68. doi: 10.1093/cvr/cvz026

21. Brahmer JR, Lacchetti C, Schneider BJ, Atkins MB, Brassil KJ, Caterino JM, et al. National Comprehensive Cancer Network. Management of immune-related adverse events in patients treated with immune checkpoint inhibitor therapy: american society of clinical oncology clinical practice guideline. *J Clin Oncol*. (2018) 36(17):1714–68. doi: 10.1200/JCO.2017.77.6385

22. Zhang L, Zlotoff DA, Awadalla M, Mahmood SS, Nohria A, Hassan MZO, et al. Major adverse cardiovascular events and the timing and dose of corticosteroids in immune checkpoint inhibitor-associated myocarditis. *Circulation*. (2020) 141(24):2031–4. doi: 10.1161/CIRCULATIONAHA.119.044703

23. Gilon D, Iakobishvili Z, Leibowitz D. The diagnosis and management of immune checkpoint inhibitor cardiovascular toxicity:myocarditis and beyond. *Vaccines (Basel)*. (2022) 10(2):304. doi: 10.3390/vaccines10020304

24. Chen DH, Tyebally S, Malloupas M, Roylance R, Spurrell E, Raja F, et al. Cardiovascular disease amongst women treated for breast cancer: traditional cytotoxic chemotherapy, targeted therapy, and radiation therapy. *Curr Cardiol Rep*. (2021) 23(3):16. doi: 10.1007/s11886-021-01446-x

25. Declercq A, Verstraete S, Vanwalleghem L, Trenson S. Case report of an ST-elevation myocardial infarction-like presentation of an immune checkpoint (PD-1/PD-L1) inhibitor-associated myocarditis. *Eur Heart J Case Rep*. (2024) 8(9):ytae429. doi: 10.1093/ehjcr/ytae429

frontiers | Frontiers in Oncology

TYPE Case Report
PUBLISHED 14 April 2025
DOI 10.3389/fonc.2025.1515950

Check for updates

OPEN ACCESS

EDITED BY
Reto Asmis,
Wake Forest University, United States

REVIEWED BY
Surendra Rajpurohit,
Augusta University, United States
Maruti Haranal,
U N Mehta Institute of Cardiology and Research, India
Catalin Constantin Badiu,
Carol Davila University of Medicine and Pharmacy, Romania

*CORRESPONDENCE
Pengtao Sun
sunpengtao@gzucm.edu.cn
Weihui Lu
weihui.lu@163.com

†These authors have contributed equally to this work

RECEIVED 23 October 2024
ACCEPTED 27 March 2025
PUBLISHED 14 April 2025

CITATION
Chen S, Cen H, Zhao J, Ran P, Lu W and Sun P (2025) Case report: Diversity of imaging in cardiac angiosarcoma: two cases with disparate enhancement and metabolic manifestations.
Front. Oncol. 15:1515950.
doi: 10.3389/fonc.2025.1515950

COPYRIGHT
© 2025 Chen, Cen, Zhao, Ran, Lu and Sun. This is an open-access article distributed under the terms of the Creative Commons Attribution License (CC BY). The use, distribution or reproduction in other forums is permitted, provided the original author(s) and the copyright owner(s) are credited and that the original publication in this journal is cited, in accordance with accepted academic practice. No use, distribution or reproduction is permitted which does not comply with these terms.

Case report: Diversity of imaging in cardiac angiosarcoma: two cases with disparate enhancement and metabolic manifestations

Sinan Chen[1†], Huan Cen[1†], Jie Zhao[2], Pengcheng Ran[3], Weihui Lu[4*] and Pengtao Sun[1*]

[1]Department of Ultrasonography, The Second Affiliated Hospital of Guangzhou University of Chinese Medicine, Guangzhou, China, [2]Department of Pathology, The Second Affiliated Hospital of Guangzhou University of Chinese Medicine, Guangzhou, China, [3]Department of Nuclear Medicine, The Second Affiliated Hospital of Guangzhou University of Chinese Medicine, Guangzhou, China, [4]Department of Cardiovascular Medicine, The Second Affiliated Hospital of Guangzhou University of Chinese Medicine, Guangzhou, China

Cardiac angiosarcoma, a rare and aggressive malignancy arising from endothelial cells, is difficult to diagnose owing to its nonspecific clinical symptoms and variable imaging features. Two cases of cardiac angiosarcoma (CA) are presented, each with different enhancement and metabolic patterns on imaging. Case 1: A 59-year-old man presented with chest tightness and lower extremity edema. Ultrasound and computed tomography (CT) imaging revealed a hypoechoic/hypodense, non-enhancing mass with pericardial thickening in the right atrium. Positron emission tomography (PET) showed minimal uptake and, given that the patient had elevated D-dimer and fibrinogen levels, a thrombus was initially suspected. However, surgical intervention ultimately led to a diagnosis of CA. Case 2: A 27-year-old man presented with dyspnea and cough. Both ultrasound and CT imaging revealed a mass in the right atrium, with mid-to-low echogenic/hypodense features, heterogeneous enhancement, and pericardial effusion, along with pericardial thickening. A PET scan showed a significant increase in radiotracer uptake within the mass, strongly suggestive of CA. Surgical intervention subsequently confirmed the diagnosis of CA. These two cases demonstrate the presence of distinct enhancement and metabolic patterns on imaging in primary CA and indicate the importance of considering a wide range of enhancement features and metabolic activities in the differential diagnosis of patients presenting with non-specific cardiac symptoms.

KEYWORDS

cardiac angiosarcoma, positron emission tomography, echocardiography, contrast-enhanced ultrasound, cardiac oncology

1 Introduction

Cardiac angiosarcoma (CA), a rare and highly aggressive malignancy originating from endothelial cells, presents significant diagnostic challenges owing to its non-specific clinical manifestations and variable imaging features. Given its biological behavior and poor prognosis, early and accurate CA diagnosis is critical for optimizing therapeutic strategies and improving patient outcomes. Multimodal imaging tools, such as transthoracic echocardiography (TTE), contrast-enhanced ultrasound (CEUS), computed tomography angiography (CTA), and positron emission tomography (PET), are indispensable for the detection, characterization, and staging of CA. While CA typically exhibits hyperenhancement and hypermetabolism on imaging, this report presents two cases of CA with contrasting enhancement and metabolic patterns, highlighting the diversity of enhancement and metabolic pattern combinations in this malignancy. By presenting these cases, we aim to underscore the importance of considering a wide range of imaging and metabolic findings in the diagnosis and management of CA.

2 Case report

2.1 Case 1

A 59-year-old Chinese American male with no prior comorbidities, 179 cm in height and weighing 79 kg, presented to the emergency department with a 4-month history of progressive chest tightness and bilateral lower extremity edema. Upon admission, the patient exhibited acute respiratory distress accompanied by chest pain and lower extremity edema. Electrocardiography (ECG) showed paroxysmal atrial fibrillation (AF), while TTE showed a hypoechoic mass in the right atrium (RA), pericardial thickening, and a left ventricular ejection fraction (LVEF) of 44% with reduced ventricular wall motion (Figure 1A, Online Supplementary Video 1). CEUS further confirmed a filling defect in the RA and an absence of wash-in within the hypoechoic mass (Figure 1B, Online Supplementary Video 2). Both TEE and CTA showed that the mass (measuring 3.0 × 3.7 cm) was located on the right posterior wall of the RA, had a broad base, and involved the superior and inferior vena cava (Figure 1C, Online Supplementary Video 3). CTA also showed hypodense filling defects without enhancement as well as pericardial thickening. A whole-body PET scan revealed an arcuate-shaped increase in radiotracer uptake in the lateral wall of the RA with a maximum standard uptake value (SUV_{max}) of 7.29, while the hypodense mass displayed no significant increase in radiotracer uptake in the PET scan (Figures 2A–C). The patient's creatine kinase (CK) and CK-MB levels were 183 and 11.4 U/L, respectively. The level of lactate dehydrogenase (LDH) was 213 U/L, that of troponin T (TNT) was 0.015 μg/L, and that of N-terminal pro-B-type natriuretic peptide (NT-proBNP) was 915.8 ng/L.

Given the increase in radioactivity in an arcuate-shaped area in the lateral wall of the RA with no significant increase in mass, elevated D-dimer or fibrinogen levels, and low serologic tumor marker levels, the atrial mass was suspected to be a thrombus. The arcuate-shaped increase in radiotracer uptake was attributed to right atrial wall

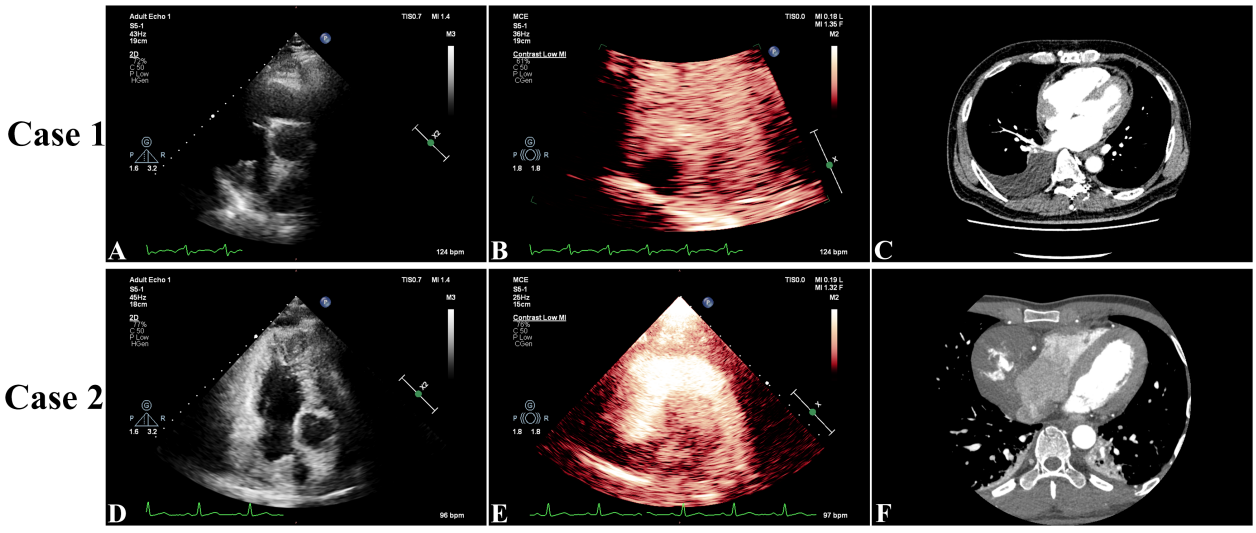

FIGURE 1
In Case 1, preoperative three-dimensional transthoracic echocardiography showed a hypoechoic mass in the right atrium (RA), pericardial thickening, and a left ventricular ejection fraction of 44% with reduced ventricular wall motion **(A)**. Contrast-enhanced ultrasound showed a filling defect in the RA and no wash-in of the hypoechoic mass **(B)**. Arterial phase computed tomography angiography showed that the mass (measuring 3.7 × 3.0 cm) was located on the right posterior wall of the RA and had a broad base **(C)**. In Case 2, transthoracic echocardiography showed a mass with medium-to-low echogenicity, with a broad basal change and an unclear border with the posterior wall of the RA, that extended toward the opening of the superior vena cava. The LVEF was measured at 60% with normal wall movement **(D)**. Contrast-enhanced ultrasound showed a filling defect in the RA with a moderately enhancing mass **(E)**. Computed tomography angiography showed a hypodense right atrial mass (measuring 7.9 × 6.0 cm) with heterogeneous enhancement and pericardial thickening **(F)**.

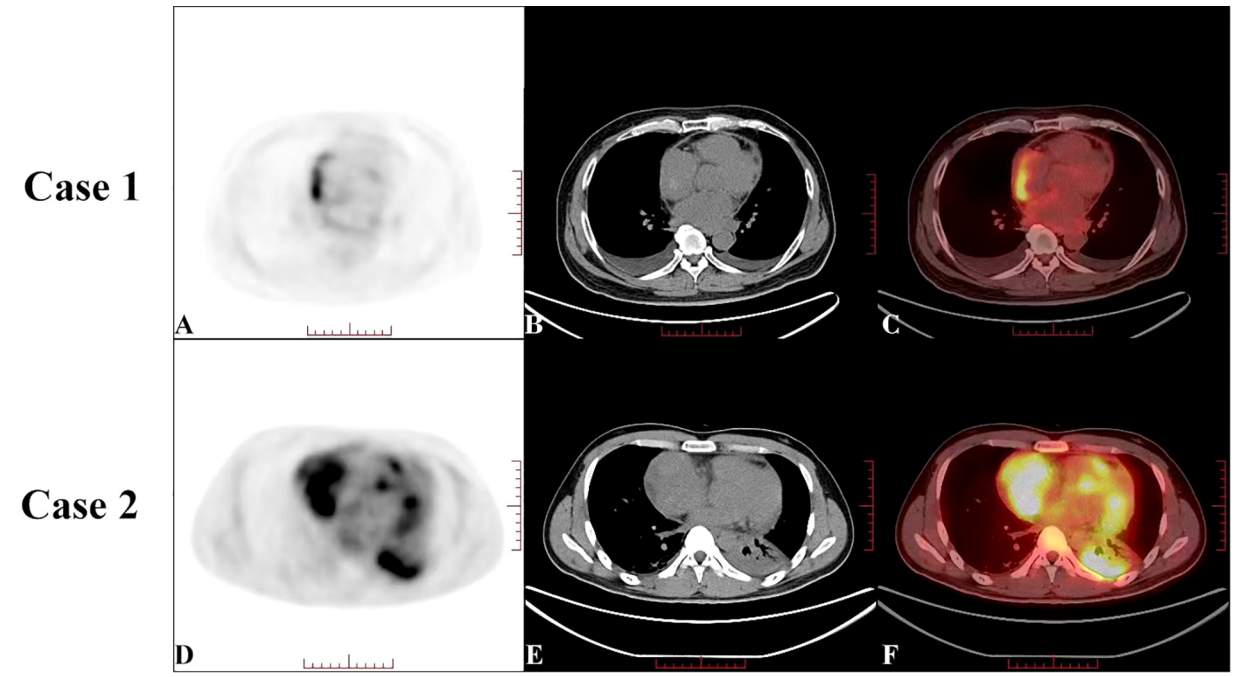

FIGURE 2
Preoperative positron emission tomography-computed tomography (PET-CT) of Case 1 **(A–C)** showed an increase in radiotracer uptake in an arcuate-shaped area in the outer wall of the right atrium, with a maximum standard uptake value (SUV_{max}) of 7.29. The hypodense mass showed no significant increase in radiotracer uptake on the PET scan. Preoperative PET-CT of Case 2 **(D–F)** showed a significant increase in radiotracer uptake in the right atrial mass, with a SUV_{max} of 9.11, which was highly suggestive of cardiac angiosarcoma.

inflammation, possibly related to AF (1, 2). After 2 months of thrombolytic therapy, the patient was readmitted to the hospital for chest tightness, chest pain, recurrent lower extremity edema, and heart failure. A repeat TTE showed a LVEF of 62%, diastolic dysfunction, pericardial thickening, and a hypoechoic mass without significant size reduction. Based on these findings, constrictive pericarditis and right atrial thrombosis were considered, and surgery was performed with a cardiopulmonary bypass time of 325 minutes. During surgery, significant thickening of the posterior wall of the RA (maximum thickness of approximately 40 mm) was observed, along with diffuse thickening of the pericardium. The mass was partially resected. Pathologic examination of the atrial tissue cross-section revealed hemorrhage and necrosis, with diffuse tumor growth and typical vascular areas. The tumor consisted of a combination of solid, epithelioid cells and spindle-shaped cells, with frequent mitotic figures (Figures 3A, B). Immunohistochemical analysis showed positivity for CD34, CD31, ERG, FLi-1, Ki-67, vimentin, EMA, and INI-1 and negativity for CK, CK7, SMA, S-100, and desmin. Based on these findings and the patient's medical history, a diagnosis of CA was made. The patient died 8 days after surgery due to hemodynamic instability and the inability to maintain blood pressure.

2.2 Case 2

A 27-year-old man, 170 cm in height and weighing 67.5 kg, presented to his local hospital with dyspnea and cough. Both TTE and enhanced CT showed significant pericardial effusion and a mass in the RA. Despite undergoing pericardial puncture drainage, his symptoms persisted, and he was transferred to our hospital for further management.

On arrival, his TTE showed a mass in the RA with mid-to-low echogenicity, a broad base, and an unclear boundary with the posterior RA wall. This mass extended toward the superior vena cava orifice, resulting in increased blood flow velocity in the superior vena cava. The LVEF was measured at 60% and wall movement was normal (Figure 1D, Online Supplementary Video 4). CEUS revealed a filling defect in the RA with a moderately enhancing mass (Figure 1E, Online Supplementary Video 5). CT showed a hypodense mass in the RA (7.9 × 6.0 cm) with heterogeneous enhancement and pericardial thickening (Figure 1F, Online Supplementary Video 6). PET revealed a significant increase in radiotracer uptake within the right atrial mass with a SUV_{max} of 9.11, highly suggestive of CA (Figures 2D–F). The patient's CK-MB level was 12.0 U/L. The concentrations of CK, LDH, TNT, and NT-proBNP were 169 U/L, 205 U/L, 0.02 μg/L, and 875.9 ng/L, respectively.

The patient underwent radical resection surgery, during which extensive adhesions between the pericardium and the RA were identified. The cardiopulmonary bypass time of the surgery was 115 minutes, with a cross-clamp time of 73 minutes. The tumor extended superiorly to parts of the superior vena cava, inferiorly to the inferior vena cava orifice, posteriorly to the anterior edge of the atrial sulcus, and left to the anterior edge of the tricuspid annulus. Pathologic examination of the atrial tissue cross-section showed no hemorrhage or necrosis; however, irregular vascular lacunar-like structures could be observed, along with characteristic

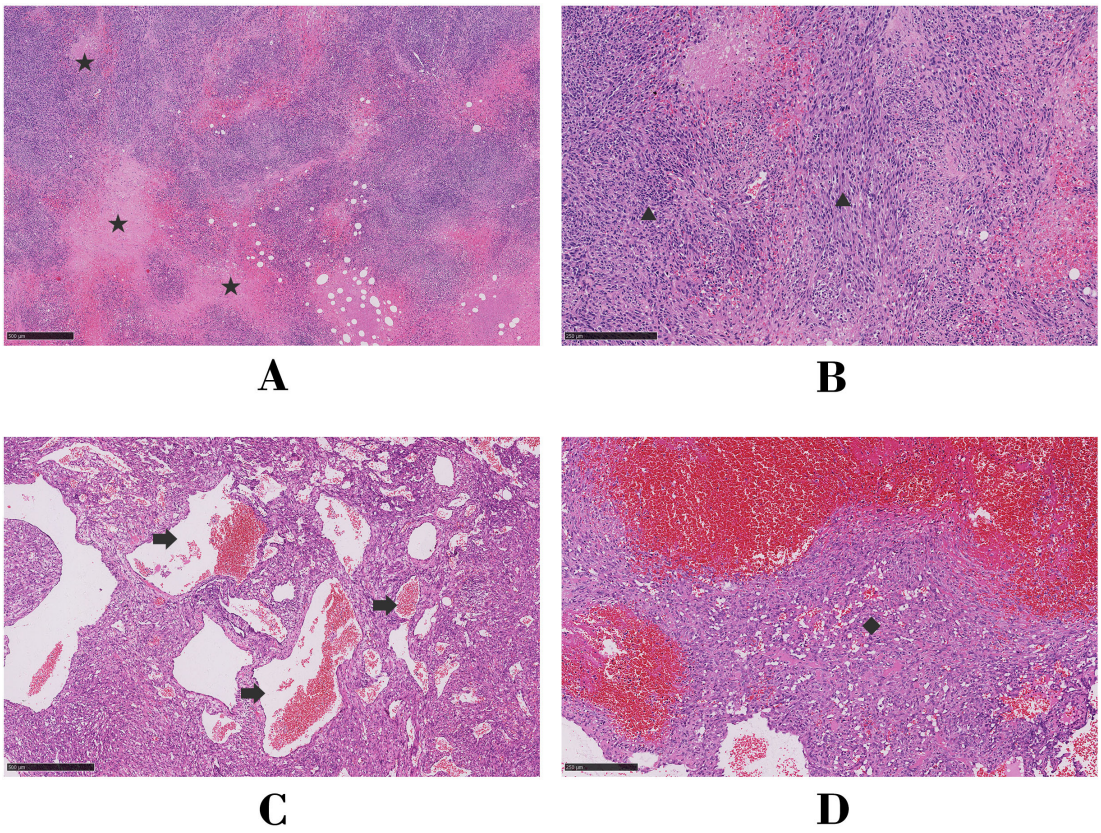

FIGURE 3
Microscopic analysis of hematoxylin and eosin-stained histologic sections for Case 1 **(A, B)** and Case 2 **(C, D)**. Asterisk, focal necrosis; triangle, fusiform tumor cells; arrow, tortuous vessels of the tumor; diamond, solid epithelioid tumor cells.

blood cavities and lakes covered by spindle-shaped endothelial cells. In some areas, endothelial cells were highly proliferative, showing clustered or papillary growth with minimal mitotic figures (Figures 3C, D). Immunohistochemical analysis showed positivity for CD34, CD31, ERG, Ki-67, SMA, and INI-1 and negativity for CK, HMB45, S-100, desmin, and Mrlan-A. Two weeks after surgery, TTE confirmed the disappearance of the original right atrial mass, unobstructed flow in both the superior and inferior vena cava, and a normal RA volume. Enhanced CT images showed no significant metastasis. Monthly follow-up measurements remained stable for eight months after discharge.

3 Discussion

Angiosarcoma is a rare and aggressive soft tissue tumor originating from endothelial cells of blood or lymphatic vessels. It is commonly detected in the extremities, particularly the lower limbs, followed by the trunk, head, and neck. CA is exceptionally rare, accounting for 25%–30% of all primary malignant cardiac tumors, with the RA being the most frequent site of origin (3). The incidence of CA is higher in males (63.1%) than females, with a median age at onset of 50.5 years (4). CA often presents with nonspecific clinical symptoms such as dyspnea, chest pain, fever, and pericardial effusion, which may result from its aggressive nature. Up to 80% of cases initially present with pericardial infiltration, potentially leading to misdiagnosis as constrictive pericarditis (5). Pericardial effusion drainage and cytological biopsy have limited diagnostic success rates for CA (6) and the gold standard for diagnosis remains immunohistochemical analysis of tissue specimens, with markers of positivity including CD31, CD34, ERG, FLI-1, and von Willebrand factor. Among these factors, FLI-1 and ERG demonstrate superior specificity and sensitivity (7, 8).

On two-dimensional echocardiography, CA typically appears as a nodular or lobulated hypoechoic mass. RA-originating CA often presents with a broad-based attachment, accompanied by pericardial effusion or thickening (9). In Case 1, CA invasion into the pericardium caused diffuse thickening and adhesion, leading to restricted movement of the ventricular free wall. In Case 2, the RA mass invaded the superior vena cava, resulting in increased blood flow velocity at the vena cava entrance. Although the diagnostic value of echocardiography for CA is limited, its specificity for detecting intracardiac tumors is as high as 95%, making it the preferred screening method for cardiac tumors (10).

Contrast-enhanced ultrasound provides critical insights into the perfusion characteristics of tumors and serves as a valuable tool for differentiating benign from malignant lesions (11). In Case 1, the complete perfusion defect initially led to misdiagnosis as an atrial thrombus. Notably, 3.6% of malignant tumors exhibit reduced

perfusion due to ischemic necrosis (12), and, in Case 1, the perfusion defect was attributed to extensive intratumoral hemorrhaging and necrosis, a hallmark of poorly differentiated CA (8). In contrast, Case 2 demonstrated moderate heterogeneous enhancement on CEUS, consistent with the histopathological findings of abundant irregular vascular lacunae and minimal necrosis. The striking disparity in CEUS enhancement patterns between the two cases (complete perfusion defect *vs*. moderate heterogeneous enhancement) underscores the significant impact of tumor vascular architecture on perfusion characteristics.

On contrast-enhanced CT, CA typically presents as a homogeneous or heterogeneously dense mass with broad-based attachment and infiltrative margins (13). Characteristic filling defects are observed when the tumor involves the tricuspid annulus or cavoatrial junctions (14). Here, Case 1 exhibited a non-enhancing hypodense lesion initially mistaken for a thrombus, while Case 2 demonstrated heterogeneous enhancement, aligning with classical CA features. These contrasting enhancement patterns—non-enhancing *versus* heterogeneously hyperenhancing—reflect the stark differences in tumor necrosis and vascular supply between these cases. Furthermore, as previously mentioned, the enhancement patterns on CEUS and CT were consistent in both cases, highlighting their complementary roles in characterizing CA vascularity.

Fluorodeoxyglucose (^{18}F-FDG) PET/CT is a crucial imaging modality for assessing tumor metabolic activity (15). Yamakuni et al. established a diagnostic threshold of SUV_{max} ≥3.5, demonstrating 100% sensitivity and 80% specificity for CA diagnosis (16). In Case 1, focal arcuate-shaped uptake (SUV_{max} 7.29) was observed in the RA lateral wall, suggestive of localized hypermetabolic activity. Wan et al. detected potential associations between atrial wall hypermetabolism and atrial fibrillation (1, 2). Given the presence of atrial fibrillation, elevated D-dimer levels, and the absence of significant metabolic activity in the RA mass, the initial diagnosis favored thrombus. However, postoperative pathological analysis revealed that the tumor primarily consisted of hemorrhagic and necrotic tissue, with atrial wall thickening and increased metabolism attributable to tumor infiltration. In contrast, Case 2 demonstrated intense heterogeneous uptake (SUV_{max} 11) within the pericardium-invading mass, consistent with typical CA findings. The marked metabolic heterogeneity between the two cases paralleled the disparities observed on CEUS and contrast-enhanced CT. Notably, Case 1 exhibited low Ki-67 levels, which correlate with the cell division cycle and differentiation status, indicative of poor differentiation (8, 17) and potentially explaining the hypometabolic phenotype.

Owing to the marked heterogeneity in CA differentiation (18), multimodal imaging analysis combining contrast-enhanced and PET metabolic patterns reveals diverse phenotypic combinations, including hyperenhancement with hypermetabolism, hypoenhancement with hypermetabolism, heterogeneous enhancement with hypermetabolism, and heterogeneous enhancement with heterogeneous metabolism. We present the first report of two CA cases exhibiting contrasting enhancement-metabolism patterns, including a rare hypoenhanced-hypometabolic phenotype (Case 1) that has not been previously documented in the literature. This striking dichotomy not only expands the imaging spectrum of CA but also highlights the considerable diversity of enhancement-metabolism pattern combinations.

4 Conclusion

CA is a rare yet highly aggressive malignancy that poses significant diagnostic challenges owing to its atypical clinical presentation. The two cases reported here demonstrated strikingly contrasting enhancement-metabolism patterns (hypoenhanced-hypometabolic *vs*. hyperenhanced-hypermetabolic), reflecting not only the diversity of imaging phenotypes and metabolic patterns but also providing critical insights into the underlying biological heterogeneity of CA.

Data availability statement

The original contributions presented in the study are included in the article/Supplementary Material. Further inquiries can be directed to the corresponding authors.

Ethics statement

The studies involving humans were approved by the Ethics Committee of Guangdong Provincial Hospital of Traditional Chinese Medicine. The studies were conducted in accordance with the local legislation and institutional requirements. The participants provided their written informed consent to participate in this study. Written informed consent was obtained from the individual(s) for the publication of any potentially identifiable images or data included in this article.

Author contributions

SC: Writing – original draft. HC: Conceptualization, Data curation, Funding acquisition, Methodology, Software, Writing – review & editing. JZ: Data curation, Writing – review & editing. PR: Conceptualization, Data curation, Writing – review & editing. WL: Writing – review & editing. PS: Conceptualization, Funding acquisition, Supervision, Writing – review & editing.

Funding

The author(s) declare that financial support was received for the research and/or publication of this article. This work was supported by the Clinical Research Fund of the Traditional Chinese Medicine Science and Technology from the Guangdong Provincial Hospital of Chinese Medicine (GPHCM) (YN2020MS11), the Zhaoyang Talent Research Project of GPHCM (ZY2022YL02), and the

Overseas High-profiled Experts Subsidy Project of Science and Technology Department of Guangdong Province.

Conflict of interest

The authors declare that the research was conducted in the absence of any commercial or financial relationships that could be construed as a potential conflict of interest.

Generative AI statement

The author(s) declare that Generative AI was used in the creation of this manuscript. The author(s) utilized DeepL Write (a generative AI tool) for language polishing and manuscript refinement.

Publisher's note

All claims expressed in this article are solely those of the authors and do not necessarily represent those of their affiliated organizations, or those of the publisher, the editors and the reviewers. Any product that may be evaluated in this article, or claim that may be made by its manufacturer, is not guaranteed or endorsed by the publisher.

Supplementary material

The Supplementary Material for this article can be found online at: https://www.frontiersin.org/articles/10.3389/fonc.2025.1515950/full#supplementary-material

References

1. Wan P, Yu W, Zhai L, Qian B, Zhang F, Liu B, et al. The relationship between right atrial wall inflammation and poor prognosis of atrial fibrillation based on (18)F-FDG positron emission tomography/computed tomography. *Quant Imaging Med Surg*. (2024) 14:1369–82. doi: 10.21037/qims-23-1129

2. Wan P, Wang B, Yu W, Zhai LS, Qian B, Zhang F, et al. Right atrial wall inflammation detected by (18)F-FDG PET/CT may be significantly associated with persistent atrial fibrillation: a prospective case-control study. *BMC Cardiovasc Disord*. (2023) 23:587. doi: 10.1186/s12872-023-03592-2

3. Luo L, Zhao W, Wang Y, Liu K. Cardiac angiosarcoma: A case report and review of the literature. *Echocardiography*. (2021) 38:2083–90. doi: 10.1111/echo.15221

4. Rahouma M, Baudo M, Khairallah S, Lau C, Gaudino M, El-Sayed Ahmed MM, et al. Surgically resected cardiac angiosarcoma: Survival analysis from the national cancer database. *J Clin Med*. (2023) 12:764. doi: 10.3390/jcm12247764

5. Farzin AO, Nejad SS. Cardiac angiosarcoma: a case report. *J Int Med Res*. (2023) 51:3000605231211772. doi: 10.1177/03000605231211772

6. Kupsky DF, Newman DB, Kumar G, Maleszewski JJ, Edwards WD, Klarich KW. Echocardiographic features of cardiac angiosarcomas: the mayo clinic experience (1976-2013). *Echocardiography*. (2016) 33:186–92. doi: 10.1111/echo.13060

7. Fang X, Zheng S. Primary cardiac angiosarcoma: a case report. *J Int Med Res*. (2021) 49:3000605211033261. doi: 10.1177/03000605211033261

8. Liu R, Chen D, Dong F, Wang H, Shang JF, Teng F. Primary cardiac angiosarcoma: a clinicopathological and molecular genetic analysis of thirteen cases. *Zhonghua Bing Li Xue Za Zhi*. (2023) 52:599–605. doi: 10.3760/cma.j.cn112151-20221019-00874

9. Tyebally S, Chen D, Bhattacharyya S, Mughrabi A, Hussain Z, Manisty C, et al. Cardiac tumors: JACC cardioOncology state-of-the-art review. *JACC CardioOncol*. (2020) 2:293–311. doi: 10.1016/j.jaccao.2020.05.009

10. Paraskevaidis IA, Michalakeas CA. Papadopoulos CH and anastasiou-nana M. Cardiac tumors. *ISRN Oncol*. (2011) 2011:208929. doi: 10.5402/2011/208929

11. Wang Q, Wang B, Zhang X, Zhong X, Chang S, Yang J, et al. The usefulness of contrast echocardiography in the evaluation of cardiac masses: a multicenter study. *BMC Cardiovasc Disord*. (2024) 24:43. doi: 10.1186/s12872-024-03708-2

12. Mao YH, Deng YB, Liu YN, Wei X, Bi XJ, Tang QY, et al. Contrast echocardiographic perfusion imaging in clinical decision-making for cardiac masses in patients with a history of extracardiac Malignant tumor. *JACC Cardiovasc Imaging*. (2019) 12:754–56. doi: 10.1016/j.jcmg.2018.08.033

13. Chen Y, Li Y, Zhang N, Shang J, Li X, Liu J, et al. Clinical and imaging features of primary cardiac angiosarcoma. *DX (Basel)*. (2020) 10:776. doi: 10.3390/diagnostics10100776

14. Chen Y, He X, Shang J, Zhang N, Li X, Liu J, et al. CT findings of pulmonary metastases from primary cardiac angiosarcoma. *Curr Med Imaging*. (2021) 17:1216–20. doi: 10.2174/1573405617666210521151753

15. Peng J, Sun PT, Cen H, Liu YX, Zhu W, Ran PC. Incremental value of combinatorial contrast echocardiography and 18F-fluorodeoxyglucose positron emission tomography/computed tomography in giant right atrial myxomas. *J Clin US*. (2022) 50:1268–70. doi: 10.1002/jcu.23360

16. Yamakuni R, Ishii S, Yamada S, Hara J, Suenaga H, Sugawara S, et al. Different prognostic outcomes in two cases of FDG-PET/CT-Positive and -negative cardiac angiosarcoma. *Fukushima J Med Sci*. (2023) 69:45–9. doi: 10.5387/fms.2022-13

17. Kumari N, Bhandari S, Ishfaq A, Butt SRR, Ekhator C, Karski A, et al. Primary cardiac angiosarcoma: A review. *Cureus*. (2023) 15:e41947. doi: 10.7759/cureus.41947

18. Kato A, Nakamoto Y, Ishimori T, Saga T, Togashi K. Prognostic value of quantitative parameters of (18)F-FDG PET/CT for patients with angiosarcoma. *AJR Am J Roentgenol*. (2020) 214:649–57. doi: 10.2214/ajr.19.21635

frontiers | Frontiers in Cardiovascular Medicine

TYPE Case Report
PUBLISHED 30 May 2025
DOI 10.3389/fcvm.2025.1455947

Check for updates

OPEN ACCESS

EDITED BY
Reto Asmis,
Wake Forest University, United States

REVIEWED BY
Didem Oguz,
University of Health Sciences, Türkiye
Fabio Miraldi,
Sapienza University of Rome, Italy

*CORRESPONDENCE
Si M. Pham
✉ pham.si@mayo.edu

RECEIVED 27 June 2024
ACCEPTED 07 May 2025
PUBLISHED 30 May 2025

CITATION
Ali M, Alomari M, El-Sayed Ahmed MM, Garg P, Pham AN and Pham SM (2025) Multiple cardiac papillary fibroelastomas: a case report and review of the literature.
Front. Cardiovasc. Med. 12:1455947.
doi: 10.3389/fcvm.2025.1455947

COPYRIGHT
© 2025 Ali, Alomari, El-Sayed Ahmed, Garg, Pham and Pham. This is an open-access article distributed under the terms of the Creative Commons Attribution License (CC BY). The use, distribution or reproduction in other forums is permitted, provided the original author(s) and the copyright owner(s) are credited and that the original publication in this journal is cited, in accordance with accepted academic practice. No use, distribution or reproduction is permitted which does not comply with these terms.

Multiple cardiac papillary fibroelastomas: a case report and review of the literature

Mostafa Ali[1], Mohammad Alomari[1], Magdy M. El-Sayed Ahmed[1,2], Pankaj Garg[1], Anthony N. Pham[1] and Si M. Pham[1]*

[1]Department of Cardiothoracic Surgery, Mayo Clinic, Jacksonville, FL, United States, [2]Department of Surgery, Zagazig University Faculty of Human Medicine, Zagazig, Egypt

Cardiac papillary fibroelastomas (PFEs) are the most common benign cardiac tumors and are typically solitary. PFEs affecting both sides of the heart are exceptionally rare, with only four cases reported in the literature. Herein, we report a case of a 63-year-old male presenting with signs and symptoms of embolic strokes and an embolism in the coronary arteries. An echocardiogram showed multiple masses on both the mitral and tricuspid valve leaflets. Because of the risk of embolism, he underwent successful valve-sparing surgical resection without complications. The follow-up echocardiogram at 6 months showed no recurrence and competence of both the mitral and tricuspid valves with minimal regurgitation.

KEYWORDS

cardiac papillary fibroelastomas, cardiac tumor, valvular abnormalities, cardiac surgery, management of heart tumors

Background

Primary cardiac tumors (PCTs) are rare; most of the epidemiological data on these tumors are derived from autopsy studies, which estimate an incidence of 0.002%–0.3% and a prevalence of 0.001%–0.03% (1). Most cases are secondary to metastasis, while PCTs account for less than 5%. Among PCTs, benign types are predominant. Within this category, myxomas are most commonly identified in autopsy series, whereas papillary fibroelastomas (PFEs) are more frequently reported through echocardiography and pathology (2). Although the exact prevalence of PFEs remains uncertain, recent investigations estimate it to be approximately 10%, with tricuspid PFEs accounting for 6%–15% of cases (3).

PFEs are small, benign endocardial lesions, primarily valvular, and are clinically significant due to their potential to cause embolic events (4). Cardiac PFEs are typically solitary, with multiple PFEs constituting less than 10% of cases. They usually present on the valvular endocardium of the left side of the heart (5). Multiple PFEs involving both sides of the heart are extremely rare, with only four reported cases in the literature (4, 6–8).

In this report, we present a case of multiple PFEs affecting both the mitral and tricuspid valves in a patient who presented with signs and symptoms of emboli in the coronary arteries and brain.

Case presentation

A 63-year-old male with a history of hyperlipidemia and tobacco use presented with chest pain for 3 days. The patient was afebrile, and the clinical examination was

unremarkable. An electrocardiogram (EKG) revealed ST elevation in leads V3 and V5, and an echocardiogram showed a mobile mass on the posterior leaflet of the mitral valve and two mobile masses on the tricuspid valve: one on the septal leaflet and one in the anterior leaflet (Figures 1, 2). There was minimal mitral and tricuspid regurgitation. Endocarditis vegetations were suspected and intravenous cefazolin was started (2 g/8 h). Brain computed tomography (CT) was obtained as part of the endocarditis evaluation and showed a few areas of decreased attenuation within the subcortical white matter concerning for acute/subacute infarcts. The brain magnetic resonance imaging (MRI) showed multiple small brain infarcts. The patient was thought to have old embolic strokes and transient embolic thrombi.

Laboratory results were within normal limits: hemoglobin 14.6 g/dl, leukocytes 5.5×10^3/µl, platelets 248×10^3/µl, C-reactive protein (CRP) <3 mg/L, erythrocyte sedimentation rate (ESR) 3 mm/h, aspartate aminotransferase (AST) 26 U/L, creatinine 0.84 mg/dl, lactate 1.6 mmol/L, and troponin 8 ng/L. Blood cultures showed no growth. The coronary angiogram revealed eccentric calcified plaques in the proximal and mid segments of the left anterior descending artery (LAD), resulting in mild luminal stenosis, while the distal LAD remained patent. The left circumflex artery (LCX) exhibited calcified and mixed plaques in the proximal segment with mild stenosis. The right coronary artery (RCA) was unremarkable (Supplementary Videos S1, S2). He was placed on systemic anticoagulation—apixaban 5 mg twice a day—and was referred for surgical removal of the cardiac masses. The patient was operated on through median sternotomy on cardiopulmonary bypass. Intraoperative findings include two masses attached to the tricuspid valve: one 8 mm × 5 mm mass

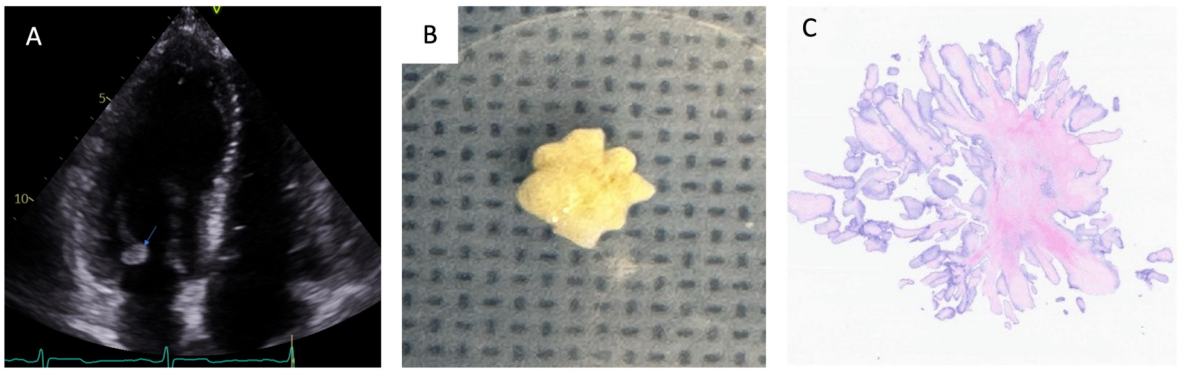

FIGURE 1
Fibroelastoma on the posterior leaflet of the mitral valve. Transthoracic echocardiography revealed a round, mobile mass (indicated by the arrow) adherent to the posterior leaflet of the mitral valve **(A)**. A macroscopic image shows a gray-white lesion measuring 1 cm in its greatest dimension **(B)**. Light microscopy (hematoxylin and eosin staining at 40× magnification) demonstrated papillary fibroelastomas with many avascular fonds lined by endothelial cells **(C)**.

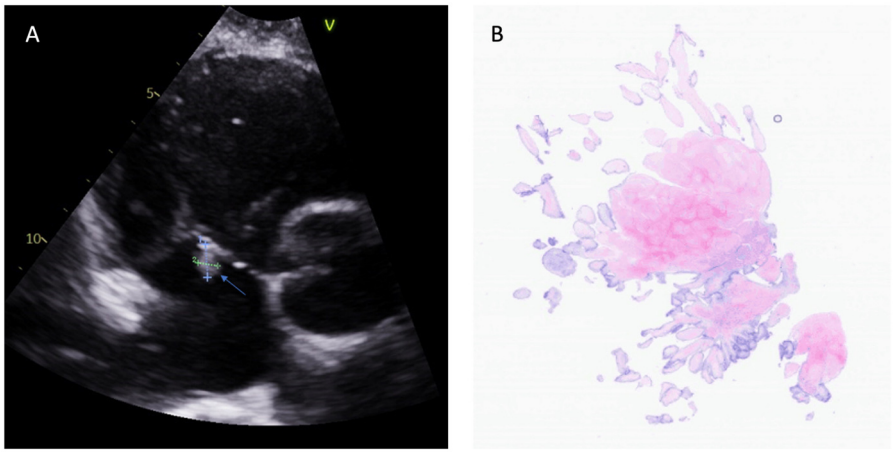

FIGURE 2
Fibroelastoma on the septal leaflet of the tricuspid valve. **(A)** Transthoracic echocardiography identified a small, mobile mass on the septal leaflet of the tricuspid valve (indicated by the arrow). **(B)** Light microscopy (hematoxylin and eosin staining of the mass at 40× magnification) revealed the characteristics of the papillary fibroelastomas.

10.3389/fcvm.2025.1455947

was attached with a stalk to the septal leaflet and a second 5 mm × 5 mm mass was attached to the posterior leaflet near the anteroposterior commissure. Both masses were excised.

In the left side of the heart, there were three discrete masses found on the mitral valve leaflets: a 10 mm × 10 mm on the posterior mitral leaflet at the P2 level, a 5 mm × 7 mm mass on the posterior mitral leaflet at the P3 level, and a third sessile mass (2 mm × 5 mm) on the anterior mitral leaflet at A2 level. In addition, there were multiple micronodules, with a sandpaper appearance on the atrial surface of the anterior leaflet of the mitral valve, covering approximately 20% surface of the anterior leaflet. Moreover, micronodules covered the tip of the medial and lateral papillary muscles. These nodules were too small to resect.

Histopathology confirmed a diagnosis of fibroelastoma (Figures 1, 2). The postoperative course was unremarkable, and the patient was discharged from the hospital on Aspirin 325 mg/day on postoperative day 4. A follow-up echocardiogram at 1 year revealed competent cardiac valves and no residual mass (Supplementary Video S3).

Discussion

Multiple PFEs involving both sides of the heart are rare; only four reported cases have been reported (Table 1). All these patients were female and were older than 40 years of age at the time of diagnosis. It has been suggested that multiple PFEs may emerge due to stimulus-driven responses to heart surgeries and abnormalities such as hypertrophic obstructive cardiomyopathy (HOCM) (8). Further, a genetic association with multiple PFEs has also been recently reported. Muyldermans et al. reported MYBPC3 gene mutation in a patient with HOCM and multiple PFEs (9).

Histopathologically, cardiac PFEs are characterized by an avascular collagenous core, which consists of proteoglycans, elastic fibers, fibroblasts, and occasionally spindle cells and calcification, enveloped by a single layer of endocardial cells. Grossly, they present as mobile papillary projections attached to a stalk (10).

They are often found incidentally through imaging, surgery, or post mortem examinations. While most cases are asymptomatic, symptomatic patients may experience embolization-related complications, with stroke being the most common presentation. In some instances, chest pain due to myocardial infarction or acute abdominal pain due to acute mesenteric ischemia may be their first presentation. Other features, including heart murmurs, dyspnea, pulmonary hypertension, and arrhythmia, were also reported (11, 12). In the four reported cases of multiple PFEs that involved both sides of the heart, one patient was asymptomatic and diagnosed incidentally during routine follow-up (6). Two patients experienced embolic events [pulmonary (8) and brain (7)], and three patients had a history of cardiac disorders, mitral prolapse (6), bradyarrhythmia (4), and Noonan syndrome with HOCM (8).

Echocardiography is highly sensitive and specific, making it the preferred diagnostic tool. PFEs appear as a small (usually not exceeding 20 mm) endocardial mass that is homogenous, well-defined, echo-dense, and mobile with uniform or irregular

TABLE 1 Characteristics of the reported cases of multiple cardiac papillary fibroelastomas.

Reference	Age/sex	Presentation	Cardiac history	Embolic events	No. of valves affected	No. of masses	Valvular insufficiency	Other surgical procedures	Follow-up (months/recurrence)
Patel et al. (4)	76 years/F	Fatigue, pedal edema, and exertional dyspnea	Bradycardia	None	Two: RA, TV, AV, and LV	10	None	None	Not reported
Vittala et al. (6)	53 years/F	Asymptomatic	MV prolapse	None	Three: MV, TV, and PV	3	MV and AV regurgitation	MV annuloplasty, AV repair	1/No
Iosifescu et al. (7)	63 years/F	Embolic stroke	None	Embolic stroke	Three: Chords, MV, TV, PV, and LV endocardium	10	MV and AV regurgitation	MV and TV replacement	Not reported
Kumar et al. (8)	41 years/F	Chest pain, exercise intolerance, and palpitation	Noonan syndrome and HOCM	Pulmonary embolism	Zero: LV and RV	35–40	Moderate PV and TV regurgitation	PV replacement	Not reported
Current case	63 years/M	Asymptomatic	None	Systemic embolism (brain and coronary artery)	Two: MV and TV	5, multiple small nodules	None	None	6/No

MV, mitral valve; TV, tricuspid valve; PV, pulmonary valve; AV, aortic valve; LV, left ventricle; HOCM, hypertrophic obstructive cardiomyopathy; RA, right atrium; RV, right ventricle.

borders and are traditionally associated with single or multiple stalks. The small size is suggestive of a thrombus or vegetation as a differential diagnosis (5). Cardiac CT and MRI can be used as adjunctive diagnostic tests.

Four patients, including ours, exhibited two or three (6, 7) valves affected by PFEs, and the number of masses was <10 (3, 6, 7). There was no valvular involvement in one patient despite 35–40 masses in the left and right ventricles (8). Even though the aortic valve is the most common valve affected with PFEs (12), in patients with multiple bilateral cardiac PFEs, aortic valve involvement has been reported in only one case (4). In patients with numerous PFEs, significant valvular regurgitation may occur and need to be addressed during surgery. In our review, three patients had significant regurgitation in their aortic (6), mitral (6, 7), tricuspid (7, 8), and pulmonary (8) valves, and the affected valve was either repaired or replaced.

Because PFEs carry a potential risk of complications, especially embolic events, complete surgical excision of all the masses is recommended (13). However, it may not be possible to safely remove all the masses without disrupting the heart's integrity, as reported by Patel et al. (4). Furthermore, due to the lack of data, the long-term outcome is unknown. Hence, after surgery, all patients with multiple cardiac PFEs should be closely followed with serial echocardiography to detect any growth of the residual masses or recurrence. Surgical approaches depend on the site, size, number of masses, and surgeon preference. There is no consensus regarding the management of asymptomatic and small right-sided PFEs. Some have suggested regular follow-up, while others have recommended surgical excision (14, 15). For solitary or multiple PFEs involving aortic valves, a minimally invasive technique is gaining popularity; however, median sternotomy remains the preferred approach for multiple PFEs involving both sides of the heart (16). All the patients in the present review underwent surgical resection without major complications; however, follow-up data regarding recurrence were not reported for two of the patients (4, 7). In patients with contraindications to surgery, antiplatelet and/or anticoagulation therapy are recommended with no supporting data (17).

In summary, multiple PFEs that occur on both sides of the heart are rare, but systemic embolization occurs frequently, therefore, surgical removal is recommended to avoid complications. Ongoing, routine follow-up is recommended to monitor for recurrence.

Data availability statement

The original contributions presented in the study are included in the article/Supplementary Material, further inquiries can be directed to the corresponding author.

Ethics statement

Written informed consent was obtained from the individual(s) for the publication of any potentially identifiable images or data included in this article.

Author contributions

MAli: Writing – original draft, Writing – review & editing. MAlo: Writing – original draft, Writing – review & editing. ME: Writing – original draft, Writing – review & editing. PG: Writing – original draft, Writing – review & editing. AP: Writing – original draft, Writing – review & editing. SP: Conceptualization, Data curation, Formal analysis, Funding acquisition, Investigation, Methodology, Project administration, Resources, Software, Supervision, Validation, Visualization, Writing – original draft, Writing – review & editing.

Funding

The author(s) declare that no financial support was received for the research and/or publication of this article.

Conflict of interest

The authors declare that the research was conducted in the absence of any commercial or financial relationships that could be construed as a potential conflict of interest.

Publisher's note

All claims expressed in this article are solely those of the authors and do not necessarily represent those of their affiliated organizations, or those of the publisher, the editors and the reviewers. Any product that may be evaluated in this article, or claim that may be made by its manufacturer, is not guaranteed or endorsed by the publisher.

Supplementary material

The Supplementary Material for this article can be found online at: https://www.frontiersin.org/articles/10.3389/fcvm.2025.1455947/full#supplementary-material

SUPPLEMENTARY VIDEO S1
Coronary angiogram: The Left Anterior Descending (LAD) artery exhibits eccentric calcified plaques in the proximal and mid segments, causing mild luminal stenosis, with the distal LAD remaining patent and free of stenosis. The Left Circumflex (LCX) artery demonstrates calcified and mixed plaques in the proximal segment with mild luminal stenosis.

SUPPLEMENTARY VIDEO S2
Coronary angiogram: The Right Coronary Artery (RCA) appears normal.

SUPPLEMENTARY VIDEO S3
Echocardiogram at the 1-year postoperative follow-up showed normal valvular function with no evidence of residual mass or recurrence.

References

1. Rahouma M, Arisha MJ, Elmously A, El-Sayed Ahmed MM, Spadaccio C, Mehta K, et al. Cardiac tumors prevalence and mortality: a systematic review and meta-analysis. *Int J Surg*. (2020) 76:178–89. doi: 10.1016/j.ijsu.2020.02.039

2. Tamin SS, Maleszewski JJ, Scott CG, Khan SK, Edwards WD, Bruce CJ, et al. Prognostic and bioepidemiologic implications of papillary fibroelastomas. *J Am Coll Cardiol*. (2015) 65(22):2420–9. doi: 10.1016/j.jacc.2015.03.569

3. Chen D, Ma X, He Y, Xie S, Xia J. Papillary fibroelastomas of tricuspid valve. *Acta Cardiol*. (2024) 12:1–2. doi: 10.1080/00015385.2024.2327139

4. Patel N, Harb S, Xu B, Soltesz E, Myles J, Faulx M. Multiple cardiac papillary fibroelastomas. *CASE (Phila)*. (2017) 1(3):104–6. doi: 10.1016/j.case.2017.03.004

5. Sun JP, Asher CR, Yang XS, Cheng GG, Scalia GM, Massed AG, et al. Clinical and echocardiographic characteristics of papillary fibroelastomas: a retrospective and prospective study in 162 patients. *Circulation*. (2001) 103(22):2687–93. doi: 10.1161/01.cir.103.22.2687

6. Vittala SS, Click RL, Challa S, Najib MQ, Khandheria BK, Edwards WD, et al. Multiple papillary fibroelastomas. *Circulation*. (2012) 126(2):242–3. doi: 10.1161/CIRCULATIONAHA.111.049569

7. Iosifescu AG, Enache R, Văleanu L, Timisescu AT, Iliescu VA. Ten tumors in the heart: papillary fibroelastoma with triple valve involvement. *Ann Thorac Surg*. (2022) 114(4):e269–72. doi: 10.1016/j.athoracsur.2021.12.047

8. Kumar TKS, Kuehl K, Reyes C, Talwar S, Moulick A, Jonas RA. Multiple papillary fibroelastomas of the heart. *Ann Thorac Surg*. (2009) 88(6):e66–67. doi: 10.1016/j.athoracsur.2009.08.005

9. Muyldermans P, de Ceuninck M, Dujardin K. Left ventricular hypertrophy and papillary fibroelastoma in a patient with a MYBPC3 gene mutation. *Acta Cardiol*. (2017) 72(1):75–6. doi: 10.1080/00015385.2017.1281550

10. Kurmann R, El-Am E, Ahmad A, Abbasi MA, Mazur P, Akiki E, et al. Cardiac masses discovered by echocardiogram; what to do next? *Struct Heart*. (2023) 7(4):100154. doi: 10.1016/j.shj.2022.100154

11. Gowda RM, Khan IA, Nair CK, Mehta NJ, Vasavada BC, Sacchi TJ. Cardiac papillary fibroelastoma: a comprehensive analysis of 725 cases. *Am Heart J*. (2003) 146(3):404–10. doi: 10.1016/S0002-8703(03)00249-7

12. Tsugu T, Nagatomo Y, Endo J, Kawakami T, Murata M, Yamazaki M, et al. Multiple papillary fibroelastomas attached to left ventricular side and aortic side of the aortic valve: a report of new case and literature review. *Echocardiography*. (2019) 36(6):1194–9. doi: 10.1111/echo.14350

13. Devanabanda AR, Lee LS. Papillary fibroelastoma. In: *StatPearls*. Treasure Island (FL): StatPearls Publishing (2024). [Updated 2023 April 26].

14. Teng P, Hu P, Yuan S, Ma L. Case report: minimally invasive excision of multifocal cardiac papillary fibroelastomas involving right atrium and aortic valve. *Front Cardiovasc Med*. (2022) 9:908567. doi: 10.3389/fcvm.2022.908567

15. Phan TQ, Pham CTV, Bui VDA, Ho TD, Le TN, Nguyen TVT, et al. Minimally invasive resection of heart valve papillary fibroelastoma: two case reports and review of the literature. *J Cardiothorac Surg*. (2023) 18(1):320. doi: 10.1186/s13019-023-02392-1

16. Harling L, Athanasiou T, Ashrafian H, Kokotsakis J, Brown V, Nathan A, et al. Minimal access excision of aortic valve fibroelastoma: a case report and review of the literature. *J Cardiothorac Surg*. (2012) 7:80. doi: 10.1186/1749-8090-7-80

17. Esteban-Lucía L, De La Fuente Batista S, Kallmeyer Mayor AM, Cortés García M. Cardioembolic stroke secondary to an aortic valve fibroelastoma: an increasingly recognized rare cause of stroke. *Stroke*. (2021) 52(4):e111–4. doi: 10.1161/STROKEAHA.120.029361

frontiers | Frontiers in Oncology

TYPE Case Report
PUBLISHED 11 June 2025
DOI 10.3389/fonc.2025.1531668

Check for updates

OPEN ACCESS

EDITED BY
Reto Asmis,
Wake Forest University, United States

REVIEWED BY
Emanuele Micaglio,
IRCCS San Donato Polyclinic, Italy
Chaoyu Wang,
Chongqing University, China

*CORRESPONDENCE
Jianping Gao
gjianping1993@163.com

†These authors have contributed equally to this work

RECEIVED 20 November 2024
ACCEPTED 19 May 2025
PUBLISHED 11 June 2025

CITATION
Du Y, Tian Y, Chen Y, Cheng S and Gao J (2025) Case Report: A very rare case of diffuse large B-cell lymphoma with cardiac and ovarian involvement. *Front. Oncol.* 15:1531668. doi: 10.3389/fonc.2025.1531668

COPYRIGHT
© 2025 Du, Tian, Chen, Cheng and Gao. This is an open-access article distributed under the terms of the Creative Commons Attribution License (CC BY). The use, distribution or reproduction in other forums is permitted, provided the original author(s) and the copyright owner(s) are credited and that the original publication in this journal is cited, in accordance with accepted academic practice. No use, distribution or reproduction is permitted which does not comply with these terms.

Case Report: A very rare case of diffuse large B-cell lymphoma with cardiac and ovarian involvement

Yadan Du[1,2†], Yuting Tian[2†], Yawen Chen[2†], Shuaihua Cheng[2] and Jianping Gao[1*]

[1]Department of Surgical Oncology, Gansu Provincial Hospital, Lanzhou, China, [2]The First School of Clinical Medicine, Gansu University of Chinese Medicine, Lanzhou, China

Background: Diffuse large B-cell lymphoma (DLBCL) is the most prevalent type of aggressive lymphoma, commonly spreading to sites such as the lymph nodes, spleen, bone marrow, liver, lungs, and central nervous system. However, metastasis to the heart and ovaries is relatively uncommon.

Case Description: A 63-year-old woman visited the hospital with abdominal pain and bloating, but showed none of the typical signs of lymphoma. Imaging scans revealed abnormal masses in both the pericardium and ovaries. A biopsy confirmed it was DLBCL, presenting in the rare form of simultaneous spread to the heart lining and ovaries. During the course of illness, she also developed atrial arrhythmia. Doctors adopted a phased treatment approach: four cycles of R-CEOD chemotherapy led to a noticeable reduction in the heart tumor and improvement in her heart rhythm. This was followed by four cycles of R-CHOP, which further shrank the cardiac lesion and cleared the abdominal tumors completely. The treatment was well tolerated, and at a three-month follow-up, there was no sign of recurrence. Her heart function remained stable, with a left ventricular ejection fraction (LVEF) of 60%.

Conclusion: This case highlights the importance of early detection of atypical metastases in DLBCL through a combination of various imaging and pathological tests. Additionally, personalized treatment strategies may contribute to better patient outcomes.

KEYWORDS

diffuse large B-cell lymphoma, non-Hodgkin lymphoma, heart, ovary, case report

Introduction

Diffuse large B-cell lymphoma (DLBCL) is the most prevalent form of aggressive non-Hodgkin lymphoma (NHL), representing 30-40% of all NHL cases (1, 2). DLBCL arises from B cells and is marked by the uncontrolled growth of tumors resulting from the monoclonal proliferation of abnormal lymphocytes (1). This type of lymphoma often metastasizes to the bone marrow, spleen, liver, bones, and central nervous system (3, 4). While DLBCL can occur throughout the body, metastasis to atypical sites like the heart and ovaries is exceedingly rare (5).

Cardiac metastasis is an uncommon complication of DLBCL, typically affecting the right atrium, right ventricle, pericardium, or major blood vessels of the heart (6). Patients may experience symptoms such as chest pain, difficulty breathing, or fainting (7). In severe cases, this can result in cardiogenic shock or arrhythmias. Because these symptoms are often subtle, early diagnosis of cardiac metastasis can be quite difficult, and the prognosis is usually poor. Imaging techniques, like PET-CT or cardiac ultrasound, are essential for diagnosis (8, 9). Although chemotherapy can help reduce tumor size to some extent, the overall mortality rate remains high (10). The ovaries are another uncommon site for DLBCL metastasis, potentially resulting from abnormalities in the local immune environment or through spread via the bloodstream (11). Ovarian metastasis usually manifests as nonspecific symptoms like abdominal bloating or lower abdominal pain, making it easy to confuse with other ovarian issues and complicating the diagnosis (12).

This article presents a rare case of DLBCL with multiple site metastases, where the lymphoma spread to both the retroperitoneal lymph nodes and affected the heart and ovaries. By thoroughly analyzing the clinical presentation, imaging characteristics, diagnosis, and treatment of this case, we hope to offer valuable insights for clinicians dealing with rare instances of multiple site metastasis in DLBCL. This could improve their ability to identify and manage such complex cases.

Case presentation

Chief complaint

The patient has been experiencing persistent abdominal pain and bloating for the past two weeks, along with a stoppage of bowel movements and gas for the last two days.

Present illness

The patient developed abdominal pain and bloating without any obvious cause about two weeks ago, mainly focused in the upper abdomen, described as a constant dull ache. The symptoms are accompanied by a loss of appetite, fatigue, occasional acid reflux, and heartburn, as well as sensations of cold and chills, although the patient's temperature is normal. The patient exhibits mild facial swelling but reports no other significant discomfort. Five days ago, the abdominal bloating intensified and spread to the entire abdomen. Two days ago, the patient stopped having bowel movements and passing gas, and also started experiencing shortness of breath and difficulty breathing. Since the onset of the condition, the patient has not noticed any significant weight changes.

Past medical history

The patient has no known chronic illnesses, no history of surgery or use of special medications, and does not smoke or drink alcohol. There is no family history of cancer or related diseases.

Physical examination

The skin and sclera appear normal, with no signs of jaundice or pallor, and there is no palpable enlargement of the superficial lymph nodes. Breath sounds in both lungs are clear, with no dry or wet rales. The heart rhythm is regular, and there are no abnormal murmurs detected in any of the valve auscultation areas. The abdomen is flat and exhibits tenderness across the entire area, with no rebound tenderness or muscle rigidity. The liver and spleen are not palpable below the ribs, and the kidneys are also not felt. Liver dullness is noted, but there is no shifting dullness. Both kidney areas show no tenderness on percussion. Bowel sounds are reduced, and no gurgling sounds are heard. There is no swelling in either lower leg.

Laboratory findings

Complete Blood Count: The patient's blood test showed a higher-than-normal white blood cell count (12.5 × 10^9/L), mainly due to a significant rise in neutrophils (9.04 × 10^9/L). Monocytes were also slightly elevated (1.22 × 10^9/L). Although the percentage of lymphocytes was lower than usual (17.7%), their absolute number remained within the normal range (2.21 × 10^9/L), suggesting no true deficiency. Eosinophils were reduced (0.2%), with their count nearing the lower normal limit (0.02 × 10^9/L). No abnormalities were found in other cell types, such as basophils.

Biochemical Results: Lactate dehydrogenase is 782.79 U/L, NT-proBNP is 2052.00 pg/ml, and high-sensitivity cardiac troponin I (hsTnI) is 0.0540 ng/ml. Interleukin-6 is 132.67 pg/ml, and procalcitonin is 0.390 ng/ml.

Imaging studies

Cardiac ultrasound: The effective volume of the right atrium is decreased, showing a circular filling defect about 43 × 34 mm in

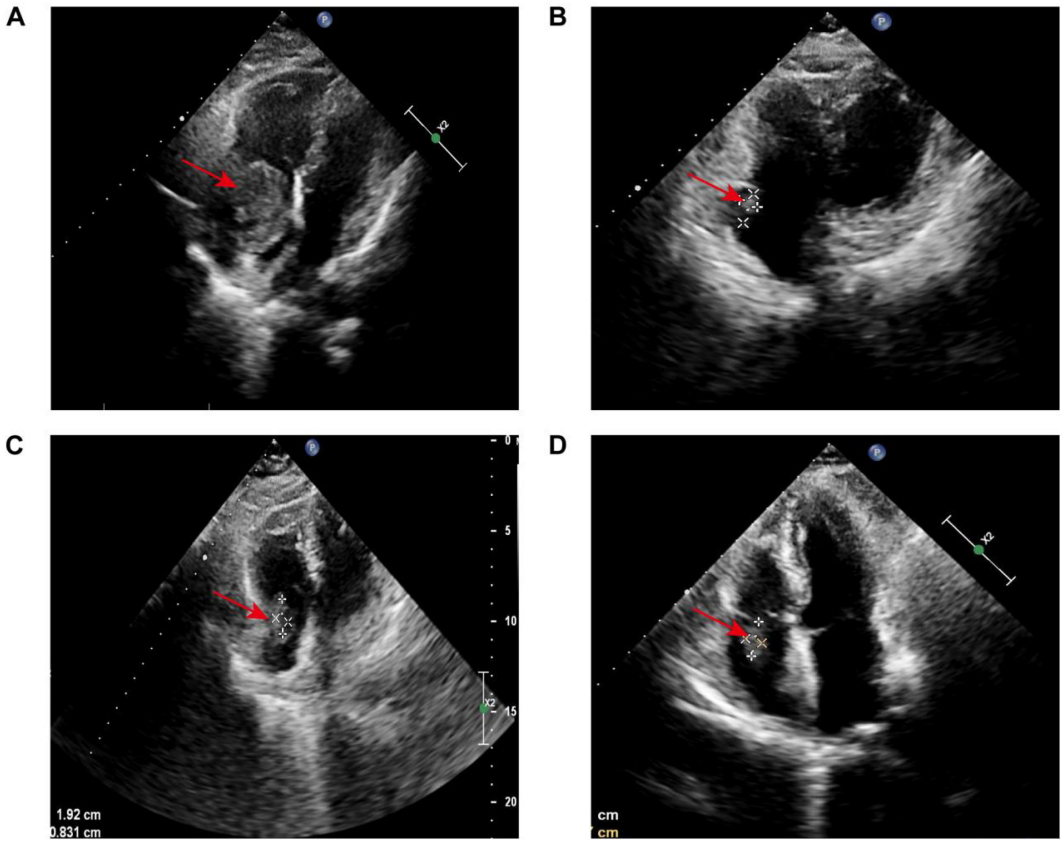

FIGURE 1
Serial echocardiographic surveillance of cardiac lesion: **(A)** Initial transthoracic echocardiography revealed a roughly oval-shaped filling defect within the right atrium, measuring approximately 43 × 34 mm. The lesion appeared to be anchored to the superior aspect of the right atrial wall. It demonstrated well-defined margins and minimal mobility, suggestive of a space-occupying mass with low dynamic activity. **(B)** Following four cycles of R-CEOD chemotherapy, reevaluation revealed a 14 × 8 mm hypoechoic-to-isoechoic lesion along the posterolateral wall of the right atrium. The lesion remained well-circumscribed, with a near-oval contour and persistently low mobility. **(C)** After an additional four cycles of R-CHOP, imaging showed the lesion to be stable in size at 19 × 8 mm. Its echogenicity remained mixed hypoechoic, and morphological characteristics (including its oval shape, sharp margins, and low mobility) were consistent with previous findings. The lesion continued to localize to the posterolateral wall of the right atrium. **(D)** At a three-month post-chemotherapy follow-up, the lesion measured 18 × 7 mm. Its acoustic properties and morphological features (mixed hypoechoic pattern, oval shape, well-defined borders, and limited mobility) remained unchanged. The basal attachment site was concordant with prior assessments.

size, likely attached to the top of the right atrium, with clear borders and minimal movement (Figure 1A). Additionally, a low-echo area measuring approximately 18 × 12 mm is noted near the right atrioventricular junction.

Enhanced CT: The right atrium is markedly enlarged, with a lobulated, well-defined mass of mixed density seen in the right pericardium and right atrium, measuring about 6.5 × 5.6 cm (Figure 2A). The contrast scan shows uneven enhancement. The mass extends from the right atrial appendage down to the entrance of the inferior vena cava. Near the phrenic angle, two enlarged lymph nodes are visible, with the larger measuring approximately 2.7 cm and showing significant enhancement with contrast. There are multiple mildly enlarged lymph nodes in both the pulmonary hila and the mediastinum. Additionally, several enlarged lymph nodes are seen near the major blood vessels in the retroperitoneum, with the largest measuring about 2.1 cm. In the adnexal region, a mixed-density mass is observed, with the larger one measuring about 42.4 × 73.5 × 50.0 mm (Figure 2B). The enhanced scan shows significant and sustained enhancement, with scattered patchy areas within the lesion that do not enhance.

Pathology findings

Immunohistochemistry: Positive for CD20, CD79, BCL-2 (60%), BCL-6, MUM1, and C-myc (40%); negative for Cyclin D1, with a Ki67 proliferation index of 70%. These results are consistent with the characteristics of non-Hodgkin DLBCL (Figure 3).

Genetic Testing: FISH analysis reveals no breakages in BCL2, BCL6, or MYC (negative) (Figures 4A–C). Clonal gene rearrangement testing suggests a monoclonal proliferation of B cells.

Final diagnosis

Non-Hodgkin lymphoma, B-cell type, stage IV, with involvement of the retroperitoneal lymph nodes, heart, and ovaries.

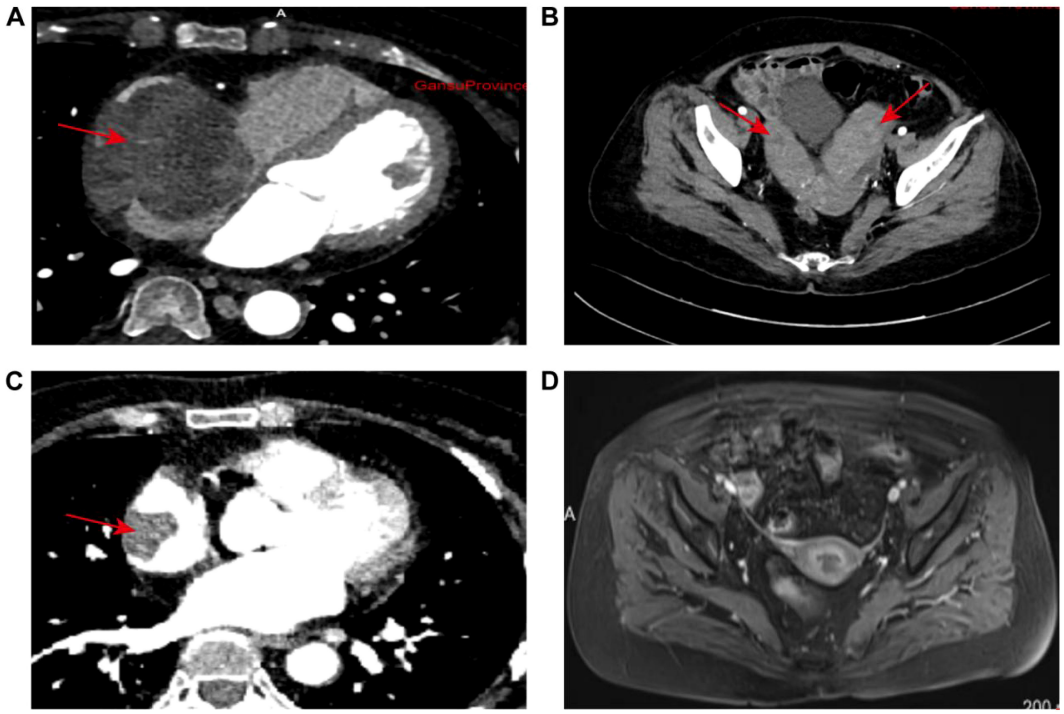

FIGURE 2
Radiological evaluation of disease dynamics: **(A)** Baseline imaging revealed marked enlargement of the right atrial chamber. A lobulated, mixed-density mass measuring approximately 6.5 × 5.6 cm was identified at the junction of the right atrium and pericardium. The lesion exhibited well-demarcated borders and demonstrated pronounced heterogeneous enhancement on contrast-enhanced scans. **(B)** Initial pelvic imaging identified bilateral adnexal masses characterized by well-defined mixed densities. The largest lesion measured 42.4 × 73.5 × 50.0 mm. Dynamic contrast-enhanced imaging revealed a pattern of persistent enhancement, interspersed with multiple non-enhancing patchy areas throughout the lesion. **(C)** Post-standard chemotherapy re-evaluation showed significant regression of the primary right atrial lesion, with a maximal axial dimension of 30 × 25 mm. Imaging characteristics were consistent with a localized filling defect. **(D)** At the final post-chemotherapy pelvic follow-up, complete resolution of bilateral adnexal lesions was observed. No abnormal enhancement or space-occupying lesions were detected. The imaging data comprehensively captured the temporal evolution of lesion morphology and enhancement characteristics throughout the treatment course.

Treatment plan

According to the guidelines, the patient met the criteria for the R-CHOP chemotherapy regimen. However, during treatment, the patient developed arrhythmias (with ECG showing junctional arrhythmia) (Figure 5A) and exhibited an increased risk to heart function. Given these cardiovascular concerns, the decision was made to switch from the R-CHOP regimen to the R-CEOD regimen to reduce cardiac toxicity and ensure the patient's safety. This regimen consisted of rituximab 600 mg, cyclophosphamide 1200 mg/m², pirarubicin 60 mg/m², and etoposide 100 mg/m², administered on days 1 through 3. Following four cycles of standardized antitumor therapy, the right atrial mass exhibited a marked reduction in size, with no recurrence of arrhythmias or other cardiac adverse events. Cardiac function parameters remained stable. Follow-up transthoracic echocardiography revealed an intracavitary right atrial mass measuring 14 × 8 mm, presenting

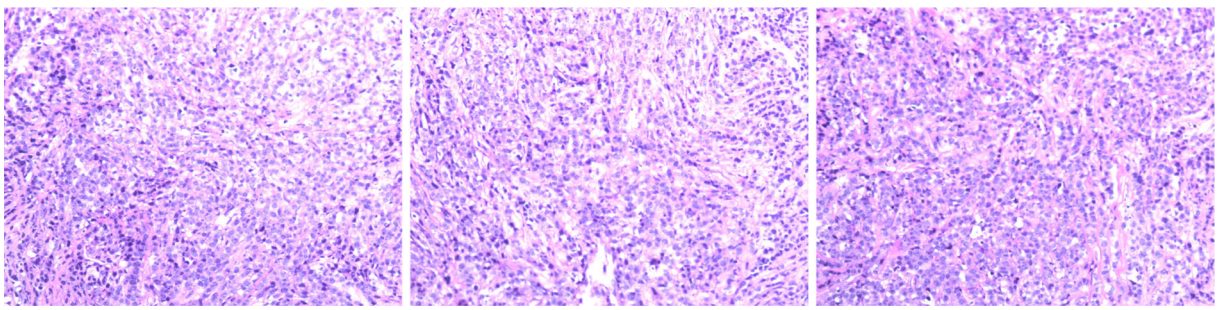

FIGURE 3
Pathological slide: Diffuse large B-Cell Lymphoma (DLBCL, NOS, Non-GCB subtype).

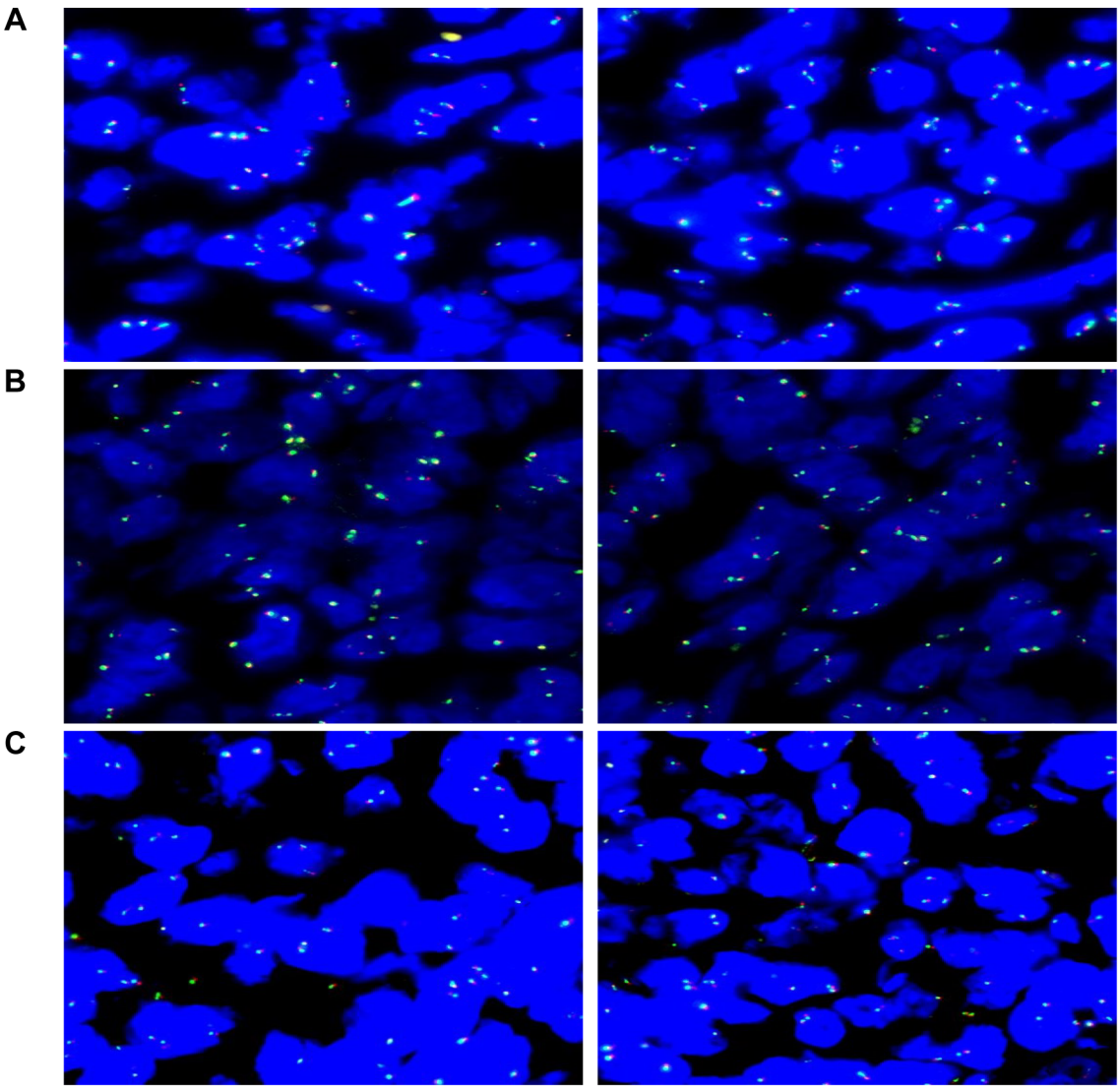

FIGURE 4
Molecular pathology diagnostic report: **(A)** Analysis of 100 tumor cells shows that 7% exhibit abnormal signal patterns, remaining below the 15% threshold, indicating no MYC gene rearrangement (negative). **(B)** Analysis of 100 tumor cells shows that 4% exhibit abnormal signal patterns, remaining below the 15% threshold, indicating no BCL6 gene rearrangement (negative). **(C)** Analysis of 100 tumor cells shows that 3% exhibit abnormal signal patterns, remaining below the 15% threshold, indicating no BCL2 gene rearrangement (negative).

as a heterogenous hypoechoic to isoechoic lesion with an irregular three-dimensional morphology, well-demarcated margins, and significantly restricted mobility (Figure 1B). Serial electrocardiographic monitoring demonstrated persistent sinus rhythm, and no evidence of atrial tachycardia, atrial fibrillation, or other abnormal atrial electrical activity was detected on ambulatory Holter recordings (Figure 5B). Following a reassessment during follow-up, the treatment was transitioned to the guideline-recommended R-CHOP regimen (cyclophosphamide, doxorubicin, vincristine and prednisone) to further enhance efficacy. Following four cycles of treatment, imaging assessment revealed a marked reduction in tumor burden. Transthoracic echocardiography showed a substantial decrease in the size of the right atrial mass, with a maximal diameter of 19 × 8 mm on two-dimensional imaging (Figure 1C). Color Doppler flow imaging did not reveal any evidence of inflow tract obstruction, the left ventricular ejection fraction (LVEF) is 62%. In contrast, contrast-enhanced CT demonstrated a larger filling defect in the right atrium, measuring up to 30 × 25 mm in maximal cross-sectional area (Figure 2C), highlighting discrepancies between anatomical measurement modalities. According to RECIST 1.1 criteria, the sum of diameters of target lesions indicated a partial response. Abdominal re-imaging showed complete resolution of the previously noted peritoneal metastases (Figure 2D), indicative of a heterogeneous response across disease sites. Given the persistence of the intracardiac mass and limitations of conventional imaging in accurately assessing residual disease, a multidisciplinary team recommended PET-CT to evaluate metabolic activity and differentiate between viable tumor and treatment-related changes. However, the patient declined this investigation.

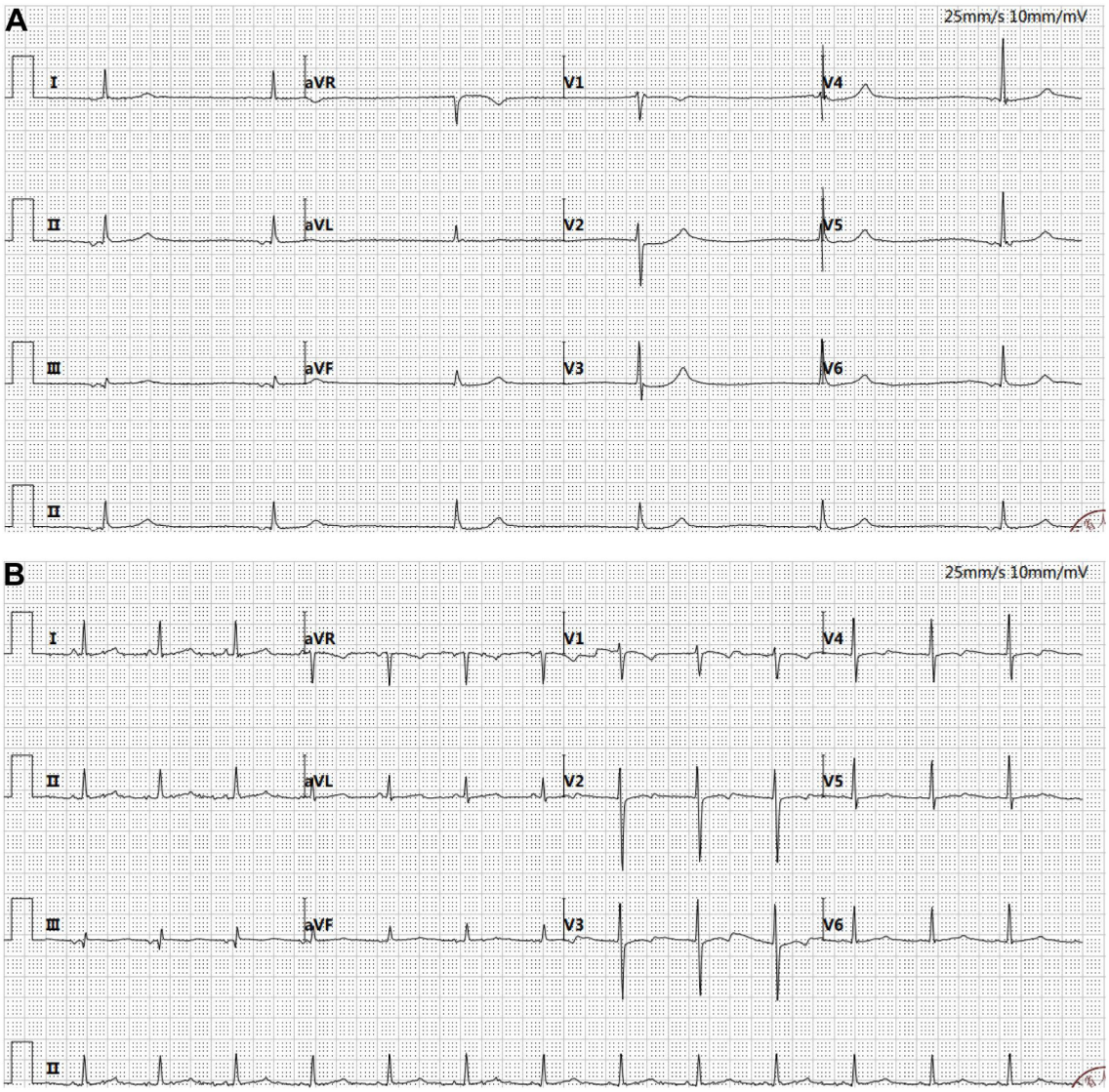

FIGURE 5
Electrocardiogram. **(A)** Atrial escape rhythm (36 bpm) and junctional escape rhythm were observed. The QT interval was prolonged (525 ms). ST segment depression of 0.05–0.1 mV was noted in leads V2–V4. RV5 amplitude was elevated at 1.28 mV, with a combined RV5 + SV1 value of 1.88 mV. The P wave duration was 82 ms, and the QRS complex measured 94 ms. **(B)** Sinus rhythm was restored (80 bpm). The QT interval normalized to 410 ms, and the ST segment changes resolved. RV5 amplitude decreased to 0.9 mV, with a combined RV5 + SV1 of 1.57 mV. The P wave measured 74 ms, and the QRS complex was 84 ms.

Planned follow-up

According to the standardized post-treatment surveillance protocol for tumors, the patient requires regular multimodal imaging assessments every three months, alongside evaluations of cardiac function. Key monitoring indicators include dynamic changes in LVEF, aimed at the early detection of chemotherapy-induced cardiotoxicity and signs of tumor recurrence. At three months following the final chemotherapy cycle, imaging review revealed a right atrial mass on echocardiography measuring 18 × 7 mm, characterized by hypoechoic to isoechoic signals, well-defined margins, and limited mobility (Figure 1D). LVEF remained preserved at 60%, suggesting compensated cardiac function. Longitudinal comparison indicated that fluctuations in the maximal diameter of the mass were within the range of technical variability. According to RECIST 1.1 criteria, given that the sum of the maximal diameters of target lesions had not increased by 20%, the current therapeutic response is assessed as stable disease.

Discussion

This case illustrates the rare metastasis of DLBCL to the heart and ovaries, underscoring the highly aggressive nature and unusual metastatic patterns of this lymphoma. The uniqueness of this case lies in the simultaneous involvement of both the heart and ovaries, a

combination rarely reported, offering valuable insights into the metastatic patterns of DLBCL. While DLBCL commonly metastasizes to the bone marrow, liver, spleen, and central nervous system, its spread to the heart and ovaries is unusual (3, 11, 13). In clinical practice, metastatic lesions in the heart and ovaries are often subtle and usually lack early symptoms, making early diagnosis particularly challenging (7, 14–16).

While there are many reports on the metastatic patterns of DLBCL, the specific mechanisms underlying its spread to the heart and ovaries remain insufficiently studied (17, 18). Cardiac metastasis is typically thought to reach the pericardial cavity via the bloodstream or direct infiltration (19), while ovarian metastasis may be linked to hematogenous or lymphatic spread (20). Furthermore, more aggressive subtypes of DLBCL may develop metastatic lesions in tissues distant from the primary site through mechanisms like invasion of vascular endothelial cells or immune evasion (21–23). In this case, the imaging findings of masses in the right atrium and right pericardium suggest that DLBCL may preferentially target areas with abundant blood supply, particularly on the right side of the heart.

The imaging features in this case clearly revealed distinct lesions in the heart and ovaries, offering critical imaging evidence for diagnosing multi-site metastasis in DLBCL. The cardiac metastasis presented as a mixed-density, lobulated mass with clear borders in the right atrium, while the ovarian metastasis appeared as an unevenly dense mass in the adnexal regions. Based on previous reports of DLBCL imaging findings, we speculate that there may be a pattern in the imaging characteristics of multi-site metastasis (24–26). To enhance the sensitivity of imaging in diagnosing multi-site metastasis in DLBCL, future efforts could focus on creating a standardized system for evaluating DLBCL imaging features, particularly with standardized descriptions for metastasis to rare sites like the heart and ovaries. This would provide clinicians with more precise information for early diagnosis and staging.

Due to the patient's arrhythmia and right atrial obstruction, the initial treatment plan of R-CHOP was reconsidered, as it could potentially increase cardiac stress. The treatment regimen was therefore adjusted to R-CEOD (27). This regimen works by inhibiting the proliferation of B-cell lymphoma through a combination of different drugs. After four cycles of treatment, the patient's tumor burden was significantly reduced. Monitoring through ECG, echocardiography, and other diagnostic methods revealed no significant cardiac toxicity. Given the patient's improvement, the treatment plan was switched back to R-CHOP to further consolidate the therapeutic effects. Based on the patient's treatment response, future therapeutic strategies may incorporate targeted therapies, such as BTK inhibitors, and immunotherapy, such as PD-1 inhibitors. Studies have shown that BTK inhibitors are highly effective in treating B-cell-related malignancies and may reduce toxicity to sensitive organs, including the heart (28). PD-1 inhibitors, as immune checkpoint inhibitors, have demonstrated promising efficacy across various cancer types, potentially clearing tumor cells by activating the patient's immune system, particularly in cases of multi-site metastasis (29, 30). Combining these targeted therapies and immunotherapies may further reduce tumor burden in metastatic sites such as the heart and ovaries, minimize treatment-related side effects, and improve patient survival. However, despite the theoretical promise of targeted therapies and immunotherapy, clinical application still requires more data from clinical trials. Future research should focus on evaluating the efficacy and safety of these treatment regimens in metastatic DLBCL patients to provide more personalized treatment options.

In this case, the presence of cardiac metastasis necessitates close monitoring of the patient's cardiac function throughout the treatment. Given that DLBCL patients with cardiac involvement may face complications like heart failure during treatment, we suggest regular monitoring of cardiac function using techniques such as ECG and cardiac ultrasound before, during, and after treatment. Additionally, monitoring changes in cardiac function with specific cardiac biomarkers (like B-type natriuretic peptide and troponin) can facilitate the early detection of potential cardiac damage, enabling prompt intervention to avoid adverse events (31, 32).

This case offers valuable clinical insights into the rare multi-site metastasis of DLBCL, highlighting the need for more extensive multicenter studies to investigate the mechanisms of DLBCL metastasis. Future research could concentrate on the following aspects. First, utilizing high-throughput gene sequencing technology could help identify molecular markers associated with multi-site metastasis of DLBCL, such as specific chemokines and cell adhesion molecules (33–35). This could provide further insights into the specific factors that contribute to the formation of metastatic lesions in organs like the heart and ovaries. Second, investigating the mechanisms of interaction between DLBCL cells and the microenvironments of the heart and ovaries could help determine whether specific conditions in these microenvironments promote the growth of DLBCL cells (36). For instance, cells that metastasize to the heart may survive more readily in the environment of cardiac myocytes, while the local immune microenvironment in the ovaries might support the growth of tumor cells (37–39). Third, it is important to develop specific biomarkers and imaging screening techniques to facilitate the early detection of metastasis in rare sites of DLBCL (33, 40, 41). Building on this, a personalized follow-up and monitoring system for patients with DLBCL metastasis could offer more targeted treatment intervention strategies.

This case offers valuable clinical insights into the rare metastasis of DLBCL, emphasizing the importance of early recognition, careful monitoring, and personalized treatment for patients with multi-site metastasis. In the future, systematically collecting similar cases and establishing standards for the diagnosis, treatment, and follow-up of multi-site metastasis in DLBCL could provide reliable clinical evidence to enhance the prognosis of these complex metastatic patients.

Conclusion

In a word, the findings of this case can provide insights into the individualized R-CEOD followed by R-CHOP regimen combined with multimodal imaging and histopathological evaluation for

DLBCL patients with atypical cardiac and ovarian metastases. However, this study is limited by its single-case nature, and future multicenter prospective studies with larger cohorts are warranted to validate these clinical strategies and explore molecular mechanisms for optimizing targeted therapies such as BTK/PD-1 inhibitors.

Data availability statement

The original contributions presented in the study are included in the article/supplementary material. Further inquiries can be directed to the corresponding author.

Ethics statement

The studies involving humans were approved by The Research Ethics Committee of Gansu Province Hospital. The studies were conducted in accordance with the local legislation and institutional requirements. The participants provided their written informed consent to participate in this study. The manuscript presents research on animals that do not require ethical approval for their study. Written informed consent was obtained from the individual(s) for the publication of any potentially identifiable images or data included in this article. Written informed consent was obtained from the participant/patient(s) for the publication of this case report.

Author contributions

YD: Methodology, Writing – original draft. YT: Investigation, Software, Visualization, Writing – original draft. YC: Data curation, Formal Analysis, Writing – original draft. SC: Methodology, Supervision, Writing – original draft. JG: Project administration, Software, Writing – review & editing.

Funding

The author(s) declare that financial support was received for the research and/or publication of this article. This work was supported by the Youth Fund of Gansu Provincial Hospital (Grant No. 20GSSY4-13), Gansu Provincial Hospital (Grant No. 22GSSYD-16) and Natural Science Foundation of Gansu Province (Grant No. 25JRRA873).

Conflict of interest

The authors declare that the research was conducted in the absence of any commercial or financial relationships that could be construed as a potential conflict of interest.

Generative AI statement

The author(s) declare that no Generative AI was used in the creation of this manuscript.

Publisher's note

All claims expressed in this article are solely those of the authors and do not necessarily represent those of their affiliated organizations, or those of the publisher, the editors and the reviewers. Any product that may be evaluated in this article, or claim that may be made by its manufacturer, is not guaranteed or endorsed by the publisher.

References

1. Wang SS. Epidemiology and etiology of diffuse large B-cell lymphoma. *Semin Hematol*. (2023) 60:255–66. doi: 10.1053/j.seminhematol.2023.11.004

2. Li S, Young KH, Medeiros LJ. Diffuse large B-cell lymphoma. *Pathology*. (2018) 50:74–87. doi: 10.1016/j.pathol.2017.09.006

3. Ollila TA, Olszewski AJ. Extranodal diffuse large B cell lymphoma: molecular features, prognosis, and risk of central nervous system recurrence. *Curr Treat options oncology*. (2018) 19:38. doi: 10.1007/s11864-018-0555-8

4. Chen DB, Shen DH, Zhang H, Wang Y, Song QJ, Yang SM, et al. Tumors of lymphoid and hematopoietic tissue of spleen: a clinicopathologic analysis of 53 cases. *Zhonghua bing li xue za zhi = Chin J pathology*. (2017) 46:775–81. doi: 10.3760/cma.j.issn.0529-5807.2017.11.008

5. Papanastasiou L, Skarakis N, Vardaka M, Dimitriadi A, Lampropoulou P, Perpinia A, et al. A very rare case of extranodal B-cell non-Hodgkin lymphoma presenting with adrenal and heart involvement. *Leukemia Res reports*. (2022) 17:100318. doi: 10.1016/j.lrr.2022.100318

6. Nasir A, Patel YB. Diffuse large B-cell lymphoma presenting as a cardiac mass. *Cureus. May*. (2024) 16:e59755. doi: 10.7759/cureus.59755

7. Qiang Y, Zeng K, Zhang B, Guan R, Liu Y, Liu Z, et al. Atypical location of primary cardiac lymphoma in the left heart with atypical clinical presentation: A case report and literature review. *Front surgery*. (2022) 9:1036519. doi: 10.3389/fsurg.2022.1036519

8. Kikuchi Y, Oyama-Manabe N, Manabe O, Naya M, Ito YM, Hatanaka KC, et al. Imaging characteristics of cardiac dominant diffuse large B-cell lymphoma demonstrated with MDCT and PET/CT. *Eur J nuclear Med Mol imaging*. (2013) 40:1337–44. doi: 10.1007/s00259-013-2436-5

9. Osmani AH, Maghfoor I. A case of diffuse large B-cell lymphoma with cardiac involvement incidently diagnosed on cardiac imaging. *J Coll Physicians Surgeons–Pakistan: JCPSP*. (2021) 31:1102–4. doi: 10.29271/jcpsp.2021.09.1102

10. Fields PA, Townsend W, Webb A, Counsell N, Pocock C, Smith P, et al. *De novo* treatment of diffuse large B-cell lymphoma with rituximab, cyclophosphamide, vincristine, gemcitabine, and prednisolone in patients with cardiac comorbidity: a United Kingdom National Cancer Research Institute trial. *J Clin oncology: Off J Am Soc Clin Oncology*. (2014) 32:282–7. doi: 10.1200/jco.2013.49.7586

11. Shen R, Xu PP, Wang N, Yi HM, Dong L, Fu D, et al. Influence of oncogenic mutations and tumor microenvironment alterations on extranodal invasion in diffuse large B-cell lymphoma. *Clin Trans medicine*. (2020) 10:e221. doi: 10.1002/ctm2.221

12. Ghadyalpatil NS, Chandrasekar R, Snehalatha D, Reddy BM. A case of primary ovarian lymphoma with autoimmune hemolytic anemia achieving complete response with Rituximab-based combination chemotherapy. *Indian J Med paediatric oncology: Off J Indian Soc Med Paediatric Oncology*. (2011) 32:207–10. doi: 10.4103/0971-5851.95142

13. Muringampurath-John D, Jaye DL, Flowers CR, Saxe D, Chen Z, Lechowicz MJ, et al. Characteristics and outcomes of diffuse large B-cell lymphoma presenting in leukaemic phase. *Br J haematology*. (2012) 158:608–14. doi: 10.1111/j.1365-2141.2012.09209.x

14. Luo B, He RQ, Peng ZG, Ma J, Feng ZB, Chen G, et al. Unusual presentation of primary ovarian diffuse large B-cell lymphoma: a case report. *J Ovarian Res*. (2022) 15:47. doi: 10.1186/s13048-022-00978-2

15. Nomoto N, Tani T, Konda T, Kim K, Kitai T, Ota M, et al. Primary and metastatic cardiac tumors: echocardiographic diagnosis, treatment and prognosis in a

15-years single center study. *J cardiothoracic surgery*. (2017) 12:103. doi: 10.1186/s13019-017-0672-7

16. Heatley MK. Mucinous tumours of the ovary–primary and metastatic. *J Clin Pathol*. (2012) 65(7):577–9. doi: 10.1136/jclinpath-2011-200407

17. Cazzola M. Introduction to a review series: the 2016 revision of the WHO classification of tumors of hematopoietic and lymphoid tissues. *Blood*. (2016) 127 (20):2361–4. doi: 10.1182/blood-2016-03-657379

18. Monterroso V, Jaffe ES, Merino MJ, Medeiros LJ. Malignant lymphomas involving the ovary. A clinicopathologic analysis of 39 cases. *Am J Surg pathology*. (1993) 17:154–70. doi: 10.1097/00000478-199302000-00007

19. Scobbo RR, Chung EK. Cardiac tumors. *Postgraduate medicine*. (1974) 56:138–41. doi: 10.1080/00325481.1974.11713809

20. Ozcivit Erkan IB, Kuru O, Turker Saricoban C, Wardak M, Hamzaoglu Canbolat K, Eskazan AE. Unusual synchronous and metachronous association of hematologic neoplasms with gynecologic neoplasms: A case series and literature review. *Int J gynaecology obstetrics: Off Organ Int Fed Gynaecology Obstetrics*. (2024) 169(3):1025–36. doi: 10.1002/ijgo.16075

21. Apollonio B, Spada F, Petrov N, Cozzetto D, Papazoglou D, Jarvis P, et al. Tumor-activated lymph node fibroblasts suppress T cell function in diffuse large B cell lymphoma. *J Clin investigation*. (2023) 133:e166070. doi: 10.1172/jci166070

22. Song MK, Park BB, Uhm J. Understanding immune evasion and therapeutic targeting associated with PD-1/PD-L1 pathway in diffuse large B-cell lymphoma. *Int J Mol Sci*. (2019) 20:1326. doi: 10.3390/ijms20061326

23. Wobser M, Siedel C, Kneitz H, Bröcker EB, Goebeler M, Houben R, et al. Microvessel density and expression of vascular endothelial growth factor and its receptors in different subtypes of primary cutaneous B-cell lymphoma. *Acta dermato-venereologica*. (2013) 93:656–62. doi: 10.2340/00015555-1589

24. Chantepie S, Hovhannisyan N, Guillouet S, Pelage JP, Ibazizene M, Bodet-Milin C, et al. (18)F-fludarabine PET for lymphoma imaging: first-in-humans study on DLBCL and CLL patients. *J nuclear medicine: Off publication Soc Nuclear Medicine*. (2018) 59:1380–5. doi: 10.2967/jnumed.117.206920

25. Lewis KL, Trotman J. Integration of PET in DLBCL. *Semin hematology*. (2023) 60:291–304. doi: 10.1053/j.seminhematol.2023.12.003

26. Capasso R, Negro A, Russo C, Zeccolini F, Muto G, Caranci F, et al. Conventional and advanced MRI techniques in the evaluation of primary CNS lymphoma. *Semin ultrasound CT MR*. (2023) 44:126–35. doi: 10.1053/j.sult.2023.02.003

27. Tilly H, Gomes da Silva M, Vitolo U, Jack A, Meignan M, Lopez-Guillermo A, et al. Diffuse large B-cell lymphoma (DLBCL): ESMO Clinical Practice Guidelines for diagnosis, treatment and follow-up. *Ann oncology: Off J Eur Soc Med Oncol*. (2015) 26 Suppl 5:v116–25. doi: 10.1093/annonc/mdv304

28. Mouhssine S, Maher N, Matti BF, Alwan AF, Gaidano G. Targeting BTK in B cell Malignancies: from mode of action to resistance mechanisms. *Int J Mol Sci*. (2024) 25:3234. doi: 10.3390/ijms25063234

29. Juárez-Salcedo LM, Sandoval-Sus J, Sokol L, Chavez JC, Dalia S. The role of anti-PD-1 and anti-PD-L1 agents in the treatment of diffuse large B-cell lymphoma: The future is now. *Crit Rev Oncology/hematology*. (2017) 113:52–62. doi: 10.1016/j.critrevonc.2017.02.027

30. Zhang T, Liu H, Jiao L, Zhang Z, He J, Li L, et al. Genetic characteristics involving the PD-1/PD-L1/L2 and CD73/A2aR axes and the immunosuppressive microenvironment in DLBCL. *J Immunotherapy Cancer*. (2022) 10:e004114. doi: 10.1136/jitc-2021-004114

31. Ananthan K, Lyon AR. The role of biomarkers in cardio-oncology. *J Cardiovasc Trans Res*. (2020) 13:431–50. doi: 10.1007/s12265-020-10042-3

32. Bojan A, Torok-Vistai T, Parvu A. Assessment and management of cardiotoxicity in hematologic Malignancies. *Dis markers*. (2021) 2021:6616265. doi: 10.1155/2021/6616265

33. de Leval L, Alizadeh AA, Bergsagel PL, Campo E, Davies A, Dogan A, et al. Genomic profiling for clinical decision making in lymphoid neoplasms. *Blood*. (2022) 140:2193–227. doi: 10.1182/blood.2022015854

34. Araf S, Korfi K, Rahim T, Davies A, Fitzgibbon J. Advances in the molecular diagnosis of diffuse large B-cell lymphoma in the era of precision medicine. *Expert Rev Mol Diagnostics*. (2016) 16:1093–102. doi: 10.1080/14737159.2016.1235974

35. Cao B, Sun C, Bi R, Liu Z, Jia Y, Cui W, et al. Mutation landscape in Chinese nodal diffuse large B-cell lymphoma by targeted next generation sequencing and their relationship with clinicopathological characteristics. *BMC Med Genomics*. (2024) 17:84. doi: 10.1186/s12920-024-01866-y

36. Takahara T, Nakamura S, Tsuzuki T, Satou A. The immunology of DLBCL. *Cancers*. (2023) 15:835. doi: 10.3390/cancers15030835

37. Ortona E, Locatelli SL, Pagano MT, Ascione B, Careddu G, Dupuis ML, et al. The natural estrogen receptor beta agonist silibinin as a promising therapeutic tool in diffuse large B-cell lymphoma. *Anticancer Res*. (2022) 42:767–79. doi: 10.21873/anticanres.15535

38. Autio M, Leivonen SK, Brück O, Mustjoki S, Mészáros Jørgensen J, Karjalainen-Lindsberg ML, et al. Immune cell constitution in the tumor microenvironment predicts the outcome in diffuse large B-cell lymphoma. *Haematologica*. (2021) 106:718–29. doi: 10.3324/haematol.2019.243626

39. Izraely S, Witz IP. Site-specific metastasis: A cooperation between cancer cells and the metastatic microenvironment. *Int J Cancer*. (2021) 148:1308–22. doi: 10.1002/ijc.33247

40. Dersh D, Phelan JD, Gumina ME, Wang B, Arbuckle JH, Holly J, et al. Genome-wide screens identify lineage- and tumor-specific genes modulating MHC-I- and MHC-II-restricted immunosurveillance of human lymphomas. *Immunity*. (2021) 54:116–131.e10. doi: 10.1016/j.immuni.2020.11.002

41. Persky DO, Li H, Stephens DM, Park SI, Bartlett NL, Swinnen LJ, et al. Positron emission tomography-directed therapy for patients with limited-stage diffuse large B-cell lymphoma: results of intergroup national clinical trials network study S1001. *J Clin oncology: Off J Am Soc Clin Oncology*. (2020) 38:3003–11. doi: 10.1200/jco.20.00999

frontiers | Frontiers in Oncology

TYPE Case Report
PUBLISHED 04 July 2025
DOI 10.3389/fonc.2025.1538786

Check for updates

OPEN ACCESS

EDITED BY
Reto Asmis,
Wake Forest University, United States

REVIEWED BY
Maria Raffaella Ambrosio,
University of Siena, Italy
Diana Mihalcea,
Carol Davila University of Medicine and Pharmacy, Romania

*CORRESPONDENCE
Xianggui Yuan
yuanxg@zju.edu.cn
Huiqing Qiu
qqson@163.com
Yun Liang
liangyun@zju.edu.cn

†These authors have contributed equally to this work

RECEIVED 03 December 2024
ACCEPTED 17 June 2025
PUBLISHED 04 July 2025

CITATION
Qiu X, Zhang L, Zhou S, Qian W, Liang Y, Qiu H and Yuan X (2025) Case Report: Primary cardiac diffuse large B-cell lymphoma with sick sinus syndrome and literature review on disease management and therapeutic strategies.
Front. Oncol. 15:1538786.
doi: 10.3389/fonc.2025.1538786

COPYRIGHT
© 2025 Qiu, Zhang, Zhou, Qian, Liang, Qiu and Yuan. This is an open-access article distributed under the terms of the Creative Commons Attribution License (CC BY). The use, distribution or reproduction in other forums is permitted, provided the original author(s) and the copyright owner(s) are credited and that the original publication in this journal is cited, in accordance with accepted academic practice. No use, distribution or reproduction is permitted which does not comply with these terms.

Case Report: Primary cardiac diffuse large B-cell lymphoma with sick sinus syndrome and literature review on disease management and therapeutic strategies

Xiaofen Qiu[1,2†], Li Zhang[1†], Shaojun Zhou[2], Wenbin Qian[2,3], Yun Liang[2*], Huiqing Qiu[1*] and Xianggui Yuan[2*]

[1]Department of Hematology and Medical Oncology, The Second People's Hospital of Quzhou, Quzhou, China, [2]Department of Hematology, The Second Affiliated Hospital, Zhejiang University School of Medicine, Hangzhou, China, [3]National Clinical Research Center for Hematologic Diseases, The First Affiliated Hospital of Soochow University, Suzhou, China

Background: Primary cardiac diffuse large B-cell lymphoma (DLBCL) is a rare but clinically challenging extranodal lymphoma. Diagnosis and management are often complicated due to its nonspecific symptoms and rarity.

Case Report: We reported a case of a 73-year-old male who initially presented with chest pain, high fever, dizziness, and amaurosis. Preliminary diagnostic assessments suggested sick sinus syndrome, necessitating the implantation of a dual-chamber pacemaker, and revealed a large mass in the interatrial septum. An endomyocardial biopsy confirmed the diagnosis of primary cardiac DLBCL. Initial treatment with R-miniCHOP chemotherapy yielded a partial response. However, due to treatment-related complications (grade 4 neutropenia and pneumonia), a change in the therapeutic regimen to OR-GemOx chemotherapy was made, leading to complete remission. A year later, the patient experienced a relapse, requiring a salvage treatment of the Pola-BR chemotherapy regimen, which again resulted in complete remission. Additionally, this review examines an in-depth literature review on the management and therapeutic strategies for this entity, focusing on the treatment recommendations for relapse/refractory disease.

Conclusion: Prompt diagnosis and effective management are crucial in treating primary cardiac DLBCL. While the emergence of new drugs has improved the prognosis by offering higher efficacy and fewer side effects, clinicians should be vigilant about potential cardiotoxicities.

KEYWORDS

primary cardiac lymphoma, diffuse large B-cell lymphoma, extranodal lymphoma, sick sinus syndrome, orelabrutinib, polatuzumab vedotin

1 Introduction

Cardiac lymphoma refers to lymphoma affecting the myocardium or pericardium, and it is a rare form of extranodal lymphoma. It is categorized into primary cardiac lymphoma (PCL) and secondary cardiac lymphoma (SCL) based on cellular origin. PCL is exceptionally rare, accounting for approximately 1.3% of all primary cardiac tumors in autopsies and 0.5% of extranodal lymphomas (1). In contrast, secondary cardiac lymphoma (SCL) is more prevalent, constituting about 20% of secondary cardiac tumors. PCLs are remarkably invasive lymphomas. The predominant histopathological type is diffuse large B-cell lymphoma, which accounts for 80% of all cases. The prognosis of PCLs is generally poor, with the median survival time of just 2.2 years according to a U.S. countrywide cancer database (2). Due to its non-specific symptoms, early diagnosis of PCLs is often challenging. Given its aggressive nature, rapid progression, and poor prognosis, timely and effective diagnosis, management, and treatment are of paramount importance.

In this report, we presented the case of a 73-year-old male diagnosed with primary cardiac DLBCL. He initially exhibited symptoms such as chest pain, continuous high fever, and progressive amaurosis. We provide a detailed account of the disease course, the diagnostic procedures employed, and the therapeutic management, which included various chemotherapy regimens such as R-miniCHOP (rituximab, cyclophosphamide, liposomal doxorubicin, vincristine, dexamethasone), OR-GemOx (orelabrutinib, rituximab, gemcitabine, oxaliplatin), and Pola-BR (polatuzumab vedotin, bendamustine, rituximab). Furthermore, we conduct an in-depth review of the existing literature to offer valuable clinical insights for the better understanding and management of this entity, focusing on the treatment recommendations for relapse/refractory disease.

2 Case report

In July 2022, a previously healthy 73-year-old male was admitted to our cardiology department presenting with chest pain for over ten days. The pain began after exertion, lasting for several seconds, and showed minimal improvement with anti-anginal therapy. Three days before hospital admission, the patient started experiencing a repeated high fever, progressive dizziness and amaurosis fugax. An electrocardiogram (ECG) revealed sinus or ectopic atrial rhythm, multiple atrial premature beats, non-specific intraventricular conduction delay, low-voltage limb leads, and mild ST-segment elevation in inferior wall leads. A 24-hour Holter monitoring indicated multiple atrial premature beats and frequent sinus arrest >4s, suggestive of sick sinus syndrome. An echocardiography showed a heterogeneous hypoechoic mass in the interatrial septum, measuring approximately 5.74*6.74*8.28cm (Figure 1B). The left ventricular ejection fraction (LVEF) was 48%. A contrast-enhanced cardiac computed tomography (CT) demonstrated mild enhanced multiple masses in the middle mediastinum invading the left and right atria, the superior vena cava, aortic root, and right pulmonary vein (Figure 1C). Laboratory examination revealed NT-ProBNP 3420 (range, <125) pg/mL, hemoglobin 109 g/L (range, 120-160), and lactate dehydrogenase (LDH) 245 U/L (range, 176-235) U/L. Cardiac biomarkers (troponin I and CK-MB) were all normal. Blood cultures were repeatedly negative during the febrile episodes. Inflammatory markers (C-reactive protein and procalcitonin) were within normal limits. Upon admission, the patient received intensive antibiotic therapy, but his fever persisted, and symptoms of dizziness and amaurosis did not alleviate. Consequently, a dual-chamber pacemaker was implanted. After the operation, the patient developed persistent atrial fibrillation refractory to amiodarone therapy, and low-molecular-weight heparin was initiated to prevent the thrombosis.

To determine the nature of the cardiac mass, an angiography-guided endomyocardial biopsy was performed. The pathological examination revealed diffuse lymphocytic proliferation. Immunohistochemistry results were as follows: ALK/P80 -, c-Myc 10%+, Bcl-6 +, CD10 -, CD19 +, CD20 +, CD21 -, CD23 -, CD3 -, CD30 -, CD35 -, CD45(LCA) +, CD45RO -, CD5 -, CD79a +, Cyclin D1 -, Ki-67 70%+, Mum-1 +, SOX11 -, Bcl-2 90%+, leading to a diagnosis of DLBCL, non-GCB subtype (Figure 2). Following this diagnosis, the patient was transferred to the hematology department for further treatment. A PET-CT scan revealed heart masses invading and compressing surrounding structures with abnormal ^{18}F-FDG uptake (SUVmax=44.2), and slightly enlarged hilar lymph nodes with increased ^{18}F-FDG uptake (Figure 1D). Bone marrow biopsy showed no lymphomatous involvement. A final diagnosis of primary cardiac DLBCL was made.

Upon diagnosis confirmation, the patient received intravenous dexamethasone 10mg QD and hydration/alkalization to prevent tumor lysis syndrome, followed by R-miniCHOP chemotherapy (Rituximab 375 mg/m^2 (d0), cyclophosphamide 600 mg/m^2 (d1), liposomal doxorubicin 40 mg/m^2 (d1), vincristine 1 mg (d1), prednisone 60 mg (d1-5)), due to the patient's advanced age and concern for cardiotoxicity from full-dose anthracyclines (3, 4). After one cycle of chemotherapy, ventricular pacing burden decreased, and atrial fibrillation resolved. The patient reported significant improvement in chest pain and dizziness. A partial response based on PET/CT was observed after four cycles of chemotherapy, as the cardiac tumor size reduced from approximately 5.74*6.74*8.28cm to 3.76*6.29*3.19cm as well as ^{18}F-FDG uptake reduced. However, treatment tolerance was suboptimal. Despite the preventive use of pegylated granulocyte colony stimulating factor, the patient developed neutropenia pneumonia requiring hospitalization after the third and fourth cycle of chemotherapy. Thereafter, the chemotherapy regimen was changed to OR-GemOx (Orelabrutinib 150 mg QD, rituximab 375 mg/m^2 (d0), gemcitabine 1000 mg/m^2 (d1), oxaliplatin 100 mg/m^2 (d1)) for 4 cycles, leveraging orelabrutinib's cardiac safety profile (5), and metabolic complete remission was achieved. The patient reported that fatigue during R-miniCHOP impacted daily activities, but OR-GemOx was better tolerated. Patient-reported grade 2 fatigue (CTCAE v5.0) resolved during OR-GemOx treatment. Then, maintenance therapy with orelabrutinib was initiated for six months.

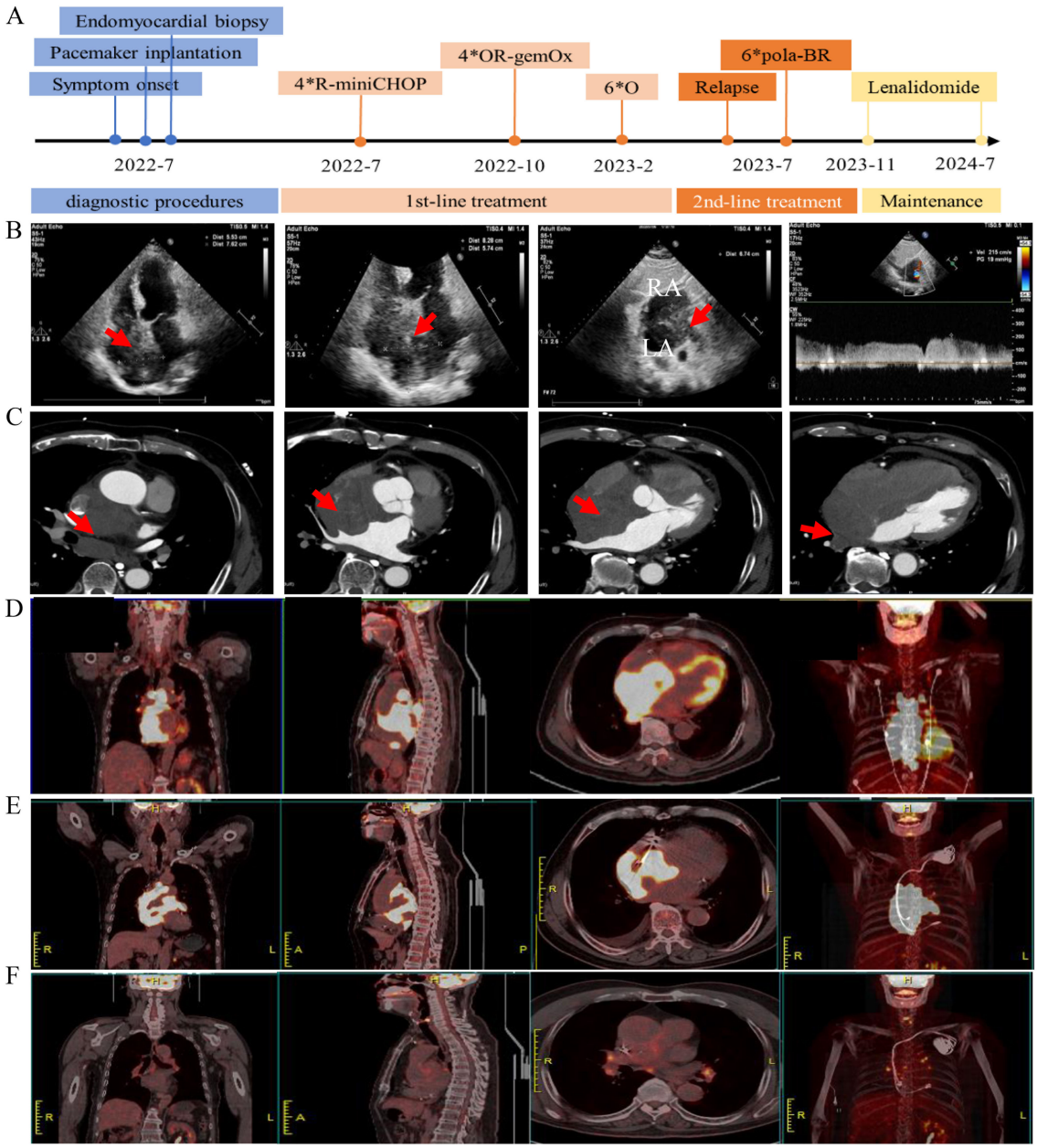

FIGURE 1
Radiological imaging before and after the treatment. **(A)** Timeline of clinical events, and interventions. **(B)** Transthoracic echocardiogram showing a large mass (red arrow) infiltrating the interatrial septum. Panel 1–3 show the apical 4-chamber and subxiphoid two-chamber views of the interatrial septal mass, panel 4 shows pulse-wave doppler imaging of the mass at the junction of the superior vena cava and the right atrium with increased blood flow velocity. **(C)** Contrast-enhanced CT scan shows a large mass (red arrow) in the middle mediastinum invading the left and right atria. **(D)** PET/CT shows increased 18-FDG-uptake heart masses invading surrounding structures at diagnosis. **(E)** PET/CT shows increased 18-FDG-uptake heart masses at relapse. **(F)** PET/CT shows no evidence of lymphoma after treatment for disease relapse.

In July 2023, the patient was admitted with a one-week history of chest tightness. A chest enhanced CT scan revealed a tumor around the superior vena cava and the right middle lobe bronchus. A PET-CT scan showed hypermetabolic masses confined to the heart (SUVmax=34.25), indicating disease recurrence (Figure 1E). The patient's condition precluded a biopsy again. Consequently, four cycles of the Pola-BR regimen [Polatuzumab vedotin 1.8 mg/kg (d1), bendamustine 70 mg/m^2 (d1-2), rituximab 375 mg/m^2 (d1)] were administered (6), achieving metabolic complete remission (Figure 1F). After two consolidation cycles of Pola-BR regimen, the patient was maintained with lenalidomide 10 mg/day. The patient underwent a structured cardiovascular follow-up protocol. Echocardiography, ECG, and NT-proBNP every 3 months, cardiac MRI (post-pacemaker adjustment to MRI-safe mode) to assess myocardial infiltration and fibrosis every 6 months, and symptom-driven troponin testing and Holter monitoring for arrhythmia recurrence. At the last follow-up in July 2024, the patient remained in a complete remission. His LVEF improved to

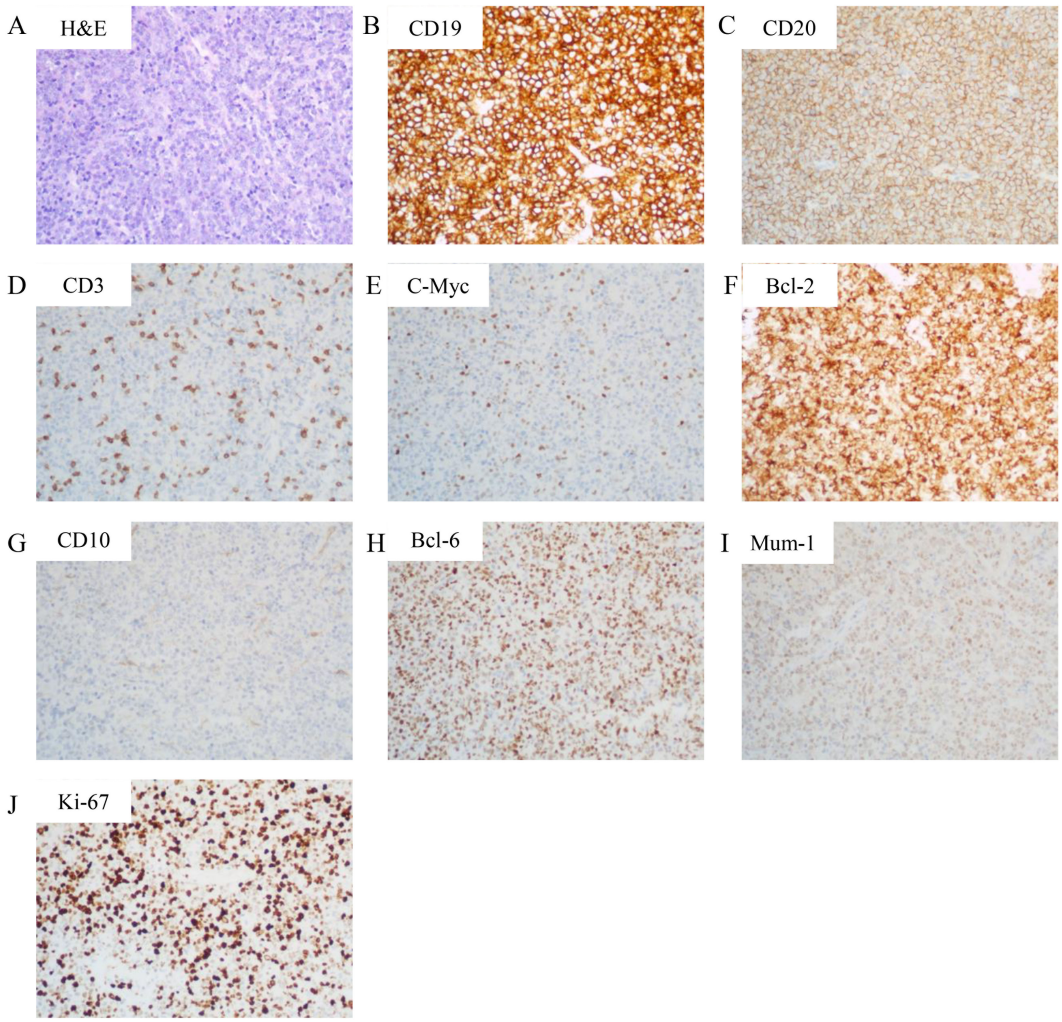

FIGURE 2
Histopathological and immunohistochemical features. **(A)** Hematoxylin and eosin (H&E) staining (200× magnification) demonstrating sheets of large atypical lymphoid cells with vesicular chromatin and prominent nucleoli, consistent with diffuse large B-cell lymphoma. **(B-I)** Immunohistochemical staining (200× magnification) revealing: **(B)** Strong CD19 positivity in neoplastic cells **(C)** Diffuse membranous CD20 expression; **(D)** CD3 negativity (internal control: background T-lymphocytes show positive staining); **(E)** c-Myc expression in 10% of tumor cells; **(F)** Bcl-2 overexpression in 90% of neoplastic cells; **(G)** CD10 negativity; **(H)** Nuclear Bcl-6 positivity; **(I)** MUM1 nuclear expression. **(J)** Ki-67 staining showing high proliferative index (70%+).

65%, with normalization of NT-proBNP and troponin-I levels post-Pola-BR. During the treatment, no cardiac events were observed. Timeline of clinical events and interventions were shown in Figure 1A.

3 Discussion

Primary cardiac DLBCL is a rare and aggressive form of extranodal lymphoma often characterized by a poor prognosis. This case presents considerable diagnostic and therapeutic challenges encountered when dealing with this entity. The patient's initial nonspecific symptoms caused a delay in diagnosis. Furthermore, biopsy was delayed by symptomatic sick sinus syndrome, necessitating pacemaker implantation prior to invasive procedures. Initial imaging suggested angiosarcoma or metastatic carcinoma. DLBCL was confirmed via biopsy after excluding infectious etiologies (e.g., infective endocarditis via repeated blood cultures) and non-lymphomatous tumors (e.g., cardiac myxoma with pathological features). The first line of treatment R-miniCHOP was chosen over full-dose R-CHOP due to age-related cardiotoxicity concerns. However, although this regimen demonstrated efficacy, but it was complicated by severe chemotherapy-related complications (grade 4 neutropenia and pneumonia). Then OR-GemOx was substituted after R-miniCHOP-induced neutropenia pneumonia, leveraging orelabrutinib's cardiac safety profile, which was successful in achieving complete remission. However, a disease recurrence called for another change in the chemotherapy regimen to Pola-BR, which also resulted in complete remission. To prevent further relapses, lenalidomide was initiated as maintenance therapy. Novel agents with improved safety profiles and higher efficacy have significantly improved the patient's prognosis.

We collected primary cardiac DLBCL case reports published from January 2009 to January 2024, collected statistics from each patient, and performed a systematic analysis (Table 1). According to the narrow definition given by the WHO in 2022 as "extranodal lymphoma involving only the heart or the pericardium", 81 cases of primary cardiac DLBCL cases in 76 reports were included (Appendix Table S1). Signs and symptoms can vary based on factors such as tumor location, size, growth rate, degree of invasion, and friability. Most symptoms are nonspecific. Dyspnea (64%), chest pain (19%) and palpitation (19%) are the most common symptoms reported. Congestive heart failure characterizes 16% of clinical presentation. Other less common manifestations include cardiogenic shock (5%), and tumor embolization (2%) and cardiac tamponade (2%). Various types of arrhythmias are also not uncommon. They often manifest as atrial fibrillation (15%), and varying degrees of atrioventricular block (21%), while sick sinus syndrome is relatively rare. One case report described a patient with cardiac lymphoma that caused atrial fibrillation and sick sinus syndrome, necessitating pacemaker therapy. After chemotherapy, ventricular pacing burden was reduced without atrial fibrillation (7). Another case report presented a patient with cardiac lymphoma and sick sinus syndrome who were successfully treated via chemotherapy without pacemaker implantation (8). This case report outlined a patient with primary cardiac DLBCL and sick sinus syndrome that did not respond to conventional treatment. However, post-chemotherapy and tumor control, the arrhythmias resolved. Although pacemaker implantation may not be entirely avoidable in case where sick sinus syndrome is present, appropriate treatment of the cardiac lymphoma may potentially restore conduction partially or completely, suggesting that the sick sinus syndrome was likely due to the reversible invasion of the sinus node by the lymphoma.

In case of suspected cardiac involvement, trans-thoracic echocardiography is the first-line imaging modality for screening. Computed tomography (CT) provides a more detailed view, capturing the morphology, location, and extent of cardiac neoplasms. Magnetic resonance imaging (MRI), on the other hand, offers superior images identifying the anatomy, blood flow, and cardiac function. Both CT and MRI offer superior contrast resolution compared to echocardiography, providing diagnostic and differential diagnoses of PCLs from angiosarcoma, metastatic tumors, and myocarditis. The gold standard to stage the disease, though, is PET/CT, which assesses the overall tumor burden and extent, detects latent cardiac involvement and determines the primary nature of cardiac lesions. It was reported that PET/CT parameters and cutoff values (SUVmean>5.17) together can help to distinguish PCLs from primary cardiac angiosarcomas with high sensitivity and specificity (9). However, there are considerable overlaps in imaging characteristics among cardiac tumors, making the initial diagnosis based on imaging features challenging. Hence, these different imaging modalities should be seen as complementary tools rather than competitive alternatives.

The definitive diagnosis of PCLs relies on pathological biopsy. Traditional open-chest biopsy (38%) carries significant risks, leading to a shift towards less invasive procedures in recent years. These include transvenous angiography-guided endomyocardial biopsy (30%), trans-thoracic CT-guided biopsy (9%), trans-thoracic echocardiography-guided biopsy (7%), transesophageal echocardiography-guided biopsy (2%), and mediastinoscopy (1%). In cases where pericardial effusion is present, cytological examination can also aid in diagnosis. The transvenous angiography-guided endomyocardial biopsy is particularly suitable for masses in the chambers or in the diffusely thickened myocardium. Recent reports from the European Society of Cardiology have shown that endomyocardial biopsy, predominantly right ventricular, carries a low complication rate and no procedure-related fatalities (10).

Currently, there are no guidelines available regarding treatment for primary cardiac DLBCL, necessitating a multidisciplinary approach involving cardiologists, oncologists, and hematologists. Generally, cardiac DLBCL is sensitive to chemotherapy. The first line treatment usually involves a combination of drugs, most commonly R-CHOP (Rituximab, cyclophosphamide, doxorubicin, vincristine, and prednisone). However, our retrospective analysis revealed 8.6% of treatment-related severe cardiac complications in PCL patients treated with R-CHOP-like regimens, suggesting that rigorous monitoring protocols coupled with risk (Appendix Table S1). Therefore, individualized treatment plans based on patient response and tolerance are highly recommended, with a focus on avoiding cardiotoxic drugs and being vigilant to cardiac events. Cardiac DLBCL is also sensitive to radiation therapy, but due to potential cardiac side effects, radiation is generally limited to cardiac masses that do not respond to chemotherapy. Cardiac DLBCL is highly likely to recurrence and eventually become refractory. Regular follow-up is crucial for monitoring signs of recurrence or progression.

Once the disease relapses, the prognosis is extremely poor. However, limited treatment recommendations are available so far for relapse/refractory(R/R) cardiac DLBCL. Bruton's tyrosine kinase (BTK) inhibitors, either alone or in combination, have been identified as a promising therapeutic option for systemic DLBCL (11, 12), particularly for cases with extranodal lesions and MCD genetic subtype. However, common cardiac side effects such atrial fibrillation or flutter (16%), cardiac failure (5%) and symptomatic ventricular arrhythmias (3%), may limit their use in R/R cardiac DLBCL. Second-generation BTK inhibitors such as orelabrutinib may minimize these cardiac events. Recent studies have shown that orelabrutinib combined with chemotherapy or immunotherapy is effective for R/R systemic DLBCL with fewer cardiac events (15.8%) (5). Polatuzumab vedotin, an antibody drug conjugates, combined with bendamustine and rituximab (Pola-BR) has yielded significantly higher CR rates and survival in R/R systemic DLBCL (6). However, a pharmacovigilance study based on the Food and Drug Administration Adverse Event Reporting System (FAERS) database indicated that it has been associated with cardiotoxicity such as cardiac failure, supraventricular tachyarrhythmias, and cardiomyopathy (13). Bispecific antibodies (Glofitamab, Blinatumomab) have shown notable success in R/R systemic DLBCL (14), but they can lead to mild sinus tachycardia (5-6%), and rare but severe cardiac adverse events (<0.5%),

TABLE 1 Summary of characteristics and outcomes of primary cardiac DLBCL cases reported from 2009 to 2024.

Characteristics	Patient number (%) (*n* 81)
Age, years, median (range)	65 (29-89)
Sex	
Male	49 (60%)
Female	32 (40%)
Symptom/findings	
Dyspnea (%)	52 (64%)
Chest pain (%)	15 (19%)
Heart failure	13 (16%)
Palpitation (%)	13 (16%)
B symptoms	11 (14%)
Syncope (%)	9 (11%)
Fatigue (%)	9 (11%)
Cough (%)	8 (10%)
Chest distress	8 (10%)
SVC syndrome (%)	7 (9%)
Edema (%)	6 (7%)
Shock (%)	4 (5%)
Dizziness (%)	3 (4%)
Pulmonary embolism (%)	2 (2%)
Cardiac tamponade (%)	2 (2%)
Arrhythmias	
Complete AV block (%)	12 (15%)
Atrial fibrillation (%)	12 (15%)
Ventricular tachycardia (%)	4 (5%)
Second degree AV block (%)	3 (4%)
First degree AV block (%)	2 (2%)
Ventricular fibrillation (%)	1 (1%)
Supraventricular tachycardia (%)	1 (1%)
Mass location	
Right atrium (%)	60 (74%)
Right ventricle (%)	44 (54%)
Pericardial effusion (%)	26 (32%)
Left atrium (%)	9 (11%)
Interatrial septum (%)	8 (10%)
Left ventricle (%)	8 (10%)
Interventricular septum (%)	3 (4%)
Others (%)	12 (15%)
Methods of diagnosis	
Open chest biopsy (%)	31 (38%)
Endomyocardial biopsy (%)	24 (30%)
CT-guided biopsy (%)	7 (9%)
Percutaneous TTE-guided biopsy (%)	6 (7%)
Pericardial fluid (%)	3 (4%)
Autopsy (%)	2 (2%)
Transesophageal echocardiography (%)	2 (2%)
Mediastinoscopy biopsy (%)	1 (1%)
Unspecified (%)	5 (6%)
Cell of Origin Subtype	
GCB (%)	5 (6%)
Non-GCB (%)	11 (14%)
Unspecified (%)	65 (80%)
Cardiac complications	
CNS Relapse	6 (7%)
Arrhythmias	1 (1%)
Sudden cardiac death	1 (1%)
Median PFS (range)	36 (13.5-58.5) months
2y-PFS rate	68.6%
Median OS (range)	Not reached
3y-OS rate	75.8%

PFS, Progression free survival; OS, Overall survival; GCB, Germinal center B-cell-like lymphoma; non-GCB, non-germinal center B-cell-like lymphoma; TTE, Transthoracic echocar-diography.

including myocardial infarction, atrial arrhythmias, congestive heart failure, cardiac arrest, and pericardial effusion (15). The FDA has also approved three CAR-T cell therapies for R/R systemic DLBCL. However, CAR-T cell therapy can also induce cardiac complications, such as cardiomyopathy (10.8%), heart failure (15%), arrhythmias (12.2%), myocardial infarction (7.1%), shock (50%), cardiac arrest (2.2%), and cardiovascular death (up to 4.3%) (16). A rare case with secondary cardiac DLBCL receiving CAR-T treatment achieved transient metabolic complete response but suffered from severe fulminant cardiotoxicity (17). In the era of novel agents, while they may effectively improve the treatment outcome for cardiac DLBCL, it is crucial to be mindful of their cardiac toxicity, warranting vigilant monitoring and tailored management. This is the first reported case utilizing orelabrutinib- and polatuzumab-based regimens for cardiac DLBCL, demonstrating feasibility in elderly patients. However, lack of molecular profiling (e.g., *MYD88* and *CD79B* mutation)

and short follow-up (24 months) preclude long-term efficacy conclusions.

In conclusion, primary cardiac DLBCL is a rare and challenging malignancy that requires prompt diagnosis and aggressive multimodality treatment. Close monitoring and individualized treatment plans are critical to optimize outcomes and prevent relapses.

Data availability statement

The original contributions presented in the study are included in the article/Supplementary Material. Further inquiries can be directed to the corresponding authors.

Ethics statement

The studies involving humans were approved by Ethics review committee of the Second Affiliated Hospital, Zhejiang University. The studies were conducted in accordance with the local legislation and institutional requirements. The participants provided their written informed consent to participate in this study. Written informed consent was obtained from the individual(s) for the publication of any potentially identifiable images or data included in this article.

Author contributions

XQ: Data curation, Formal analysis, Writing – original draft. LZ: Data curation, Formal analysis, Validation, Writing – review & editing. SZ: Validation, Writing – review & editing. WQ: Funding acquisition, Supervision, Writing – review & editing. YL: Resources, Writing – review & editing. HQ: Conceptualization, Funding acquisition, Supervision, Writing – review & editing. XY: Conceptualization, Funding acquisition, Supervision, Writing – original draft.

Funding

The author(s) declare that financial support was received for the research and/or publication of this article. The present study was funded by the National Natural Science Foundation of China (No. 82350104), Natural Science Foundation of Zhejiang Province of China (No. BY24ZH080013) and Zhejiang Province's medical and health science and technology program (a special county area) (No. 2023XY220).

Conflict of interest

The authors declare that the research was conducted in the absence of any commercial or financial relationships that could be construed as a potential conflict of interest.

Generative AI statement

The author(s) declare that no Generative AI was used in the creation of this manuscript.

Publisher's note

All claims expressed in this article are solely those of the authors and do not necessarily represent those of their affiliated organizations, or those of the publisher, the editors and the reviewers. Any product that may be evaluated in this article, or claim that may be made by its manufacturer, is not guaranteed or endorsed by the publisher.

Supplementary material

The Supplementary Material for this article can be found online at: https://www.frontiersin.org/articles/10.3389/fonc.2025.1538786/full#supplementary-material

References

1. Burke A, Jeudy J, Virmani R. Cardiac tumours: an update: Cardiac tumours. *Heart*. (2008) 94:117–23. doi: 10.1136/hrt.2005.078576

2. Yin K, Brydges H, Lawrence KW, Wei Y, Karlson KJ, McAneny DB, et al. Primary cardiac lymphoma. *J Thorac Cardiovasc Surg*. (2022) 164(2):573–80.e1. doi: 10.1016/j.jtcvs.2020.09.102

3. Italiano A, Jardin F, Peyrade F, Saudes L, Tilly H, Thyss A. Adapted CHOP plus rituximab in non-Hodgkin's lymphoma in patients over 80 years old. *Haematologica*. (2005) 90:1281–3.

4. Peyrade F, Jardin F, Thieblemont C, Thyss A, Emile J-F, Castaigne S, et al. Attenuated immunochemotherapy regimen (R-miniCHOP) in elderly patients older than 80 years with diffuse large B-cell lymphoma: a multicentre, single-arm, phase 2 trial. *Lancet Oncol*. (2011) 12:460–8. doi: 10.1016/S1470-2045(11)70069-9

5. Wei R, Wu Y, Jiang S, Zhang A, Zhang L, Liu L, et al. Efficacy and safety of Orelabrutinib-based regimens in diffuse large B-cell lymphoma: a single-center retrospective analysis. *Clin Exp Med*. (2023) 23:4609–21. doi: 10.1007/s10238-023-01231-w

6. Sehn LH, Herrera AF, Flowers CR, Kamdar MK, McMillan A, Hertzberg M, et al. Polatuzumab vedotin in relapsed or refractory diffuse large B-cell lymphoma. *J Clin Oncol*. (2020) 38:155–65. doi: 10.1200/JCO.19.00172

7. Kondo S, Osanai H, Sakamoto Y, Uno H, Tagahara K, Hosono H, et al. Secondary cardiac lymphoma presenting as sick sinus syndrome and atrial fibrillation which required leadless pacemaker implantation. *Intern Med*. (2021) 60:431–4. doi: 10.2169/internalmedicine.5573-20

8. Hirakawa Y, Tsuda S, Sugimoto T. Treatment of sick sinus syndrome in a patient with cardiac lymphoma via chemotherapy without pacemaker implantation: A case report. *Clin Case Rep*. (2022) 10:e05649. doi: 10.1002/ccr3.5649

9. Liu E, Huang J, Dong H, Chen Z, Liu C, Xie Q, et al. Diagnostic challenges in primary cardiac lymphoma, the opportunity of 18F-FDG PET/CT integrated with contrast-enhanced CT. *J Nucl Cardiol*. (2022) 29:2378–89. doi: 10.1007/s12350-021-02723-6

10. Caforio ALP, Kaski JP, Gimeno JR, Elliott PM, Laroche C, Tavazzi L, et al. Endomyocardial biopsy: safety and prognostic utility in paediatric and adult

myocarditis in the European Society of Cardiology EURObservational Research Programme Cardiomyopathy and Myocarditis Long-Term Registry. *Eur Heart J*. (2024) 45:2548–69. doi: 10.1093/eurheartj/ehae169

11. Wilson WH, Young RM, Schmitz R, Yang Y, Pittaluga S, Wright G, et al. Targeting B cell receptor signaling with ibrutinib in diffuse large B cell lymphoma. *Nat Med*. (2015) 21:922–6. doi: 10.1038/nm.3884

12. Wilson WH, Wright GW, Huang DW, Hodkinson B, Balasubramanian S, Fan Y, et al. Effect of ibrutinib with R-CHOP chemotherapy in genetic subtypes of DLBCL. *Cancer Cell*. (2021) 39(12):1643–53.e3. doi: 10.1016/j.ccell.2021.10.006

13. Long P, Li S, Pan L, Wang Y, Chen W, Wang X. Cardiovascular adverse events associated with antibody-drug conjugates (ADCs): a pharmacovigilance study based on the FAERS database. *Front Pharmacol*. (2024) 15:1378010. doi: 10.3389/fphar.2024.1378010

14. Dickinson MJ, Carlo-Stella C, Morschhauser F, Bachy E, Corradini P, Iacoboni G, et al. Glofitamab for relapsed or refractory diffuse large B-cell lymphoma. *N Engl J Med*. (2022) 387:2220–31. doi: 10.1056/NEJMoa2206913

15. Kantarjian H, Stein A, Gökbuget N, Fielding AK, Schuh AC, Ribera J-M, et al. Blinatumomab versus chemotherapy for advanced acute lymphoblastic leukemia. *N Engl J Med*. (2017) 376:836–47. doi: 10.1056/NEJMoa1609783

16. Palaskas NL, Ali H-J, Koutroumpakis E, Ganatra S, Deswal A. Cardiovascular toxicity of immune therapies for cancer. *BMJ*. (2024) 385:e075859. doi: 10.1136/bmj-2023-075859

17. Koch C, Montrasio G, Scherr BF, Schimmer R, Matter CM, Bühler KP, et al. Fulminant cardiotoxicity in a patient with cardiac lymphoma treated with CAR-T cells. *JACC CardioOncol*. (2022) 4:708–12. doi: 10.1016/j.jaccao.2022.07.012

frontiers | Frontiers in Oncology

TYPE Case Report
PUBLISHED 17 July 2025
DOI 10.3389/fonc.2025.1567625

Check for updates

OPEN ACCESS

EDITED BY
Reto Asmis,
Wake Forest University, United States

REVIEWED BY
George Lazaros,
Hippokration General Hospital, Greece
Catalin Constantin Badiu,
Carol Davila University of Medicine and Pharmacy, Romania

*CORRESPONDENCE
Wei Li
lwyljbyfy@126.com

RECEIVED 27 January 2025
ACCEPTED 26 June 2025
PUBLISHED 17 July 2025

CITATION
Dong W, Du Z, Liu D, Yang L and Li W (2025) Case report: Cardiac myxoid fibrosarcoma: a report of two cases. *Front. Oncol.* 15:1567625. doi: 10.3389/fonc.2025.1567625

COPYRIGHT
© 2025 Dong, Du, Liu, Yang and Li. This is an open-access article distributed under the terms of the Creative Commons Attribution License (CC BY). The use, distribution or reproduction in other forums is permitted, provided the original author(s) and the copyright owner(s) are credited and that the original publication in this journal is cited, in accordance with accepted academic practice. No use, distribution or reproduction is permitted which does not comply with these terms.

Case report: Cardiac myxoid fibrosarcoma: a report of two cases

Weikai Dong[1], Zhaoqi Du[1], Dianxiao Liu[1], Lijuan Yang[2] and Wei Li[1]*

[1]Department of Cardiovascular Surgery, Binzhou Medical University Hospital, Binzhou, Shandong, China, [2]Department of Medical Research Center, Binzhou Medical University Hospital, Binzhou, Shandong, China

Introduction: The research into cardiac tumors can be traced back to the 18th century, when Bonet first introduced the relevant concept. It was not until 1936 that the first successful resection of a cardiac tumor was performed. From a pathological origin perspective, cardiac tumors can be categorized into two main types: primary tumors, which originate from the heart itself, and secondary tumors, which result from metastases of malignant tumors in other tissues or organs. Primary cardiac tumors are exceedingly rare, among primary cardiac tumors, roughly 75% are benign, while the remainder are malignant. In contrast, approximately 75% of primary malignant cardiac tumors are sarcomas. Cardiac myxoid fibrosarcoma stands out as a particularly rare diagnosis in this domain.

Case report: Case one: A 25-year-old man presented with chest pain and tightness. After initial treatment, his symptoms recurred and worsened. Imaging revealed a large mass in the left atrium obstructing the mitral valve. He underwent surgical resection of the tumor, thrombectomy, and tricuspid valvuloplasty. Pathology diagnosed myxoid fibrosarcoma. The patient was readmitted 7 months later with hemoptysis due to tumor recurrence and was lost to follow-up after symptomatic treatment. Case two: A 67-year-old woman was admitted with cough, chest tightness, and shortness of breath. Physical examination and imaging showed a mass in the left atrium causing mitral valve obstruction. She underwent surgical resection of the tumor. Pathology confirmed myxoid fibrosarcoma. After 6 months of follow-up, there was no tumor recurrence or metastasis.

Discussion: Myxoid fibrosarcoma located in the left atrium can lead to mitral valve obstruction, causing symptoms of mitral stenosis such as dyspnea, cough, hemoptysis, and reduced exercise tolerance. Surgery remains the primary treatment for primary left atrial malignant tumors. Once the diagnosis is confirmed, active surgical intervention should be performed to relieve blood flow obstruction, remove pericardial effusion, and alleviate cardiac compression, which can extend patients' lives in the short term and improve their quality of life. Despite advancements in diagnostic techniques and surgical methods, the prognosis for patients with cardiac tumors still depends on the histology and location of the tumor.

KEYWORDS

cardiac myxoid fibrosarcoma, diagnosis, surgery, treatment, prognosis

Introduction

Cardiac myxoid fibrosarcoma is a rare and aggressive malignancy that typically originates in the left atrium. It is characterized by symptoms such as chest tightness, dyspnea, cough, and hemoptysis, often leading to mitral valve obstruction and mimicking mitral stenosis. The tumor's rapid progression and serious consequences necessitate prompt diagnosis and treatment. Imaging modalities like echocardiography, CT, and MRI are crucial for visualizing the tumor's size, location, and relationship with surrounding tissues. Pathological examination, including immunohistochemical staining for markers like Vimentin, SMA, and Desmin, confirms the diagnosis. Surgical resection is the primary treatment, aiming to remove the tumor, alleviate cardiac compression, and restore normal function. Despite advancements, the prognosis remains poor due to high recurrence and mortality rates. Long-term follow-up with regular imaging and laboratory tests is essential for monitoring recurrence and metastasis. Multidisciplinary collaboration is vital for managing this complex condition, and future research is needed to improve diagnostic and therapeutic strategies.

Case one

A 25-year-old man presented with unexplained chest pain and tightness three months ago. His condition improved after receiving anti-infection treatment and closed thoracic drainage at another hospital. However, the chest tightness recurred, and he was admitted to the hospital one week ago due to a worsening of his original symptoms. The patient had no history of other diseases or treatments. Physical examination revealed coarse breath sounds in both lungs, with no dry or wet rales detected. His heart rate was 114 beats per minute, with a regular rhythm and hyperactive P2 tone. A grade III/VI diastolic murmur was heard in the mitral valve auscultation area, and there was no edema in either lower limb.

Auxiliary examinations revealed the following findings: A cardiac color Doppler ultrasound (Figures 1E, F) detected a mass in the left atrium measuring 50mm×43mm×56mm. The mass appeared relatively homogeneous with poor activity. Its pedicle seemed to be connected to the mitral valve, causing obstruction of the mitral valve orifice during diastole. A computed tomography angiography (CTA) of the pulmonary artery showed a large hypodense shadow in the left atrium, with a maximum diameter

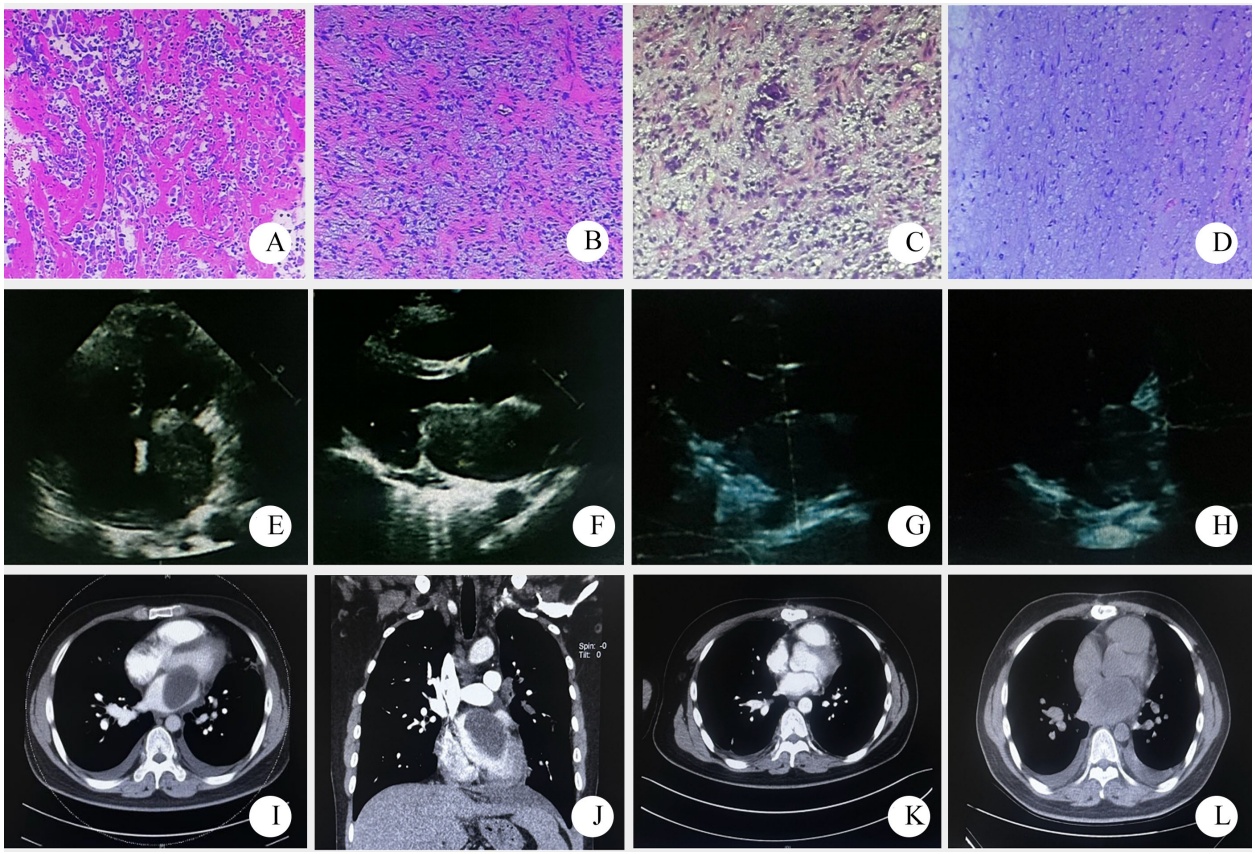

FIGURE 1
Pathological and imaging data of patient one (**(A–D)** pathological HE stained sections, 10×10; **(E, F)** a mass echo of 50mm×43mm×56mm was detected in the left atrium by echocardiography before operation. **(G, H)** postoperative cardiac color Doppler ultrasound; **(I, J)** preoperative pulmonary artery CTA showed large patchy low density shadow in the left atrium; **(K)** postoperative CTA; **(L)** 7 months later, chest CT showed low density shadow in the left atrium, considering recurrence).

of approximately 54mm×51mm. Part of the shadow protruded into the left ventricle, and no enhancement was observed (Figures 1I, J). An electrocardiogram (ECG) revealed sinus tachycardia (Figure 2). Upon admission, the following laboratory findings were noted: creatine kinase isoenzyme was 13.4 U/L, creatine kinase was 39.3 U/L, NT-proBNP was 927.70 pg/mL, alkaline phosphatase was 126.7 U/L, γ-glutamyl transpeptidase was 55.6 U/L, and C-reactive protein was 43.10 mg/L. All other indicators were within the normal range.

Surgical procedure: The patient underwent left atrial tumor resection, pulmonary vein thrombectomy, and tricuspid valvuloplasty (Figures 1G, H, K). Upon opening the pericardium, external cardiac exploration revealed significant dilation of the right atrium and ventricle. The ascending aorta measured approximately 3.5 cm in diameter, and the main pulmonary artery measured about 3.0 cm in diameter, with no other external cardiac malformations observed. Generalized hepatic congestion was noted. Extracorporeal circulation was established, and 1000 mL of HTK cardioplegic solution was infused. The pericardial cavity was packed with ice slush. The right atrium and interatrial septum were incised, revealing a mass within the left atrium, measuring approximately 8 cm × 6 cm × 5 cm. The mass was solid, firm in texture, encapsulated, with a broad base, infiltrating the superior and lateral walls of the left atrium and completely obstructing the orifice of the left upper pulmonary vein. Numerous satellite nodules of varying sizes, ranging from 0.5 cm to 1.5 cm in diameter, were observed around the tumor, with some involvement of the right upper pulmonary vein orifice. Intraoperatively, the tumor was suspected to be malignant, with a high likelihood of sarcoma. The majority of the tumor was resected at its base, and the resulting defect was treated with electrocautery. Thrombus formation was detected within the left upper pulmonary vein and was thoroughly removed. The mitral valve was tested for competence and found to be satisfactory without intervention. Moderate tricuspid regurgitation was noted, and the tricuspid valve was repaired by folding the posterior leaflet to create a bicuspid configuration, with satisfactory results. The interatrial septum was closed with 3–0 Prolene suture, and the right atrial incision was closed with 5–0 Prolene suture. The superior and inferior vena cava were unclamped, the patient was rewarmed, and the left heart was vented. The ascending aorta was then unclamped. The heart spontaneously resumed beating with ventricular fibrillation, which was successfully converted to sinus rhythm with a single 20-joule defibrillation. Circulatory support was continued until hemodynamic stability was achieved. All cardiac cannulas were sequentially removed, and protamine was administered to neutralize heparin. The patient was on bypass for 132 minutes, with aortic cross-clamp time of 68 minutes. Urine output during the procedure was 200 mL, and ultrafiltration volume was 4500 mL, with no hemoglobinuria observed. Postoperatively, the patient was safely transferred to the intensive care unit with an initial blood pressure of 103/36 mmHg, heart rate of 120 beats per minute, and oxygen saturation of 100%.

Pathological diagnosis: The tumor was identified as a left atrial sarcoma. Immunohistochemical results revealed positive staining for Vimentin, weakly positive for SMA, and positive in a few cells for Desmin. S-100, CD31, and CD34 were all negative. The Ki-67 proliferation index was approximately 10%, leading to a diagnosis of myxoid fibrosarcoma (Figures 1A–D).

Prognosis: The patient was readmitted to the hospital 7 months after surgery due to hemoptysis. Imaging suggested tumor recurrence (Figure 1L). The symptoms were slightly relieved after symptomatic and supportive treatment. The patient was lost to follow-up after discharge.

Case two

A 67-year-old female patient was admitted to the hospital due to a 1-month history of cough and expectoration, and 15 days of chest tightness and shortness of breath. The patient was unable to lie flat and had reduced exercise tolerance. Physical examination revealed weak breath sounds in both lungs, with dry and wet rales heard. There was no precordial bulge, the apex beat was normally positioned, no pericardial friction was noted, no cardiac thrill was palpable, and the cardiac dullness was normal on percussion. The

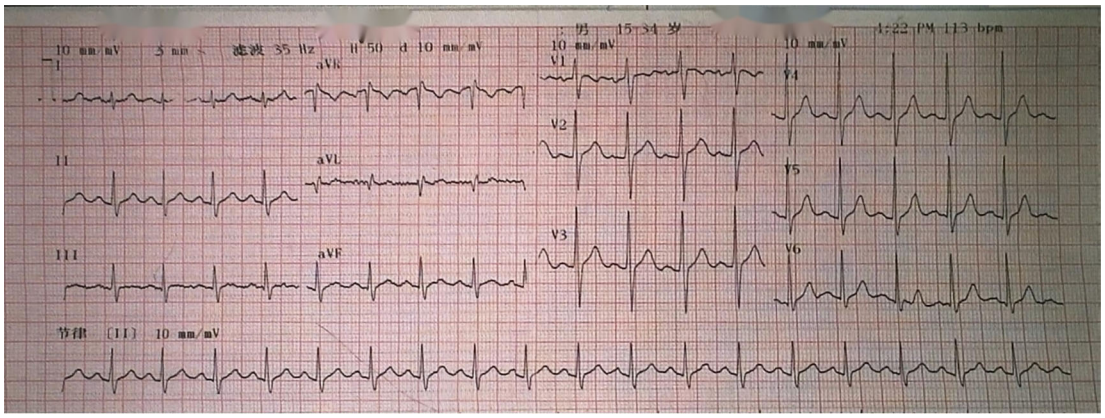

FIGURE 2
Patient one had sinus tachycardia on an ECG.

heart rate was 106 beats per minute, with a regular rhythm, hyperactive P2, a diastolic murmur heard in the mitral valve area, and moderate pitting edema in both lower limbs.

Auxiliary examination: Cardiac color doppler ultrasound (Figures 3E, F) revealed a moderately low echo mass in the left atrium, approximately 59mm×17mm in size, with a loose texture and connected to the atrial septum. During diastole, the mass protruded into the left ventricle, obstructing the mitral valve orifice, with an ejection fraction (EF) of 60%. Chest CT (Figures 3I, J) showed enlargement of the left atrium and right pleural effusion. An electrocardiogram (ECG) demonstrated sinus rhythm with low T waves (Figure 4). Upon admission, the following laboratory findings were noted: hemoglobin concentration was 101 g/L, hematocrit level was 33.8%, lymphocyte percentage was 14.0%, neutrophil percentage was 79.5%, fibrinogen concentration was 5.02 g/L, D-dimer level was 0.99 mg/L FEU, and total bilirubin was 27.40μmol/L. All other indicators were within the normal range.

Surgical procedure: The patient underwent left atrial tumor resection (Figures 3G, H). Upon opening the pericardium, external cardiac exploration revealed a mildly enlarged heart with edema of the epicardium and adventitia of the vessels. The ascending aorta measured approximately 4.0 cm in diameter, and the main pulmonary artery measured about 3.5 cm in diameter, with increased tension. Extracorporeal circulation was established, and 1000 mL of HTK cardioplegic solution was infused. The pericardial cavity was packed with ice slush for cooling. Access to the left atrium was achieved via a right atrial–septal incision, and a left heart decompression catheter was placed through the right upper pulmonary vein. Exploration revealed a tumor located in the left atrium, with its pedicle attached to the anterior margin of the foramen ovale. The main body of the tumor was resected along the pedicle. The tumor base measured approximately 3 cm in diameter, was bilobed, pale yellow, partially translucent with a jelly-like appearance, and had an intact capsule. After tumor removal, further exploration showed that the anterior, superior, and inferior margins of the foramen ovale were involved by the tumor pedicle. Residual tissue was carefully removed. The anterior and posterior leaflets of the mitral valve, as well as the anterior annulus, were densely adherent to the tumor. A 0.5 cm×1.0 cm tumor was present on the free edge of the anterior leaflet (A2 region), causing localized mitral valve insufficiency. The tumor and adherent tissue on the annulus and leaflets were meticulously removed, and the mitral valve was tested with water injection, showing no significant

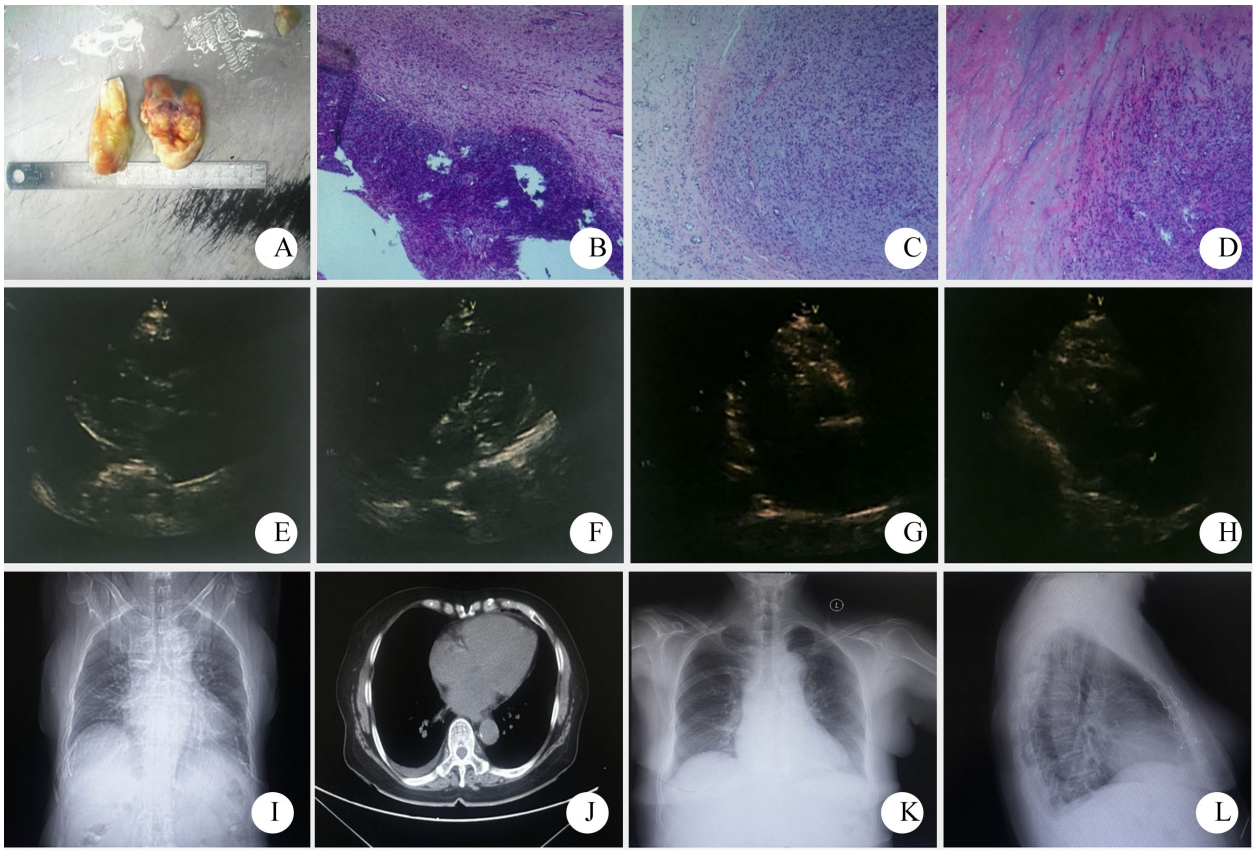

FIGURE 3
Pathological and imaging data of patient two (**(A–D)** gross observation and HE stained sections of the tumor, 4×10, 10×10, 10×10; **(E, F)** preoperative echocardiography showed a moderate to low echo of about 59mm×17mm in the left atrium. **(G–H)** postoperative cardiac color Doppler ultrasound; **(I, J)** Preoperative chest CT showed left atrial enlargement and right pleural effusion. **(K, L)** Chest X-ray reexamination at 6 months after surgery showed no obvious abnormalities after cardiac surgery).

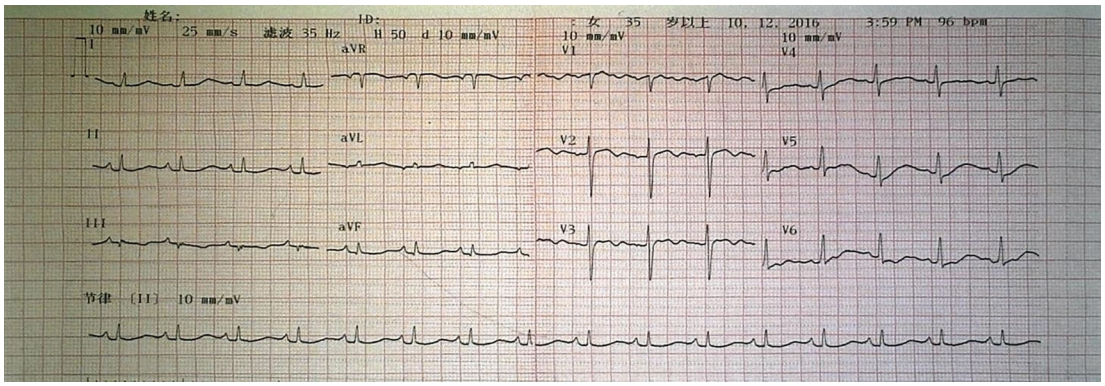

FIGURE 4
The ECG of patient two showed sinus rhythm with low T wave.

regurgitation. The left atrium and ventricle were thoroughly irrigated, and no residual tumor was found. Exploration via the right atrial incision revealed that the tricuspid annulus could accommodate three transverse fingers of the surgeon, and water injection testing showed no significant regurgitation. Rewarming was initiated, the interatrial septal incision was closed, the left heart was fully vented, and the ascending aorta was unclamped. The heart spontaneously resumed beating with sinus rhythm, a ventricular rate of 50 beats per minute, and multiple atrial premature contractions. An epicardial pacing lead was therefore sutured for temporary pacing. The right atrial incision was closed, the superior and inferior vena cava were unclamped, and circulatory support was continued until hemodynamic stability was achieved. The patient was gradually weaned from bypass, protamine was administered to neutralize heparin, and meticulous hemostasis was ensured. The patient was on bypass for 110 minutes, with aortic cross-clamp time of 50 minutes. Urine output during the procedure was 400 mL, and ultrafiltration volume was 2000 mL, with no hemoglobinuria observed. The patient was safely transferred to the intensive care unit postoperatively with an initial blood pressure of 101/64 mmHg, heart rate of 62 beats per minute, and oxygen saturation of 100%.

Pathological diagnosis: The tumor was identified as a left atrial sarcoma. Immunohistochemical results showed positive staining for Vimentin, weakly positive for SMA, and positive in some cells for Desmin. S-100 was negative, while CD31 and CD34 were positive in the vascular components. The Ki-67 proliferation index was approximately 30%, leading to a diagnosis of myxoid fibrosarcoma (Figures 3A–D).

Prognosis: The patient has been followed up for 6 months (Figures 3K, L), and no tumor recurrence or metastasis was observed during this period.

Discussion

Cardiac tumors are a rare condition with an extremely low incidence rate, ranging from 0.0017% to 0.28% (1). Among these tumors, malignant ones account for 25%, with 95% being sarcomas and the remaining 5% consisting of lymphomas and mesotheliomas (2). Cardiac sarcomas make up 75% of malignant cardiac tumors and often present with atypical symptoms. The most common symptom is dyspnea, while others include chest pain, congestive heart failure, fever, general fatigue, and weight loss (3). Kim et al. (4) reported that cardiac sarcomas can be characterized on echocardiography by the following features: 1) The tumor does not occur in the septum. 2) The sarcoma can invade the pulmonary vein. 3) Multiple sarcomas. 4) Extensive attachment to the left atrial wall. 5) Tumor liquefaction can occur. Studies have found that CT and MRI enhancement is prominent and heterogeneous, with dynamic enhanced scans showing progressive enhancement. Primary cardiac fibrosarcoma is a malignant mesenchymal tumor, also known as myxofibrosarcoma due to its rich mucoid matrix. Primary myxofibrosarcoma is rarely found in the heart, accounting for only about 3% of cardiac malignant tumors and most often involving the left atrium (5). This tumor is distinguished from fibrosarcoma by the presence of giant cells and spindle or whorled cells (9). Currently, the pathogenesis of this tumor remains unclear. Some studies suggest that it originates from multipotential endothelial reserve cells (6), which is a type of myxoma with malignant transformation of latent malignant cells within the tumor during growth (7, 8). Myxoid fibrosarcoma located in the left atrium can cause mitral valve obstruction and cause symptoms of mitral stenosis, such as dyspnea, cough, hemoptysis, and decreased exercise tolerance (9). Surgical operation is still the main treatment (10, 11). After the diagnosis is confirmed, active surgical treatment should be performed to relieve blood flow obstruction, remove pericardial effusion and relieve the compression of the heart. Despite advances in diagnostic techniques and surgical approaches, this disease still has a poor prognosis.

The diagnosis of cardiac myxoid fibrosarcoma primarily relies on imaging and pathological examinations. Imaging modalities encompass echocardiography, CT, and MRI. Color doppler echocardiography can delineate the tumor's size, shape, location, and activity, though early-stage tumors may be challenging to detect. CT and MRI offer clearer visualization of the tumor's boundaries and its relationship with surrounding tissues, aiding in the assessment of tumor invasion and staging. Pathological examination stands as the gold standard for diagnosing cardiac myxoid fibrosarcoma. Tumor tissue, obtained via surgical resection

or needle biopsy, undergoes histological and immunohistochemical analyses. Immunohistochemical examination identifies specific tumor cell markers, such as Vimentin, SMA, Desmin, etc., which assist in determining the tumor type and origin.

The two patients with cardiac myxoid fibrosarcoma reported in this paper presented with tumors located in the left atrium, symptoms of chest tightness, and P2 accentuation on auscultation. At initial diagnosis, both patients had heart rates exceeding 100 beats per minute, with electrocardiography showing sinus rhythm, indicative of sinus tachycardia. The maximum diameter of the tumors was greater than 5.0cm, and the tumors obstructed the mitral valve during diastole. There was no significant change in ejection fraction (EF). Chest CT revealed left atrial enlargement. The tumors were encapsulated and pedicled. During surgery, it was found that the tumors had infiltrated surrounding tissues, indicating strong invasiveness. The tumors were not easily detected by non-invasive examinations (such as cardiac color Doppler ultrasound) in the early stage. The histopathological features of the tumor were characterized by a heterogeneous cellular morphology, comprising spindle-shaped cells, round cells, and multinucleated giant cells, all embedded within a myxoid stromal matrix. Immunohistochemical staining revealed positive expression of vimentin, smooth muscle actin (SMA), and desmin, while S-100 protein was negative.

The primary treatment for cardiac myxoid fibrosarcoma is surgical resection, which aims to remove the tumor as completely as possible, alleviate the compression of the heart and great vessels, and restore normal cardiac function. Owing to the rarity of these tumors, surgical treatment is often referenced from the management of other types of cardiac sarcomas. Lars Niclauss et al. (12) retrospectively analyzed the clinical data of 9 patients with cardiac sarcoma and found that the 1-year mortality rate of cardiac sarcoma was 44%. However, surgery could significantly alleviate cardiac symptoms and improve survival rates. Complete tumor resection, absence of metastasis, and low-grade sarcoma types were associated with better prognosis. Rieneke Moeri-Schimmel et al. (13) reported two cases of primary cardiac sarcoma and reviewed the data of patients treated in three sarcoma centers in the Netherlands from 2005 to 2019. They concluded that surgery combined with postoperative radiotherapy was feasible for resectable cardiac sarcomas, although distant metastasis occurred frequently. For unresectable cardiac sarcomas, initial radiotherapy should be considered. Shusaku Maeda et al. (14) reported a case of a 19-year-old male patient with left ventricular synovial sarcoma. The patient presented with dyspnea and orthopnea. Imaging revealed a heterogeneous enhancing mass over 15 cm in the left ventricle, severely compressing the left atrium. Despite surgical resection and adjuvant chemotherapy and radiotherapy, the patient died of local recurrence 36 months postoperatively, indicating a poor prognosis for cardiac synovial sarcoma, especially in patients with extensive necrotic tissue. This is also similar to the treatment situation of case one in our study. A review by Pietro Scicchitano et al. (15) on Primary Soft Tissue Sarcoma of the Heart (pSTS-h) indicated that surgery is the primary treatment for pSTS-h, although chemotherapy and radiotherapy can also be effective in certain circumstances. All the above studies emphasize that surgery remains the mainstay of treatment for cardiac sarcomas. In addition, Hua Li (16) retrospectively analyzed 46 patients with non-metastatic primary cardiac sarcoma treated with heart transplantation and found that the median survival of heart transplant recipients was 16 months. Among them, the median survival of patients with angiosarcoma was 9 months, significantly lower than that of patients with other histological types (36 months). Low-grade and low-invasive histological subtypes benefited more from heart transplantation. Hassiba Smail et al. (17) reported a case of a patient who underwent total cardiac resection and total artificial heart implantation due to tumor invasion of the ventricle. They suggested that total artificial heart implantation is an effective treatment for unresectable cardiac tumors. These two studies indicate that heart transplantation can also be considered for patients with unresectable primary cardiac sarcoma.

Walid K. Abu Saleh et al. (18) retrospectively analyzed the clinical data of 44 patients with right-sided cardiac sarcoma from 1990 to 2015. Among them, 32 patients received neoadjuvant chemotherapy. The median survival of patients who received neoadjuvant chemotherapy was 20 months, significantly higher than that of patients who did not receive chemotherapy (9.5 months). The median survival of patients with complete resection (R0) was 53.5 months, significantly higher than that of patients with partial resection (R1) (9.5 months). They concluded that neoadjuvant chemotherapy combined with radical surgery could significantly improve the survival rate of patients with right-sided cardiac sarcoma. Gal Aviel et al. (19) introduced a novel treatment method—endovascular brachytherapy. They treated a 35-year-old male patient diagnosed with unresectable high-grade endocardial sarcoma involving the right ventricle and pulmonary artery. After three cycles of doxorubicin and ifosfamide treatment, the patient's right heart failure symptoms worsened. Through a femoral vein approach, a brachytherapy catheter was placed in the right ventricle, main pulmonary artery, and right pulmonary artery, delivering a dose of 20 Gy for 10 minutes. Ten months later, imaging showed a significant reduction in tumor volume, an increase in the cross-sectional area of the pulmonary artery, a significant decrease in pulmonary artery pressure, and complete relief of heart failure symptoms. They concluded that endovascular brachytherapy is a new, safe, and effective treatment for unresectable primary cardiac sarcoma, which can be used to relieve obstruction or reduce tumor volume to achieve complete resection. These two studies provide valuable insights into the efficacy of chemotherapy. Anna Romanowska et al. (20) conducted intensity-modulated radiation therapy on two male patients with cardiac intimal sarcoma (CIS) and found that radiotherapy might be effective and tolerable in the treatment of CIS. However, given the risk of radiation-induced heart disease (RIHD) due to high-dose radiation directly targeting the heart, patients are expected to develop RIHD earlier than reported in the literature. Therefore, regular cardiovascular assessments are required.

Therefore, we believe that for patients with cardiac myxoid fibrosarcoma that have not developed distant metastasis, aggressive surgical treatment should be undertaken. During the surgical procedure, every effort should be made to achieve complete

resection of the tumor tissue, thereby aiming for a radical cure and potentially delaying the risk of tumor recurrence or metastasis. For tumors that cannot be completely resected, palliative surgery may be considered to alleviate symptoms and improve quality of life. Moreover, adjuvant chemotherapy should be administered postoperatively, and radiotherapy may be employed when necessary. The primary chemotherapy regimen should be based on anthracycline agents. Additionally, the use of sensitizers (21, 22) or dendritic cell (DC) nanovaccines (23) may be considered as alternative therapeutic approaches.

Cardiac myxoid fibrosarcoma has a poor prognosis, characterized by high recurrence and mortality rates. Recurrent tumors tend to be more malignant and less responsive to treatment. Therefore, long-term postoperative follow-up with regular imaging and laboratory tests is essential to monitor for tumor recurrence and metastasis. Timely treatment should be administered if recurrence or metastasis is detected. Moreover, the patient's psychological state and quality of life are crucial, necessitating psychological support and rehabilitation guidance to help patients better cope with the disease and treatment. Cardiac myxoid fibrosarcoma is a rare and highly malignant cardiac tumor, and its diagnosis and treatment require multidisciplinary collaboration. Early diagnosis, active surgical intervention, and comprehensive adjuvant therapy are key to improving patient survival rates and quality of life. Future research should focus on further investigating the pathogenesis and biological characteristics of cardiac myxoid fibrosarcoma, as well as exploring new diagnostic and therapeutic methods to enhance patient prognosis.

Data availability statement

The original contributions presented in the study are included in the article/Supplementary Material. Further inquiries can be directed to the corresponding author.

Ethics statement

The studies involving humans were approved by Binzhou Medical University Hospital ethics committee. The studies were conducted in accordance with the local legislation and institutional requirements. The participants provided their written informed consent to participate in this study. Written informed consent was obtained from the individual(s) for the publication of any potentially identifiable images or data included in this article.

Author contributions

WD: Data curation, Project administration, Writing – original draft, Writing – review & editing. ZD: Data curation, Formal Analysis, Writing – review & editing. DL: Data curation, Formal Analysis, Methodology, Writing – review & editing. LY: Data curation, Formal Analysis, Writing – review & editing. WL: Formal Analysis, Funding acquisition, Project administration, Writing – review & editing.

Funding

The author(s) declare that financial support was received for the research and/or publication of this article. This work was supported by TCM Science and Technology Development Plan of Shandong Province (grant number 2020Z24).

Conflict of interest

The authors declare that the research was conducted in the absence of any commercial or financial relationships that could be construed as a potential conflict of interest.

Generative AI statement

The author(s) declare that no Generative AI was used in the creation of this manuscript.

Publisher's note

All claims expressed in this article are solely those of the authors and do not necessarily represent those of their affiliated organizations, or those of the publisher, the editors and the reviewers. Any product that may be evaluated in this article, or claim that may be made by its manufacturer, is not guaranteed or endorsed by the publisher.

Supplementary material

The Supplementary Material for this article can be found online at: https://www.frontiersin.org/articles/10.3389/fonc.2025.1567625/full#supplementary-material

References

1. Vassiliadis N, Vassiliadis K, Karkavelas G. Sudden death due to cardiac myxoma. *Med Sci Law*. (1997) 37:76–8. doi: 10.1177/002580249703700116

2. Bruce CJ. Cardiac tumours: diagnosis and management. *Heart*. (2011) 97:151–60. doi: 10.1136/hrt.2009.186320

3. Shanmugam G. Primary cardiac sarcoma. *Eur J Cardiothorac Surg*. (2006) 29:925–32. doi: 10.1016/j.ejcts.2006.03.034

4. Kim JT, Baek WK, Kim KH, Yoon YH, Kim DH, Lim HK, et al. A primary cardiac sarcoma preoperatively presented as a benign left atrial myxoma. *Yonsei Med J*. (2003) 44:530–3. doi: 10.3349/ymj.2003.44.3.530

5. Lazaros GA, Matsakas EP, Madas JS, Toli DI, Nikas DJ, Kershaw MA, et al. Primary myxofibrosarcoma of the left atrium: case report and review of the literature. *Angiology*. (2008) 59:632–5. doi: 10.1177/0003319707306079

6. Kelly M, Bhagwat AG. Ultrastructural features of a recurrent endothelial myxoma of the left atrium. *Arch Pathol*. (1972) 93:219–26.

7. Read RC, White HJ, Murphy ML, Williams D, Sun CN, Flanagan WH. The Malignant potentiality of left atrial myxoma. *J Thorac Cardiovasc Surg*. (1974) 68:857–68. doi: 10.1016/S0022-5223(19)39681-3

8. Hishitani T, Ogawa K, Hoshino K, Kido S, Nakamura Y, Ogawa Y. Malignant fibrosarcoma with features of myxoma. *Pediatr Cardiol*. (2001) 22:258–9. doi: 10.1007/s002460010218

9. Zhang W, Zheng X, Ni B, Gu W, Sun H, Shao Y, et al. Myxoid fibrosarcoma of the left atrium and ventricle in pregnancy. *Ann Thorac Surg*. (2014) 98:1818–9. doi: 10.1016/j.athoracsur.2013.11.056

10. Kuroczyński W, Peivandi AA, Ewald P, Pruefer D, Heinemann M, Vahl CF, et al. Cardiac myxomas: short- and long-term follow-up. *Cardiol J*. (2009) 16:447–54.

11. Müller S, Feuchtner G, Bonatti J, Müller L, Laufer G, Hiemetzberger R, et al. Value of transesophageal 3D echocardiography as an adjunct to conventional 2D imaging in preoperative evaluation of cardiac masses. *Echocardiography*. (2008) 25:624–31. doi: 10.1111/j.1540-8175.2008.00664.x

12. Niclauss L, Montemurro M, Kirsch M, Prêtre R. Sarcoma of the heart: survival after surgery. *Interact Cardiovasc Thorac Surg*. (2018) 27:198–201. doi: 10.1093/icvts/ivy045

13. Moeri-Schimmel R, Pras E, Desar I, Krol S, Braam P. Primary sarcoma of the heart: case report and literature review. *J Cardiothorac Surg*. (2020) 15:104. doi: 10.1186/s13019-020-01157-4

14. Maeda S, Takano H, Yamauchi T, Tanaka K, Suzuki K, Fushimi H, et al. Primary synovial sarcoma of the left heart with large amount of necrotic tissue. *Gen Thorac Cardiovasc Surg*. (2018) 66:365–7. doi: 10.1007/s11748-017-0828-3

15. Scicchitano P, Sergi MC, Cameli M, Miglioranza MH, Ciccone MM, Gentile M, et al. Primary soft tissue sarcoma of the heart: an emerging chapter in cardio-oncology. *Biomedicines*. (2021) 9:774. doi: 10.3390/biomedicines9070774

16. Li H, Yang S, Chen H, Yang Z, Hong T, Hou Y, et al. Survival after heart transplantation for non-metastatic primary cardiac sarcoma. *J Cardiothorac Surg*. (2016) 11:145. doi: 10.1186/s13019-016-0540-x

17. Smail H, Monteagudo-Vela M, Stock U, Simon A. Total artificial heart implantation after right ventricular intimal spindle cell sarcoma. *Eur J Cardiothorac Surg*. (2019) 56:1014–5. doi: 10.1093/ejcts/ezz117

18. Abu Saleh WK, Ramlawi B, Shapira OM, Al Jabbari O, Ravi V, Benjamin R, et al. Improved outcomes with the evolution of a neoadjuvant chemotherapy approach to right heart sarcoma. *Ann Thorac Surg*. (2017) 104:90–6. doi: 10.1016/j.athoracsur.2016.10.054

19. Aviel G, Meirovitz A, Planer D, Cohen D, Gilon D, Feldman J, et al. Endovascular brachytherapy for extensive right-heart and pulmonary artery sarcoma - a case report. *J Contemp Brachytherapy*. (2019) 11:579–83. doi: 10.5114/jcb.2019.91226

20. Romanowska A, Lewicka E, Sławiński G, Jankowska H, Zaucha R. Case report: adjuvant radiotherapy can be an effective treatment for intimal sarcoma of the heart. *Front Oncol*. (2021) 11:621289. doi: 10.3389/fonc.2021.621289

21. Baird SK, Rigopoulos A, Cao D, Allan L, Renner C, Scott FE, et al. Integral membrane protease fibroblast activation protein sensitizes fibrosarcoma to chemotherapy and alters cell death mechanisms. *Apoptosis*. (2015) 20:1483–98. doi: 10.1007/s10495-015-1166-5

22. Sampson ER, Amin V, Schwarz EM, O'Keefe RJ, Rosier RN. The histone deacetylase inhibitor vorinostat selectively sensitizes fibrosarcoma cells to chemotherapy. *J Orthop Res*. (2011) 29:623–32. doi: 10.1002/jor.21274

23. Wang Z, Miao F, Gu L, Zhang R, Ma Y, Li Y, et al. Stimulator of interferon genes-activated biomimetic dendritic cell nanovaccine as a chemotherapeutic booster to enhance systemic fibrosarcoma treatment. *ACS Nano*. (2024) 18:24219–35. doi: 10.1021/acsnano.4c05657

Frontiers in
Cardiovascular Medicine

Innovations and improvements in cardiovascular treatment and practice

Focuses on research that challenges the status quo of cardiovascular care, or facilitates the translation of advances into new therapies and diagnostic tools.

Discover the latest Research Topics

See more →

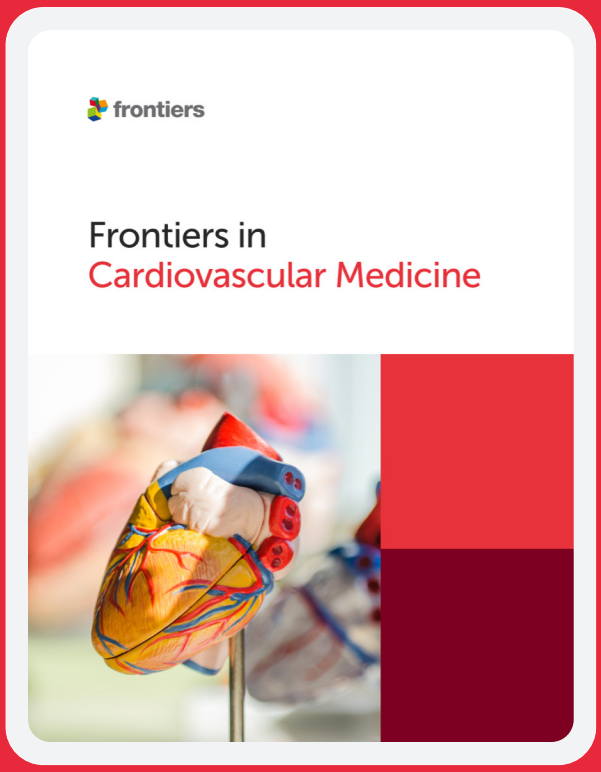

Frontiers

Avenue du Tribunal-Fédéral 34
1005 Lausanne, Switzerland
frontiersin.org

Contact us

+41 (0)21 510 17 00
frontiersin.org/about/contact